NACA TN 3671

TECH LIBRARY KAFB, NM
0066385

NATIONAL ADVISORY COMMITTEE FOR AERONAUTICS

TECHNICAL NOTE 3671

WIND-TUNNEL INVESTIGATION OF THE EFFECT OF CLIPPING THE TIPS OF TRIANGULAR WINGS OF DIFFERENT THICKNESS, CAMBER, AND ASPECT RATIO - TRANSONIC BUMP METHOD

By Horace F. Emerson

Ames Aeronautical Laboratory
Moffett Field, Calif.

Washington
June 1956

AFMDC
FL 2011

TECH LIBRARY KAFB, NM

0066385

U

NATIONAL ADVISORY COMMITTEE FOR AERONAUTICS

TECHNICAL NOTE 3671

WIND-TUNNEL INVESTIGATION OF THE EFFECT OF CLIPPING THE TIPS OF TRIANGULAR WINGS OF DIFFERENT THICKNESS, CAMBER, AND ASPECT RATIO - TRANSONIC BUMP METHOD[1]

By Horace F. Emerson

SUMMARY

The investigation reported herein was conducted on a transonic bump to determine the aerodynamic characteristics of a series of triangular wings. Four basic triangular-wing plan forms having aspect ratios of 2.0, 2.5, 3.0, and 4.0 were tested. The tips of these wings were progressively clipped to provide taper ratios of 0.1, 0.2, 0.3, 0.4, and in some cases 0.5. The NACA 63A00X profile was used with thickness-to-chord ratios of 0.02, 0.04, and 0.06. Wings having the NACA 63A(1.5)04 section were also investigated for each aspect ratio. Data were obtained over a Mach number range from 0.60 to 1.10 corresponding to a test Reynolds number range from 1.85 million to 2.90 million. Lift, drag, and pitching-moment coefficients are presented for each of the wings investigated.

In general, the greatest decrease in drag-rise factor appeared with the change in taper ratio from 0 to 0.1.

INTRODUCTION

The objective of the investigation reported herein was to provide lift, drag, and pitching-moment data through the transonic speed range on a series of triangular wings whose tips were clipped progressively. All the basic data obtained are presented, but only a limited analysis is included.

[1]Supersedes NACA RM A53L03 by Horace F. Emerson, 1953.

The investigation was conducted on a transonic bump in the Ames 16-foot high-speed wind tunnel. Figure 1 shows plan-view drawings of the wing models tested and provides a graphic indication of the scope of this investigation in which 56 wings were tested.

NOTATION

C_D drag coefficient, $\frac{\text{twice semispan drag}}{qS}$

C_L lift coefficient, $\frac{\text{twice semispan lift}}{qS}$

C_m pitching-moment coefficient, referred to $0.25\bar{c}$, $\frac{\text{twice semispan pitching moment}}{qS\bar{c}}$

A aspect ratio, $\frac{b^2}{S}$

M Mach number

R Reynolds number based on wing mean aerodynamic chord

S total wing area (twice wing area of semispan model), sq ft

V velocity, ft/sec

b twice span of semispan model, ft

c local chord, ft

$\bar{c}$ mean aerodynamic chord, $\frac{\int_0^{b/2} c^2 dy}{\int_0^{b/2} c\, dy}$, ft

q dynamic pressure, $\frac{1}{2}\rho V^2$, lb/sq ft

y spanwise distance from plane of symmetry, ft

α angle of attack, deg

ρ air density, slugs/cu ft

λ taper ratio, $\frac{\text{tip chord}}{\text{root chord}}$

Λ leading-edge sweep angle, deg

$\frac{dC_L}{d\alpha}$ slope of the lift curve measured through zero lift, per deg

$\frac{dC_m}{dC_L}$ slope of the pitching-moment curve measured through zero lift

$\frac{dC_D}{dC_L^2}$ drag-rise factor, measured on the linear part of curves of C_L^2 versus C_D (This linear part extended from a C_L of about 0 to at least 0.3.)

APPARATUS

Wind Tunnel and Equipment

The tests were conducted on a transonic bump in the Ames 16-foot high-speed wind tunnel. A description of the bump is available in reference 1. Aerodynamic forces and moments were measured by means of a six-component strain-gage balance in which the gages were essentially free of interactions.

Models

All models were machined from 4130 steel. Models having other than pointed tips were obtained by successive cutting of the wing tips. Figure 1 shows the plan forms and sections investigated and table I presents pertinent dimensional data.

A fence (2.75 inches wide and 12 inches long with semicircular ends) located 3/16 inch from the bump surface was used to reduce the effects of leakage which resulted from the clearance between the wing and the bump surface required for operation of the balance. Figure 2 is a photograph of one of the models tested in this investigation (aspect ratio 2.46, taper ratio 0.1) and typifies the model installation.

TESTS AND PROCEDURE

Range of Variables

The aerodynamic characteristics of the wings were investigated over a Mach number range from 0.60 to 1.10. The variation of test Reynolds number with Mach number is shown in figure 3. The angle-of-attack range was from -4° to a positive angle limited either by the capacity

of the equipment or by the strength of the model. For the majority of the tests, the upper limit of the angle-of-attack range was 26°.

Reduction of Data

The test data have been reduced to standard NACA coefficients. The drag data have been corrected to account for the fence tares. Tare values were ascertained by cutting the wing semispan to zero and testing the fence alone. The measured fence tare drag was independent of angle of attack but varied with Mach number.

An angle-of-attack correction of -0.6° was applied to the data to account for the inclination of flow over the bump. Interference effects of the fence and effects of leakage around the fence are not known and no corrections for these effects have been made. A boundary layer, which was approximately 3/4 inch thick at the location of the model, existed over the surface of the transonic bump. No account has been taken to its effect on the aerodynamic characteristics.

Comparisons between data obtained utilizing the 16-foot wind-tunnel transonic bump and data obtained at Mach numbers between 0.60 and 0.94 using other testing techniques have shown no significant differences. (See, e.g., ref. 2.)

Typical Mach number contours of the flow over the bump without a model in place are shown in figure 4. The outline of the wing having an aspect ratio of 3 and a taper ratio of 0 is superposed to indicate the Mach number variation over the model. The test Mach number was taken to be the average of the Mach number contours passing over the model.

RESULTS AND DISCUSSION

Figures 5 through 16 present the variation of angle of attack, drag coefficient, and pitching-moment coefficient with lift coefficient for all the wings investigated. Figures 17 through 19 present the variation of lift-curve slope, drag-rise factor, and pitching-moment-curve slope with aspect ratio. Although not considered to be within the scope of this report, some comparisons with theory have been made, and from a very limited check they indicate that qualitative agreement exists over the aspect-ratio range investigated. The interested reader is directed to references 3 and 4. Table II presents a figure index.

Figure 17 shows the variation of lift-curve slope as a function of aspect ratio for various taper ratios at three Mach numbers. The differences in values of lift-curve slope corresponding to constant values of aspect ratio are attributable to differences in taper and in leading-edge sweep. With the exception of the wings having a taper ratio of 0 and an aspect ratio of 4.0 at a Mach number of 0.98, it can be seen that neither the thickness-to-chord ratios investigated nor the camber had significant effects on the lift-curve slope.

Figure 18 presents the variation of drag-rise factor with aspect ratio at three Mach numbers. It can be observed that the wings with pointed tips had higher drag-rise factors than did the wings with clipped tips. In some cases, for example between aspect ratios of 2 and 3 at a Mach number of 0.98 for the NACA 63A002 wing, the data indicate that the first tip cut provided substantial reductions in the drag-rise factor; whereas subsequent increases in taper ratio failed to produce similar gains. Again, for constant values of aspect ratio, differences in drag-rise factor are attributable to differences in both leading-edge sweep and taper ratio. The data presented in figure 18 indicate that, generally, the most significant gains were realized when the taper ratio was increased from 0 to 0.1. It can be seen that the cambered wings investigated had consistently lower values of the drag-rise factor for all Mach numbers and aspect ratios.

Figure 19 shows the variation of pitching-moment-curve slope with aspect ratio for three Mach numbers. Almost without exception, the increase in taper ratio resulted in a less negative value of the pitching-moment-curve slope.

Figure 19 indicates that the variation of pitching-moment-curve slope with aspect ratio for the 6-percent wings was much different than the variation for the 2-percent wings. The pitching-moment-curve slopes show that between aspect ratios of 2 and 2.5, the aerodynamic center of the 6-percent wing was behind that for the 2-percent wing. Between aspect ratios of 2.5 and 3.0, the aerodynamic center of the thicker wing moved rapidly forward to a point where it was ahead of the center for the thinner wing, remaining ahead as the aspect ratio was increased to 4.0.

CONCLUSIONS

For aspect ratios of 2.0 or greater, the wings having pointed tips had lift-curve slopes that were consistently lower than those for the wings with clipped tips. Values of drag-rise factor were higher in each case for the wings having taper ratios of 0 than for any other values of taper ratio. Generally, the most significant decreases in drag-rise factor were realized when the taper ratio was increased from 0 to 0.1.

The cambered wings had consistently lower values of drag-rise factor than the plane wings.

In general, the values of pitching-moment-curve slope became less negative with increasing taper ratio. The aerodynamic centers of the 6-percent-thick wings were behind those for the 2-percent-thick wings for aspect ratios between 2.0 and 2.5. Between aspect ratios of 2.5 and 3.0, the aerodynamic centers of the 6-percent wings moved forward of those for the 2-percent wings and remained there as the aspect ratio was increased to 4.0.

Ames Aeronautical Laboratory
National Advisory Committee for Aeronautics
Moffett Field, Calif., Dec. 3, 1953

REFERENCES

1. Axelson, John A., and Taylor, Robert A.: Preliminary Investigation of the Transonic Characteristics of an NACA Submerged Inlet. NACA RM A50C13, 1950.

2. Nelson, Warren H., and McDevitt, John B.: The Transonic Characteristics of 17 Rectangular, Symmetrical Wing Models of Varying Aspect Ratio and Thickness. NACA RM A51A12, 1951.

3. DeYoung, John: Theoretical Additional Span Loading Characteristics of Wings with Arbitrary Sweep, Aspect Ratio, and Taper Ratio. NACA TN 1491, 1947.

4. Lapin, Ellis: Charts for the Computation of Lift and Drag of Finite Wings at Supersonic Speeds. Douglas Report No. SM-13480. Oct. 14, 1949.

TABLE I.- PERTINENT MODEL DIMENSIONS

Taper ratio	Aspect ratio	Mean aerodynamic chord, ft	Semispan wing area, sq ft
0	2.00	0.5556	0.174
.1	1.64	.5606	.172
.2	1.33	.5740	.167
.3	1.08	.5940	.158
.4	.86	.6191	.146
0	2.50	.5556	.217
.1	2.05	.5606	.215
.2	1.67	.5740	.208
.3	1.35	.5940	.197
.4	1.07	.6191	.182
0	3.00	.5556	.260
.1	2.46	.5606	.258
.2	2.00	.5740	.250
.3	1.62	.5940	.237
.4	1.29	.6191	.219
.5	1.00	.6481	.195
0	4.00	.5556	.347
.1	3.27	.5606	.344
.2	2.67	.5740	.333
.3	2.15	.5940	.316
.4	1.71	.6191	.292
.5	1.33	.6481	.260

Fence area for all wings, 0.218 sq ft
Root chord for all wings, 0.8333 ft

NACA

TABLE II.- FIGURE INDEX

Aspect ratio	Taper ratio	Figure numbers											
		63A002			63A004			63A006			63A(1.5)04		
		C_L	C_D	C_m	C_L	C_D	C_m	C_L	C_D	C_m	C_L	C_D	C_m
2.00	0	5(a)	6(a)	7(a)	5(f)	6(f)	7(f)	5(j)	6(j)	7(j)	5(k)	6(k)	7(k)
1.64	.1	5(b)	6(b)	7(b)	5(g)	6(g)	7(g)				5(l)	6(l)	7(l)
1.33	.2	5(c)	6(c)	7(c)	5(h)	6(h)	7(h)				5(m)	6(m)	7(m)
1.08	.3	5(d)	6(d)	7(d)	5(i)	6(i)	7(i)				5(n)	6(n)	7(n)
.86	.4	5(e)	6(e)	7(e)									
2.50	0	8(a)	9(a)	10(a)	8(f)	9(f)	10(f)	8(k)	9(k)	10(k)	8(m)	9(m)	10(m)
2.05	.1	8(b)	9(b)	10(b)	8(g)	9(g)	10(g)	8(l)	9(l)	10(l)	8(n)	9(n)	10(n)
1.67	.2	8(c)	9(c)	10(c)	8(h)	9(h)	10(h)				8(o)	9(o)	10(o)
1.35	.3	8(d)	9(d)	10(d)	8(i)	9(i)	10(i)				8(p)	9(p)	10(p)
1.07	.4	8(e)	9(e)	10(e)	8(j)	9(j)	10(j)						
3.00	0	11(a)	12(a)	13(a)	11(d)	12(d)	13(d)	11(j)	12(j)	13(j)	11(k)	12(k)	13(k)
2.46	.1	11(b)	12(b)	13(b)	11(e)	12(e)	13(e)				11(l)	12(l)	13(l)
2.00	.2	11(c)	12(c)	13(c)	11(f)	12(f)	13(f)				11(m)	12(m)	13(m)
1.62	.3				11(g)	12(g)	13(g)						
1.29	.4				11(h)	12(h)	13(h)						
1.00	.5				11(i)	12(i)	13(i)						
4.00	0	14(a)	15(a)	16(a)	14(d)	15(d)	16(d)	14(j)	15(j)	16(j)	14(k)	15(k)	16(k)
3.27	.1	14(b)	15(b)	16(b)	14(e)	15(e)	16(e)				14(l)	15(l)	16(l)
2.67	.2	14(c)	15(c)	16(c)	14(f)	15(f)	16(f)				14(m)	15(m)	16(m)
2.15	.3				14(g)	15(g)	16(g)						
1.71	.4				14(h)	15(h)	16(h)						
1.33	.5				14(i)	15(i)	16(i)						

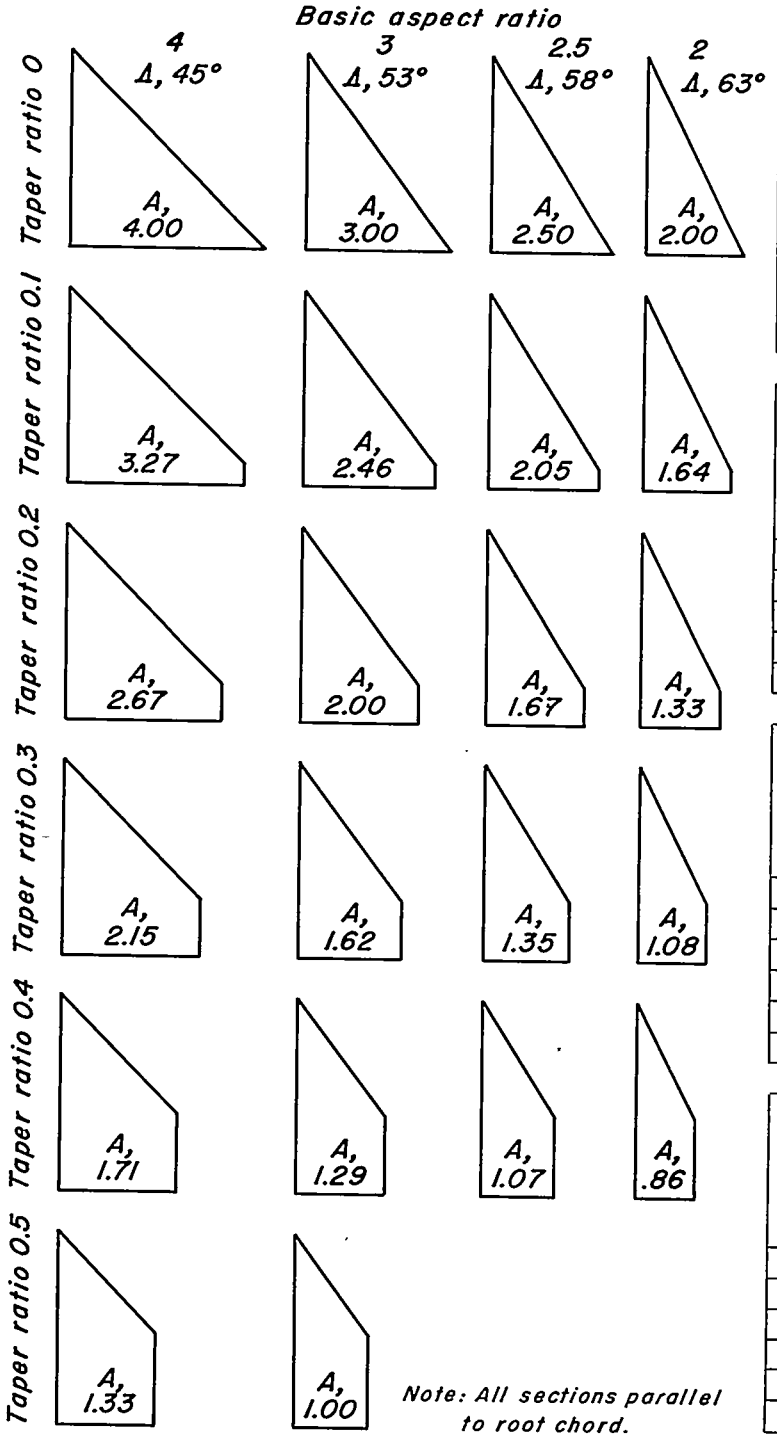

Taper ratio	Basic aspect ratio 2			
	63A002	63A004	63A006	63A(1.5)04
0	x	x	x	x
.1	x	x		x
.2	x	x		x
.3	x	x		x
.4	x			

Taper ratio	Basic aspect ratio 2.5			
	63A002	63A004	63A006	63A(1.5)04
0	x	x	x	x
.1	x	x	x	x
.2	x	x		x
.3	x	x		x
.4	x	x		

Taper ratio	Basic aspect ratio 3			
	63A002	63A004	63A006	63A(1.5)04
0	x	x	x	x
.1	x	x		x
.2	x	x		x
.3		x		
.4		x		
.5		x		

Taper ratio	Basic aspect ratio 4			
	63A002	63A004	63A006	63A(1.5)04
0	x	x	x	x
.1	x	x		x
.2	x	x		x
.3		x		
.4		x		
.5		x		

Figure 1.- Plan-view drawings of the wing models and a table of profiles tested for each plan form.

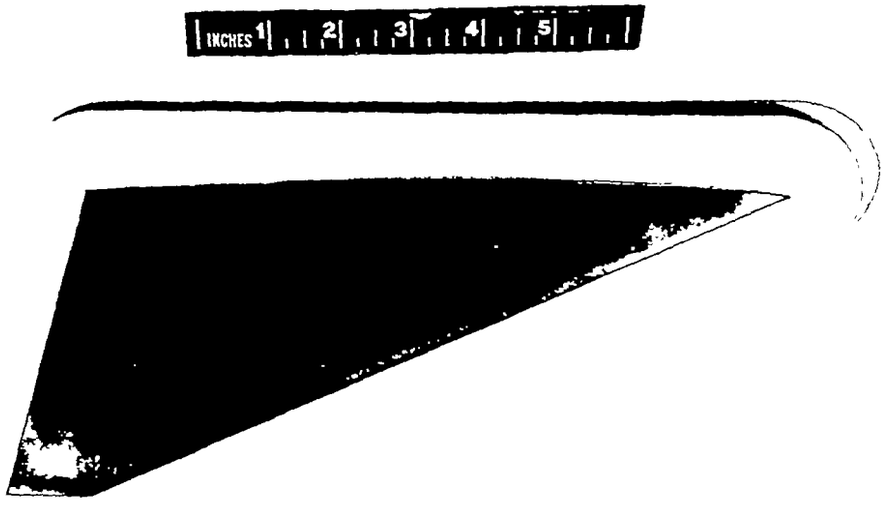

A-17992

Figure 2.- Photograph of one of the wings tested having an aspect ratio of 2.46 and a taper ratio of 0.1 mounted on the Ames 16-foot high-speed wind-tunnel transonic bump.

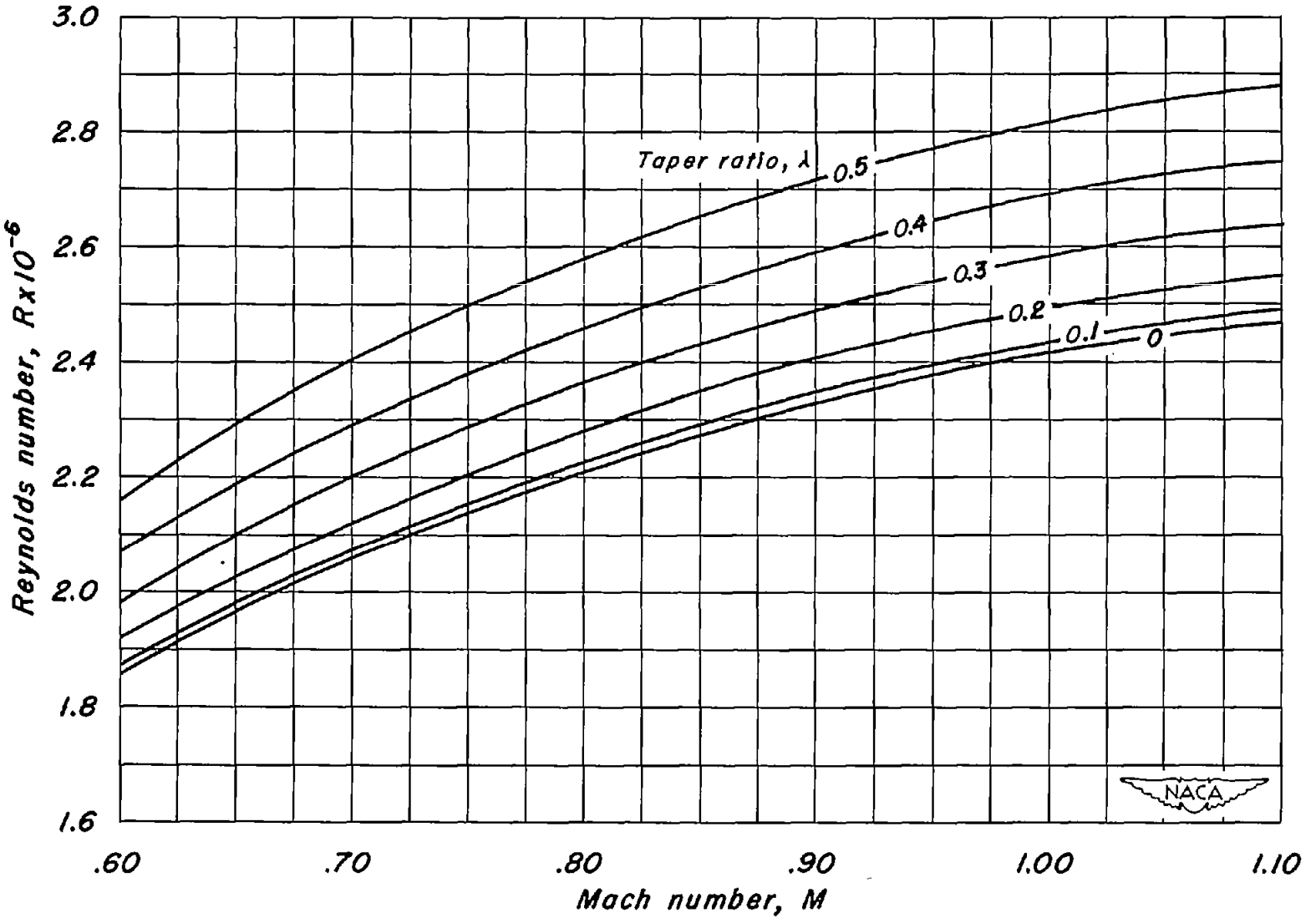

Figure 3.- Variation of Reynolds number with Mach number.

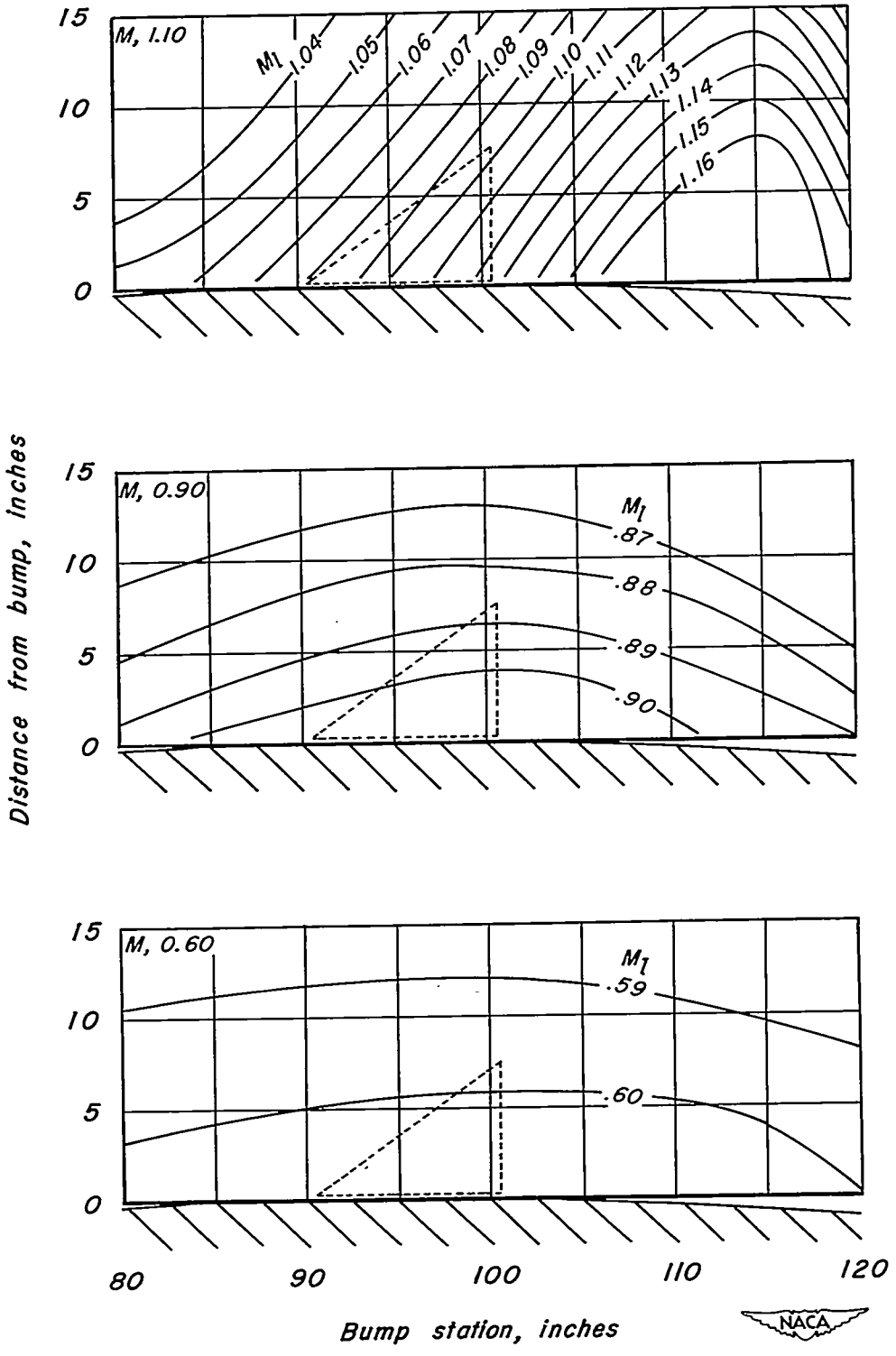

Figure 4.– Typical Mach number contours over the transonic bump in the Ames 16-foot high-speed wind tunnel.

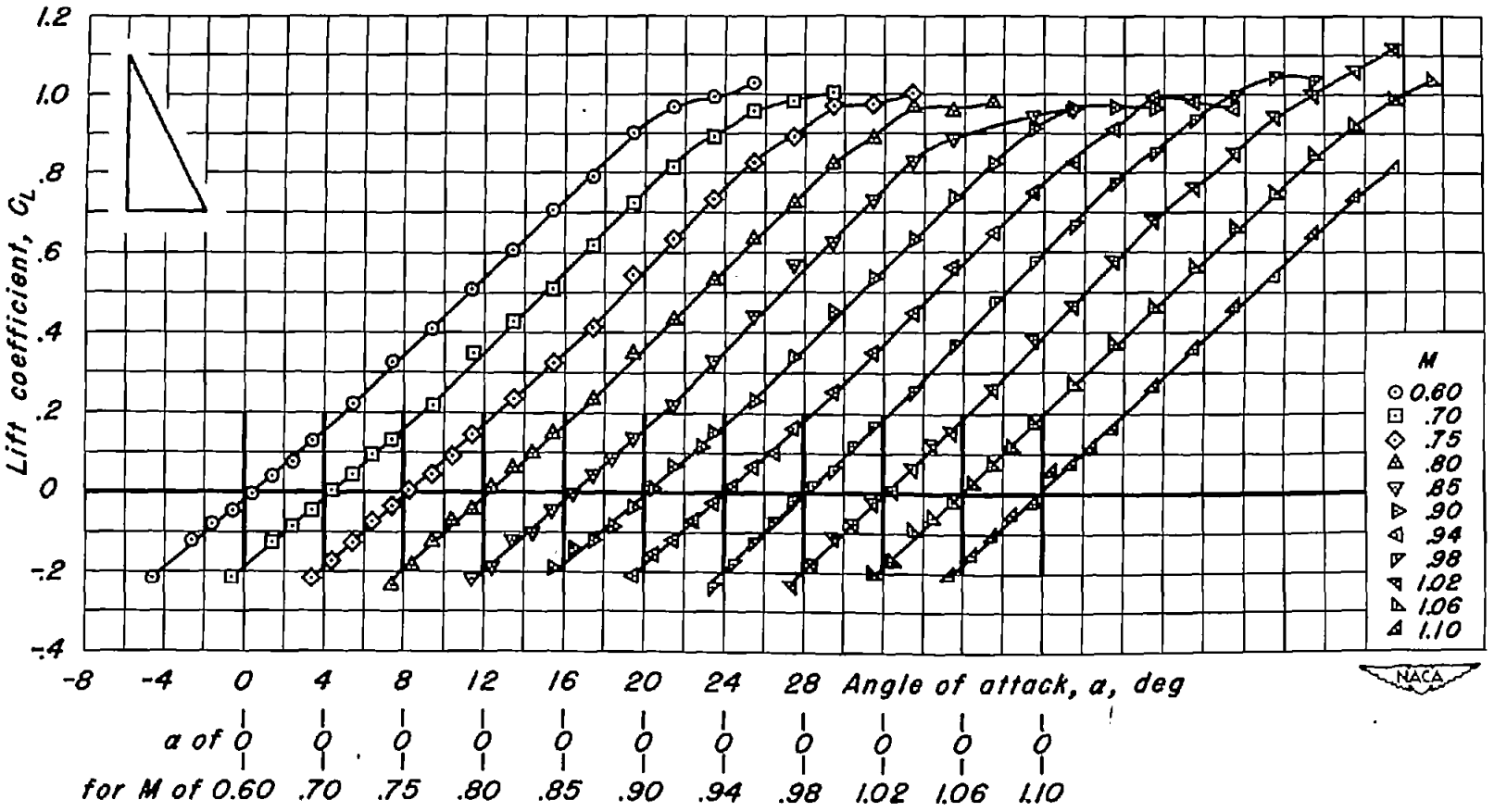

(a) NACA 63A002; λ, 0; A, 2.00.

Figure 5.- Variation of lift coefficient with angle of attack for the wings of basic aspect ratio 2.

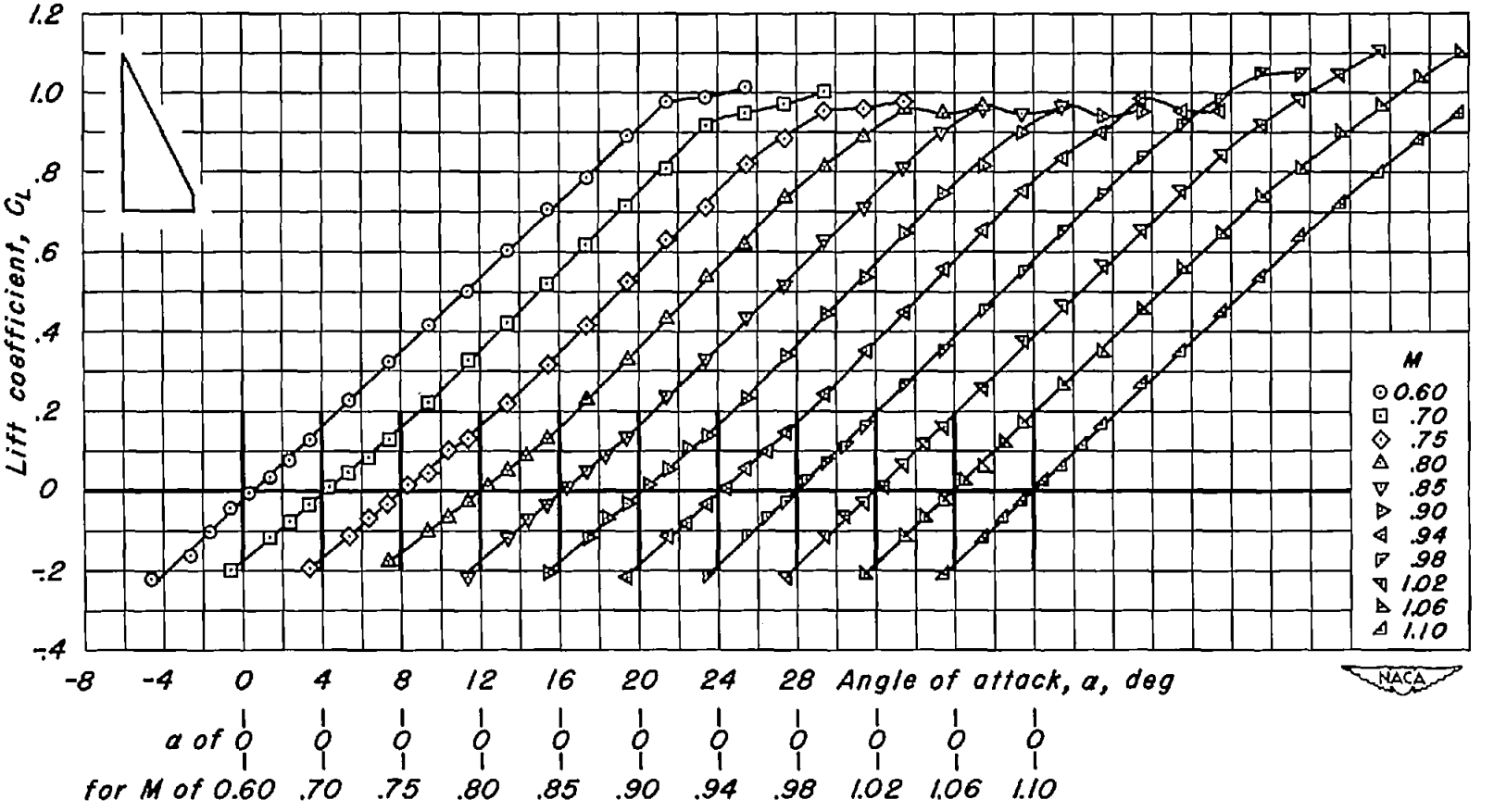

(b) NACA 63A002; λ, 0.1; A, 1.64.
Figure 5.- Continued.

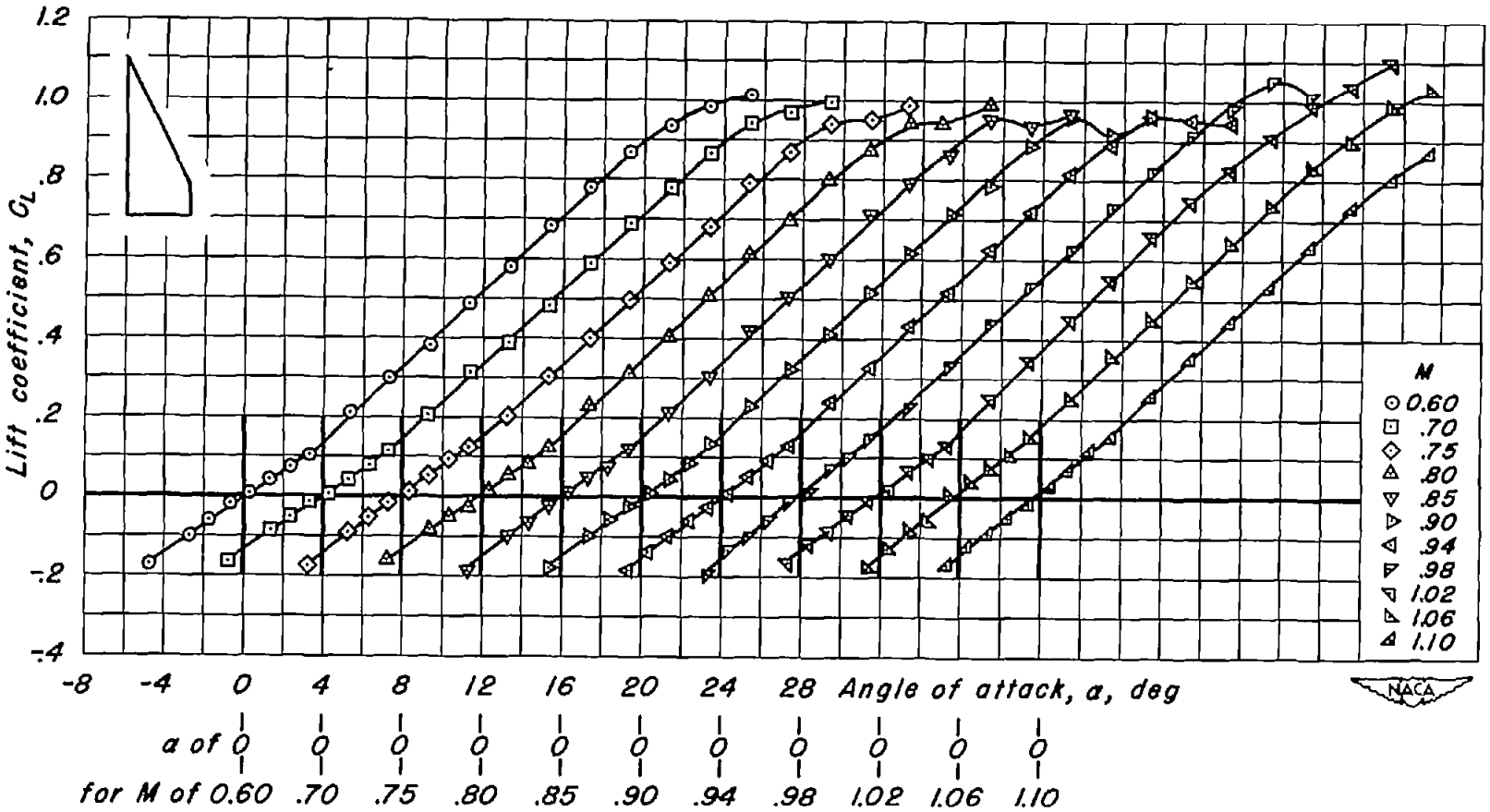

(c) NACA 63A002; λ, 0.2; A, 1.33.
Figure 5.- Continued.

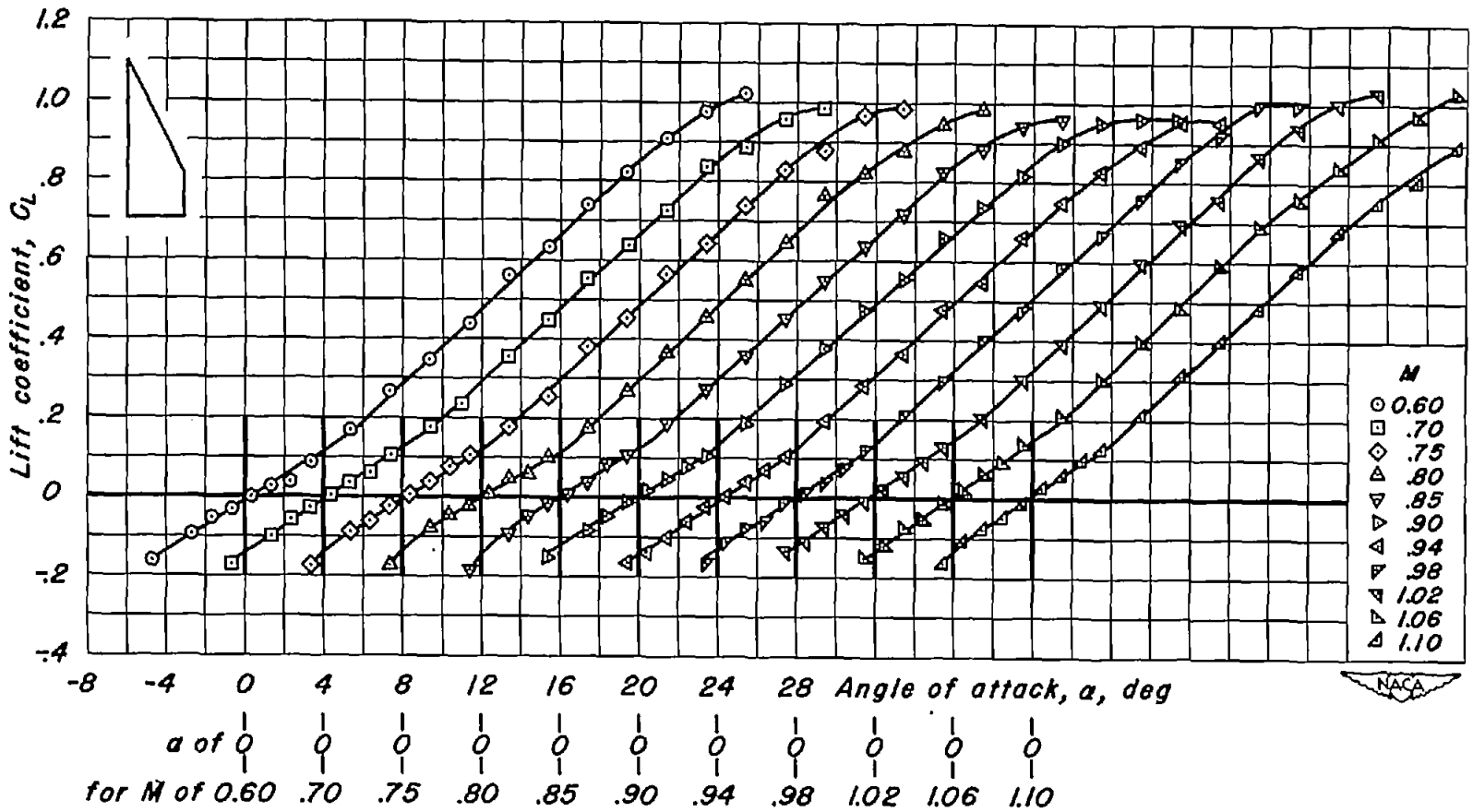

(d) NACA 63A002; λ, 0.3; A, 1.08.
Figure 5.- Continued.

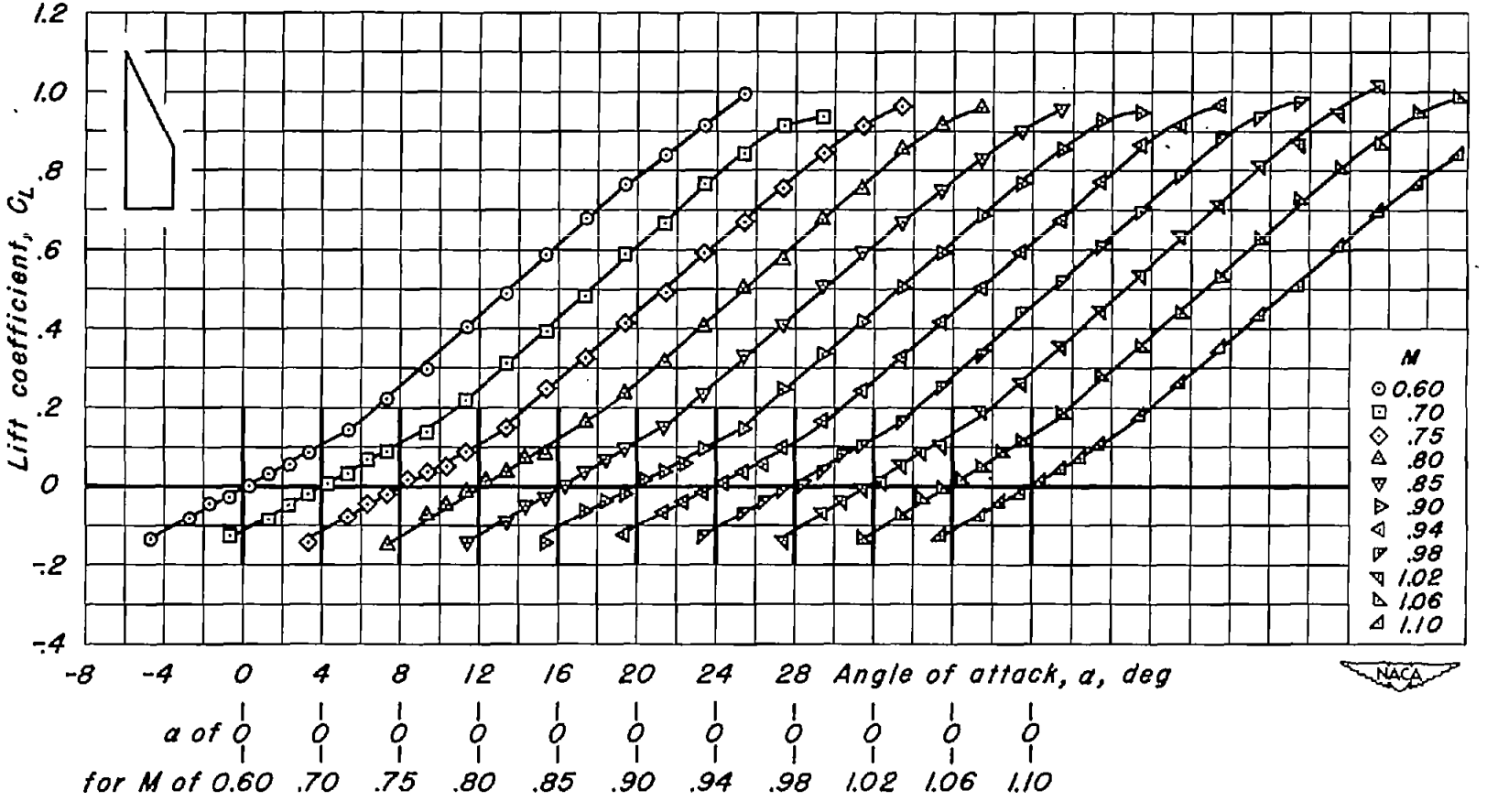

α of	0	0	0	0	0	0	0	0	0	0	0
for M of	0.60	.70	.75	.80	.85	.90	.94	.98	1.02	1.06	1.10

(e) NACA 63A002; λ, 0.4; A, 0.86.
Figure 5. Continued.

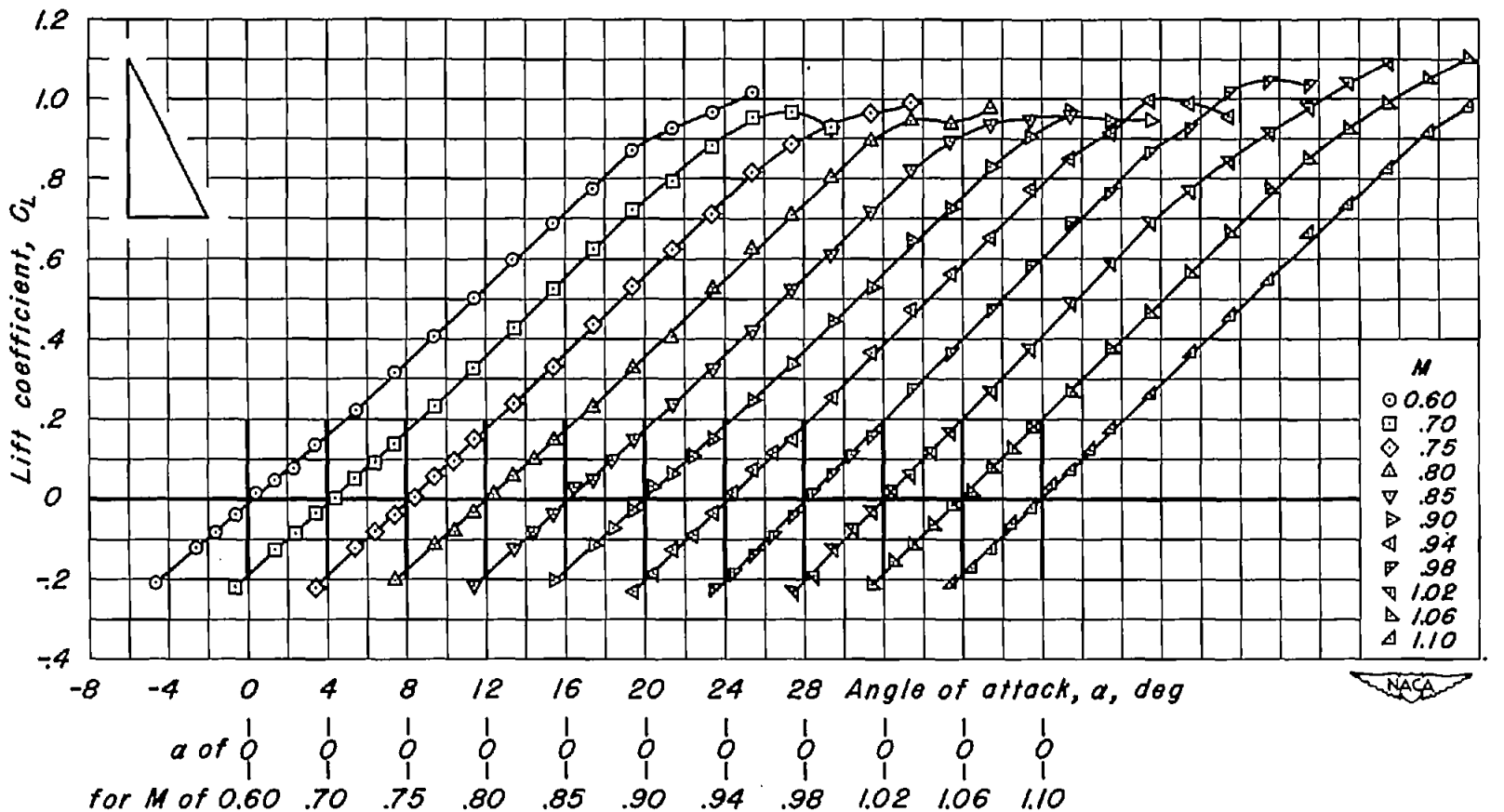

(f) NACA 63A004; λ, 0; A, 2.00.
Figure 5.- Continued.

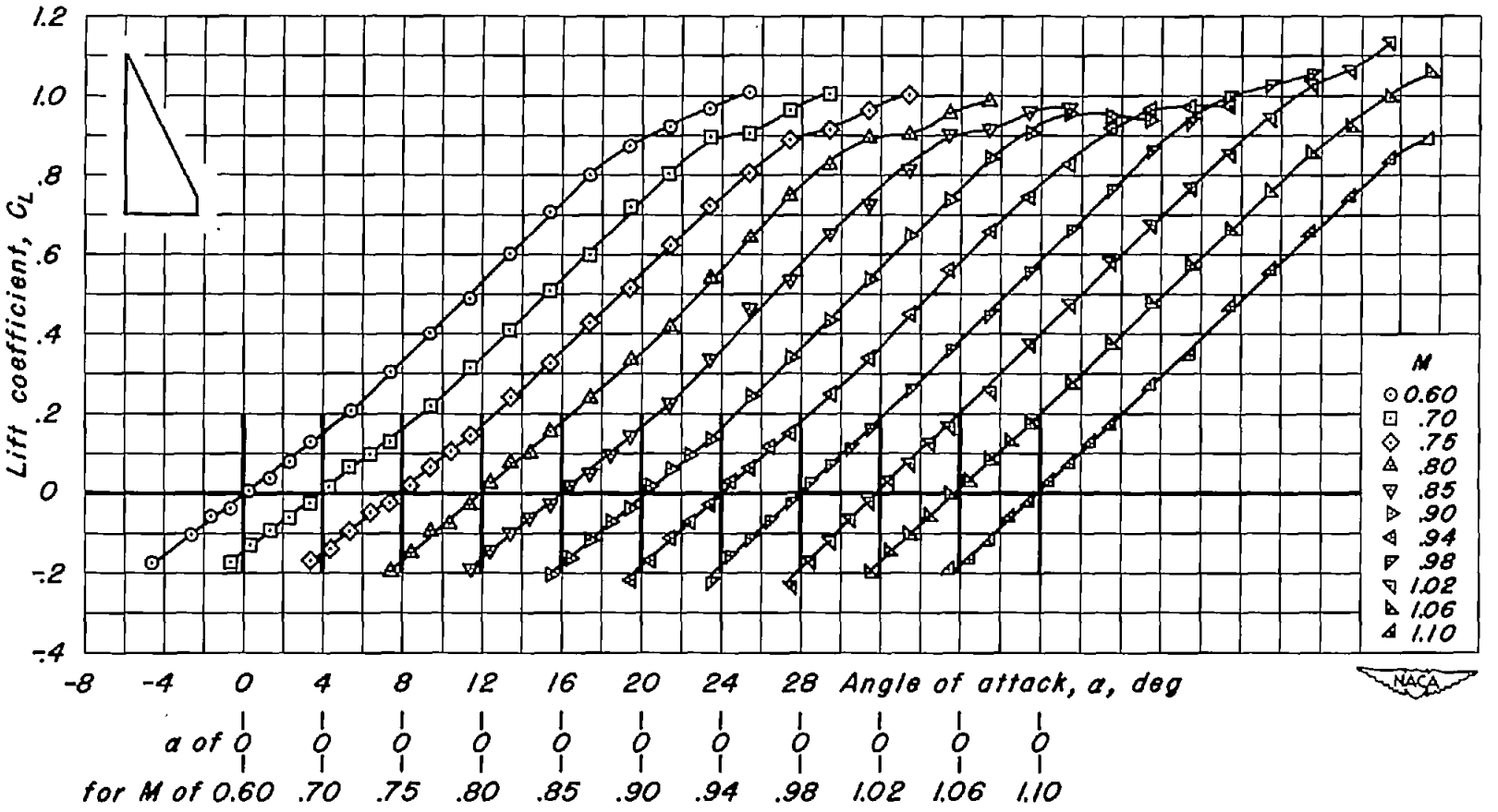

(g) NACA 63A004; λ, 0.1; A, 1.64.
Figure 5.- Continued.

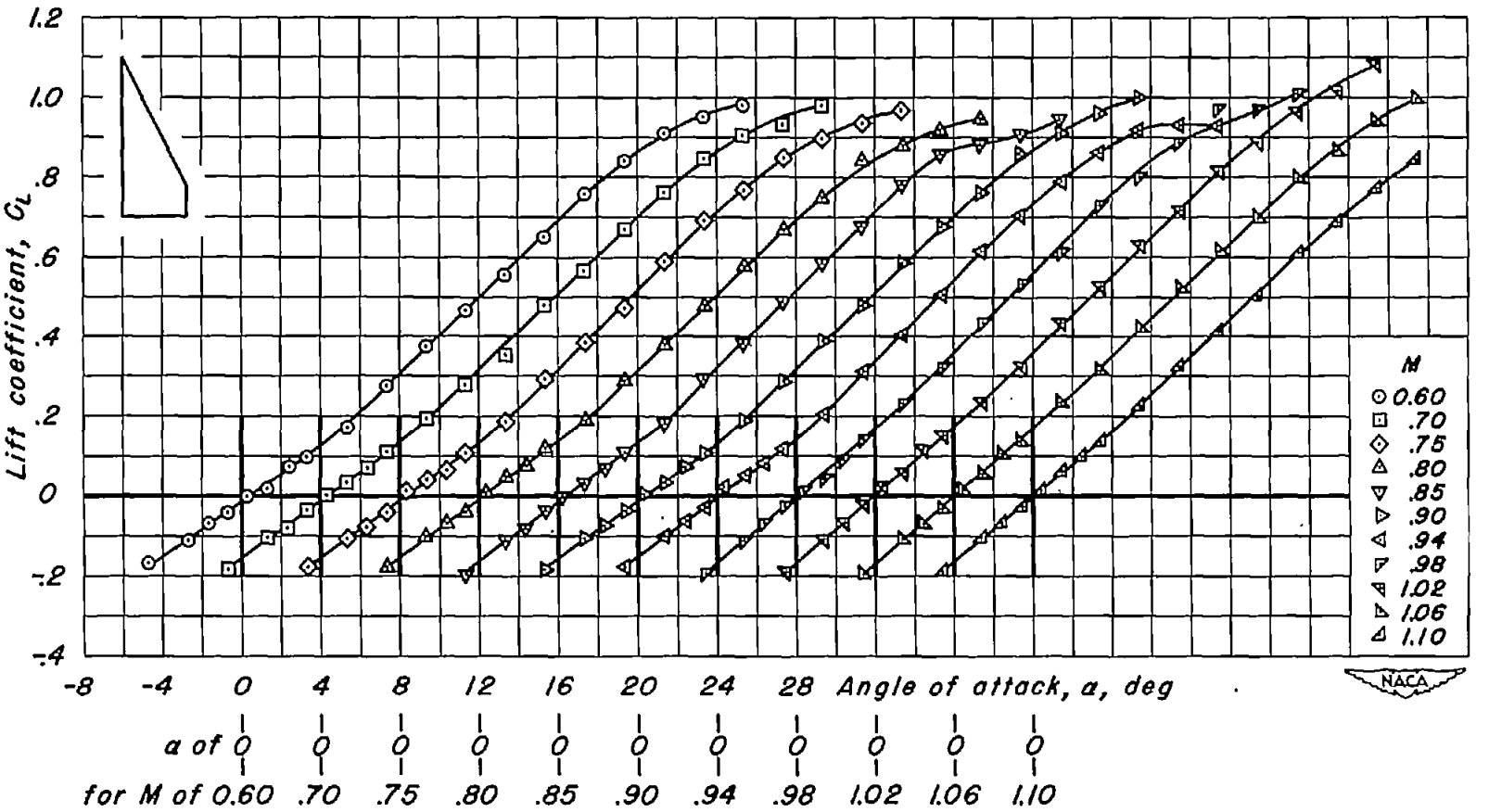

(h) NACA 63A004; λ, 0.2; A, 1.33.
Figure 5.- Continued.

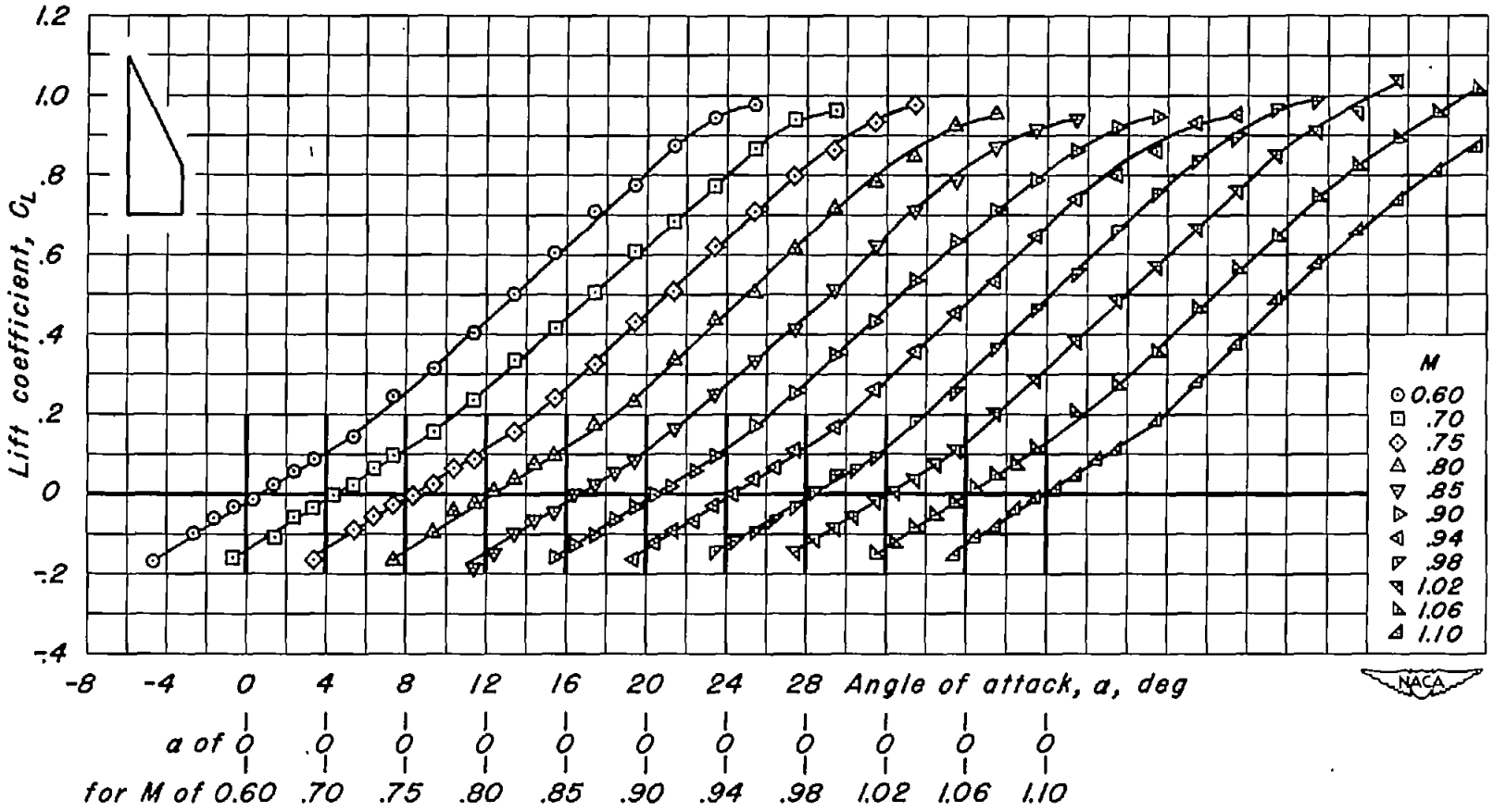

(l) NACA 63A004; λ, 0.3; A, 1.08.
Figure 5.- Continued.

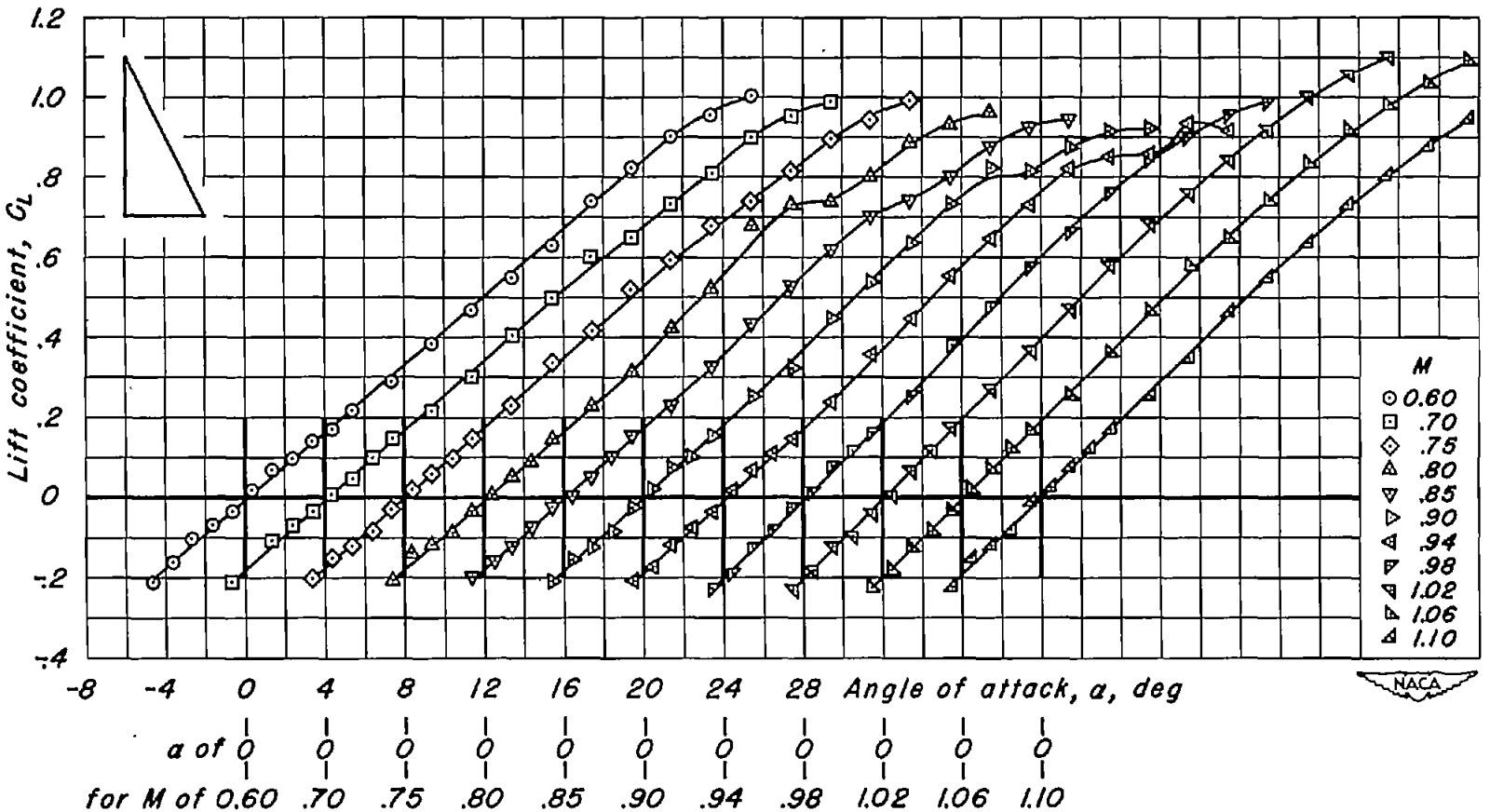

(j) NACA 63A006; λ, 0; A, 2.00.
Figure 5.- Continued.

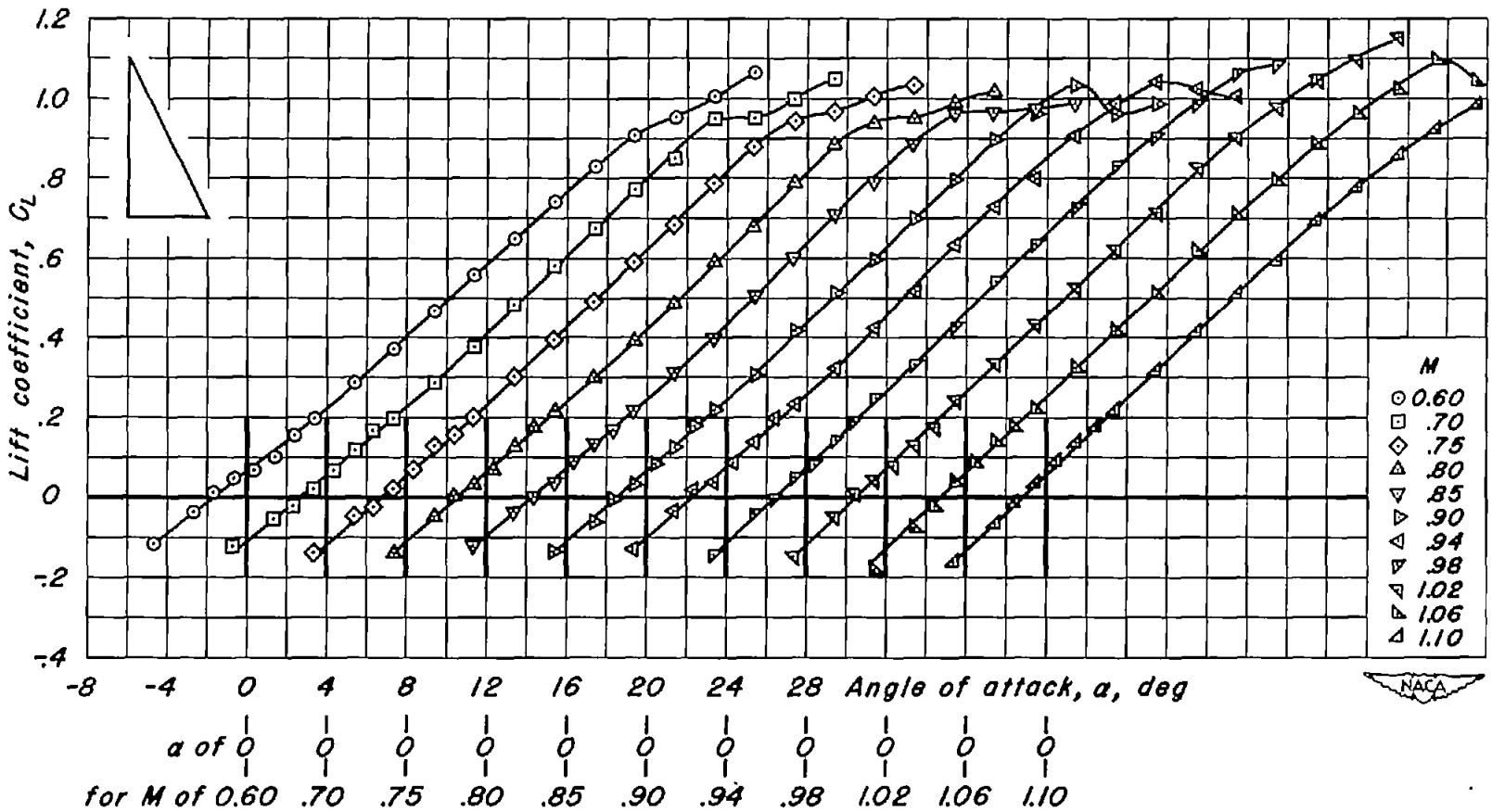

(k) NACA 63A(1.5)04; λ, 0; A, 2.00.
Figure 5.- Continued.

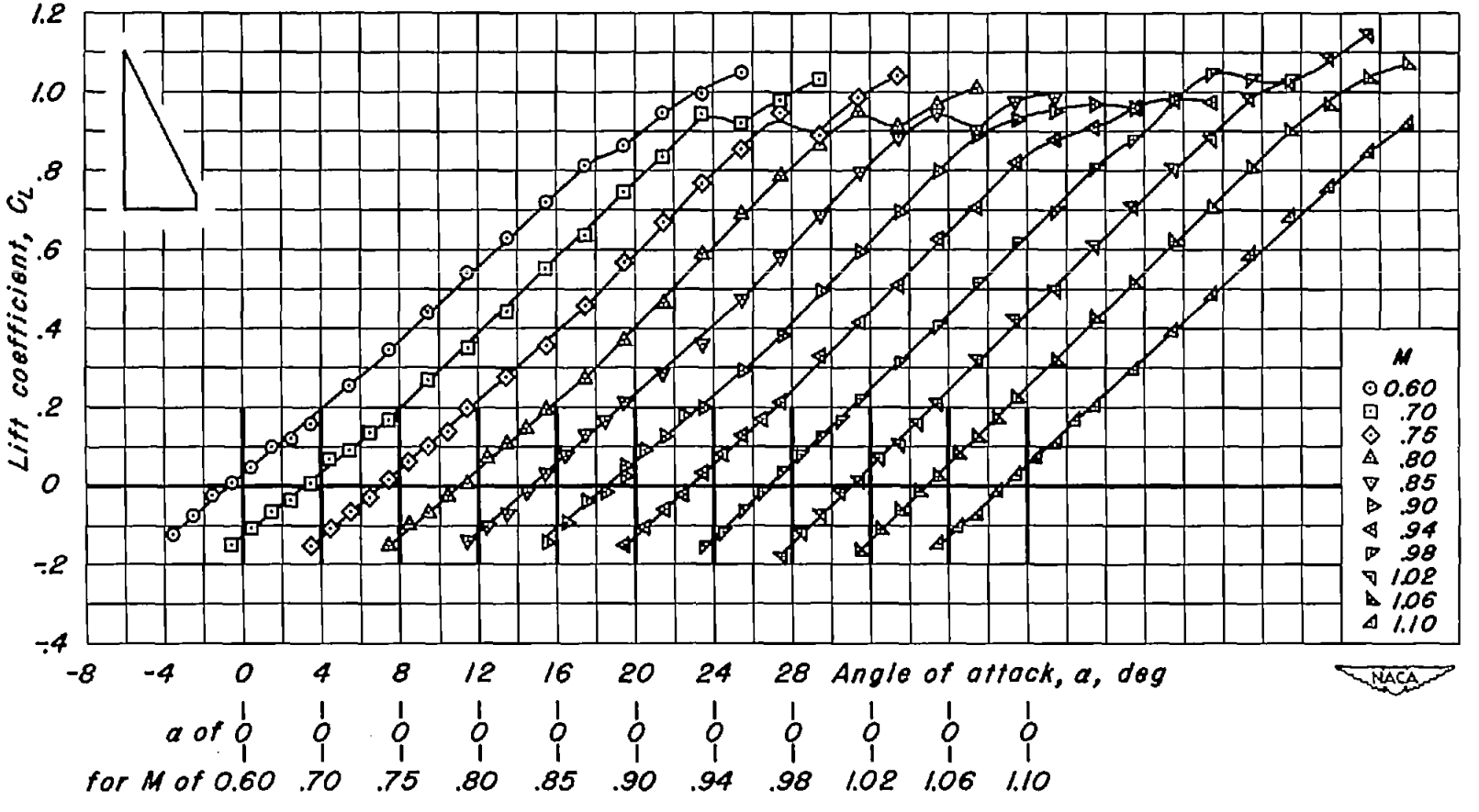

(l) NACA 63A(1.5)04; λ, 0.1; A, 1.64.
Figure 5.- Continued.

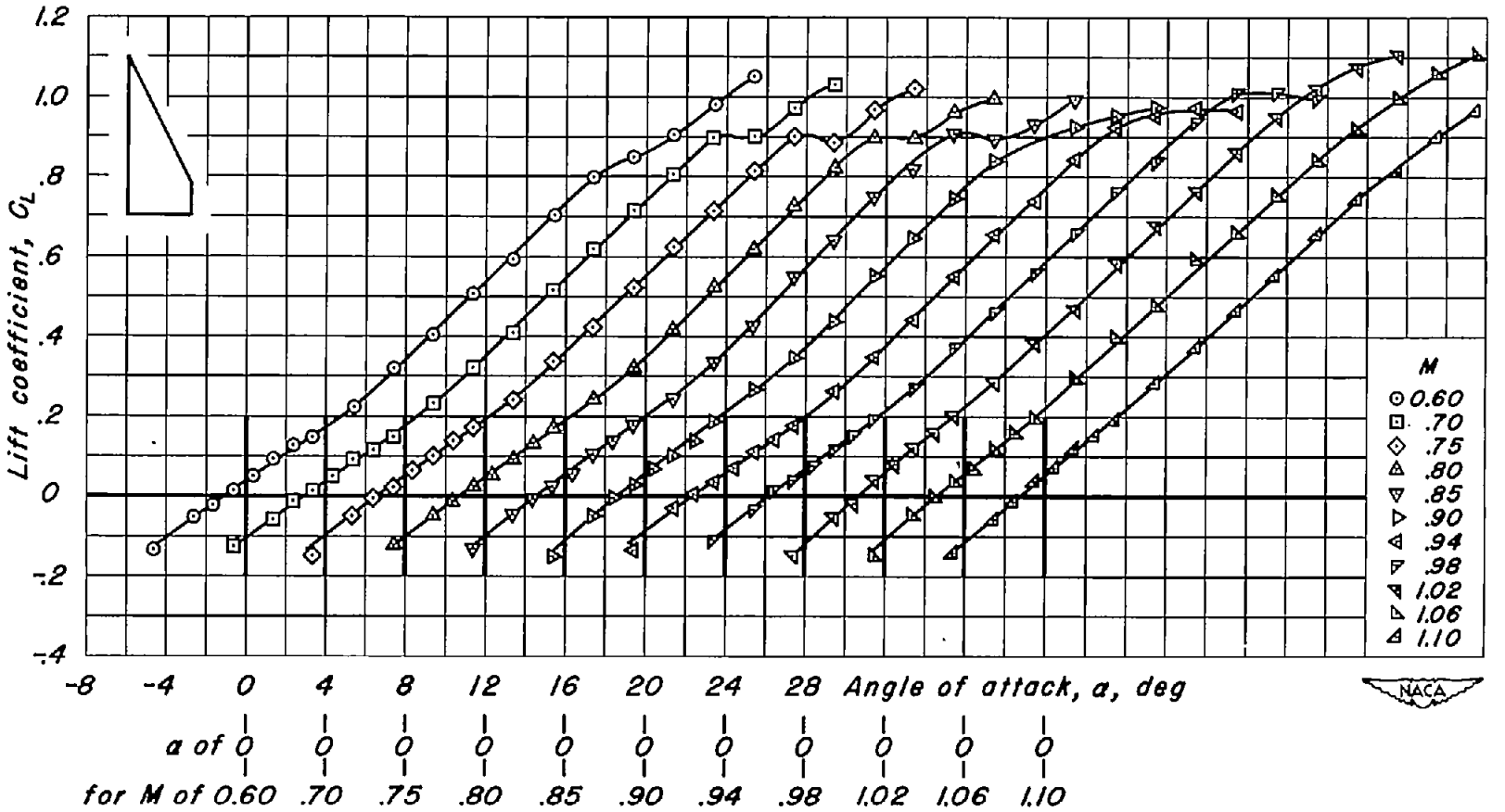

(m) NACA 63A(1.5)04; λ, 0.2; A, 1.33.
Figure 5.- Continued.

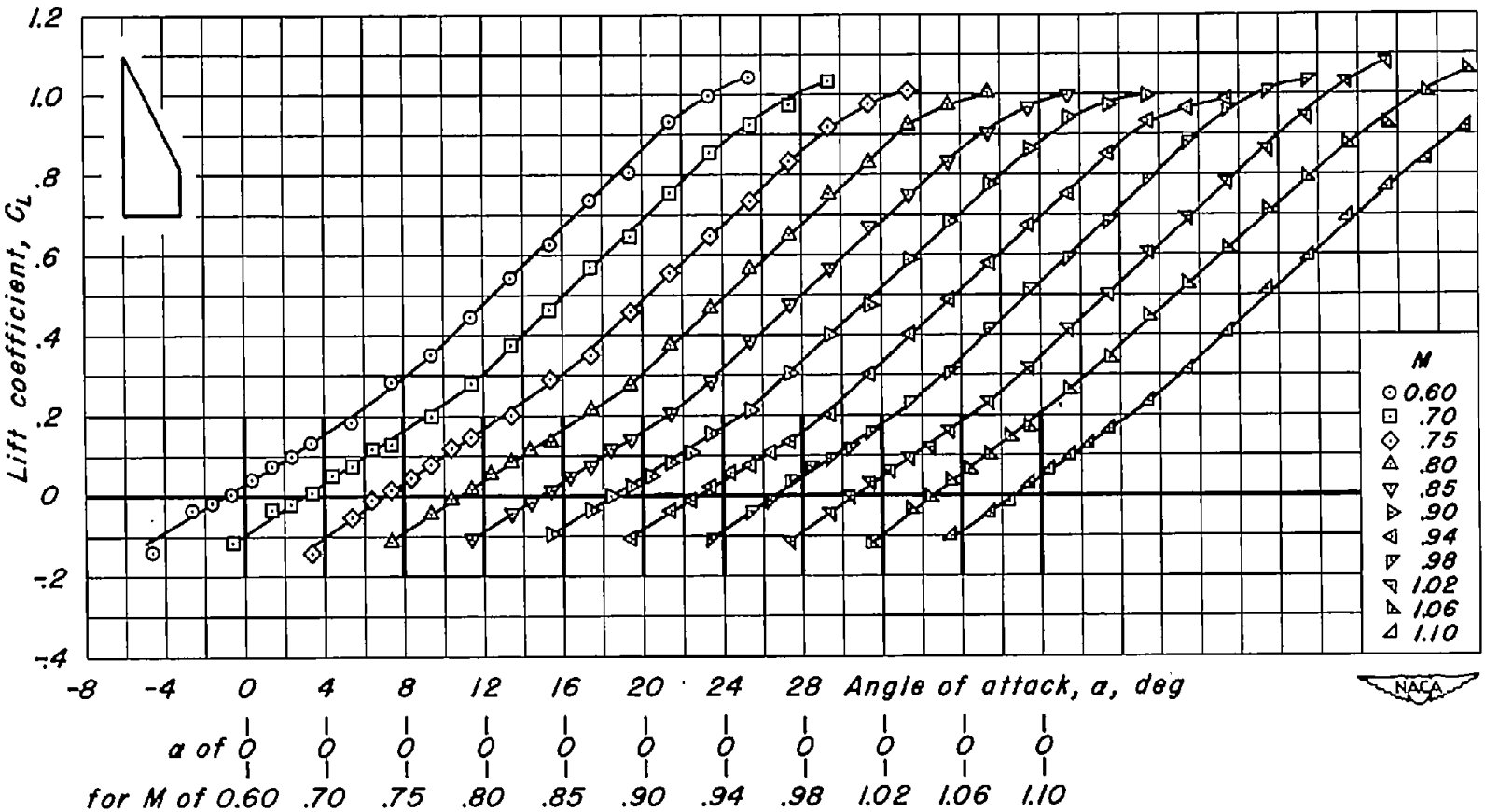

(n) NACA 63A(1.5)04; λ, 0.3; A, 1.08.
Figure 5.- Concluded.

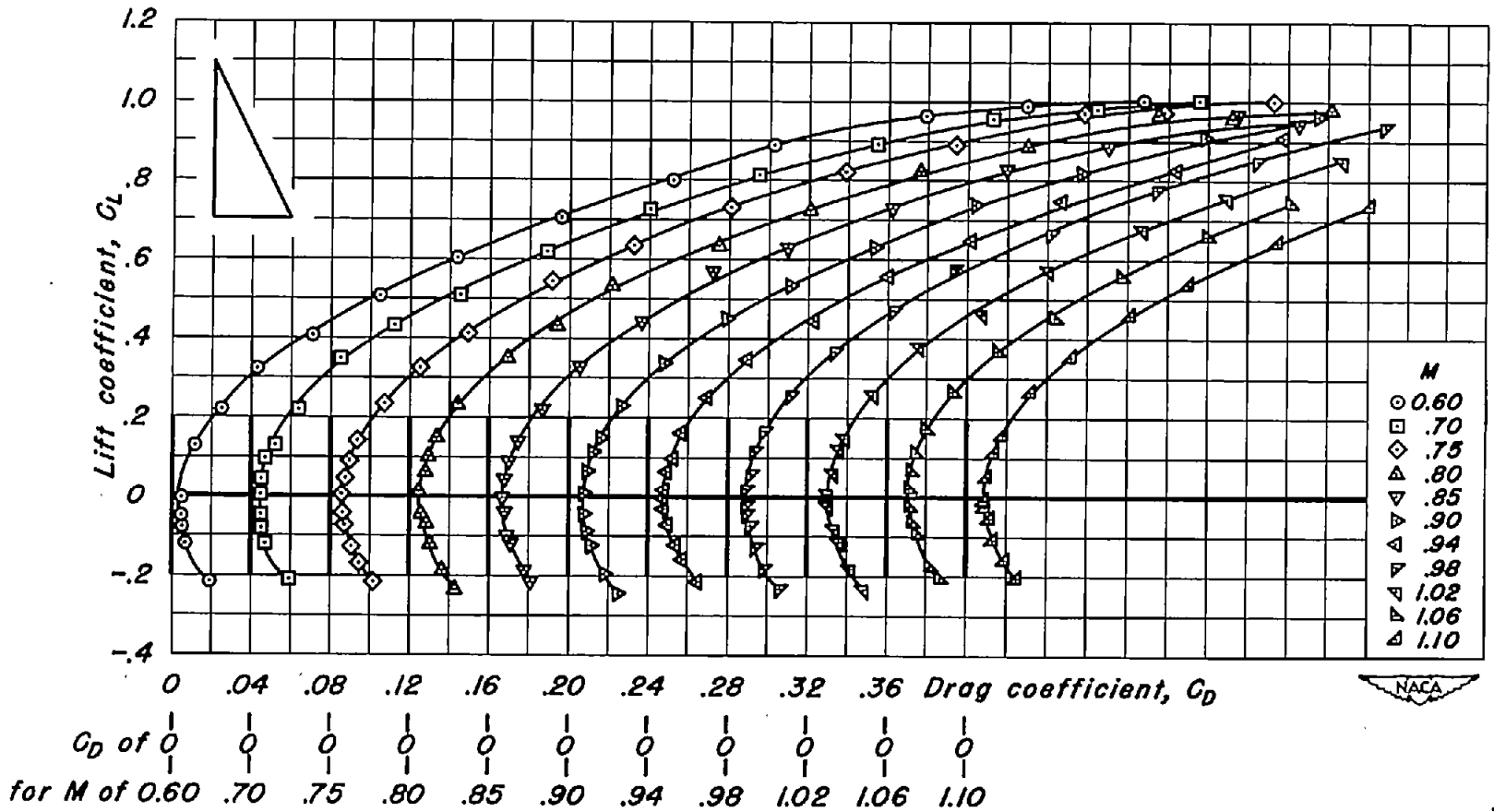

(a) NACA 63A002; λ, 0; A, 2.00.

Figure 6.- Variation of drag coefficient with lift coefficient for the wings of basic aspect ratio 2.

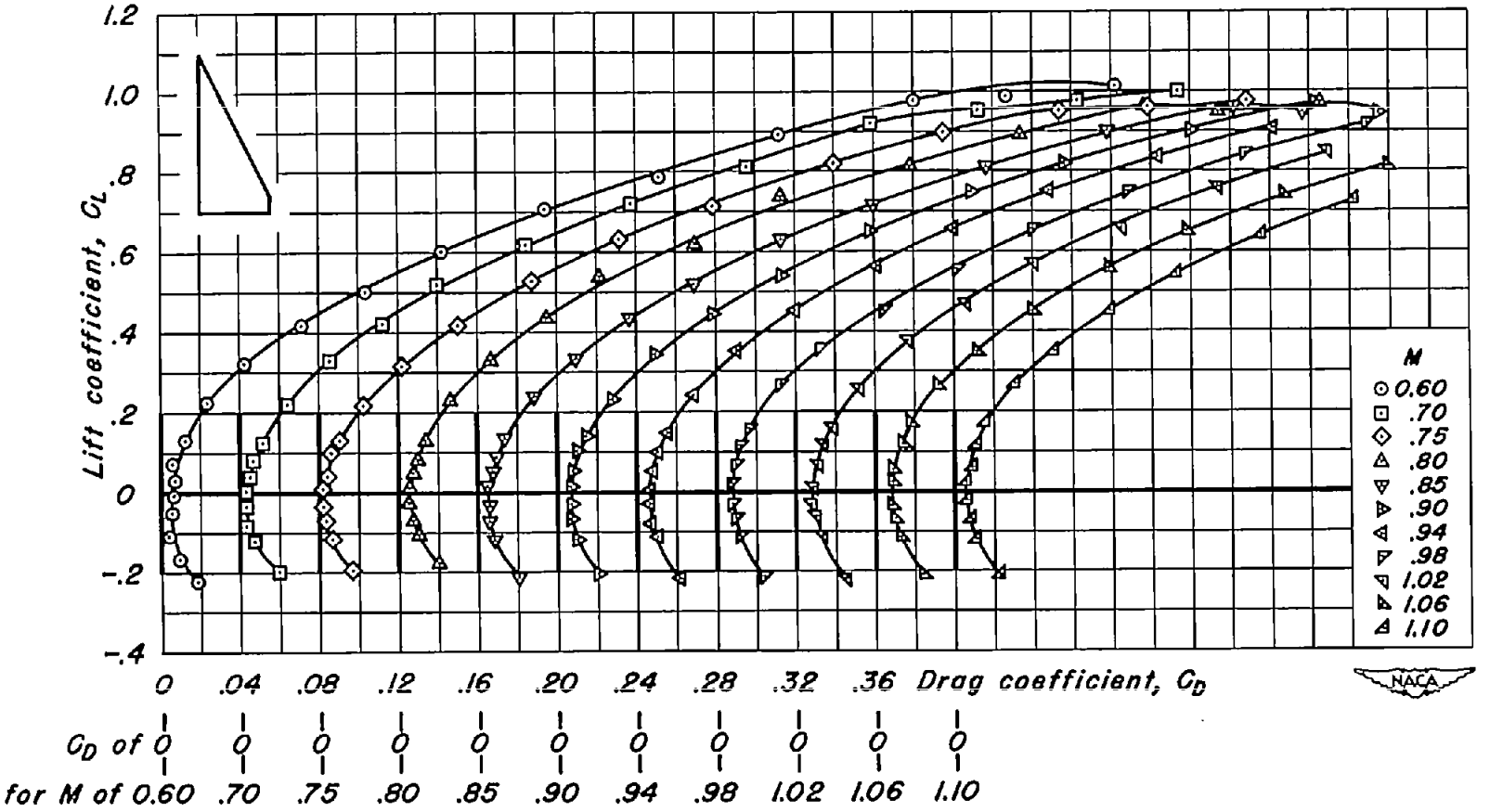

C_D of 0 0 0 0 0 0 0 0 0 0 0
for M of 0.60 .70 .75 .80 .85 .90 .94 .98 1.02 1.06 1.10

(b) NACA 63A002; λ, 0.1; A, 1.64.
Figure 6.- Continued.

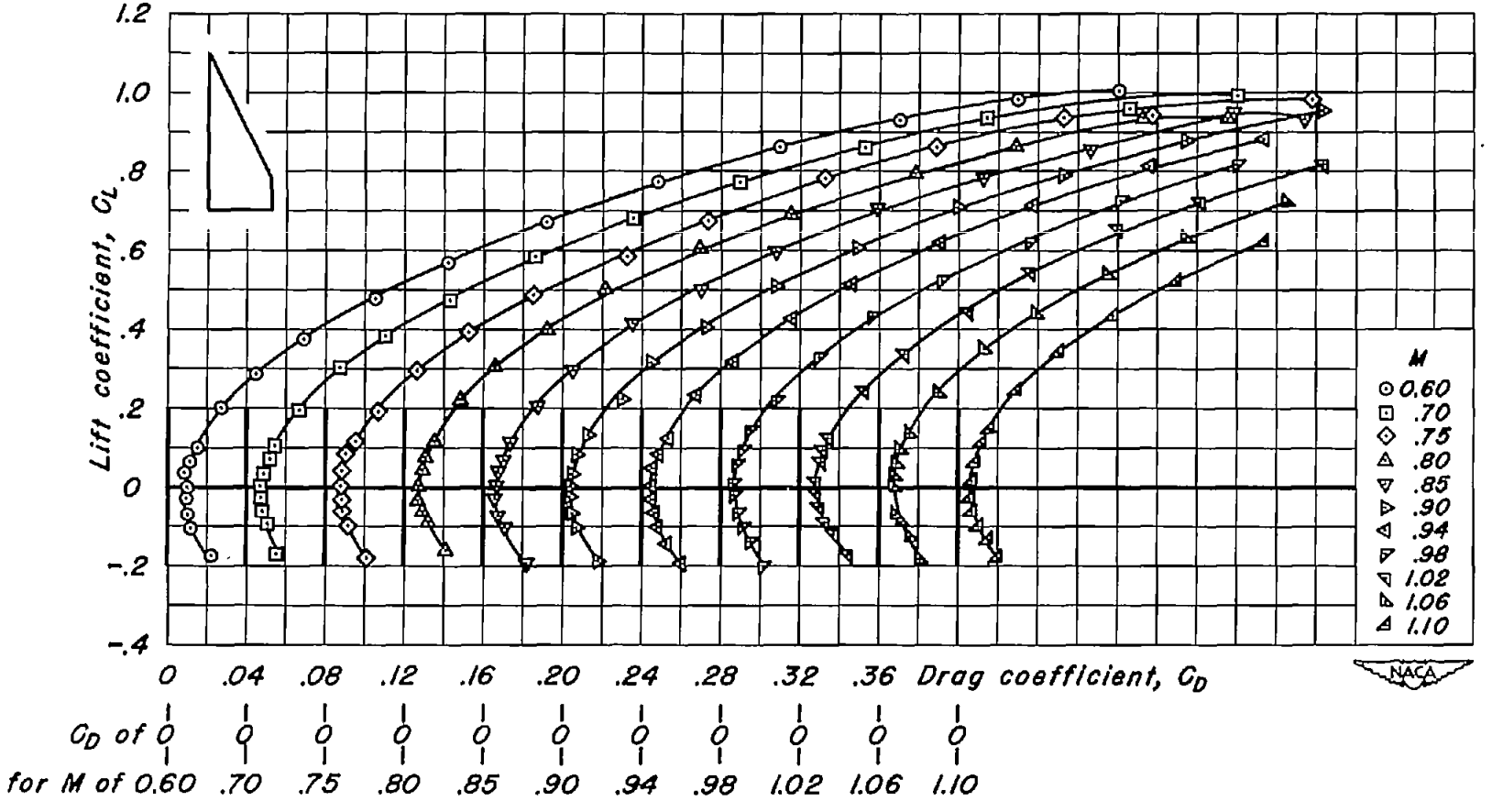

C_D of 0	0	0	0	0	0	0	0	0	0	0
for M of 0.60	.70	.75	.80	.85	.90	.94	.98	1.02	1.06	1.10

(c) NACA 63A002; λ, 0.2; A, 1.33.
Figure 6.- Continued.

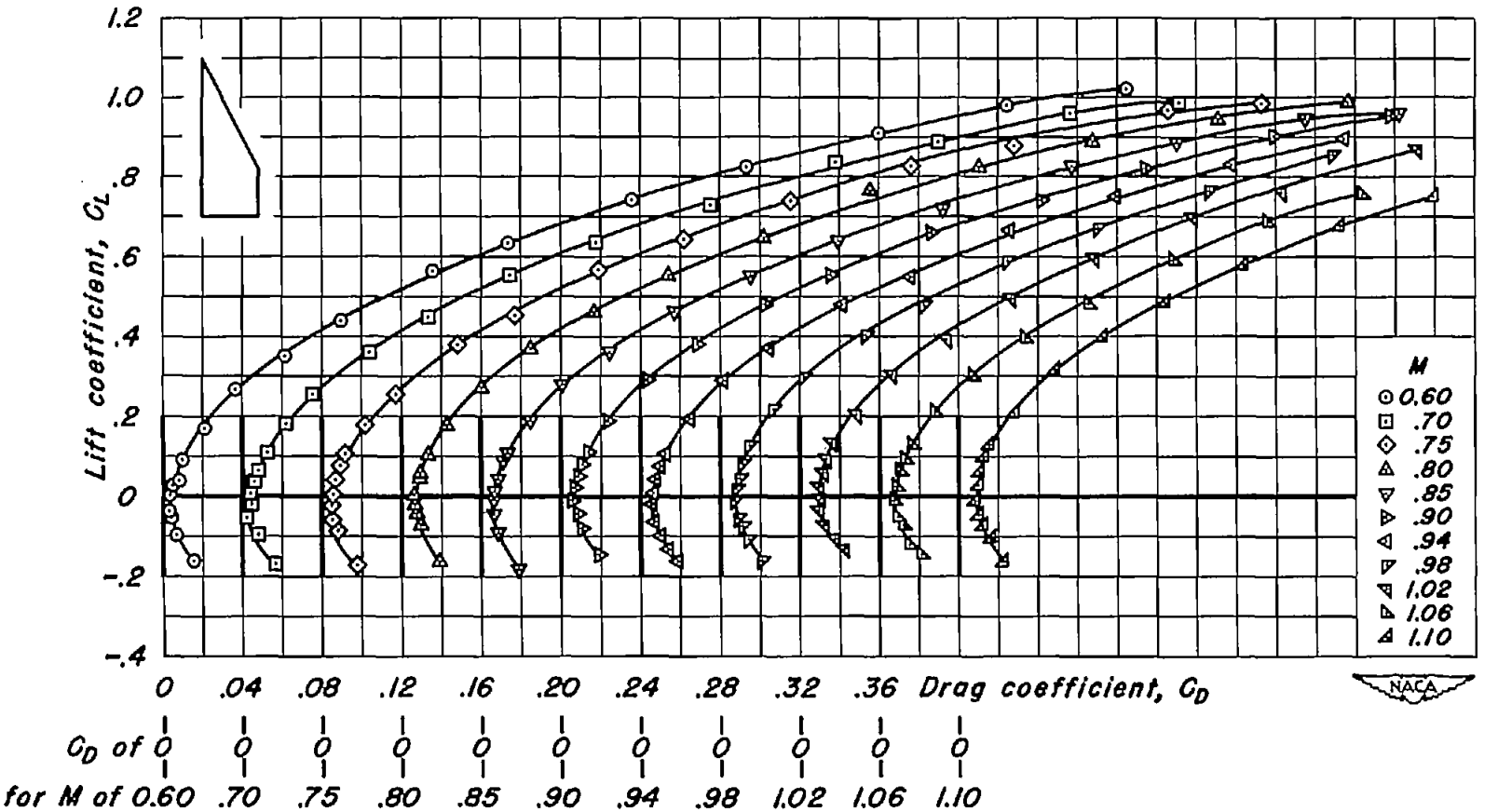

(d) NACA 63A002; λ, 0.3; A, 1.08.
Figure 6.- Continued.

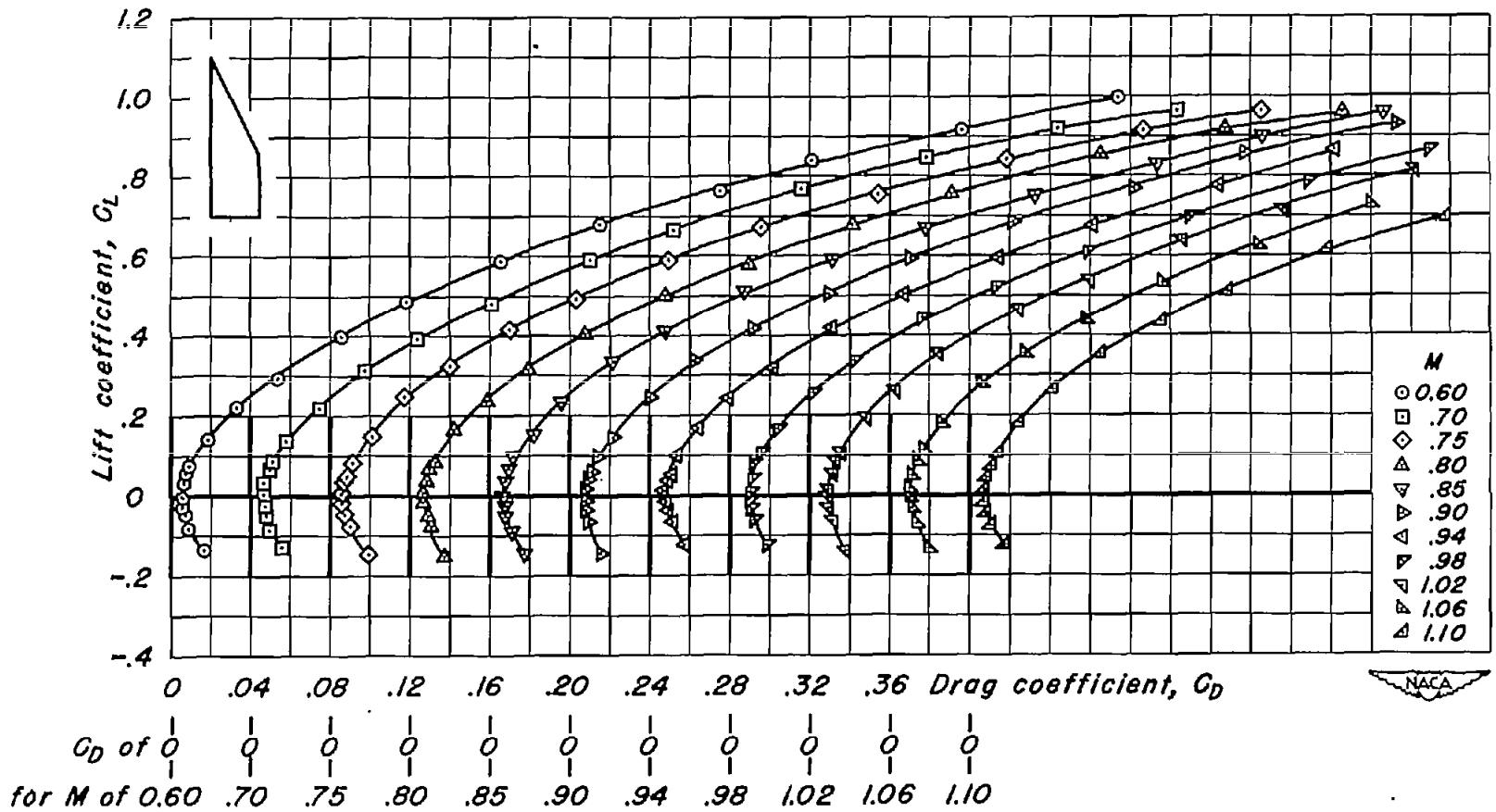

(e) NACA 63A002; λ, 0.4; A, 0.86.
Figure 6.- Continued.

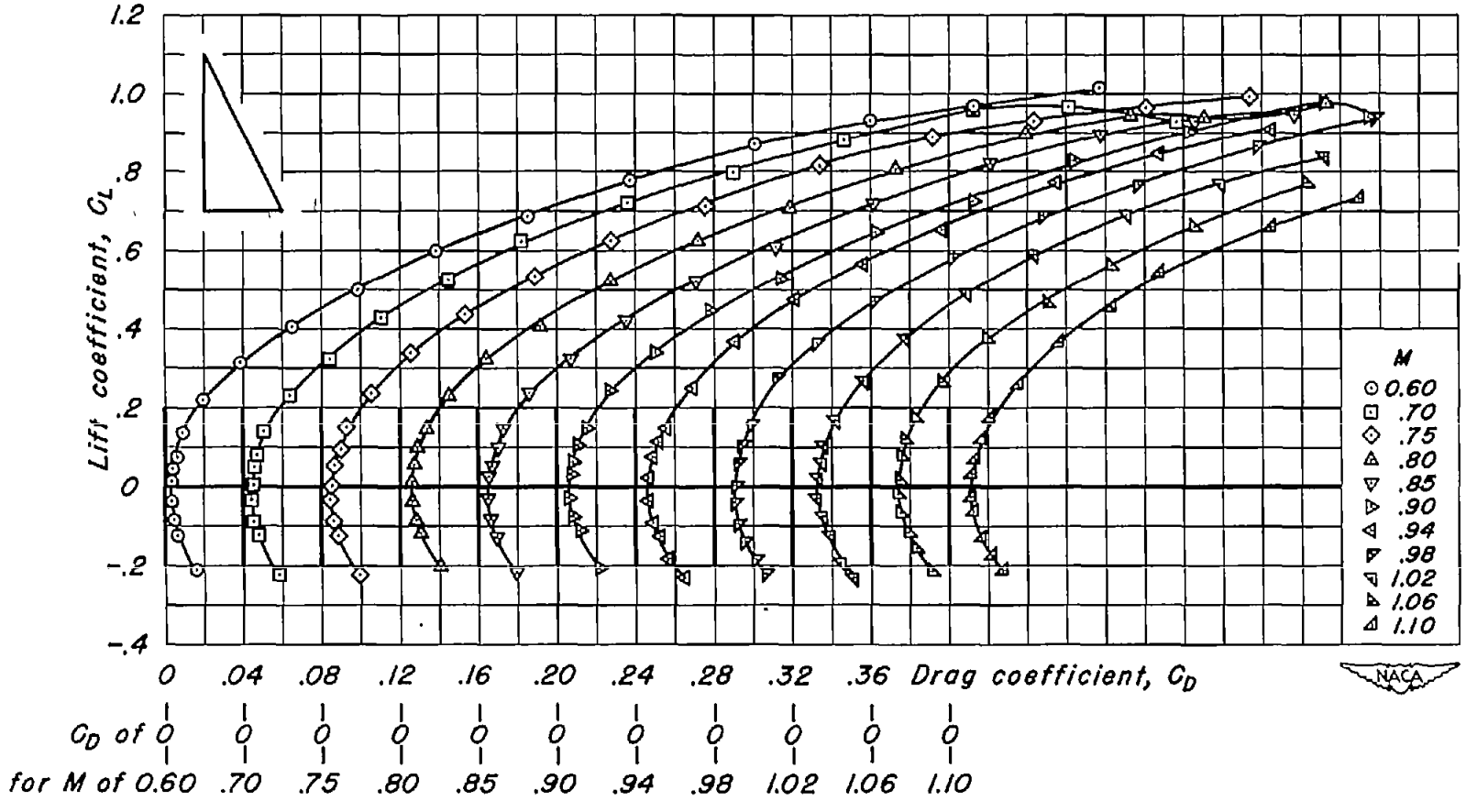

(f) NACA 63A004; λ, 0; A, 2.00.
Figure 6.- Continued.

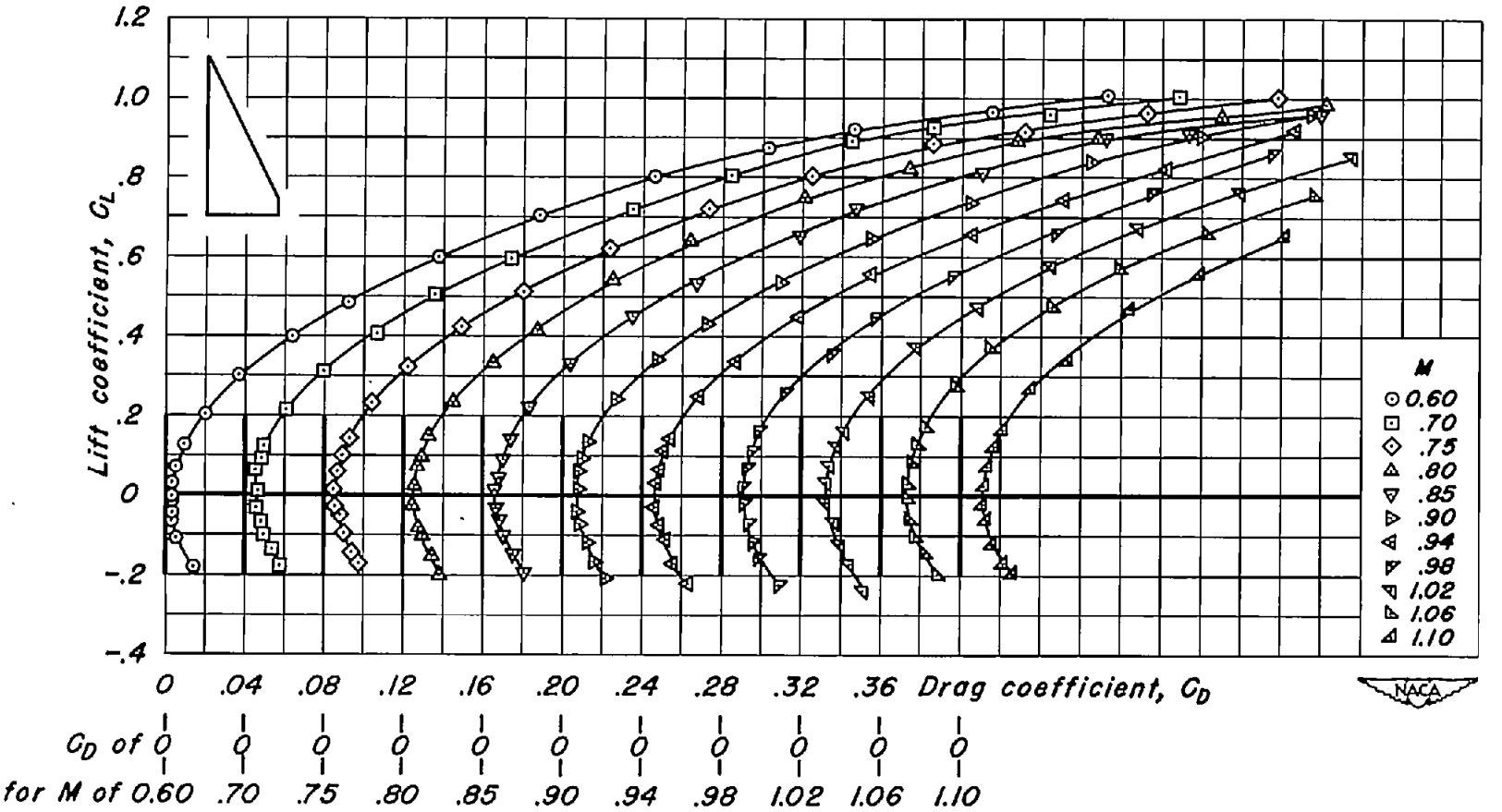

C_D of 0 0 0 0 0 0 0 0 0 0 0
for M of 0.60 .70 .75 .80 .85 .90 .94 .98 1.02 1.06 1.10

(g) NACA 63A004; λ, 0.1; A, 1.64.
Figure 6.- Continued.

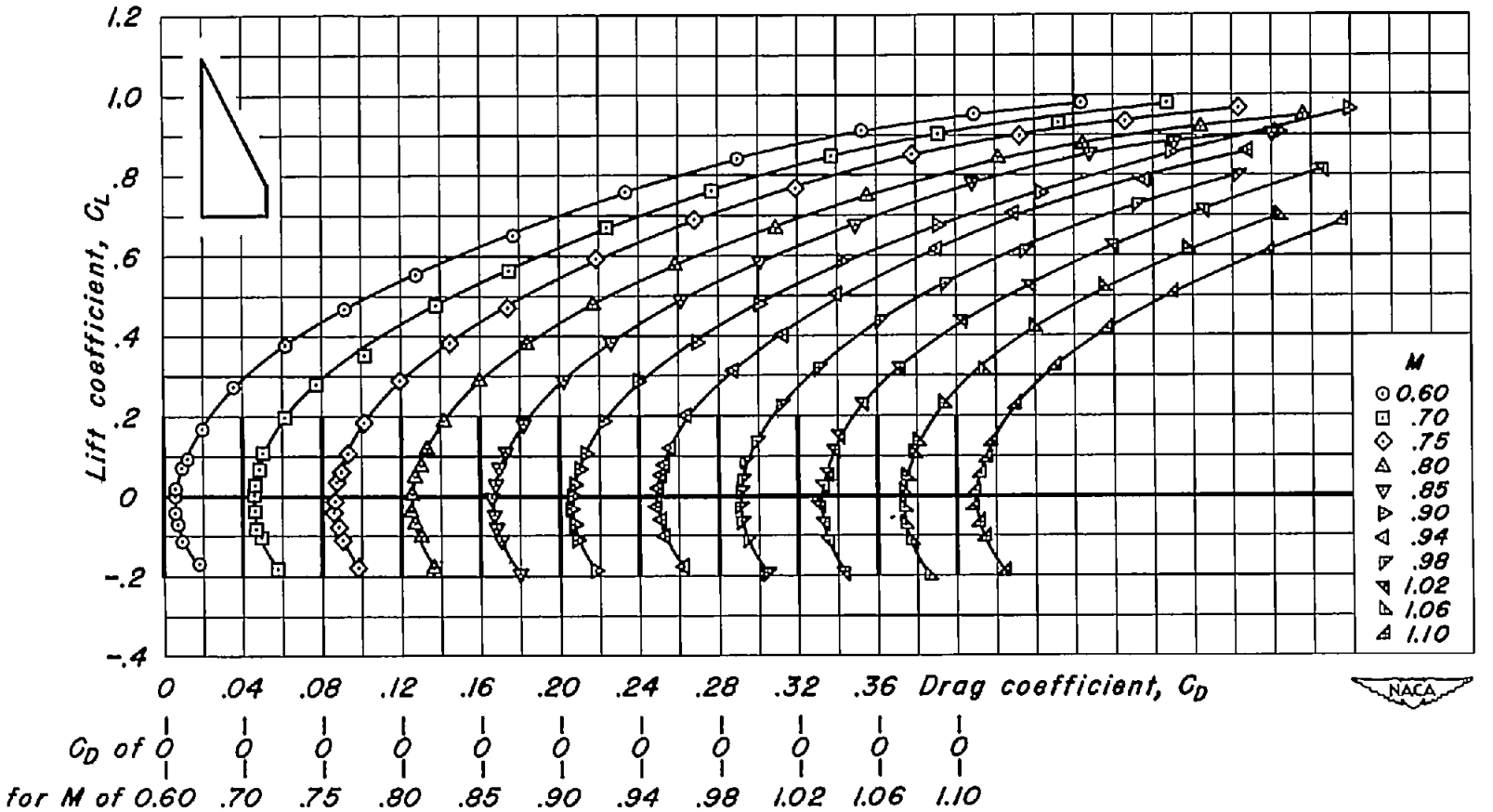

(h) NACA 63A004; λ, 0.2; A, 1.33.
Figure 6.- Continued.

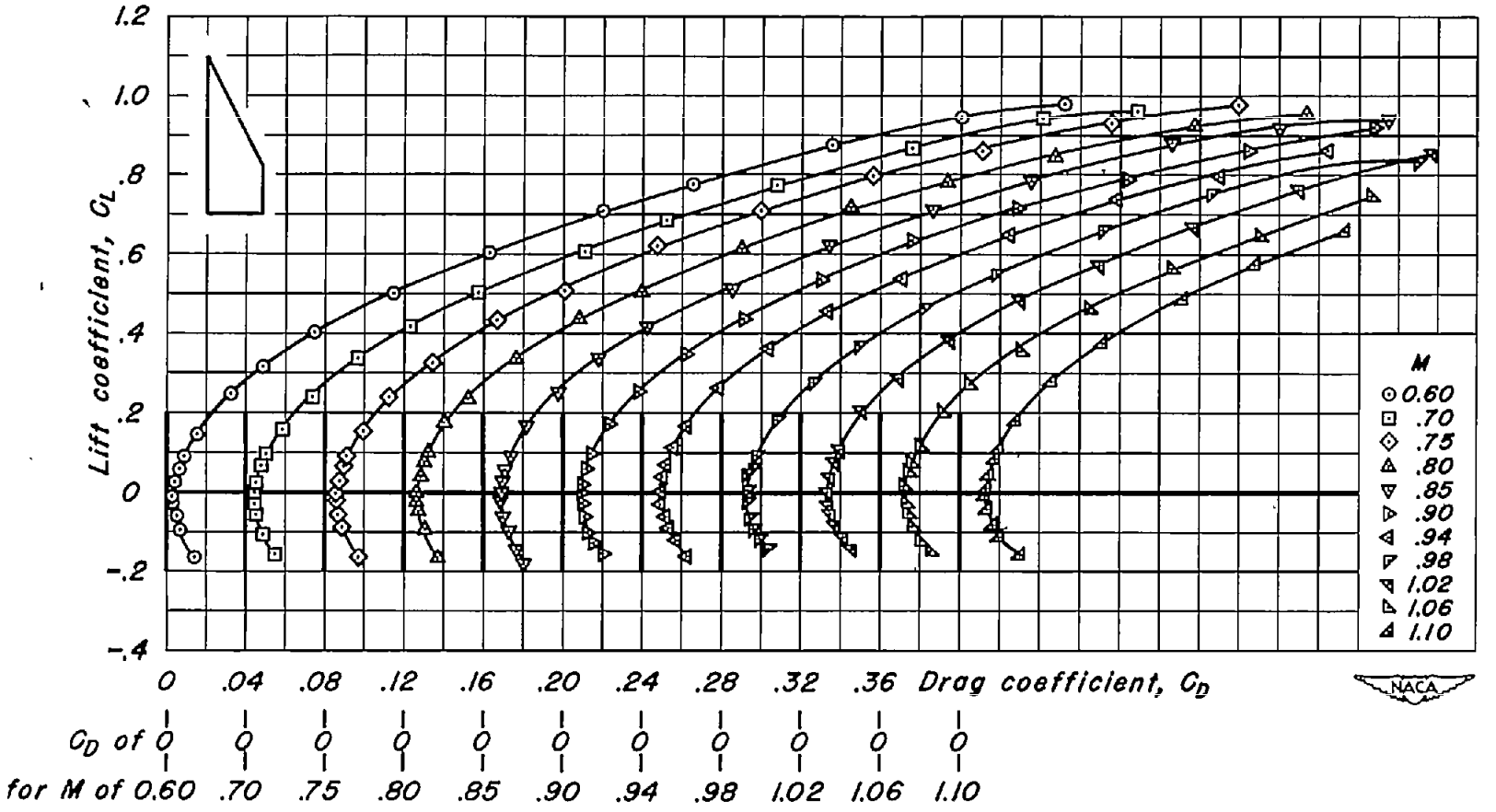

(i) NACA 63A004; λ, 0.3; A, 1.08.
Figure 6.- Continued.

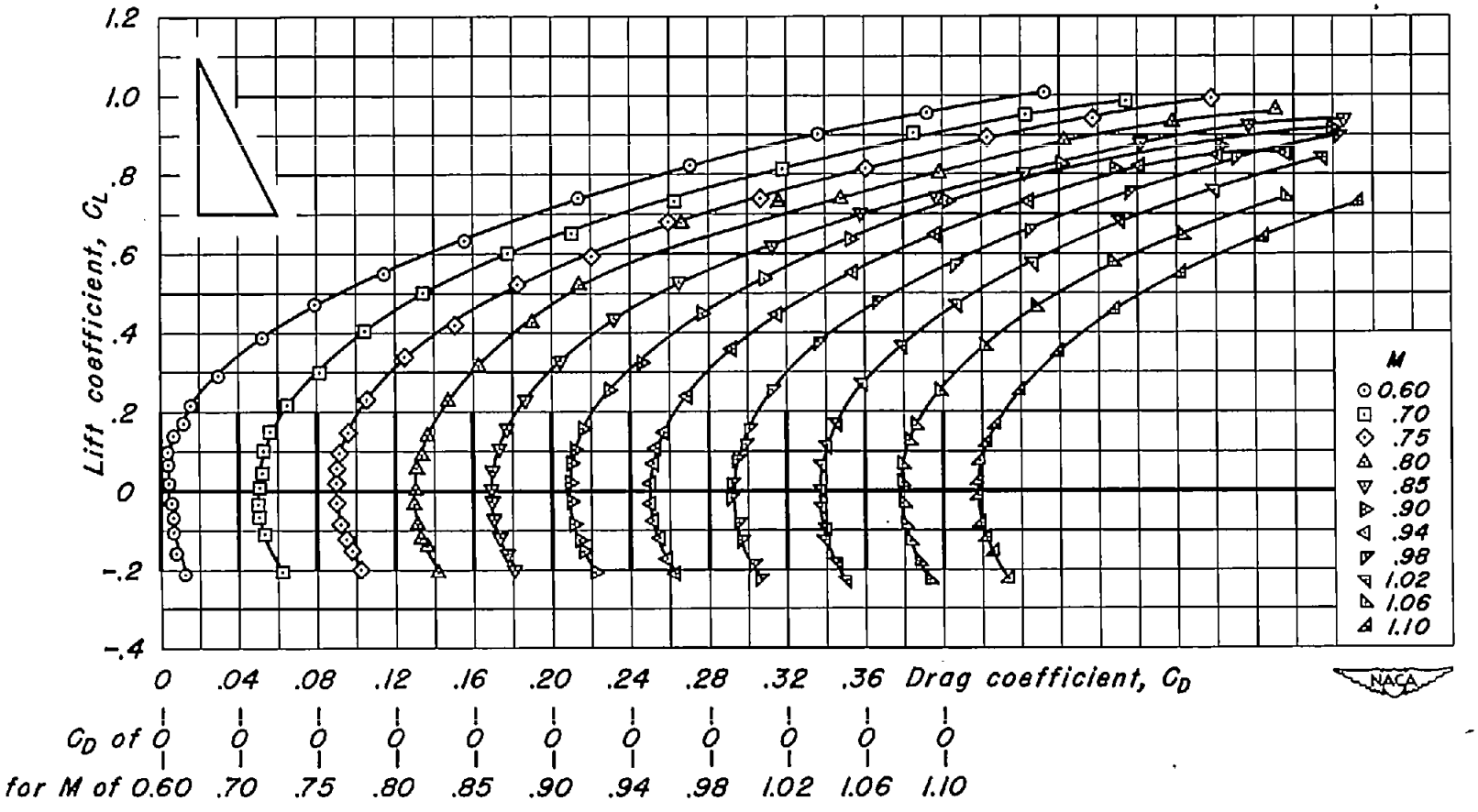

C_D of	0	0	0	0	0	0	0	0	0	0	0
for M of	0.60	.70	.75	.80	.85	.90	.94	.98	1.02	1.06	1.10

(j) NACA 63A006; λ, 0; A, 2.00.
Figure 6.- Continued.

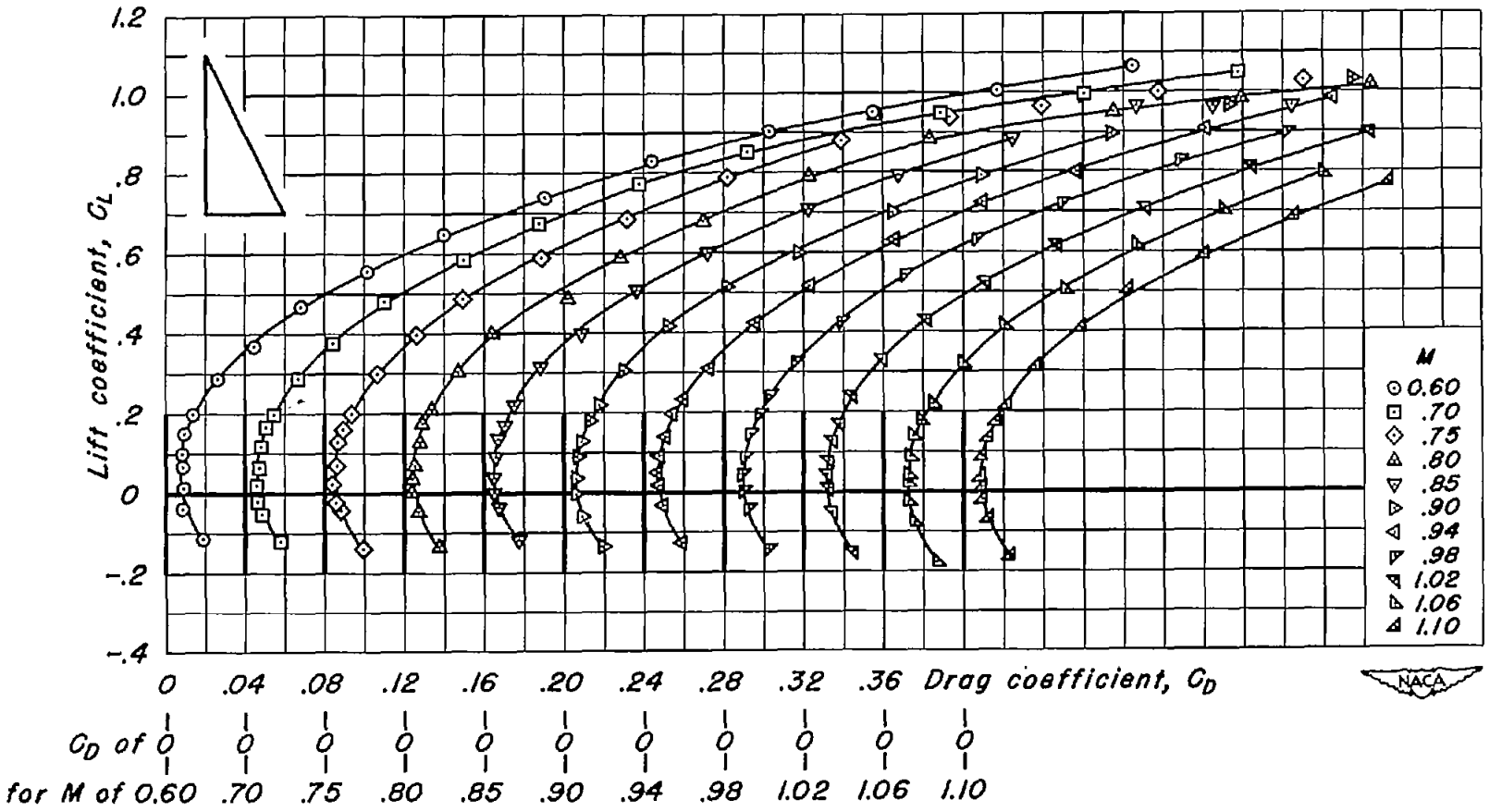

C_D of	0	0	0	0	0	0	0	0	0	0
for M of	0.60	.70	.75	.80	.85	.90	.94	.98	1.02	1.06	1.10

(k) NACA 63A(1.5)04; λ, 0; A, 2.00.
Figure 6.- Continued.

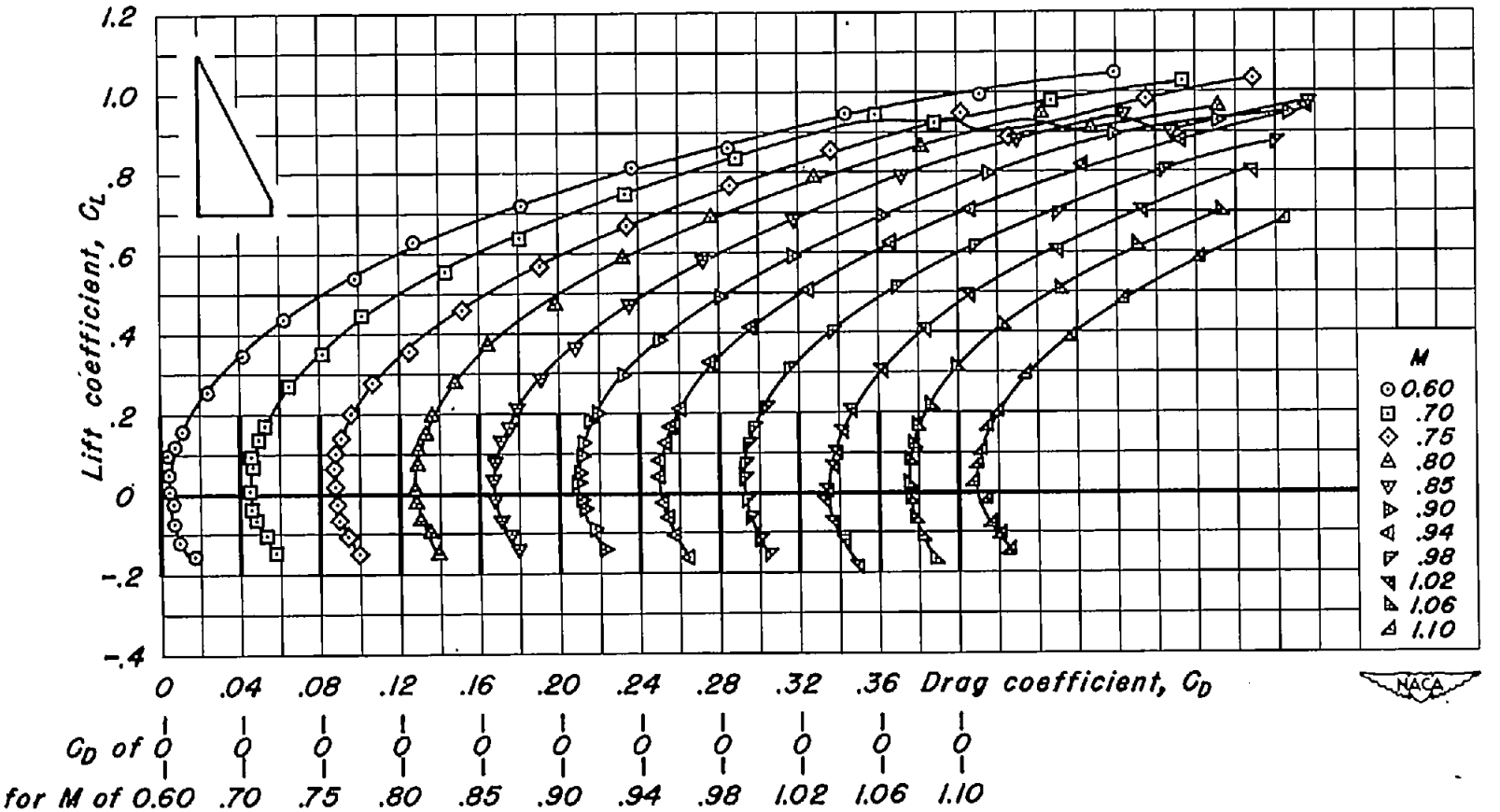

(l) NACA 63A(1.5)04; λ, 0.1; A, 1.64.
Figure 6.- Continued.

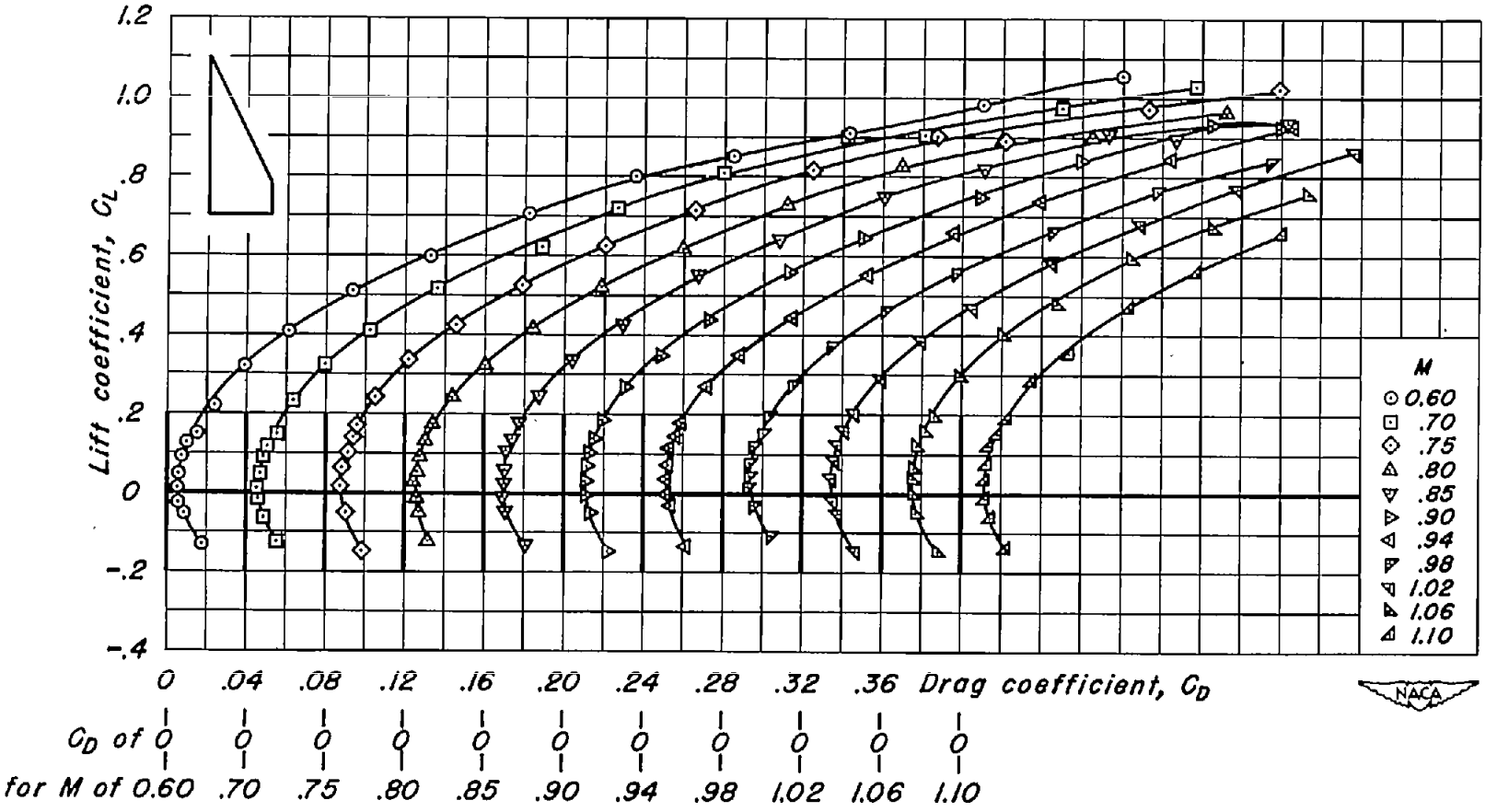

C_D of	0	0	0	0	0	0	0	0	0	0	0
for M of	0.60	.70	.75	.80	.85	.90	.94	.98	1.02	1.06	1.10

(m) NACA 63A(1.5)04; λ, 0.2; A, 1.33.
Figure 6.- Continued.

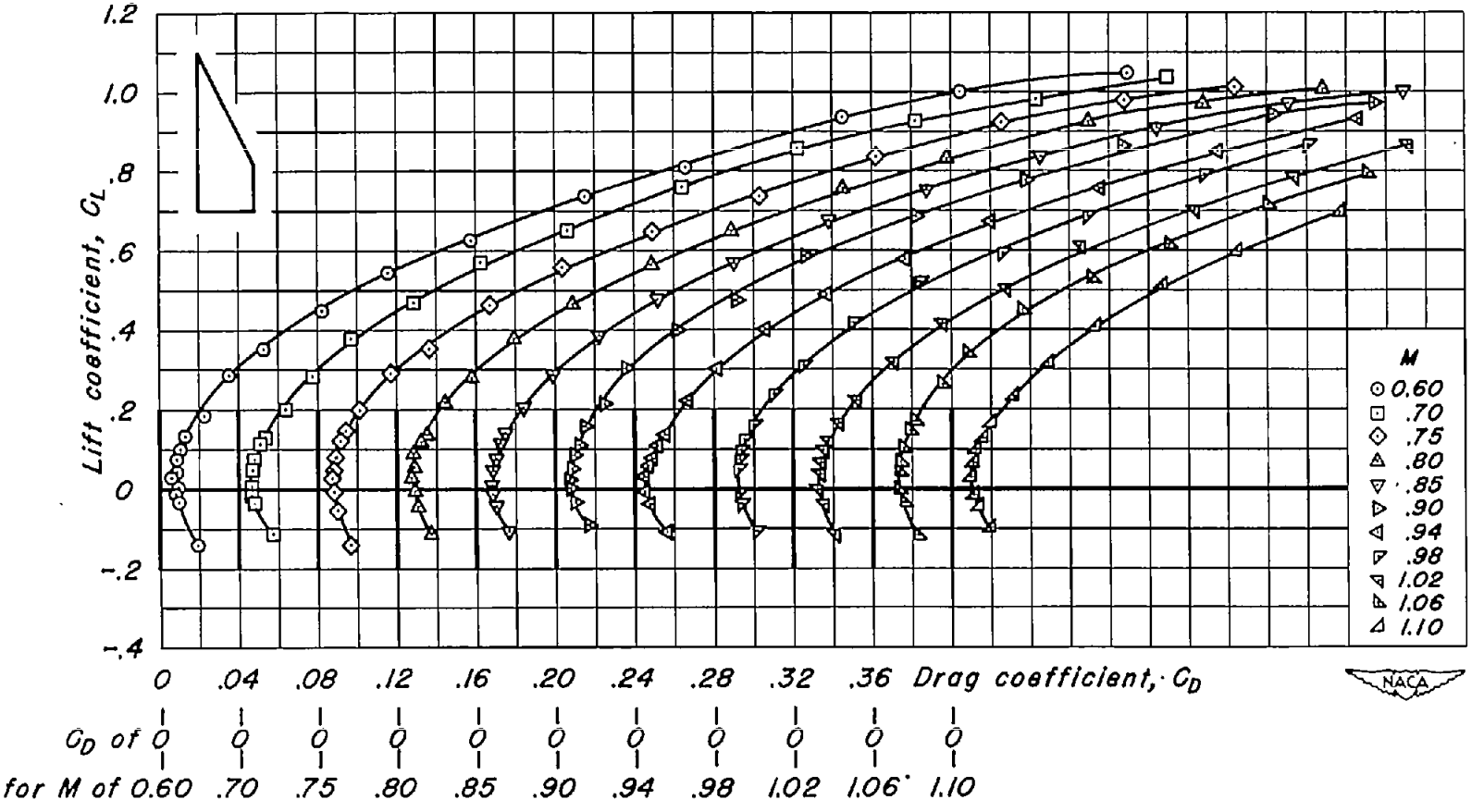

(n) NACA 63A(1.5)04; λ, 0.3; A, 1.08.
Figure 6.- Concluded.

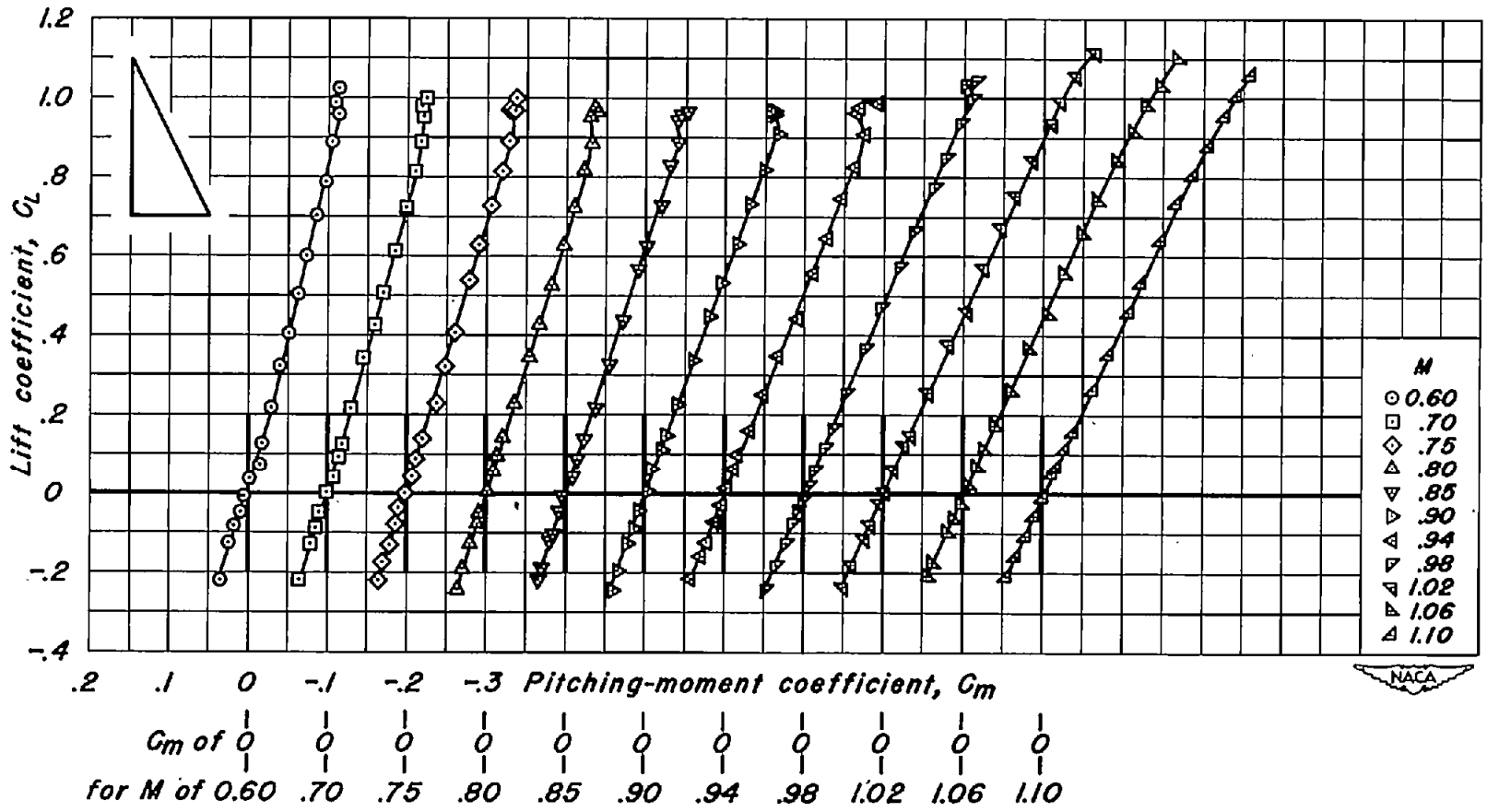

(a) NACA 63A002; λ, 0; A, 2.00.

Figure 7.- Variation of pitching-moment coefficient with lift coefficient for the wings of basic aspect ratio 2.

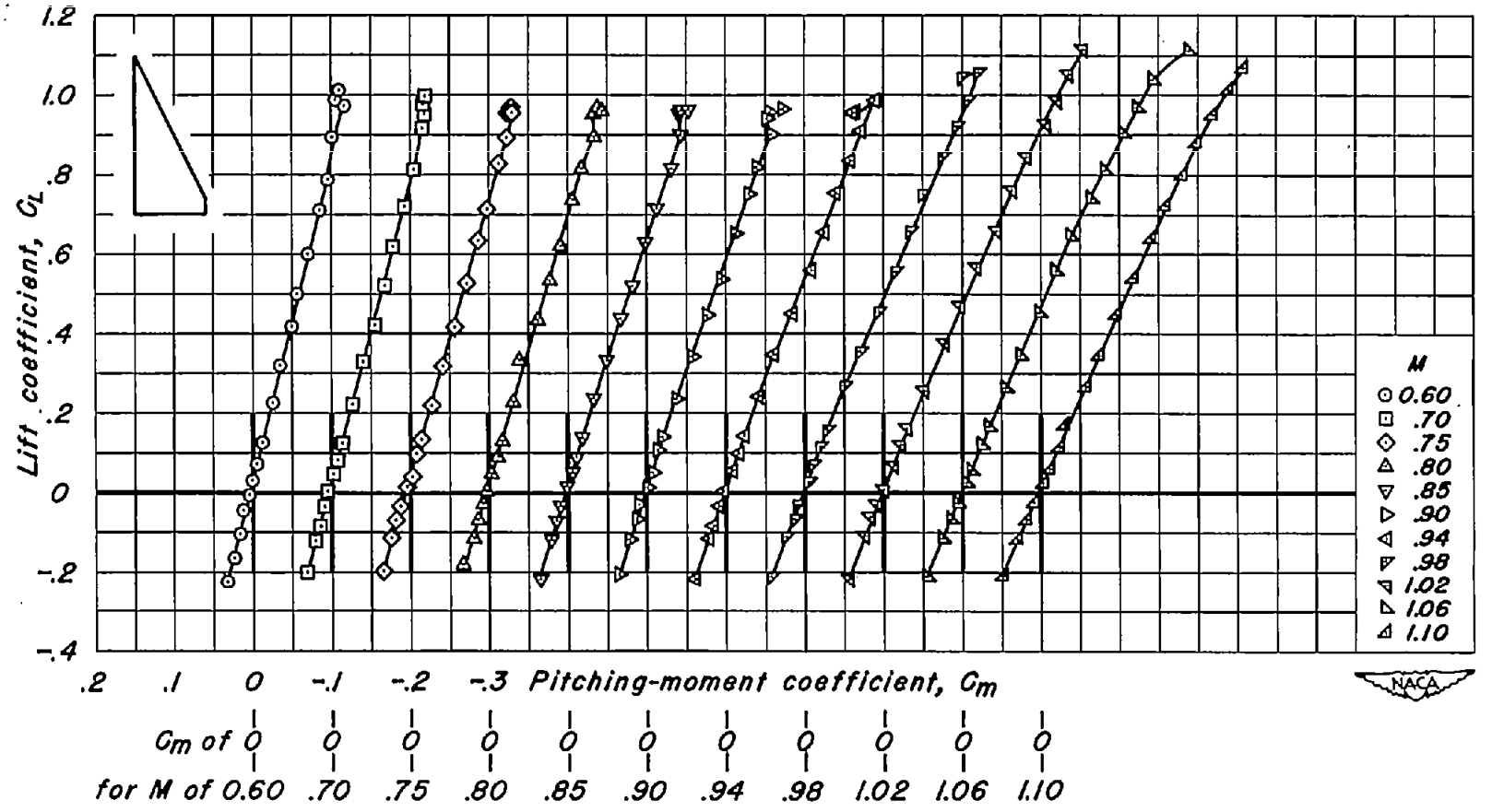

(b) NACA 63A002; λ, 0.1; A, 1.64.
Figure 7.- Continued.

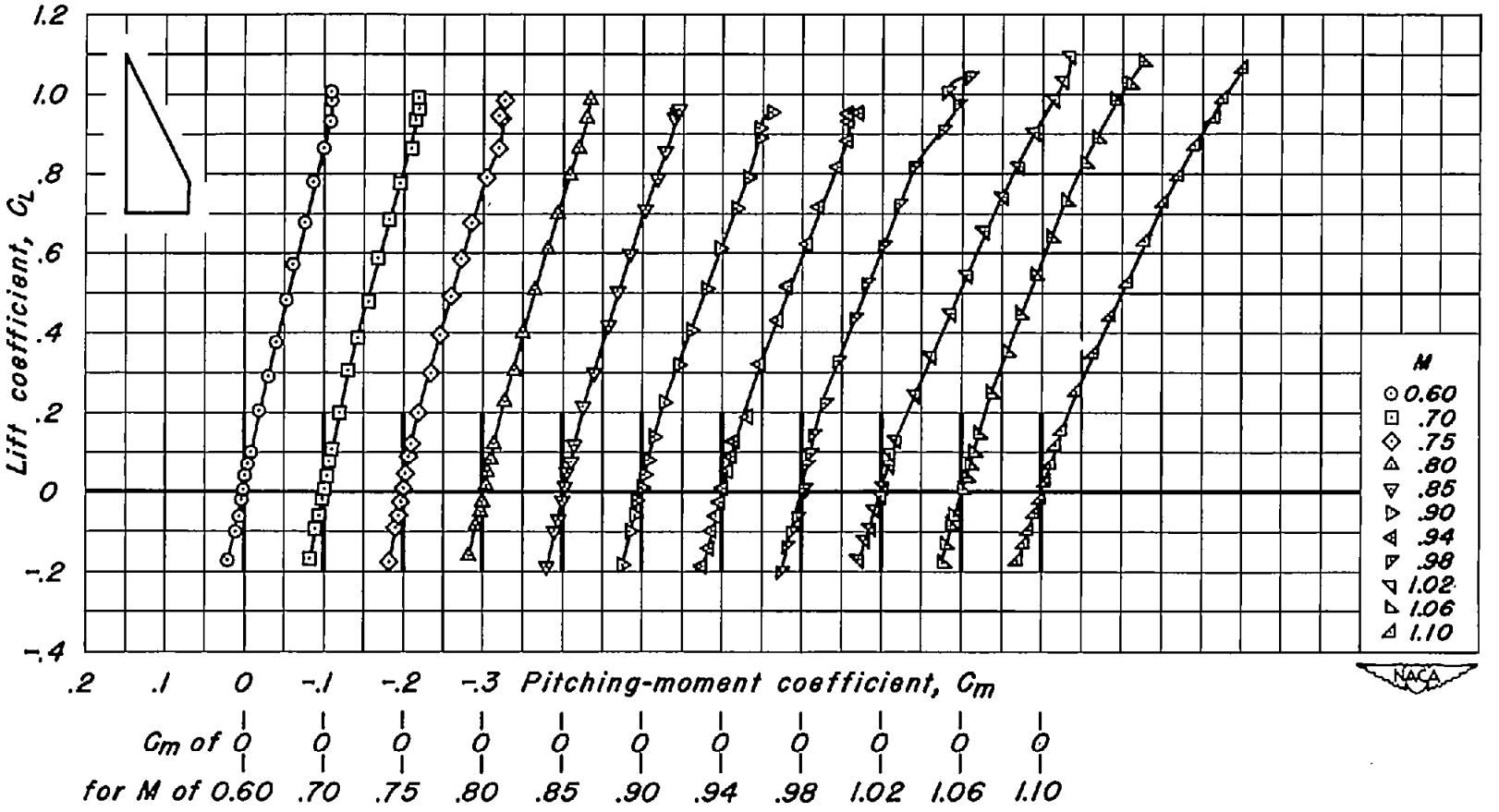

(c) NACA 63A002; λ, 0.2; A, 1.33.
Figure 7.- Continued.

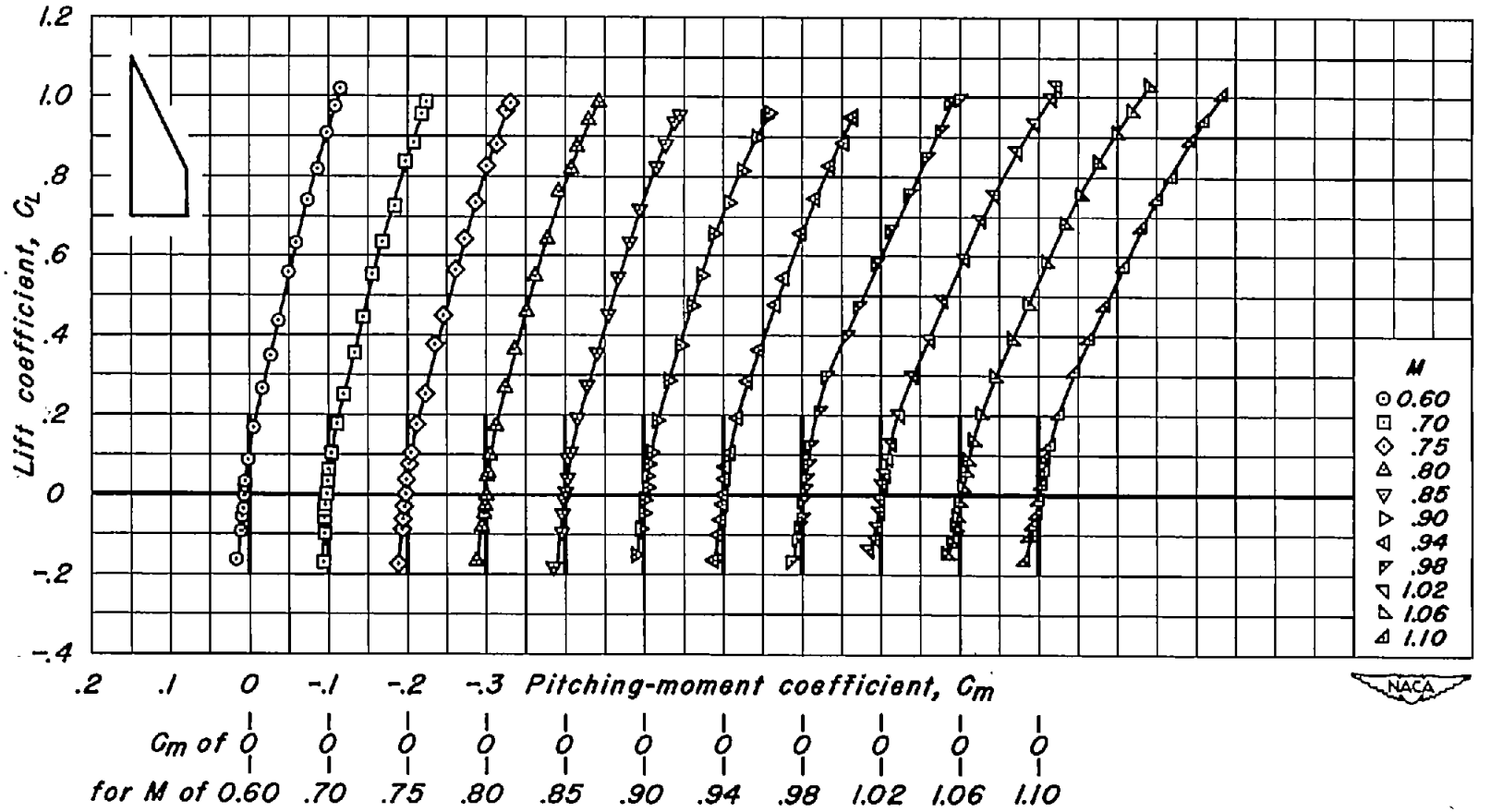

(d) NACA 63A002; λ, 0.3; A, 1.08.
Figure 7.- Continued.

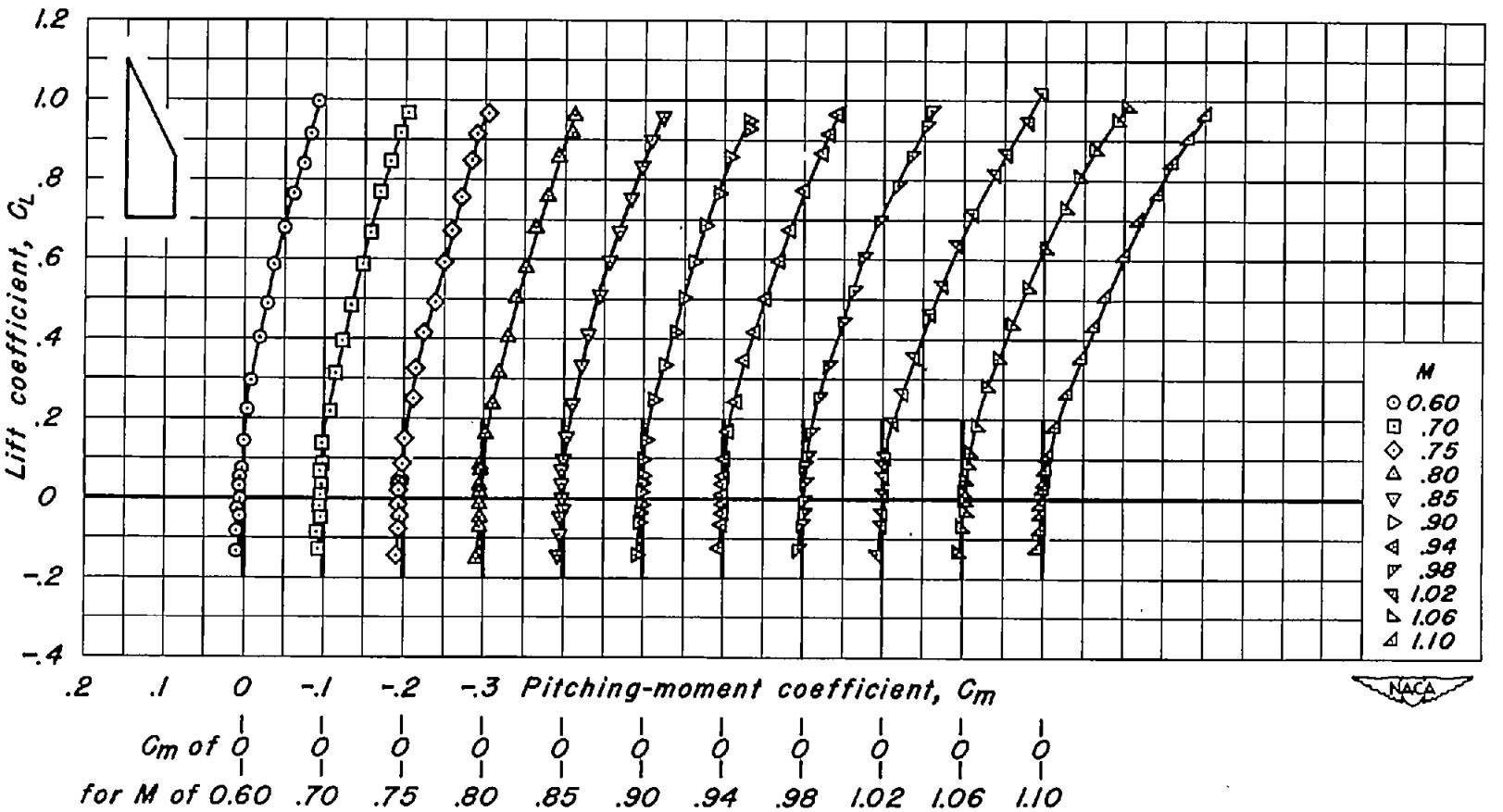

(e) NACA 63A002; λ, 0.4; A, 0.86.
Figure 7.- Continued.

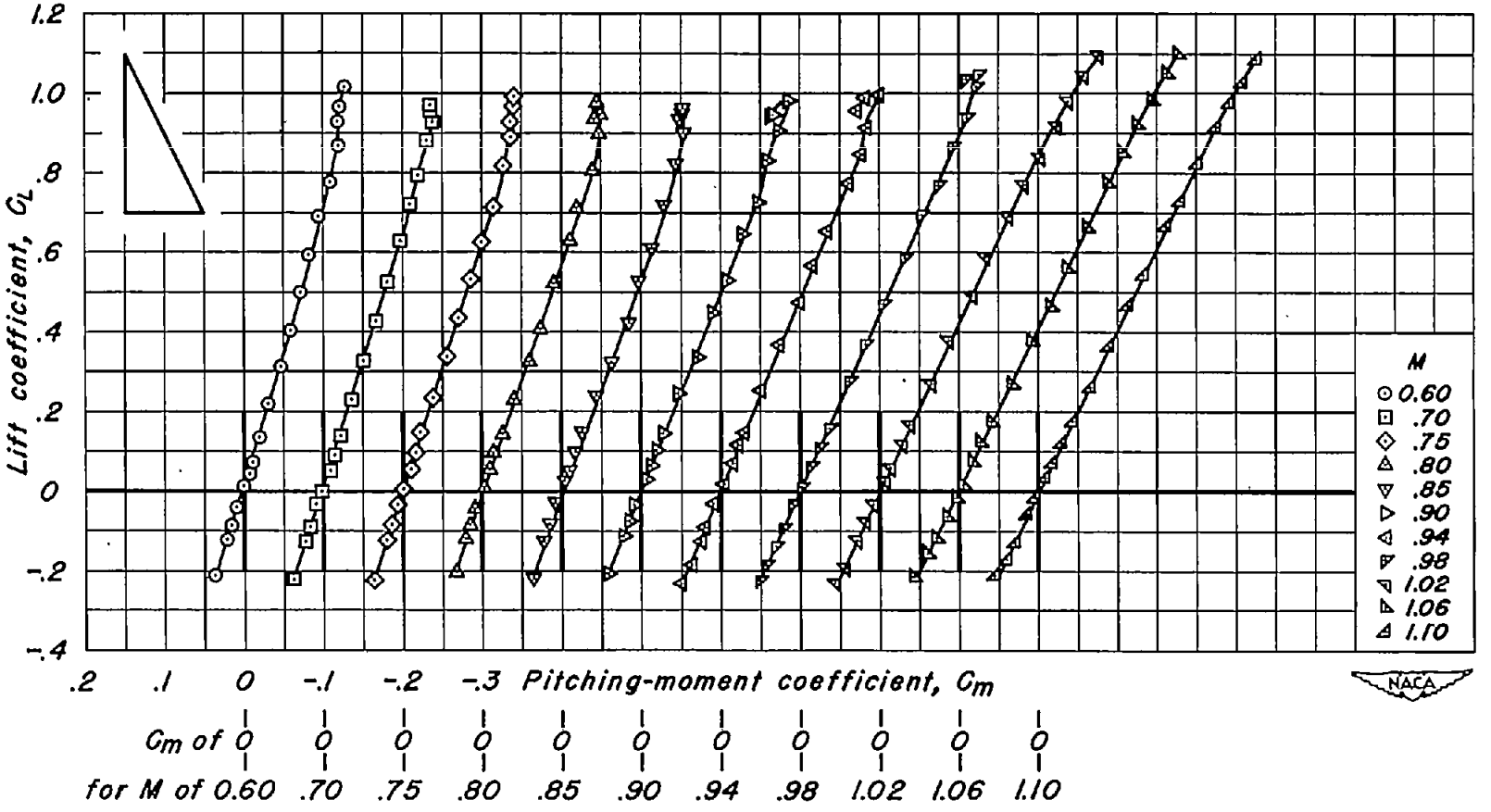

(f) NACA 63A004; λ, 0; A, 2.00.
Figure 7.- Continued.

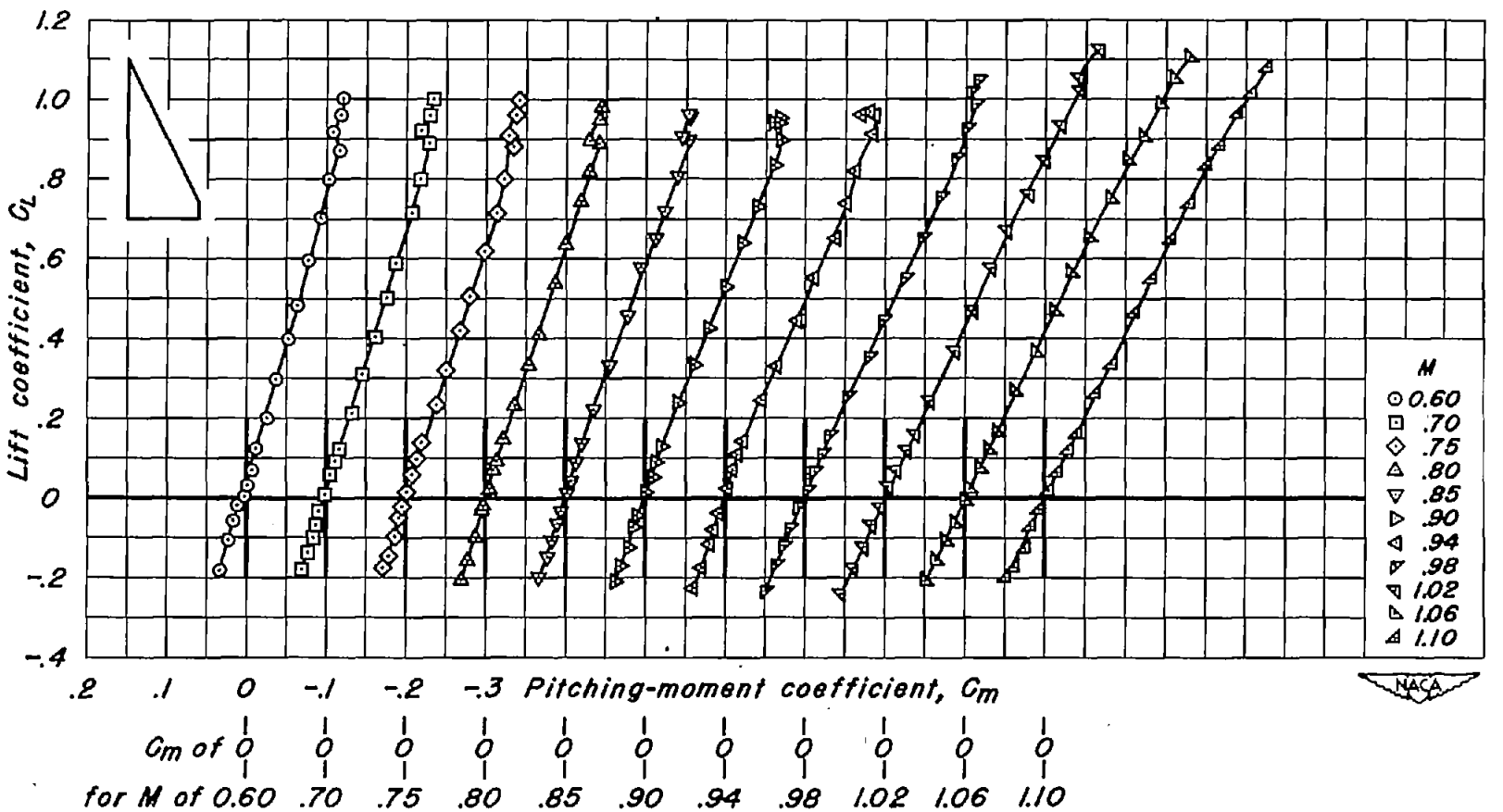

(g) NACA 63A004; λ, 0.1; A, 1.64.
Figure 7.- Continued.

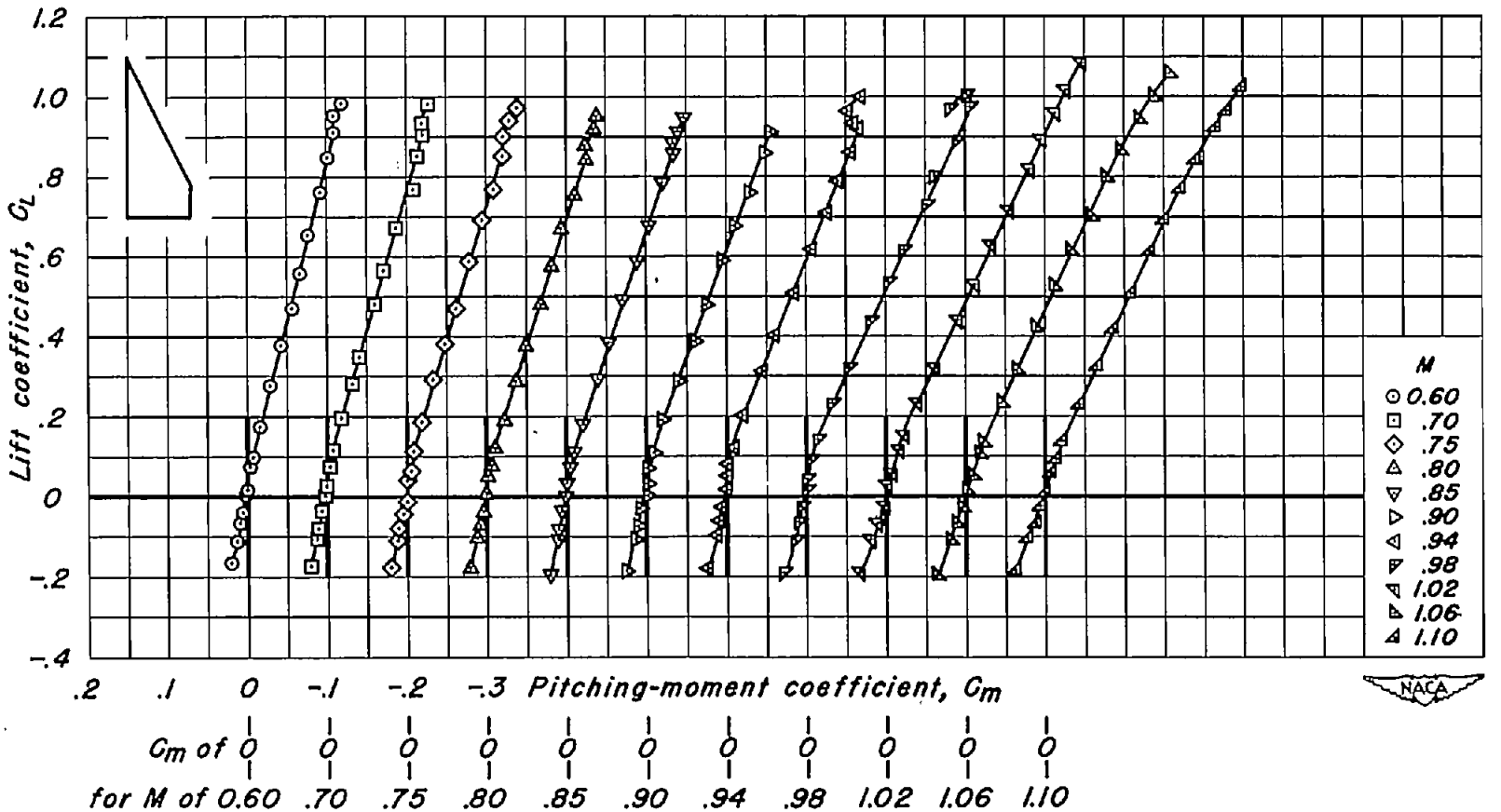

(h) NACA 63A004; λ, 0.2; A, 1.33.
Figure 7.- Continued.

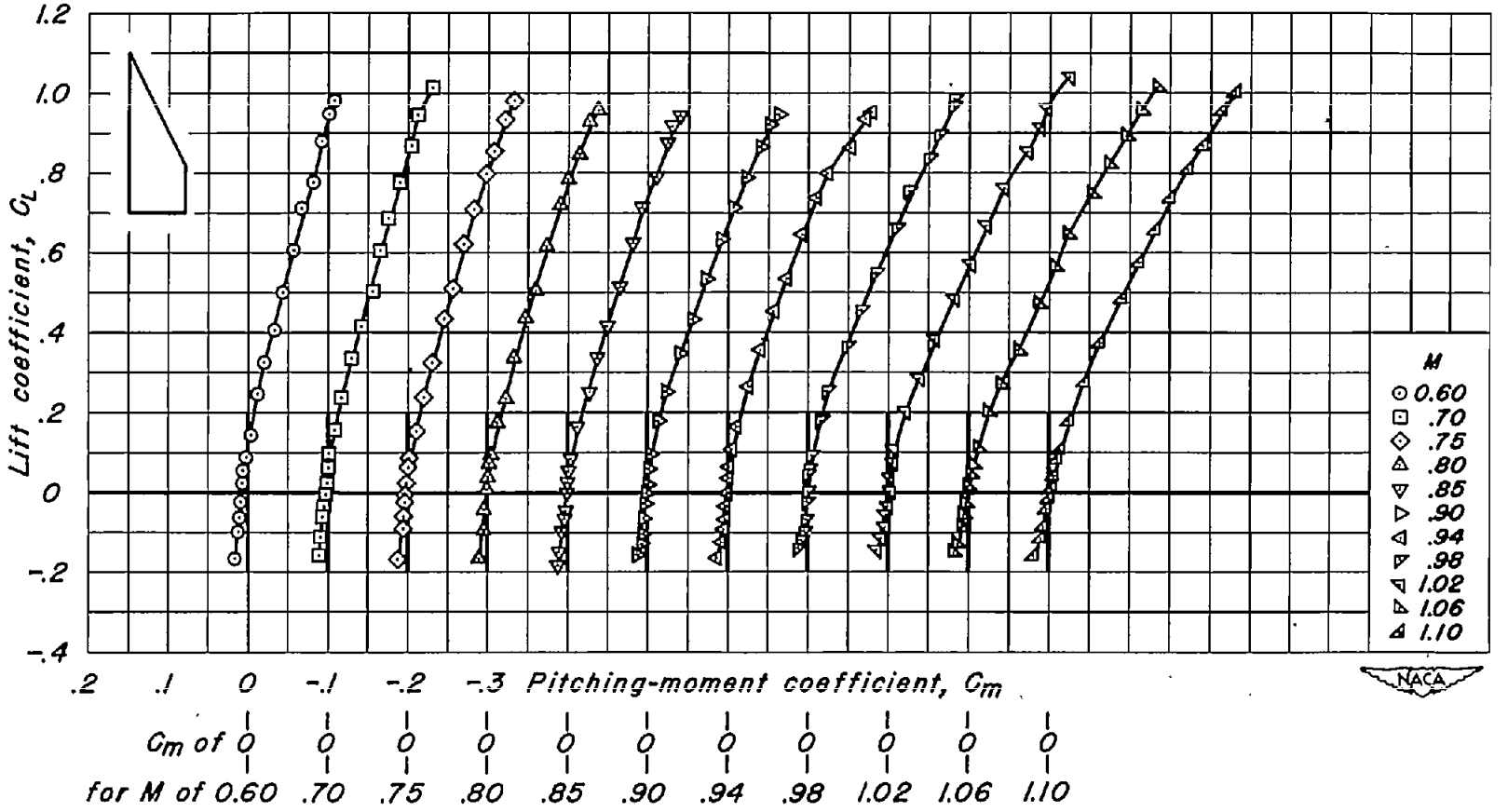

(i) NACA 63A004; λ, 0.3; A, 1.08.
Figure 7.- Continued.

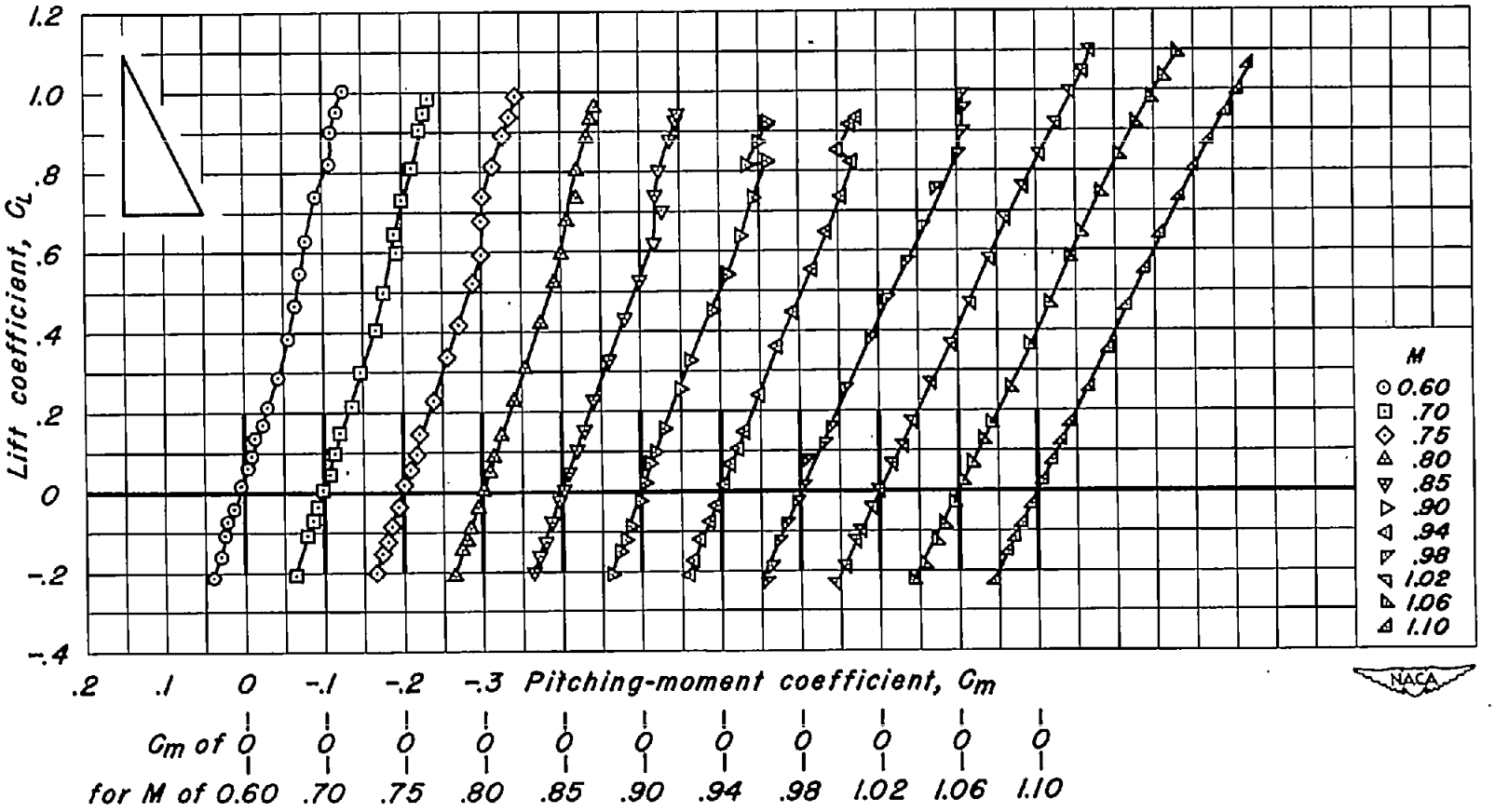

(j) NACA 63A006; λ, 0; A, 2.00.
Figure 7.- Continued.

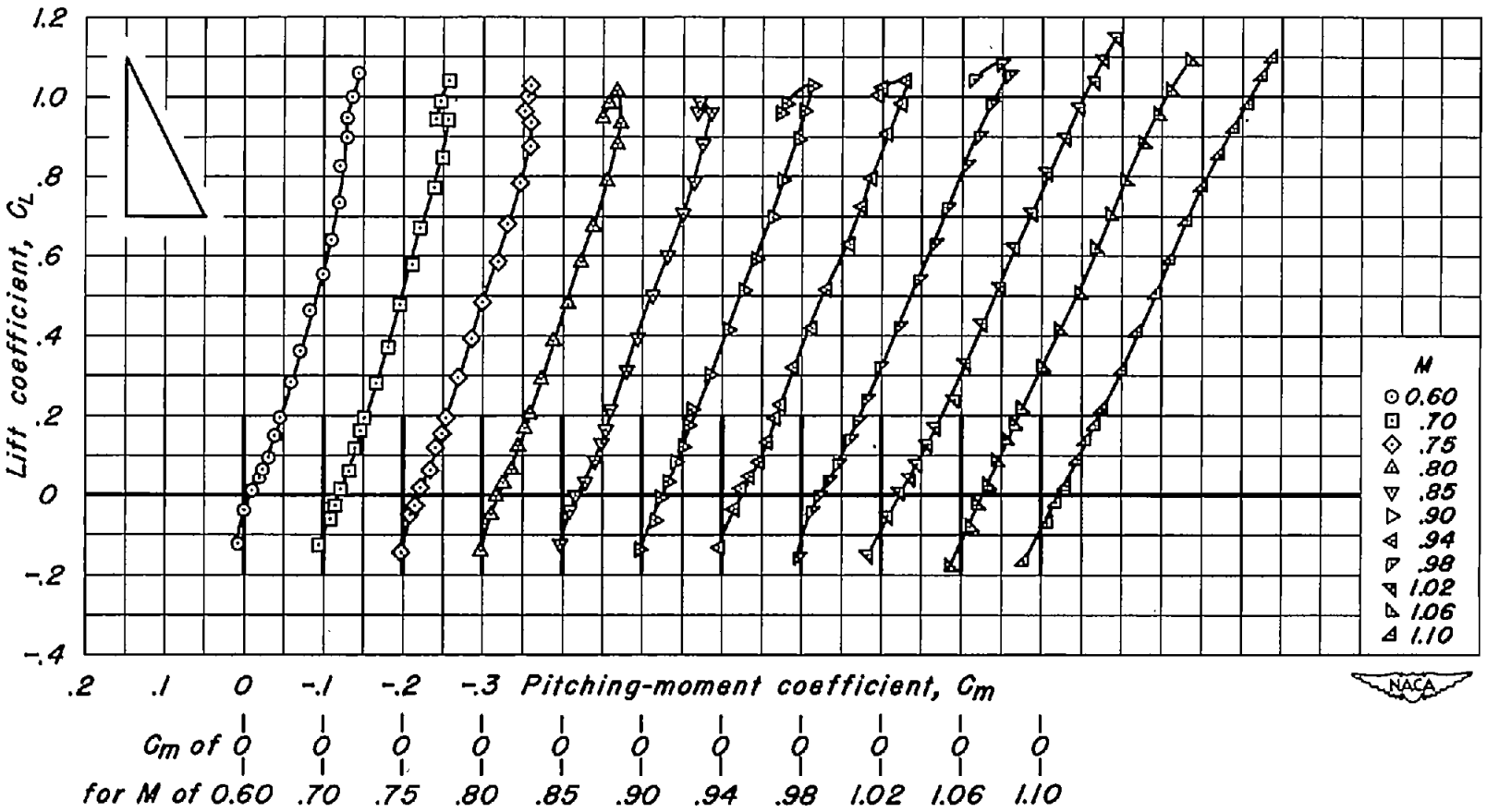

(k) NACA 63A(1.5)04; λ, 0; A, 2.00.
Figure 7.- Continued.

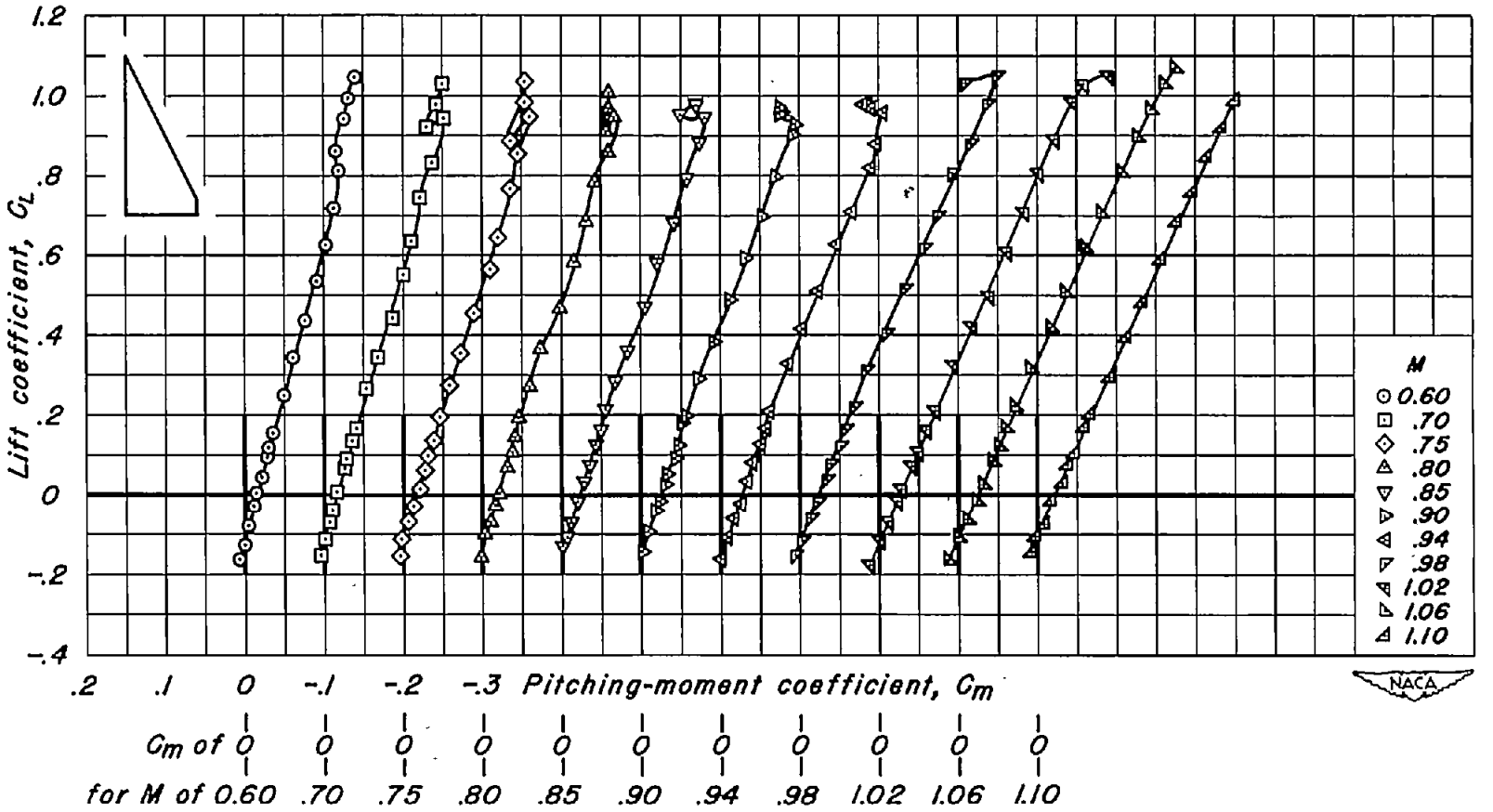

(l) NACA 63A(1.5)04; λ, 0.1; A, 1.64.
Figure 7.- Continued.

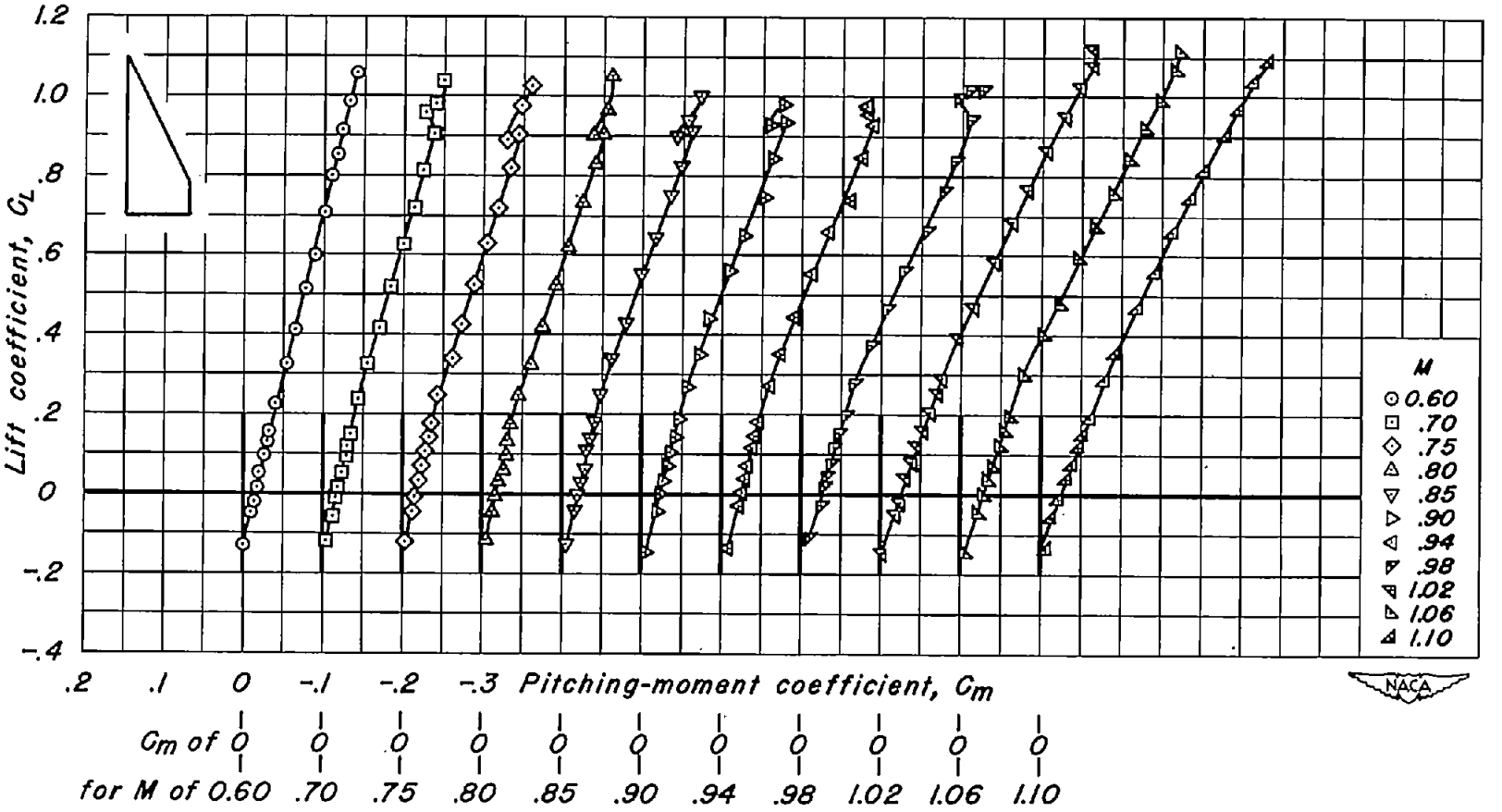

(m) NACA 63A(1.5)04; λ, 0.2; A, 1.33.
Figure 7.- Continued.

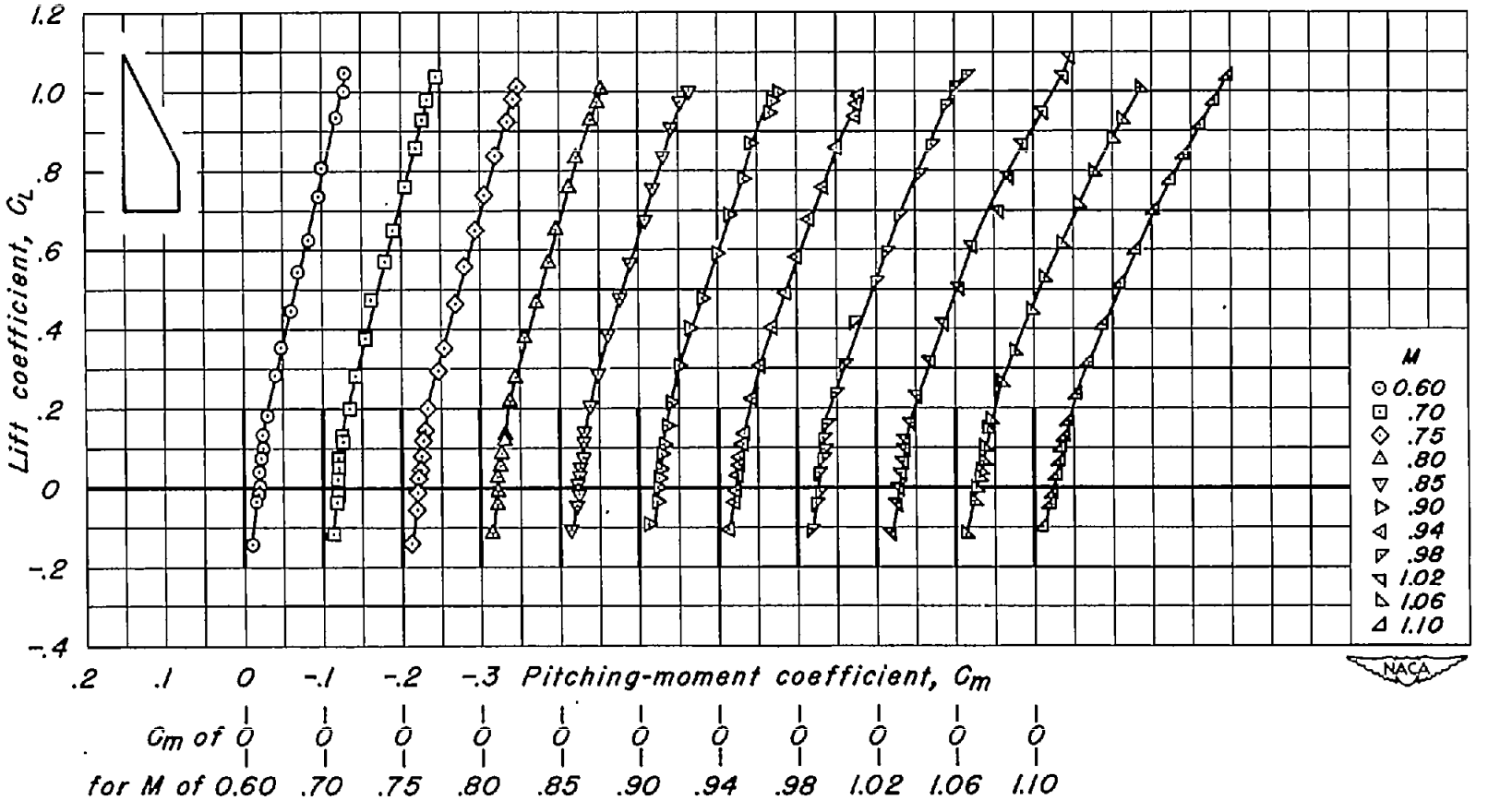

(n) NACA 63A(1.5)04; λ, 0.3; A, 1.08.
Figure 7.- Concluded.

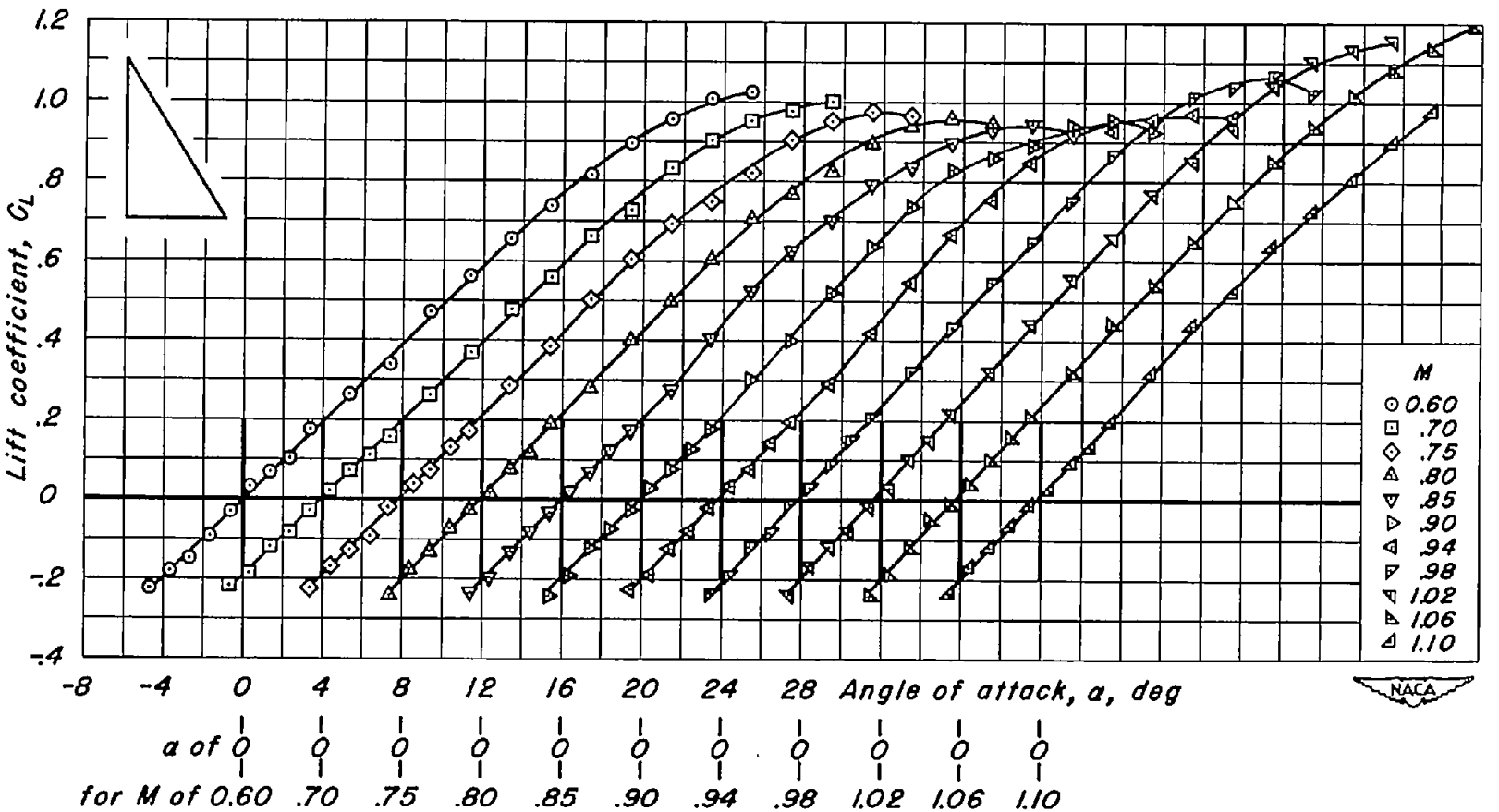

(a) NACA 63A002; λ, 0; A, 2.50.

Figure 8.- Variation of lift coefficient with angle of attack for the wings of basic aspect ratio 2.5.

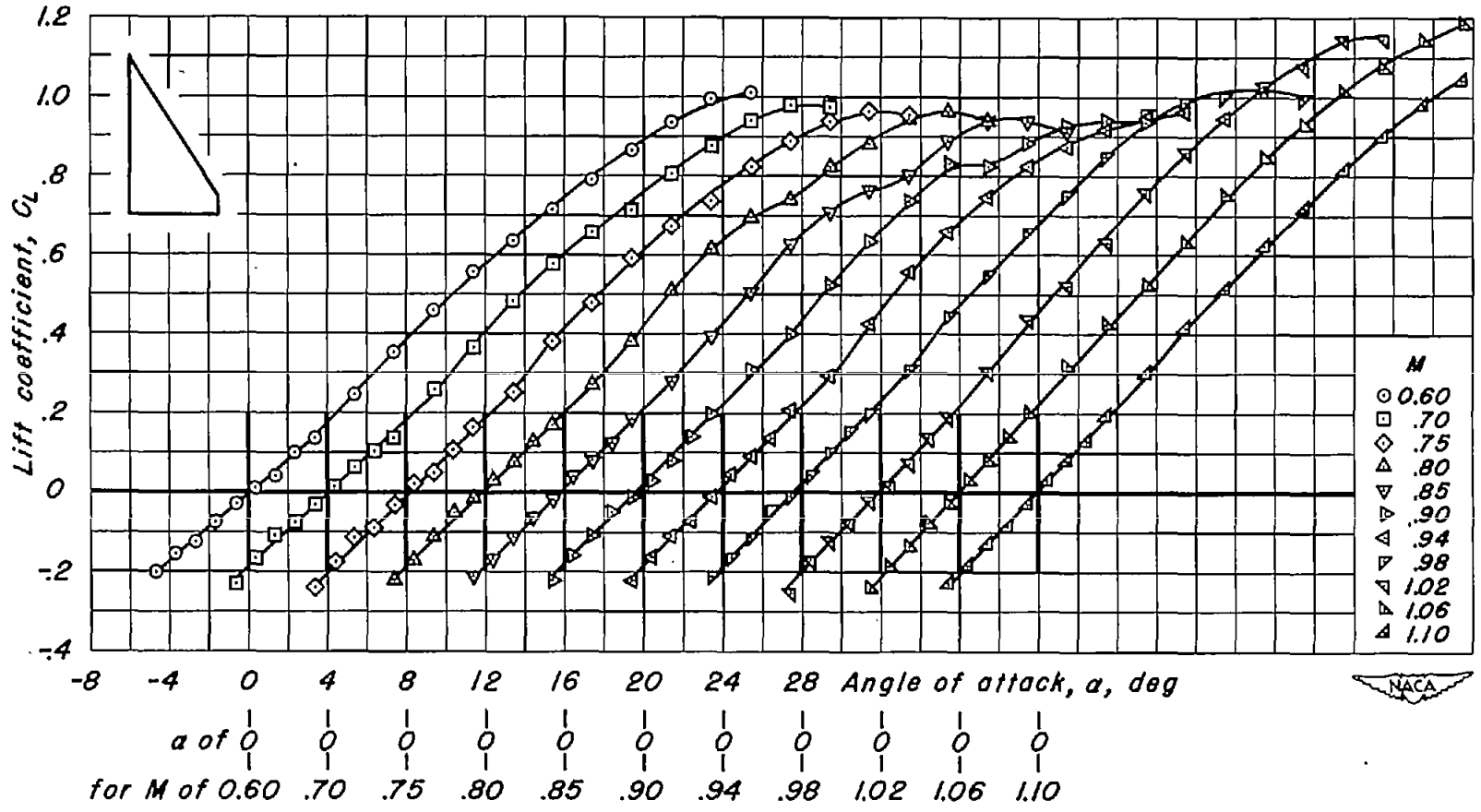

(b) NACA 63A002; λ, 0.1; A, 2.05.
Figure 8.- Continued.

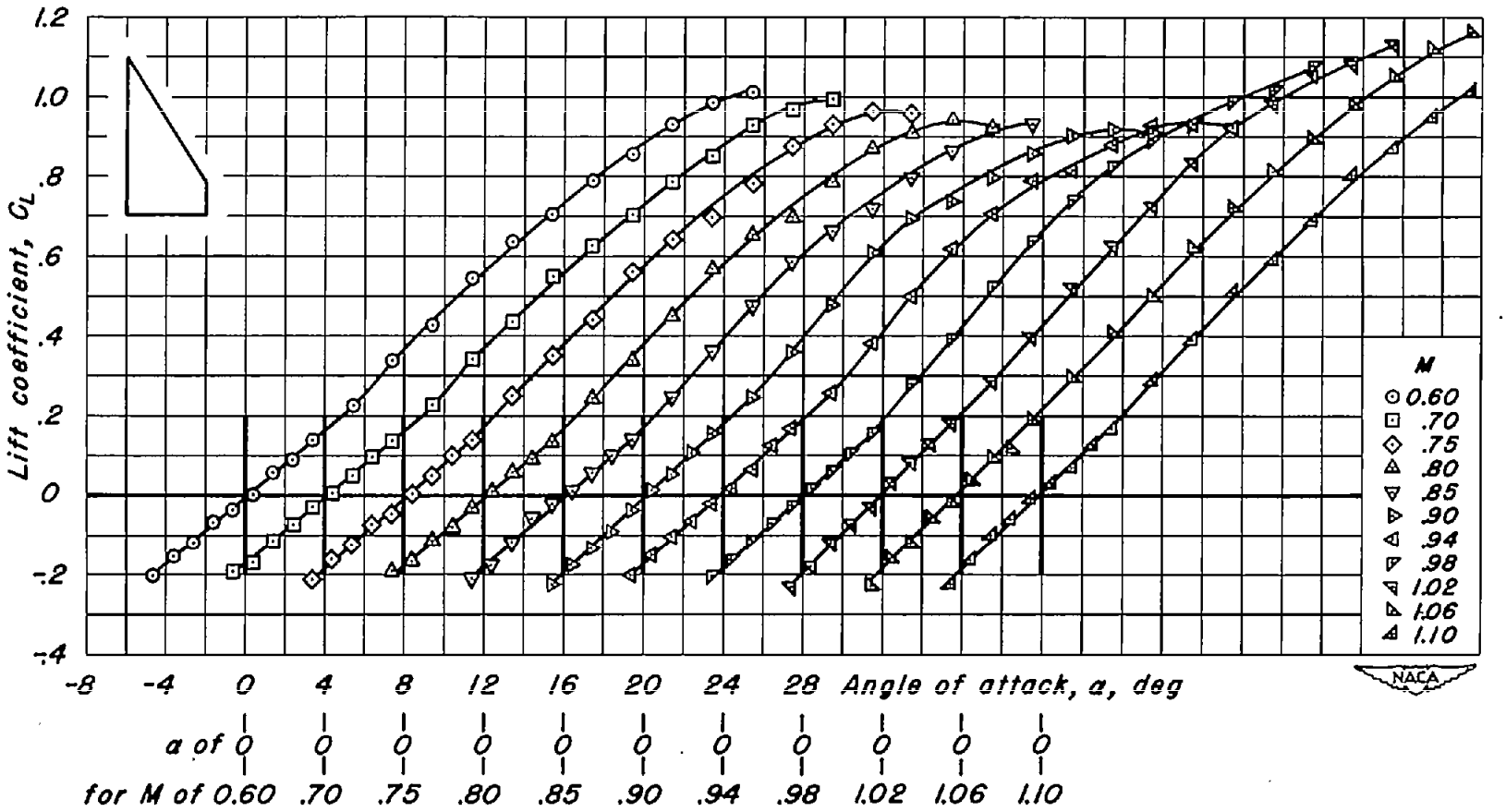

α of	0	0	0	0	0	0	0	0	0	0
for M of	0.60	.70	.75	.80	.85	.90	.94	.98	1.02	1.06	1.10

(c) NACA 63A002; λ, 0.2; A, 1.67.
Figure 8.- Continued.

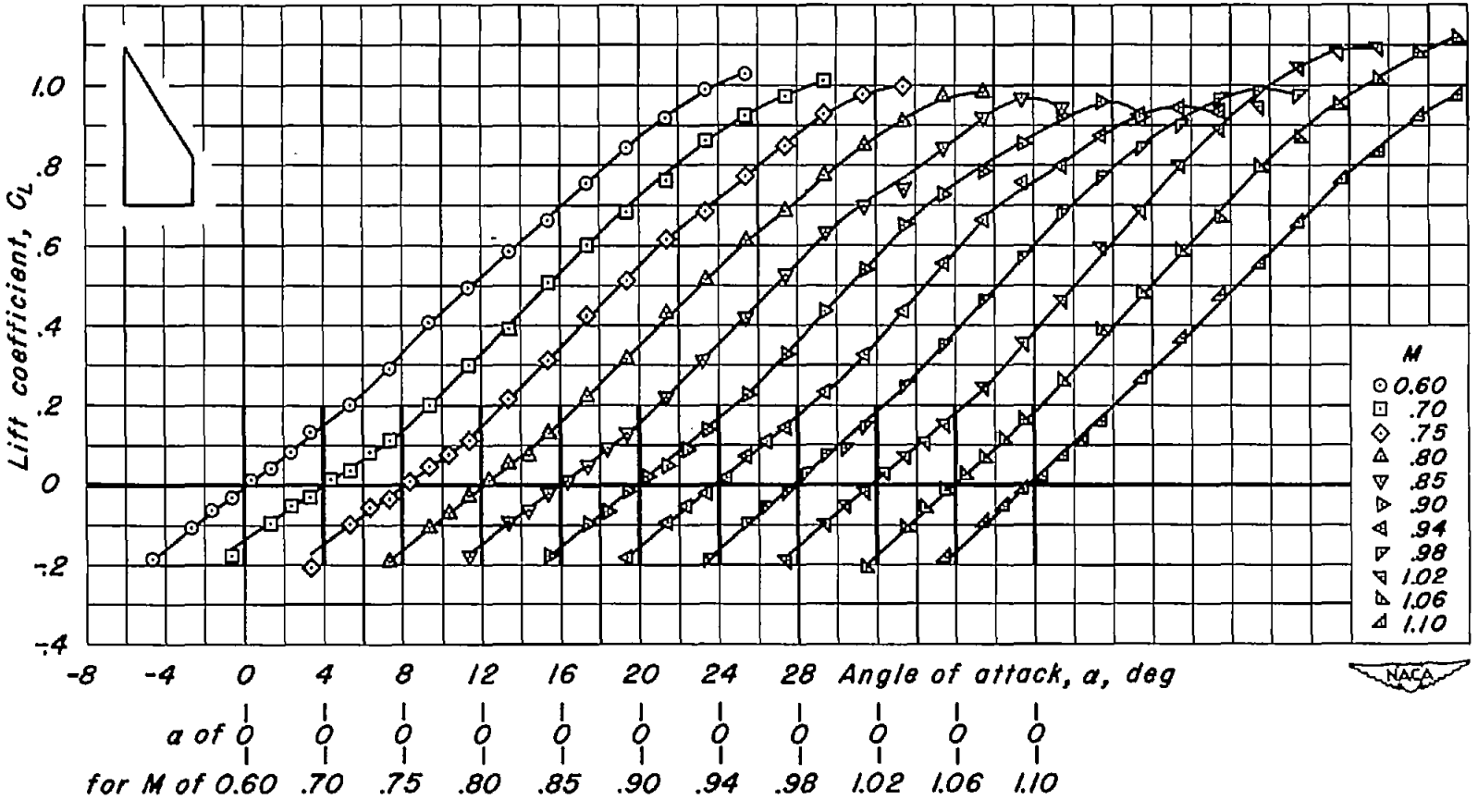

(d) NACA 63A002; λ, 0.3; A, 1.35.
Figure 8.- Continued.

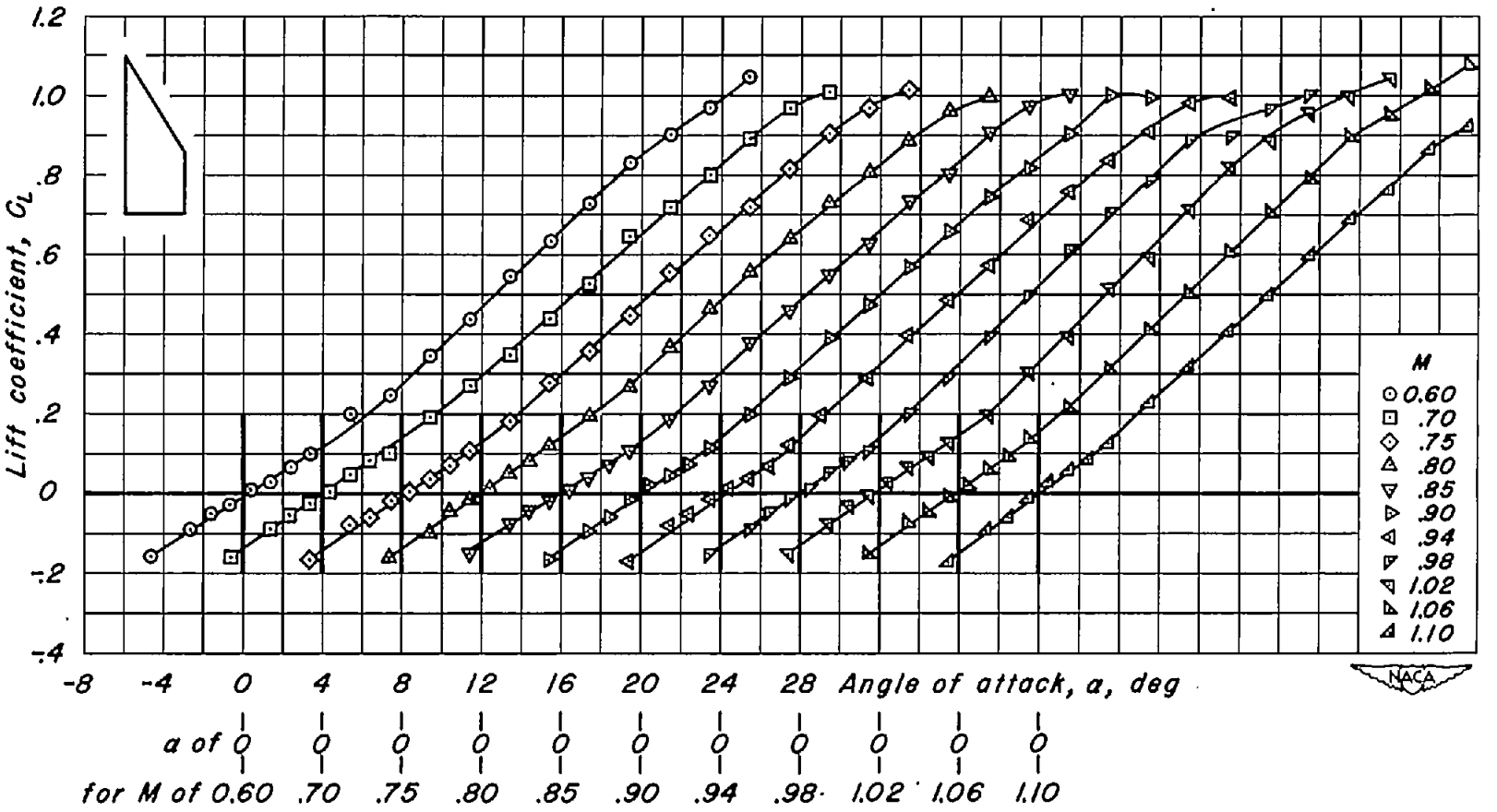

α of	0	0	0	0	0	0	0	0	0	0	0
for M of	0.60	.70	.75	.80	.85	.90	.94	.98	1.02	1.06	1.10

(e) NACA 63A002; λ, 0.4; A, 1.07.
Figure 8.- Continued.

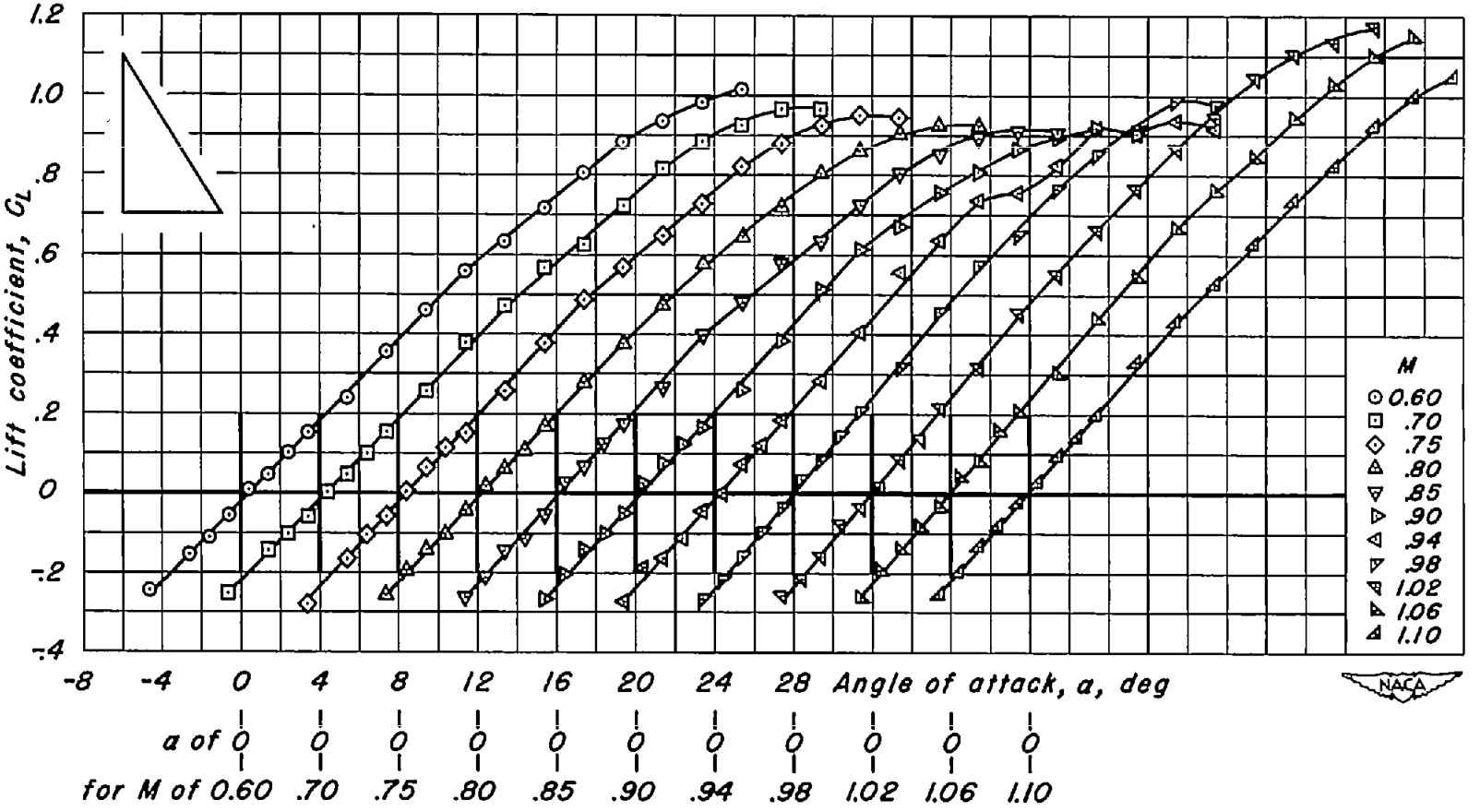

(f) NACA 63A004; λ, 0; A, 2.50.
Figure 8.- Continued.

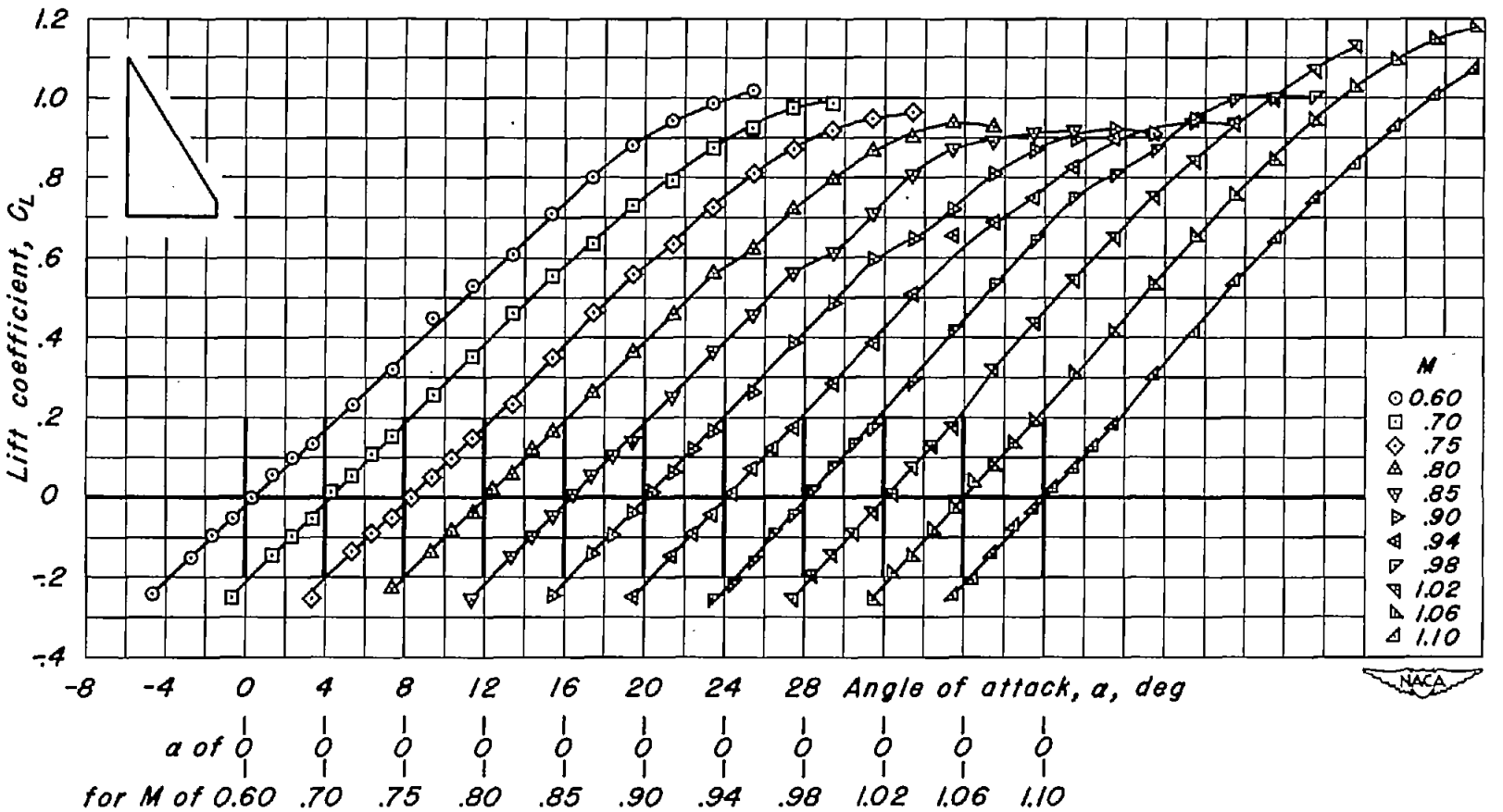

(g) NACA 63A004; λ, 0.1; A, 2.05.
Figure 8.- Continued.

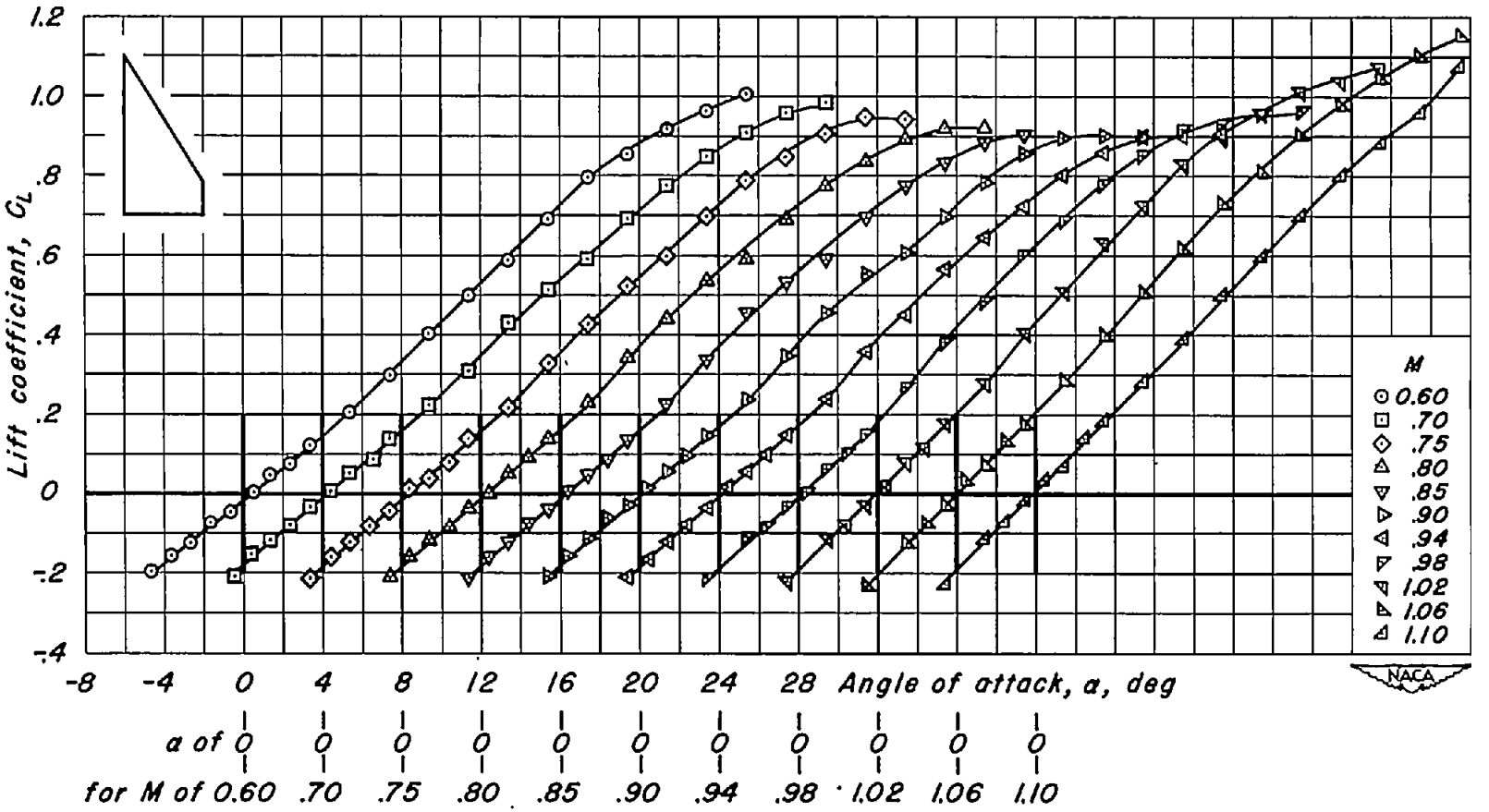

(h) NACA 63A004; λ, 0.2; A, 1.67.
Figure 8.- Continued.

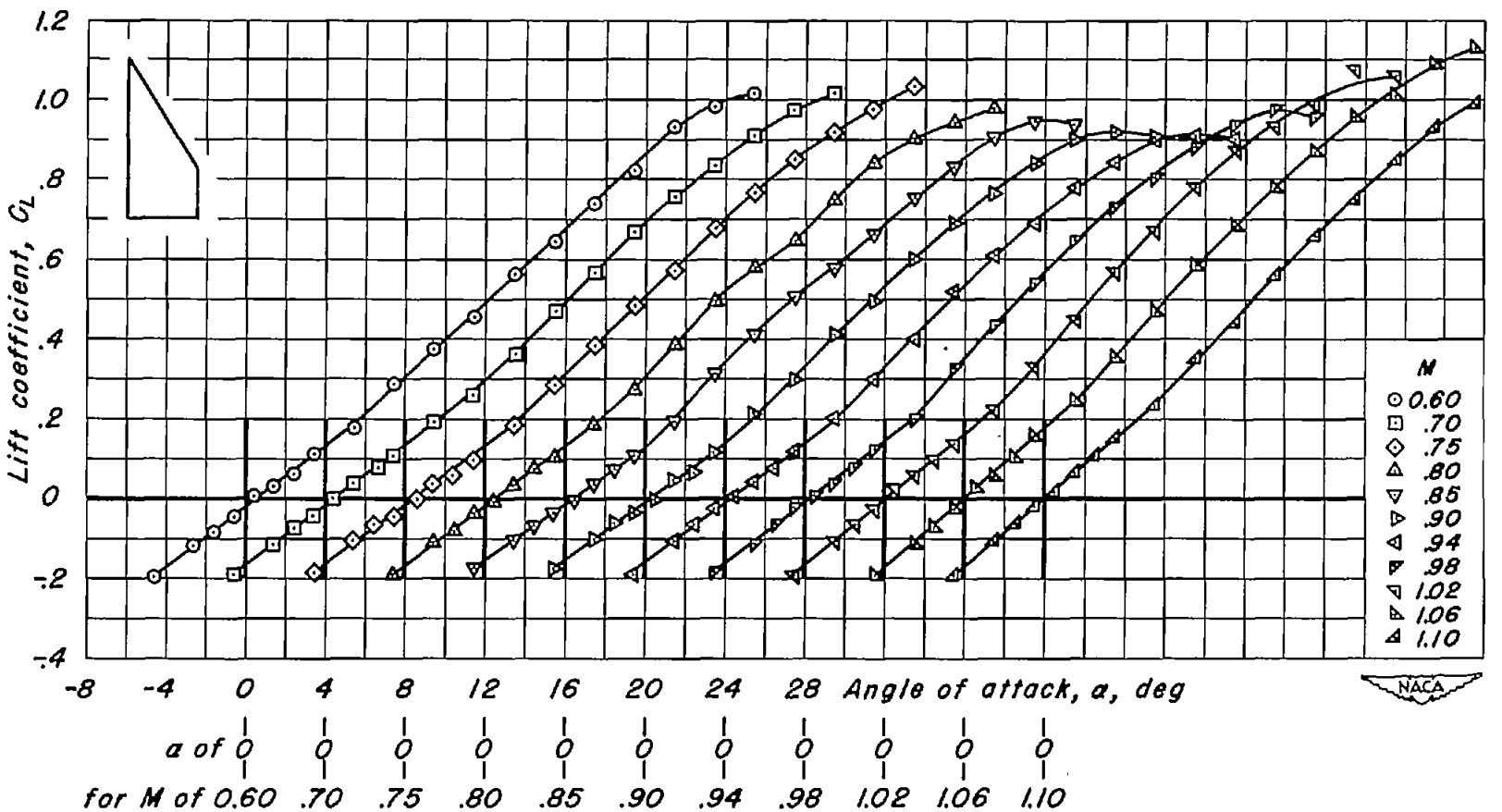

(i) NACA 63A004; λ, 0.3; A, 1.35.
Figure 8.- Continued.

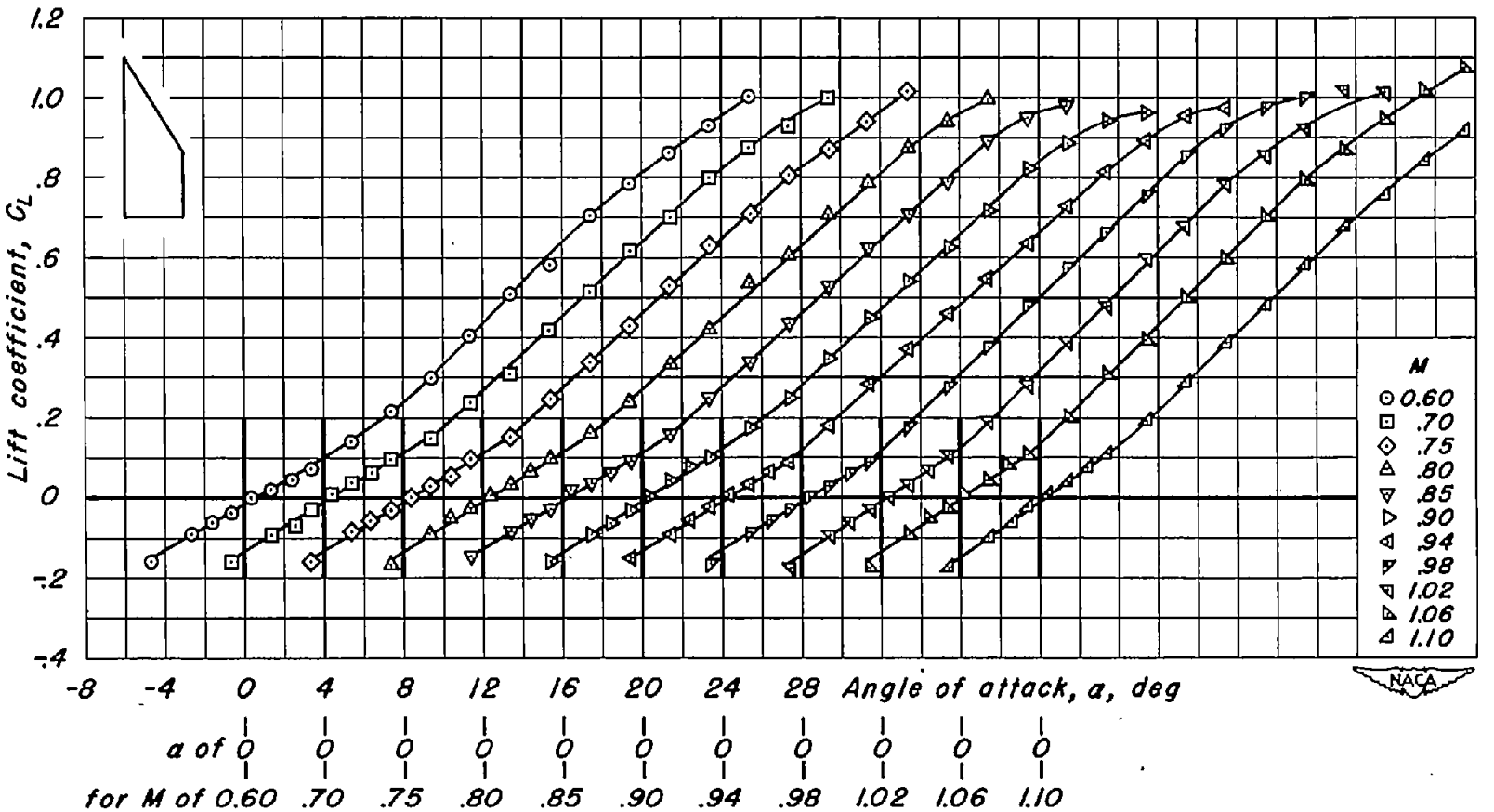

(j) NACA 63A004; λ, 0.4; A, 1.07.
Figure 8.- Continued.

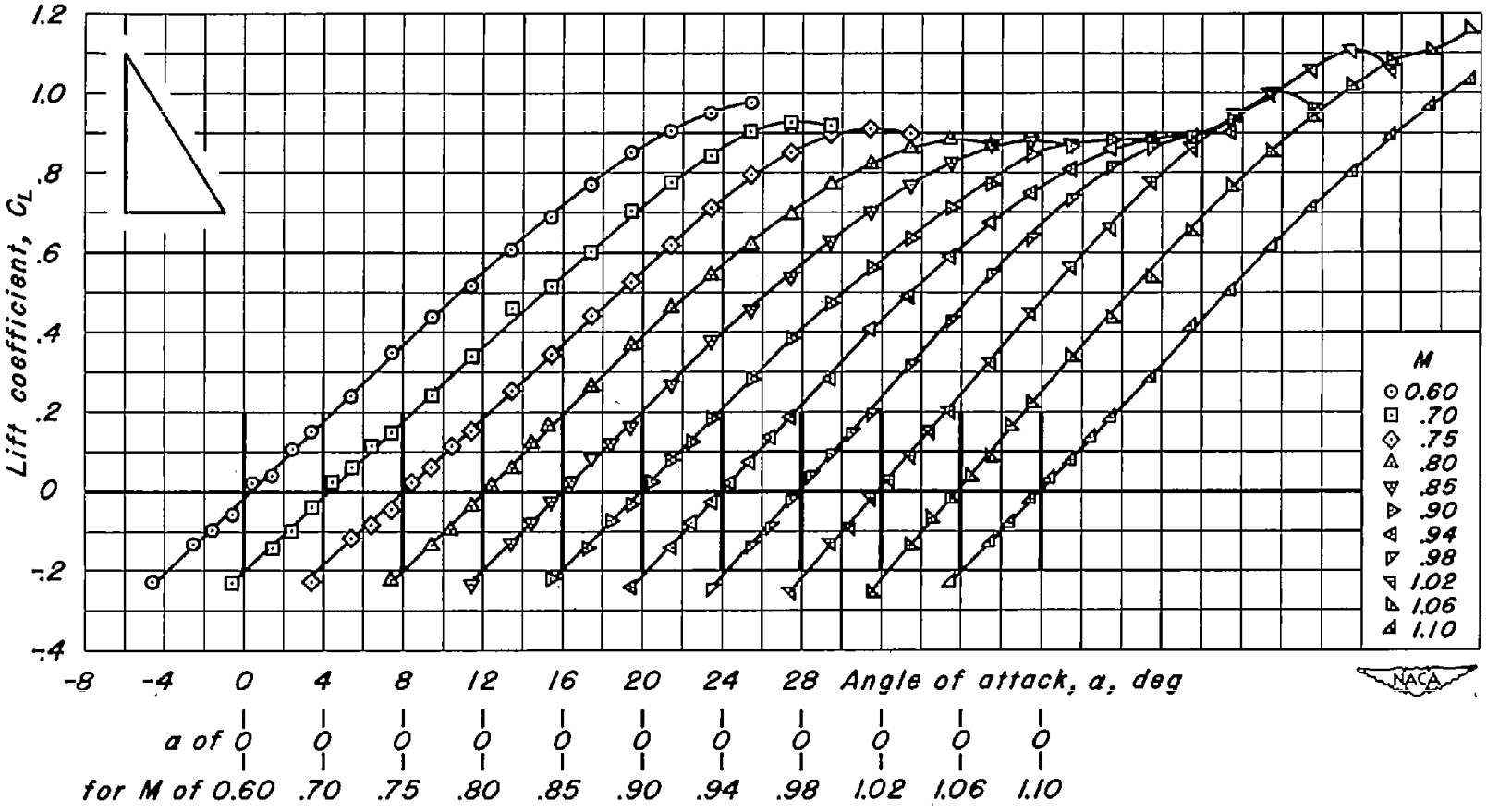

(k) NACA 63A006; λ, 0; A, 2.50.
Figure 8.- Continued.

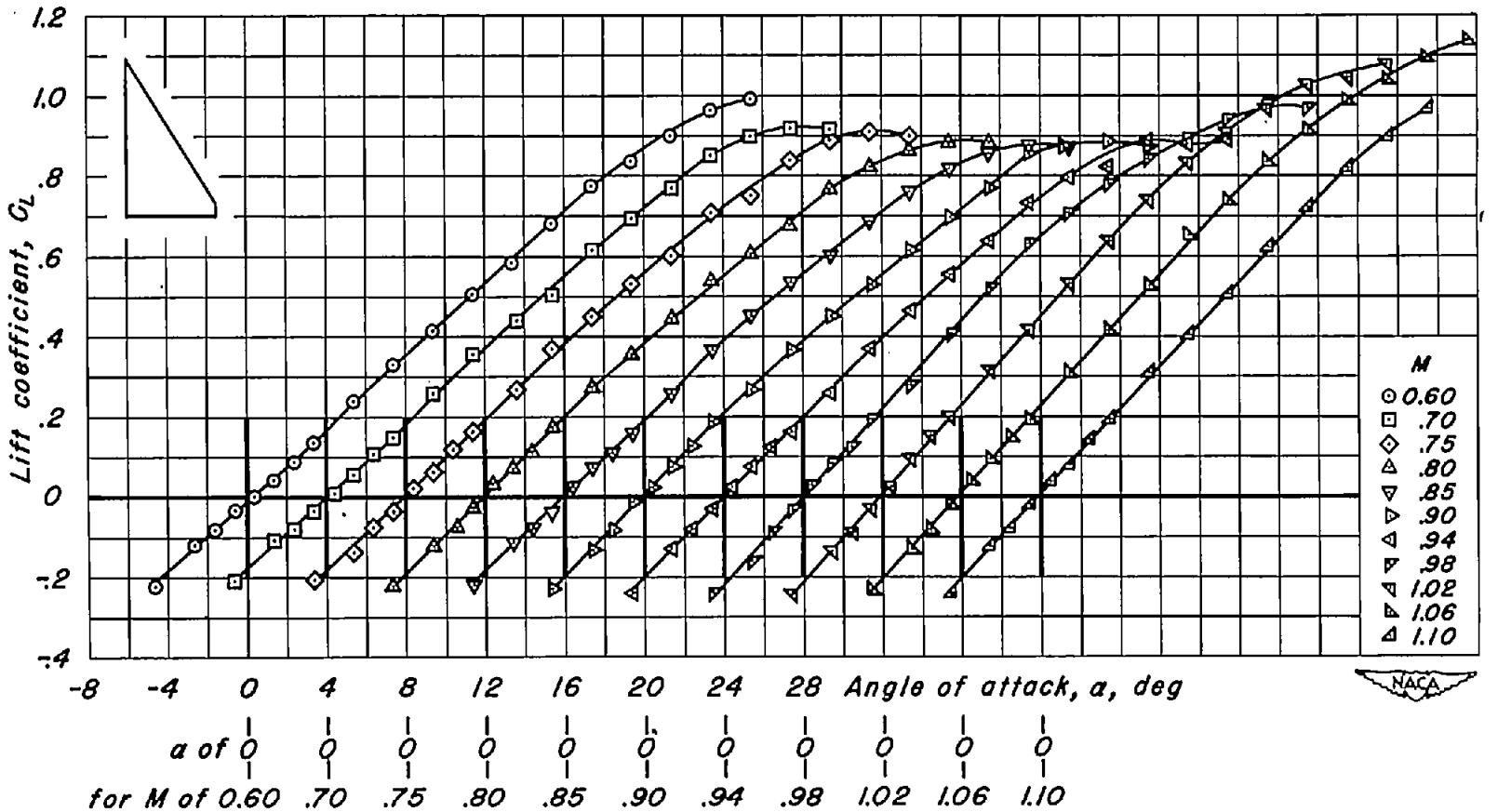

(l) NACA 63A006; λ, 0.1; A, 2.05.
Figure 8.- Continued.

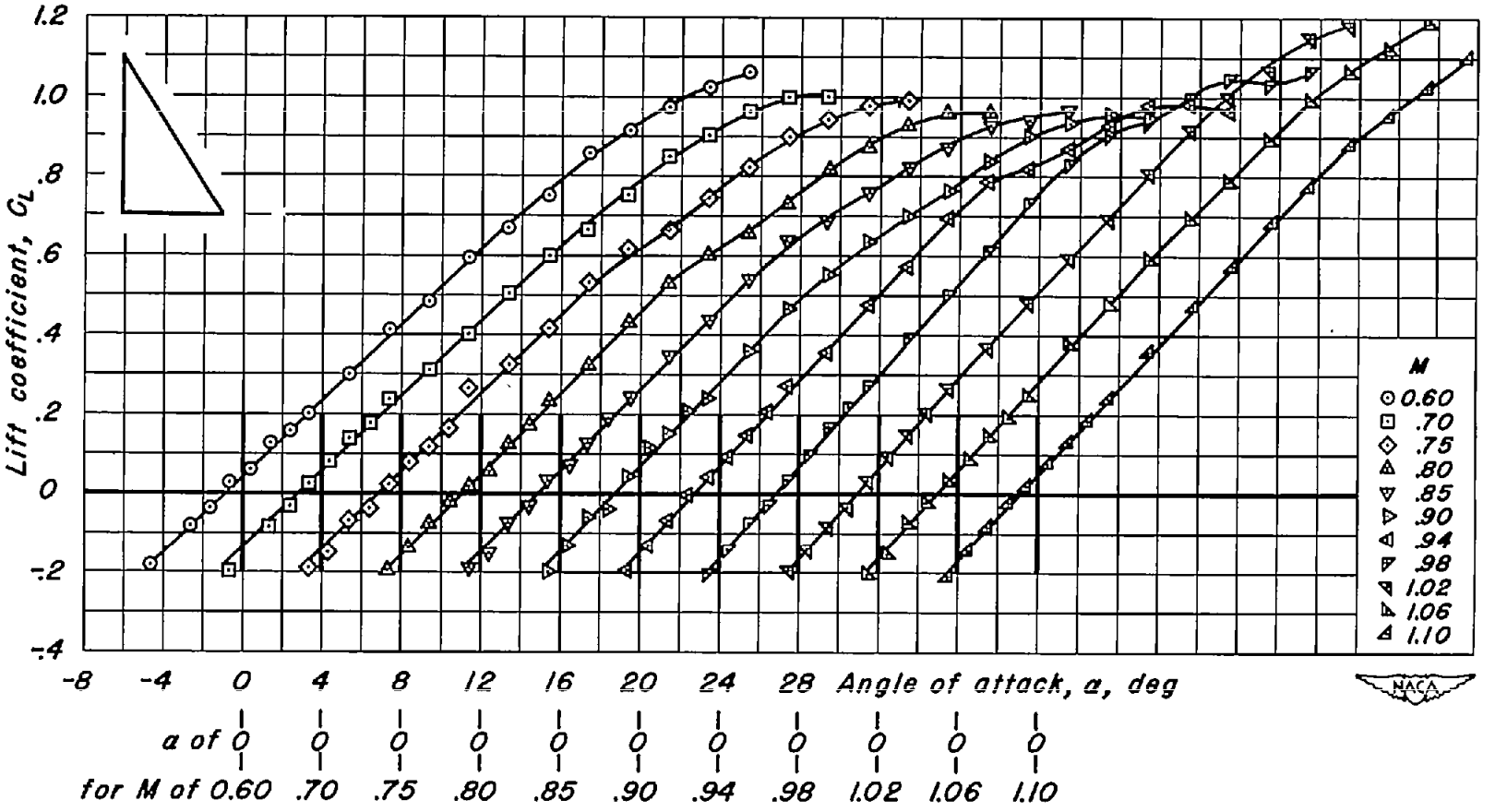

(m) NACA 63A(1.5)04; λ, 0; A, 2.50.
Figure 8.- Continued.

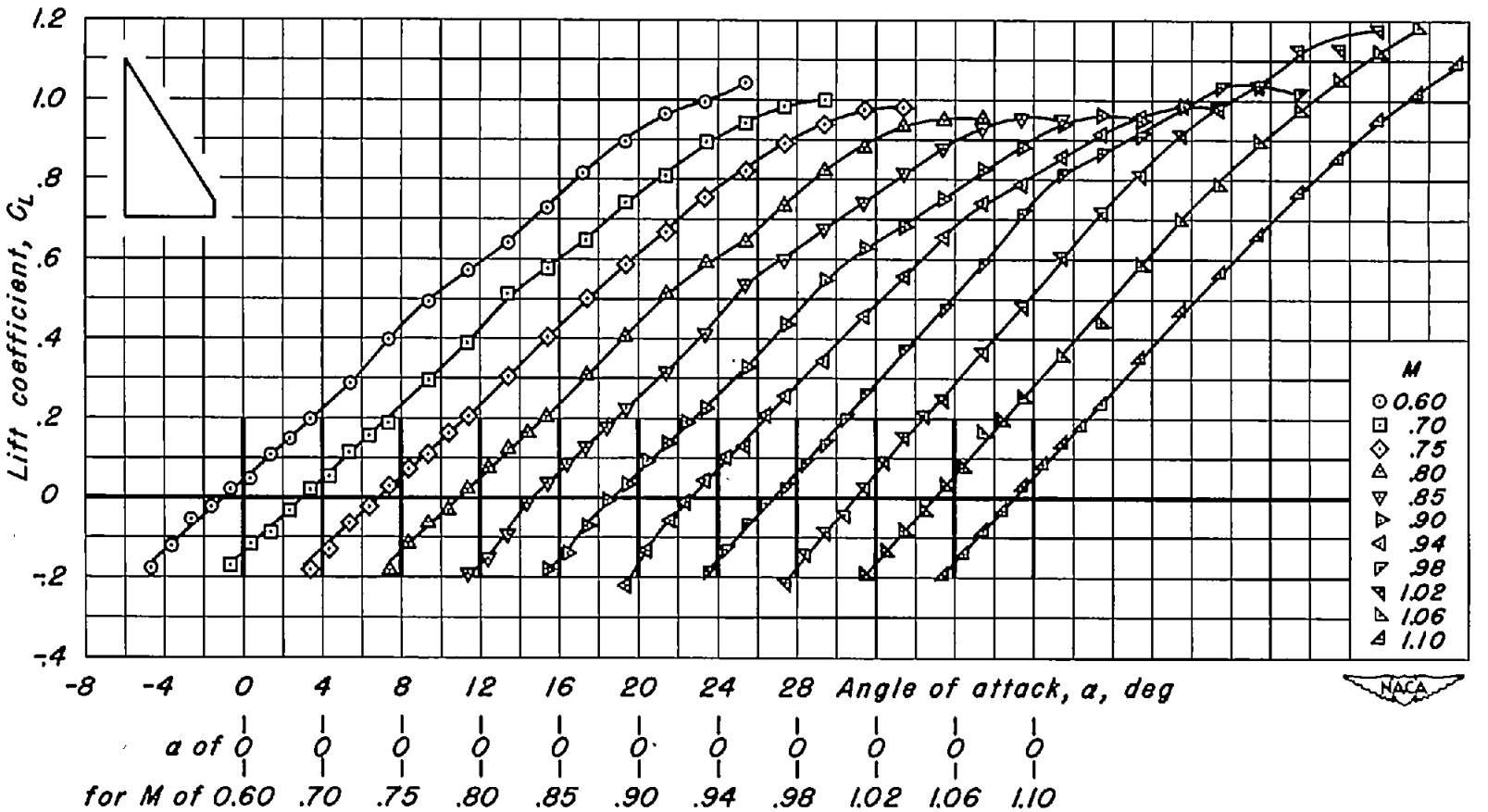

(n) NACA 63A(1.5)04; λ, 0.1; A, 2.05.
Figure 8.- Continued.

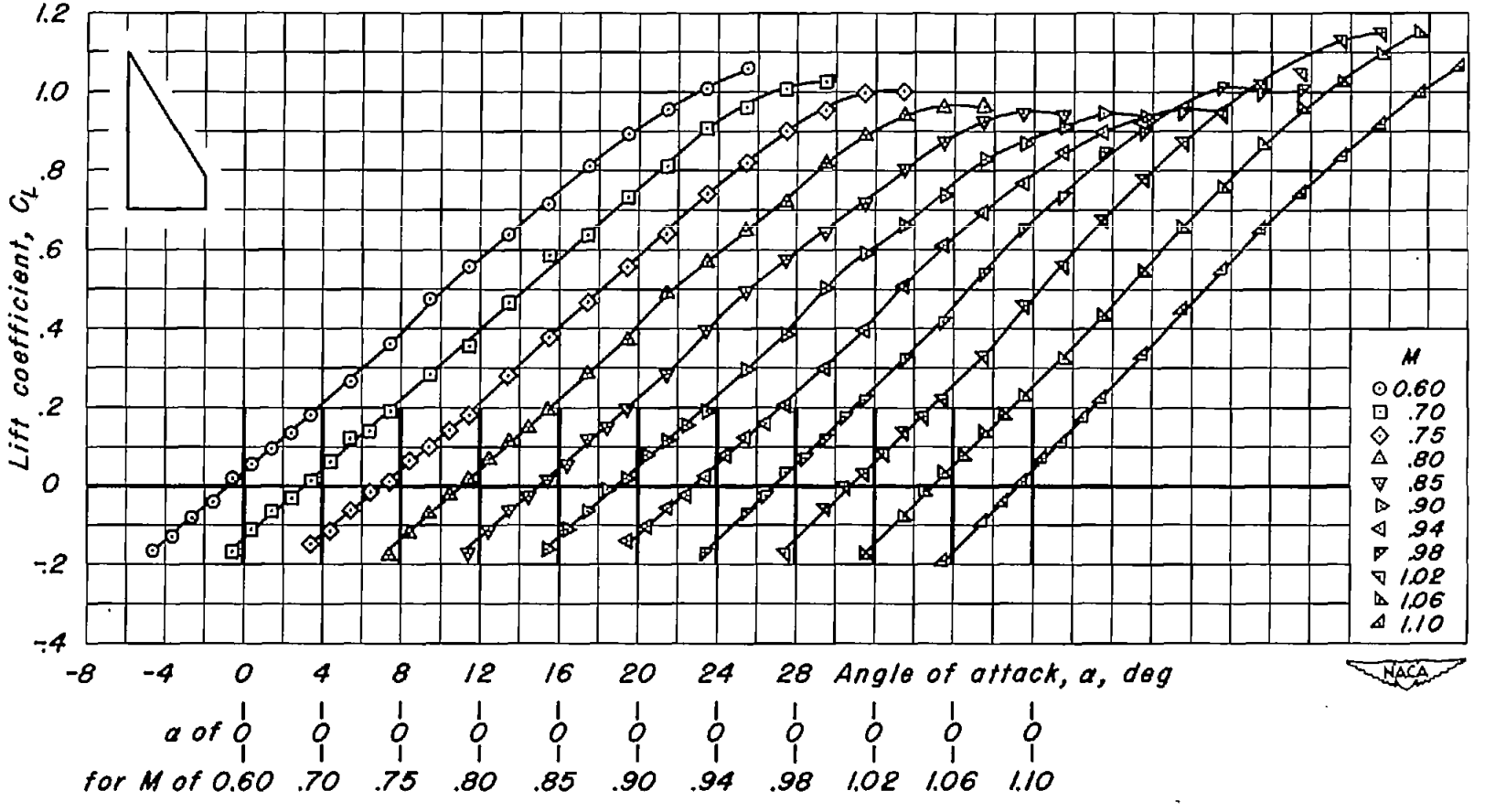

(o) NACA 63A(1.5)04; λ, 0.2; A, 1.67.
Figure 8.- Continued.

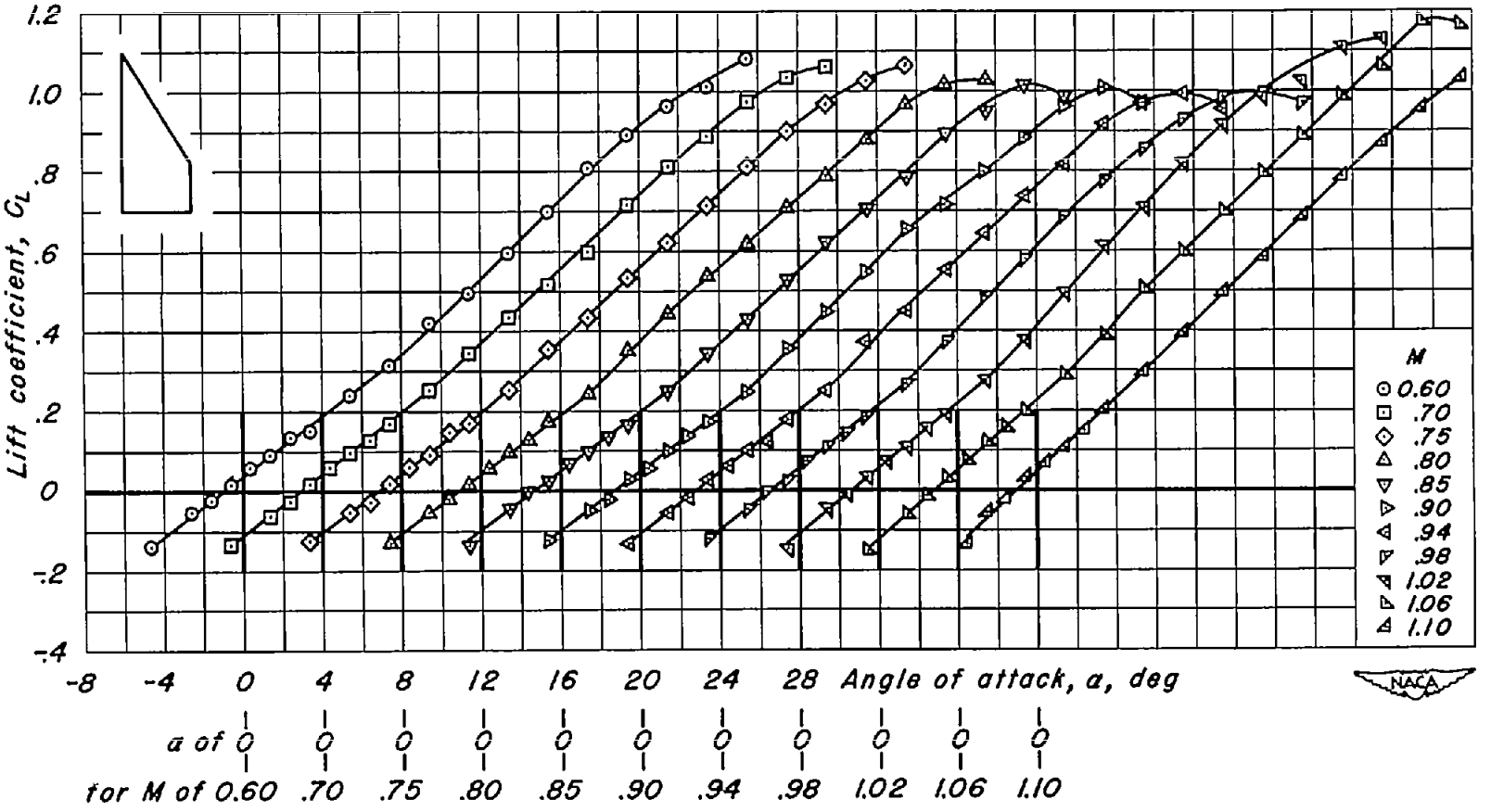

(p) NACA 63A(1.5)04; λ, 0.3; A, 1.35.
Figure 8.- Concluded.

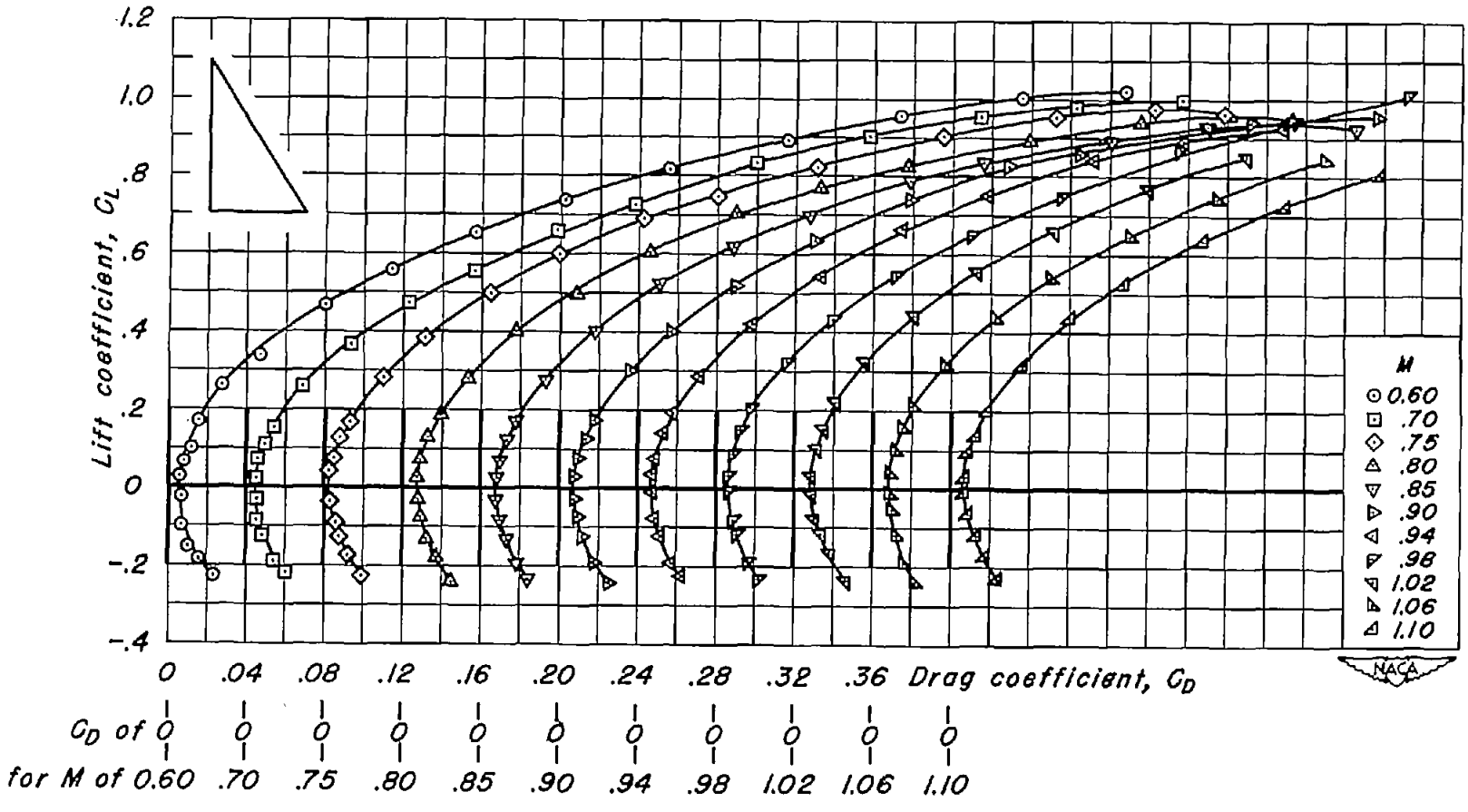

C_D of	0	0	0	0	0	0	0	0	0	0	0
for M of	0.60	.70	.75	.80	.85	.90	.94	.98	1.02	1.06	1.10

(a) NACA 63A002; λ, 0; A, 2.50.

Figure 9.- Variation of drag coefficient with lift coefficient for the wings of basic aspect ratio 2.50.

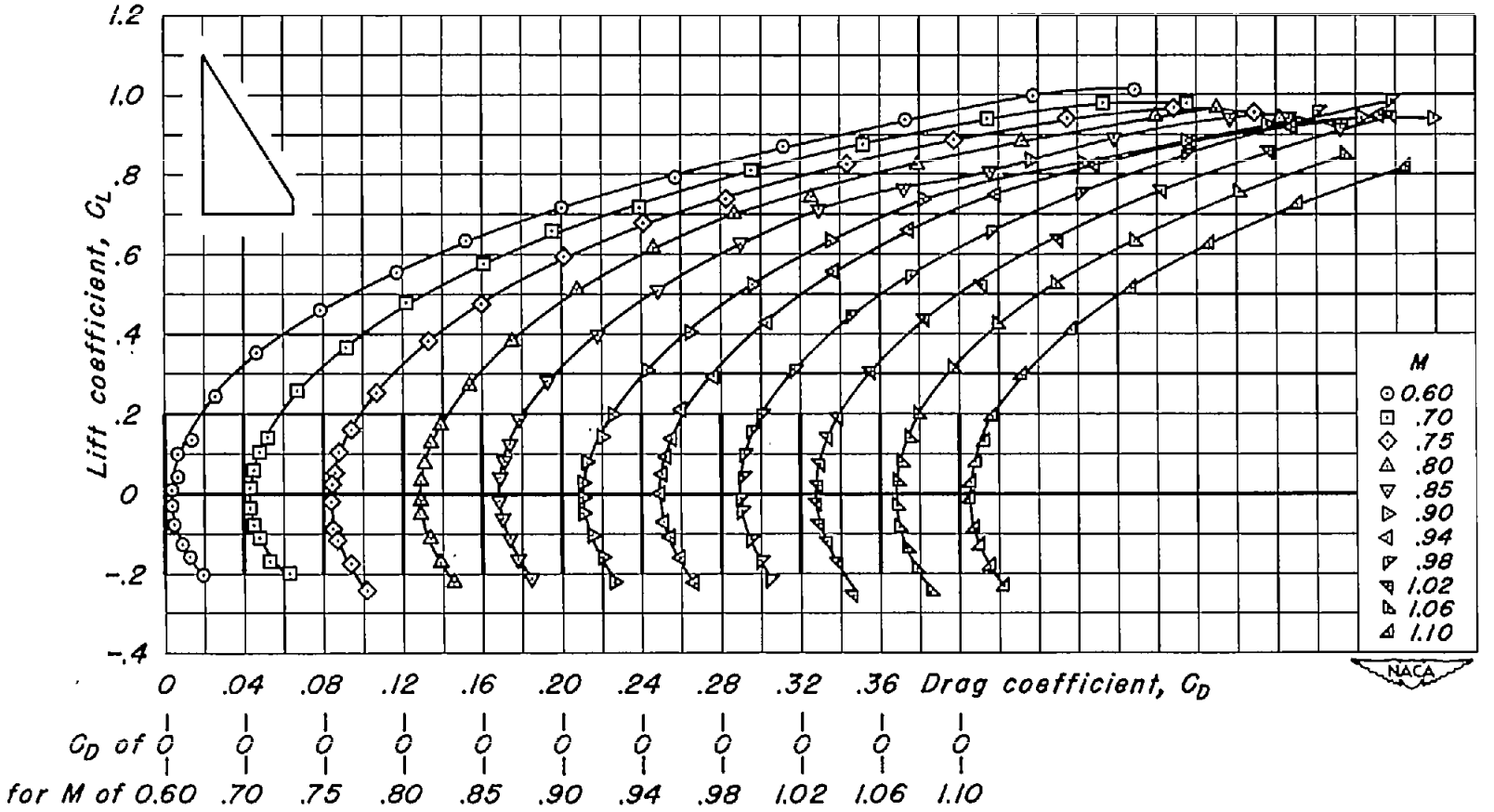

(b) NACA 63A002; λ, 0.1; A, 2.05.
Figure 9.- Continued.

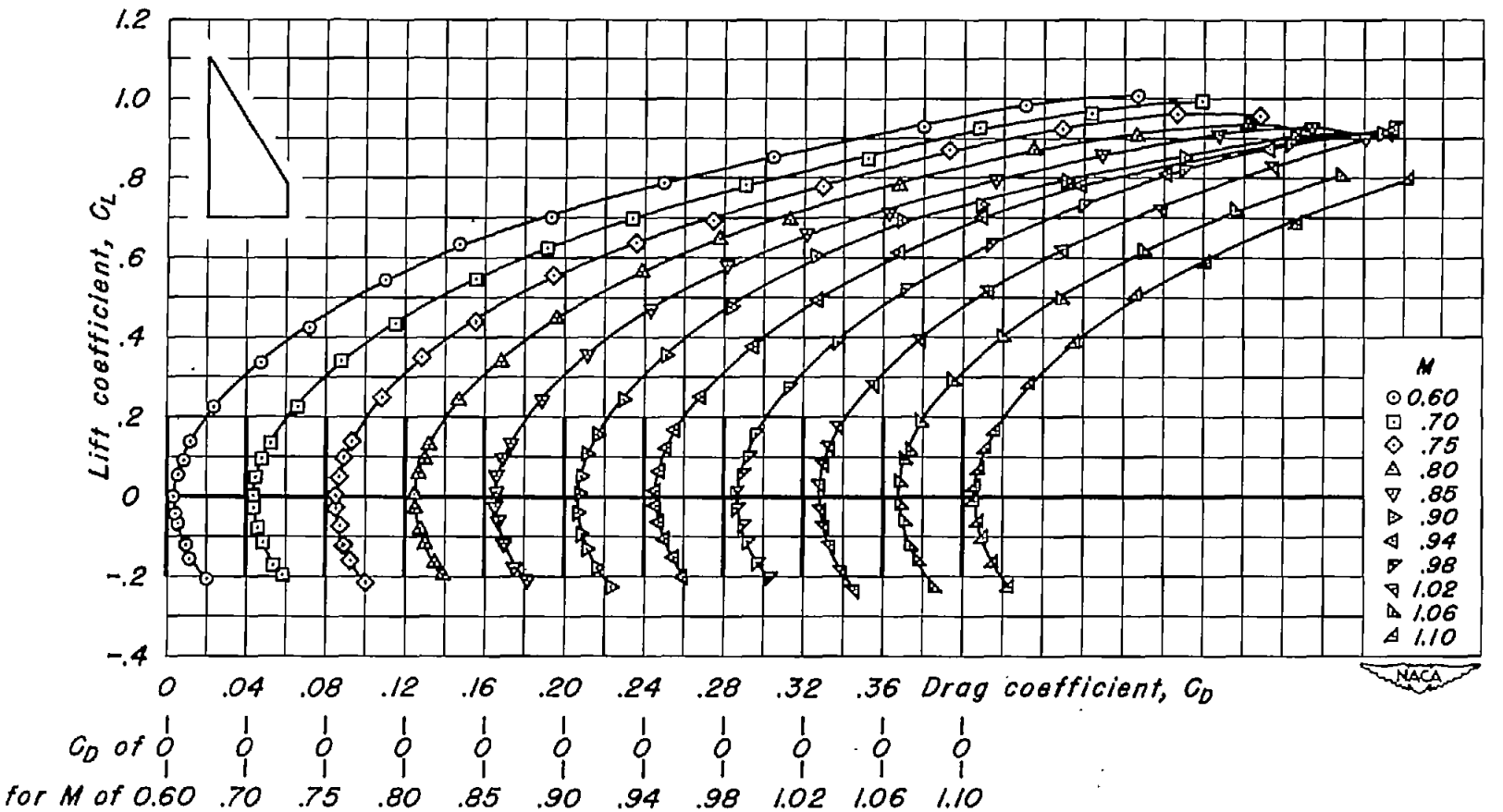

C_D of	0	0	0	0	0	0	0	0	0	0	0
for M of	0.60	.70	.75	.80	.85	.90	.94	.98	1.02	1.06	1.10

(c) NACA 63A002; λ, 0.2; A, 1.67.
Figure 9.- Continued.

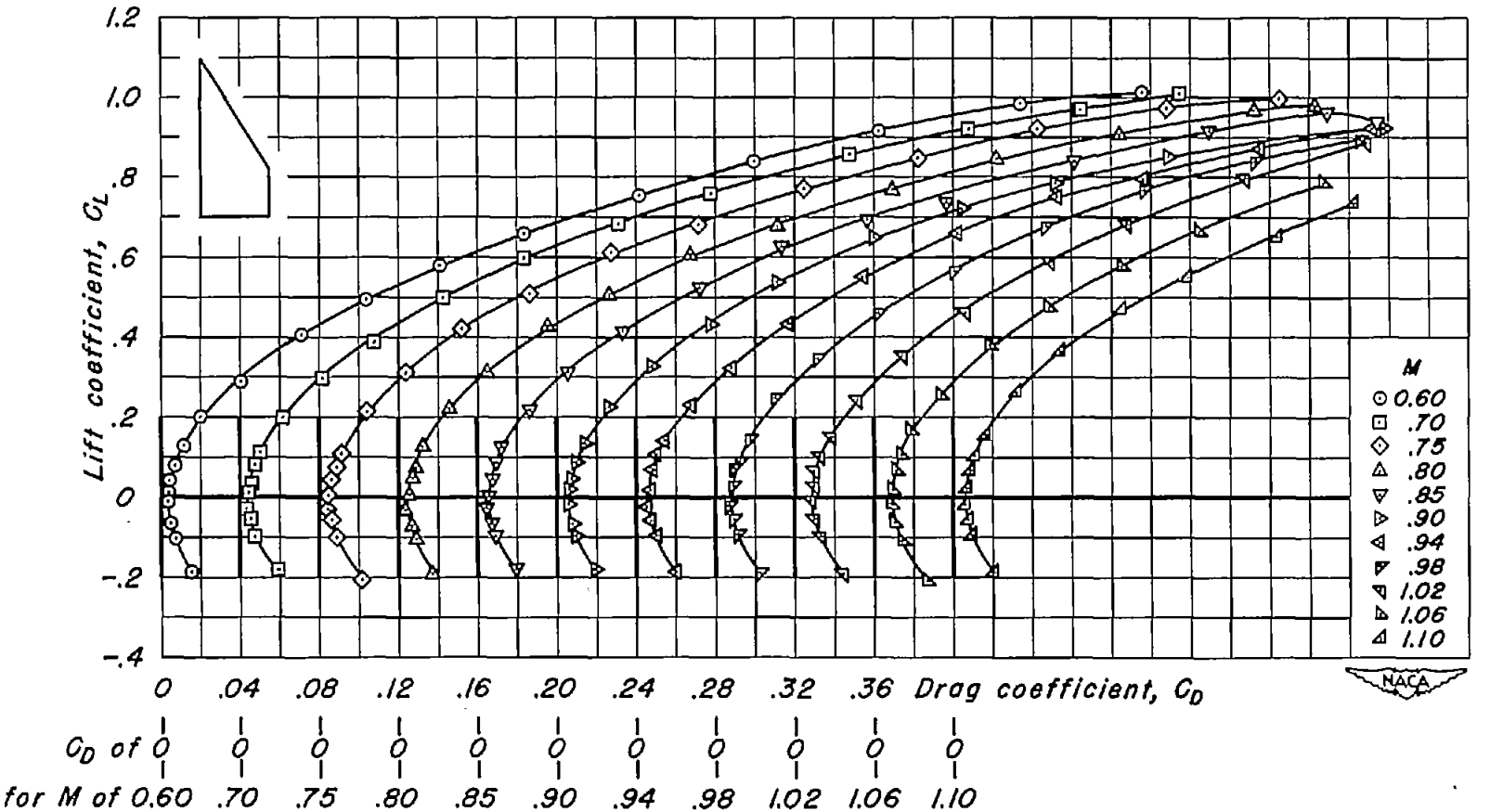

C_D of	0	0	0	0	0	0	0	0	0	0	0
for M of	0.60	.70	.75	.80	.85	.90	.94	.98	1.02	1.06	1.10

(d) NACA 63A002; λ, 0.3; A, 1.35.
Figure 9.- Continued.

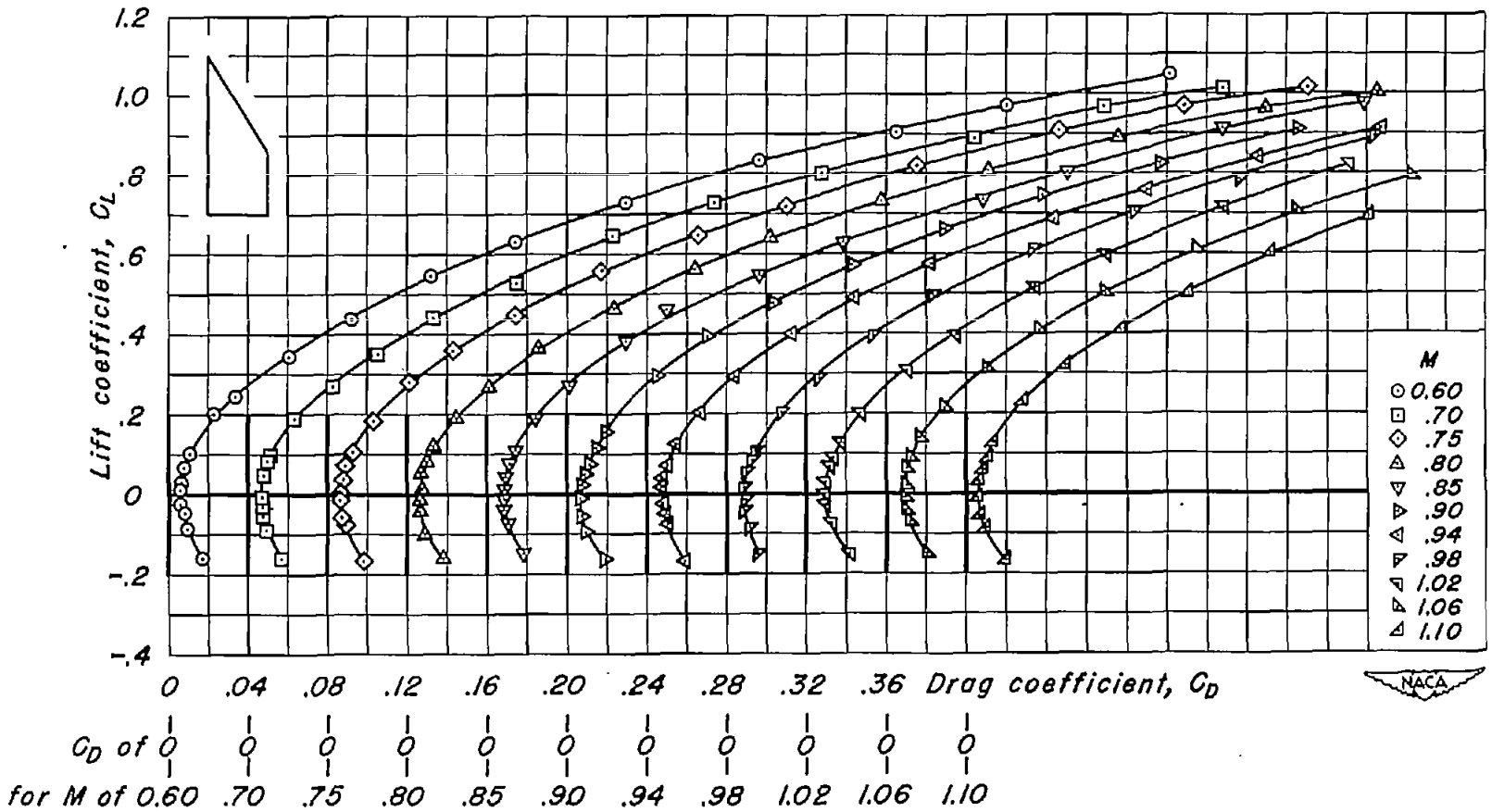

(e) NACA 63A002; λ, 0.4; A, 1.07.
Figure 9.- Continued.

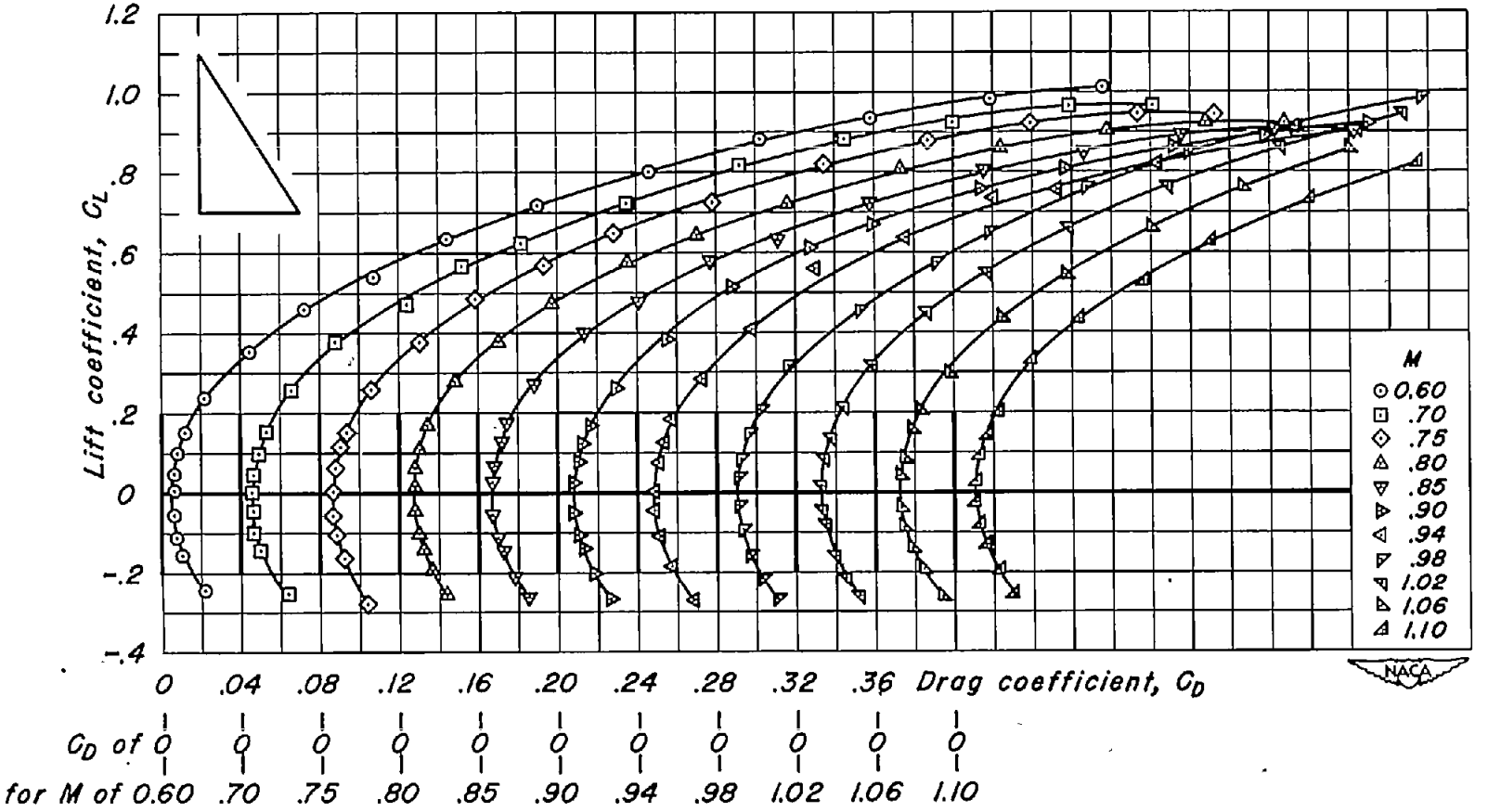

(f) NACA 63A004; λ, 0; A, 2.50.
Figure 9.- Continued.

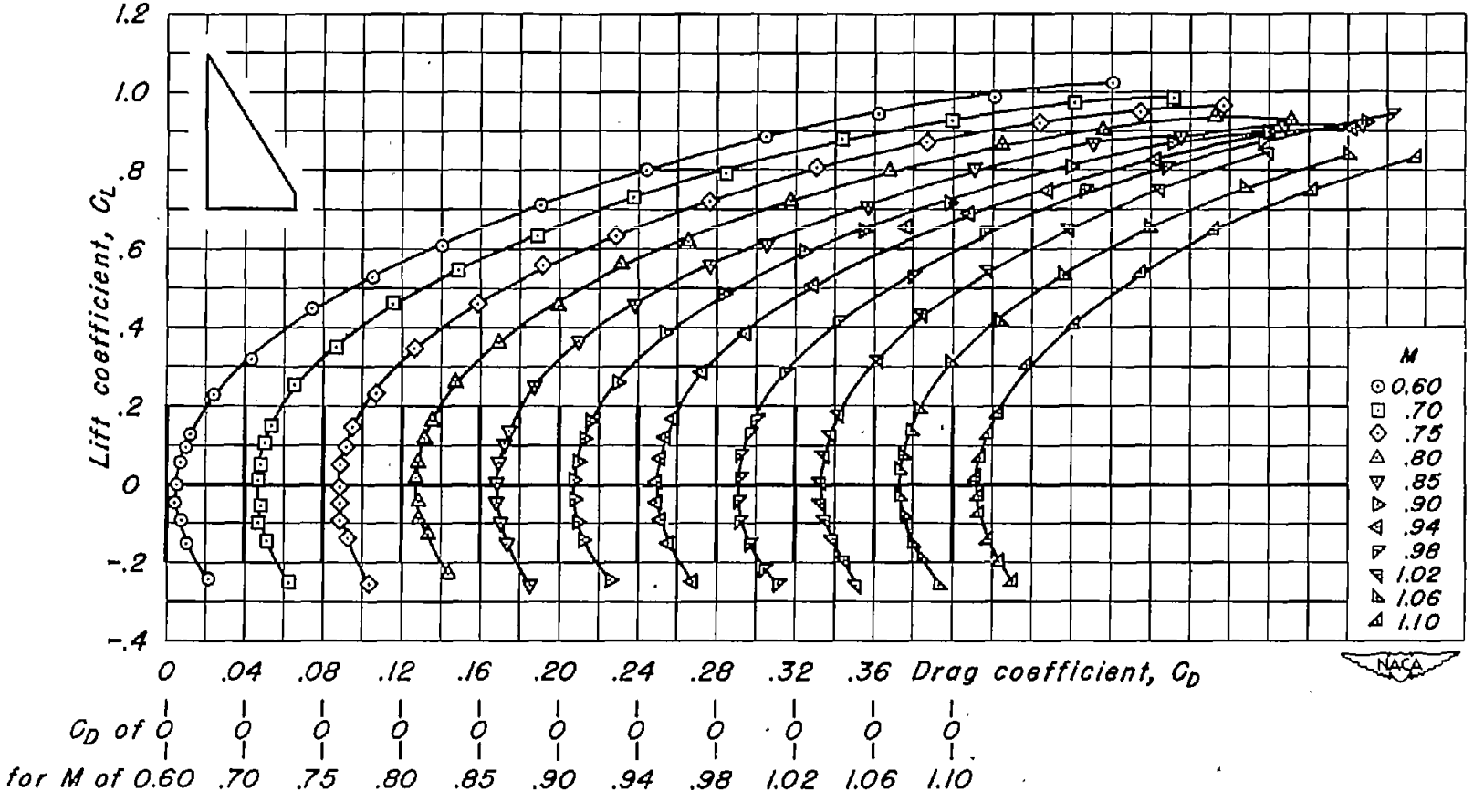

(g) NACA 63A004; λ, 0.1; A, 2.05.
Figure 9.- Continued.

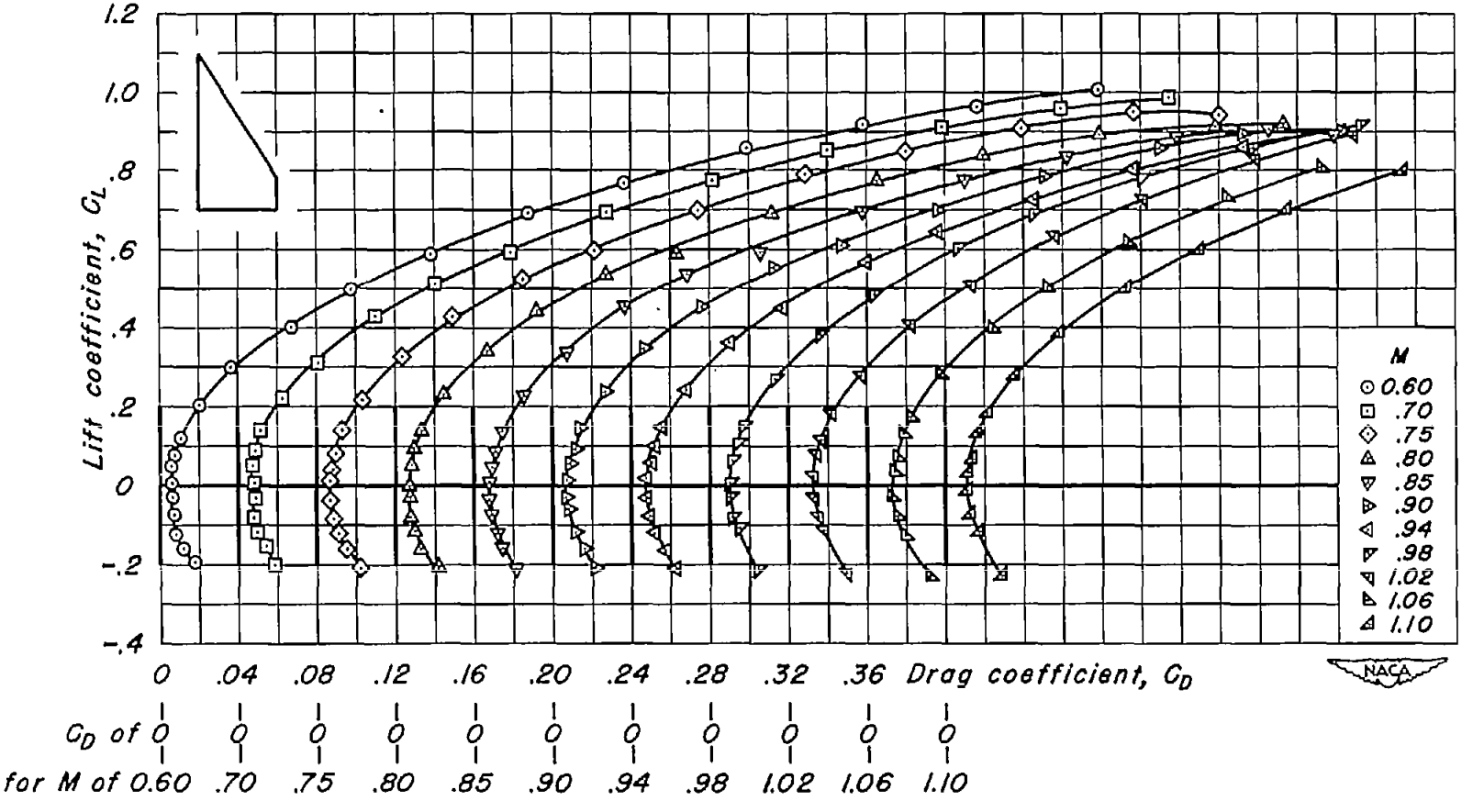

(h) NACA 63A004; λ, 0.2; A, 1.67.
Figure 9.- Continued.

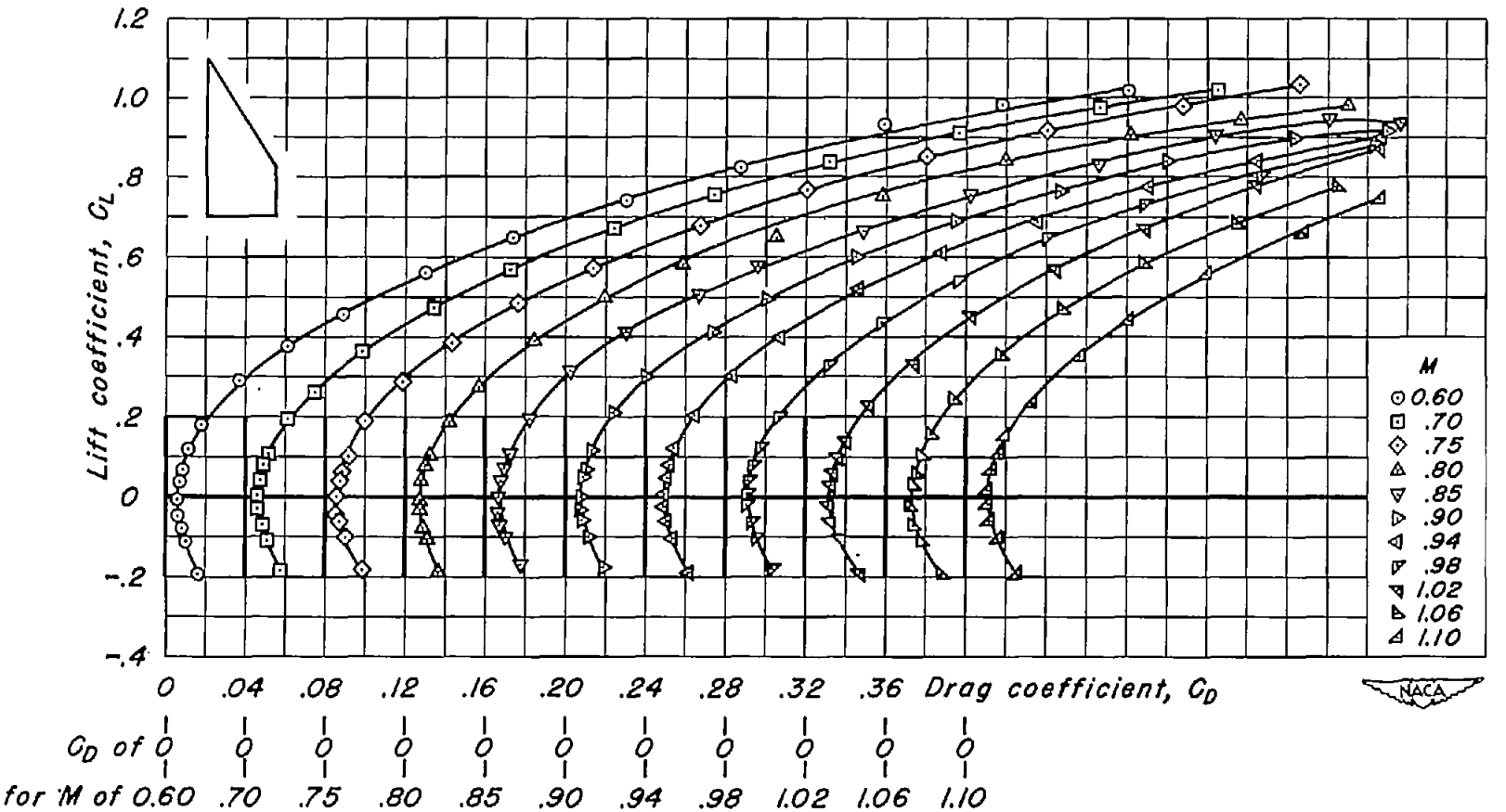

(i) NACA 63A004; λ, 0.3; A, 1.35.
Figure 9.- Continued.

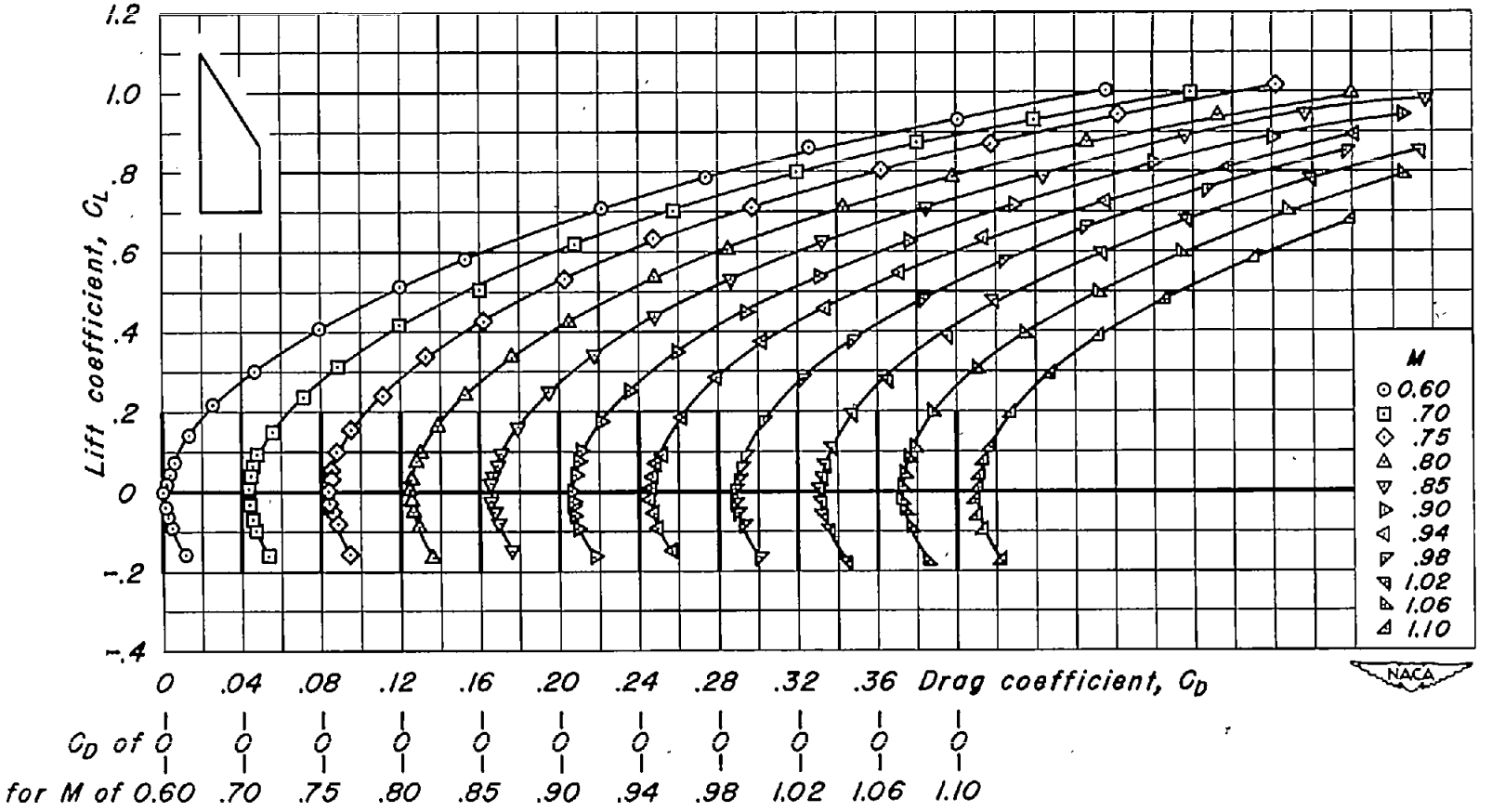

(j) NACA 63A004; λ, 0.4; A, 1.07.
Figure 9.- Continued.

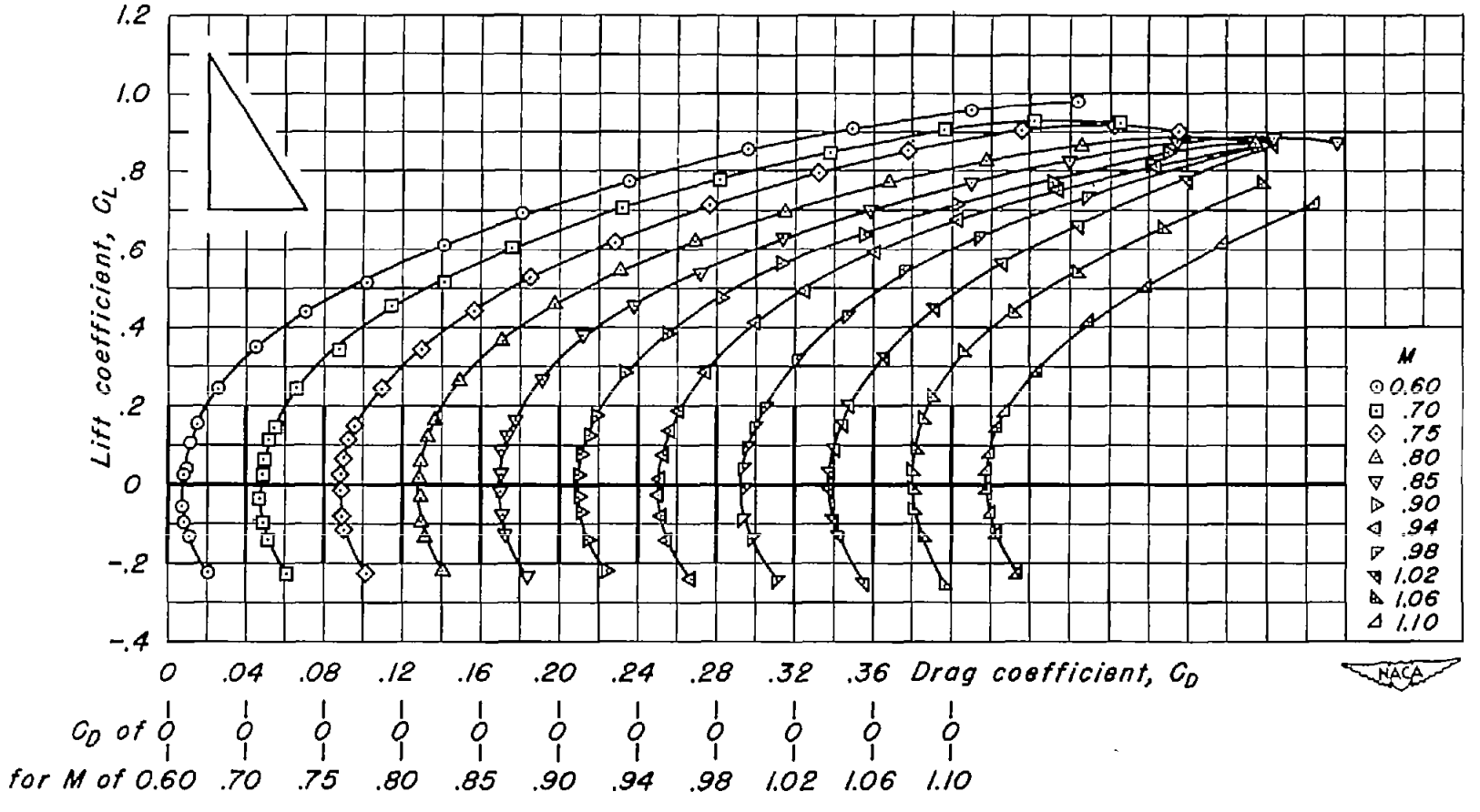

C_D of 0 0 0 0 0 0 0 0 0 0 0

for M of 0.60 .70 .75 .80 .85 .90 .94 .98 1.02 1.06 1.10

(k) NACA 63A006; λ, 0; A, 2.50.
Figure 9.- Continued.

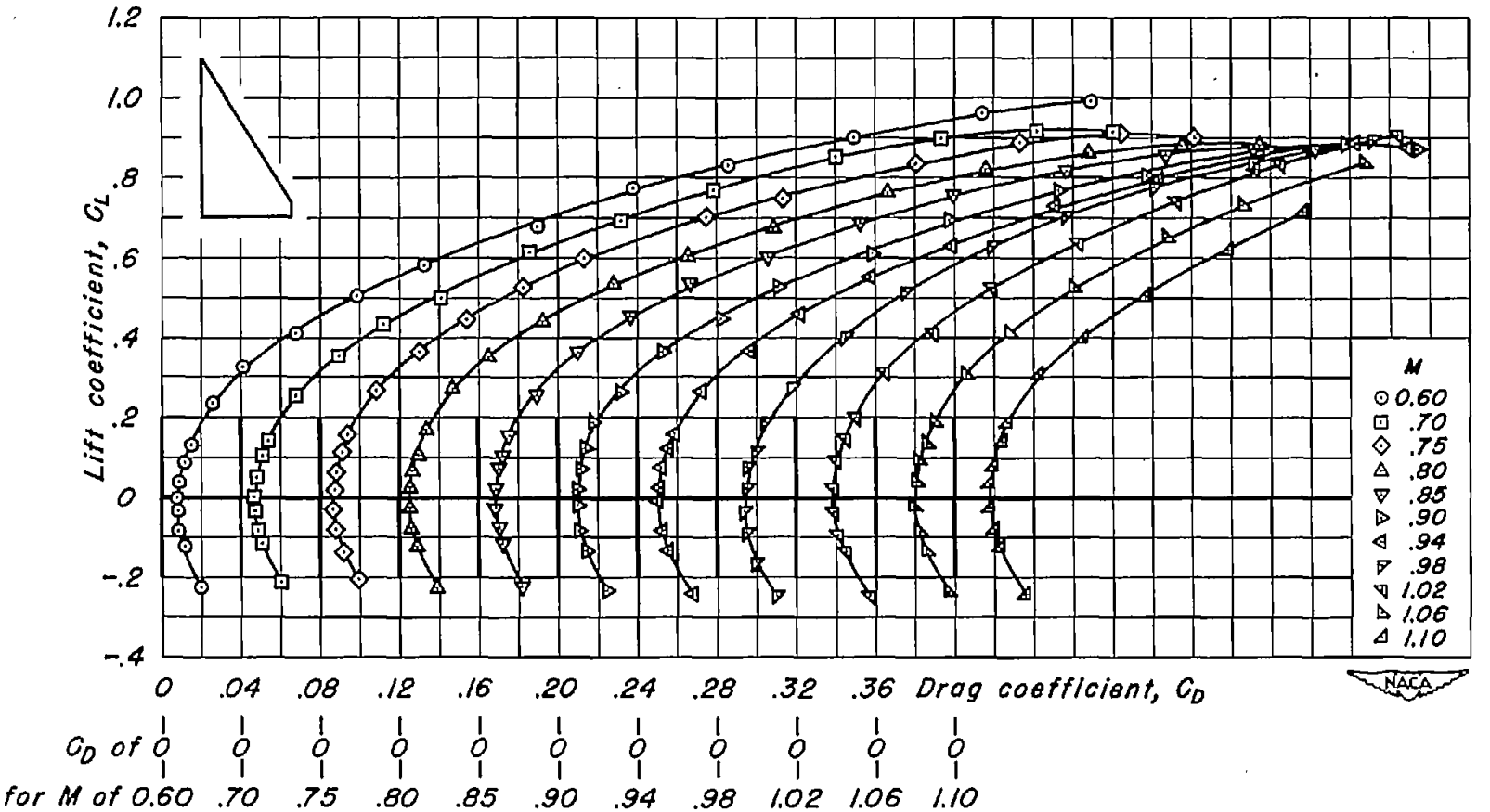

(l) NACA 63A006; λ, 0.1; A, 2.05.
Figure 9.- Continued.

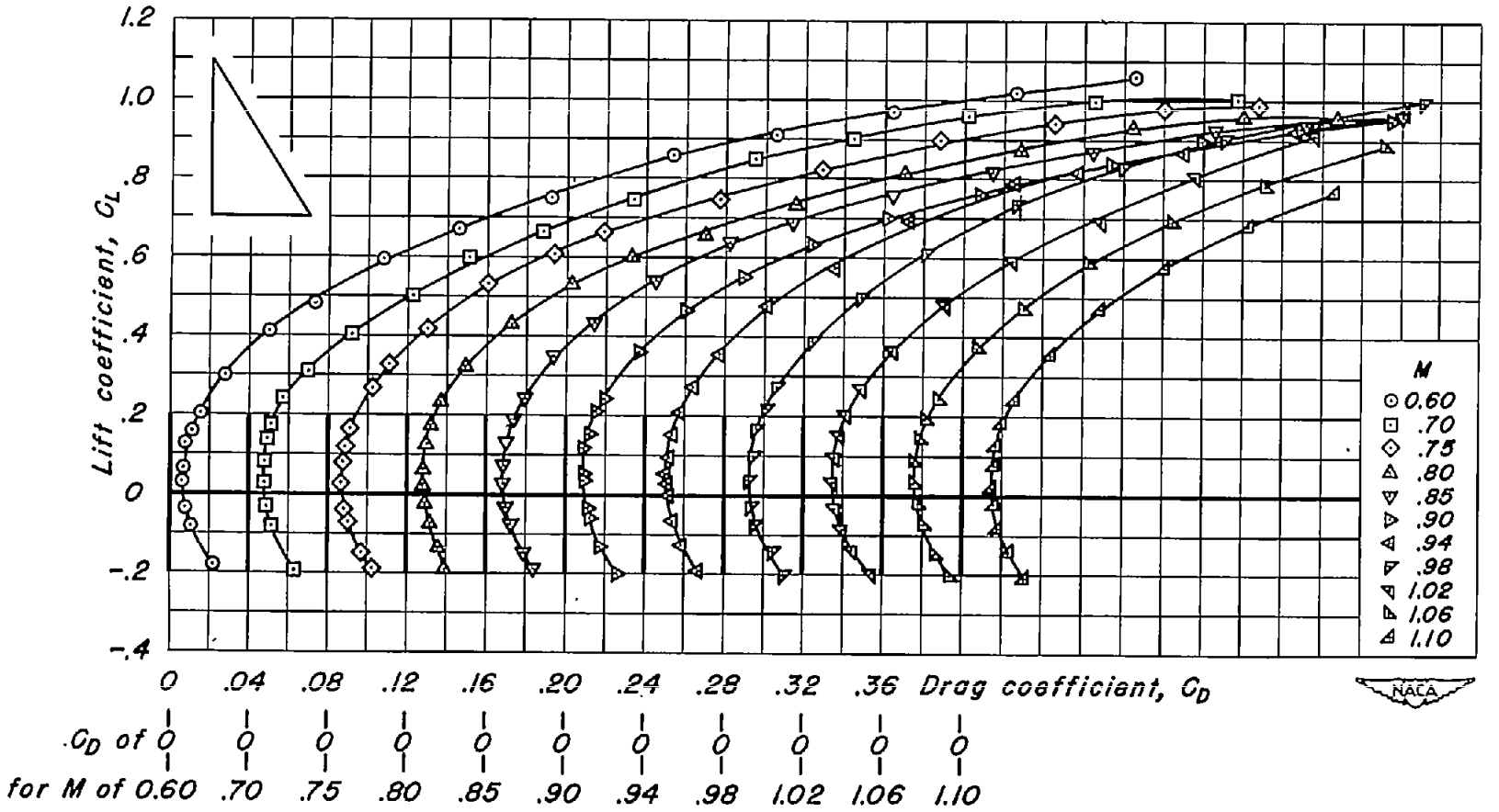

(m) NACA 63A(1.5)04; λ, 0; A, 2.50.
Figure 9.- Continued.

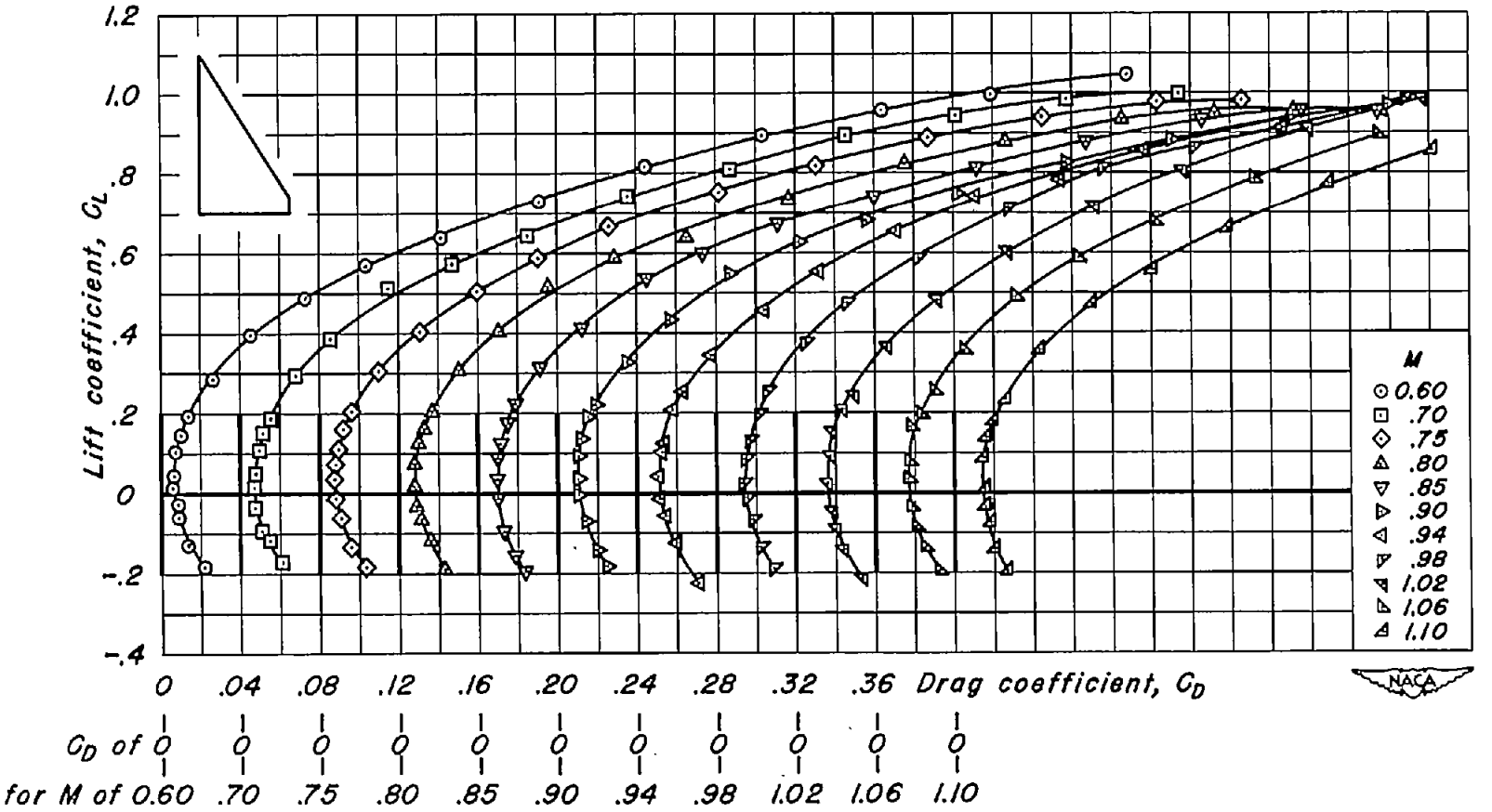

(n) NACA 63A(1.5)04; λ, 0.1; A, 2.05.
Figure 9.- Continued.

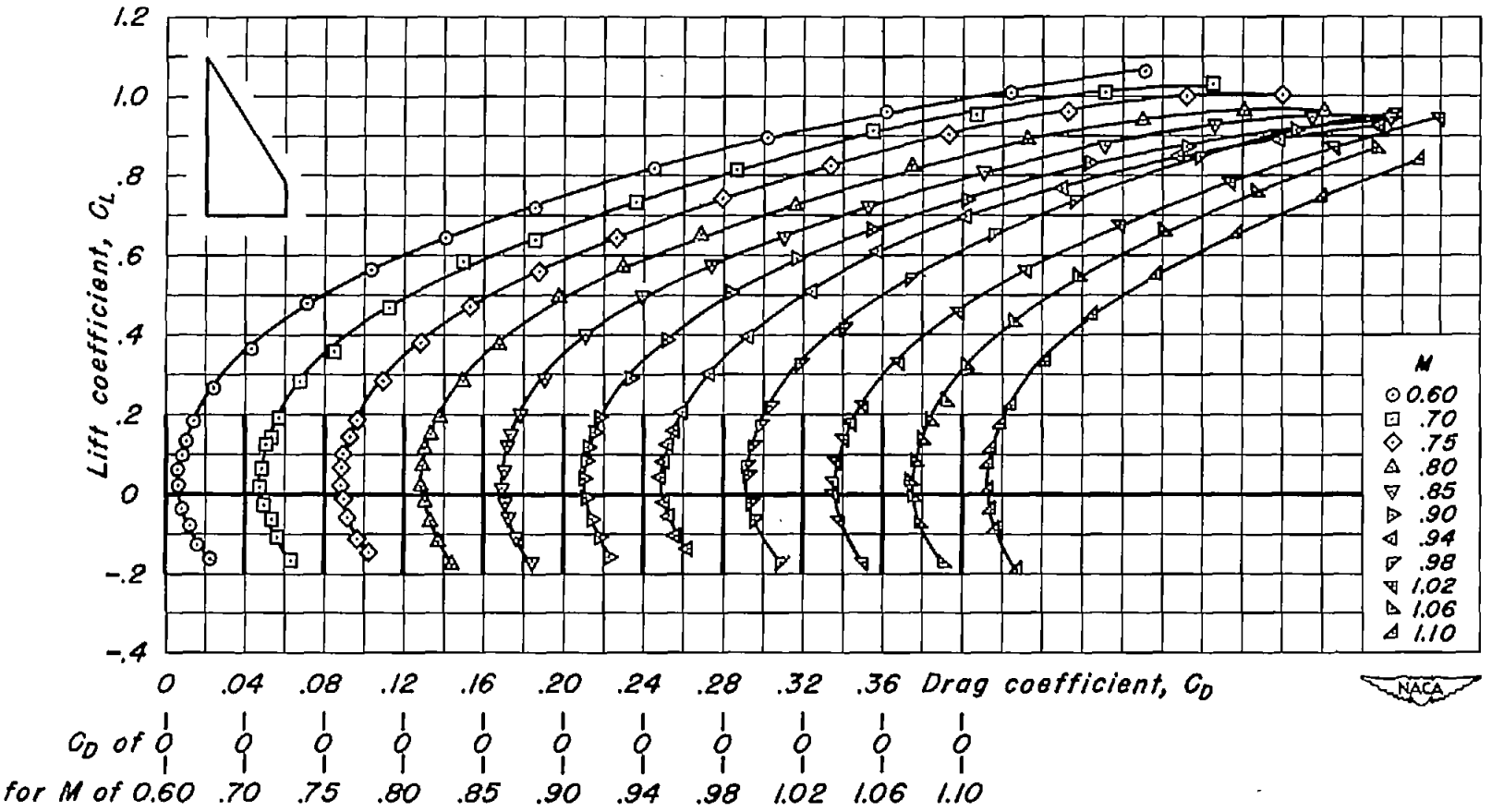

(o) NACA 63A(1.5)04; λ, 0.2; A, 1.67.
Figure 9.- Continued.

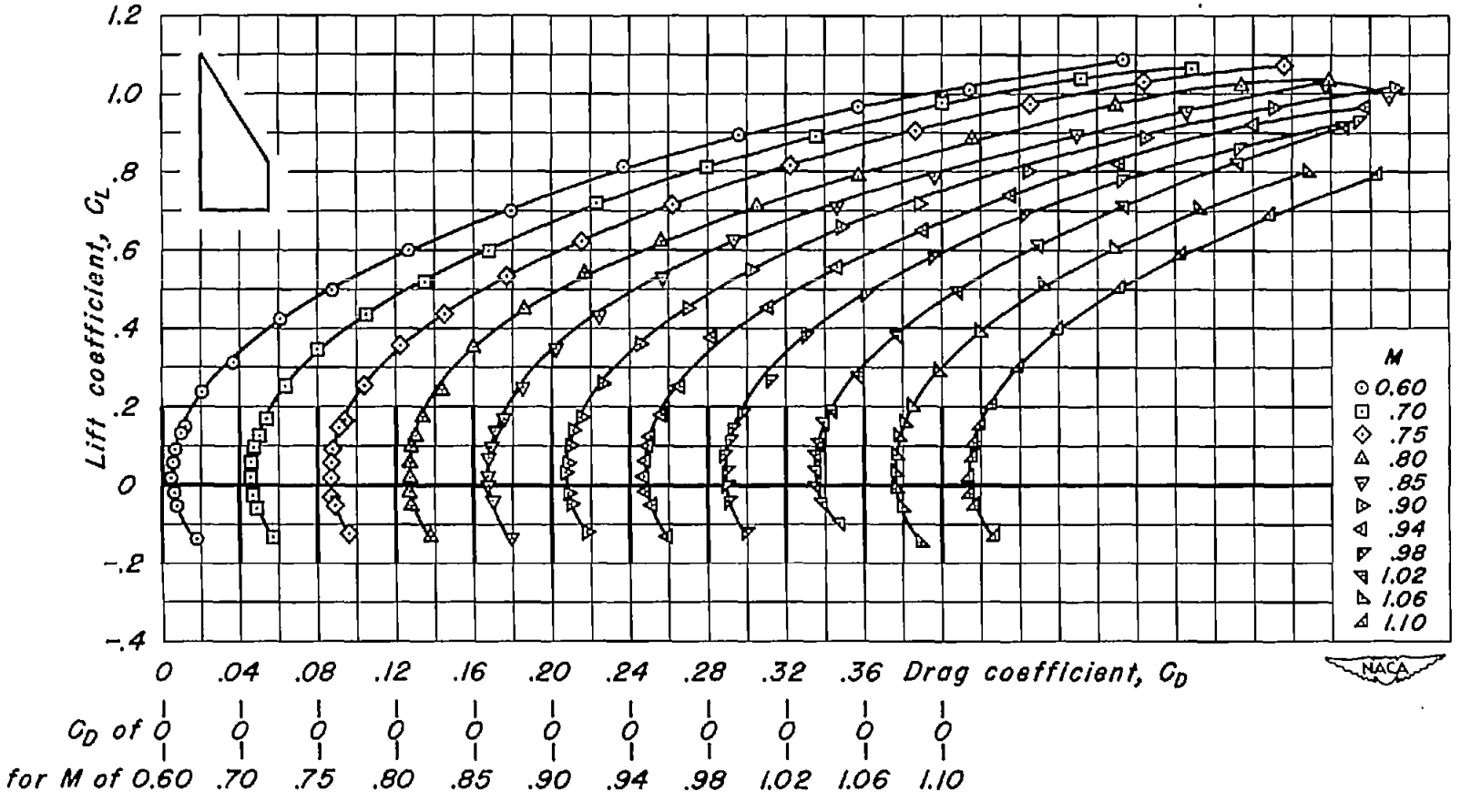

C_D of	0	0	0	0	0	0	0	0	0	0	0
for M of	0.60	.70	.75	.80	.85	.90	.94	.98	1.02	1.06	1.10

(p) NACA 63A(1.5)04; λ, 0.3; A, 1.35.
Figure 9.- Concluded.

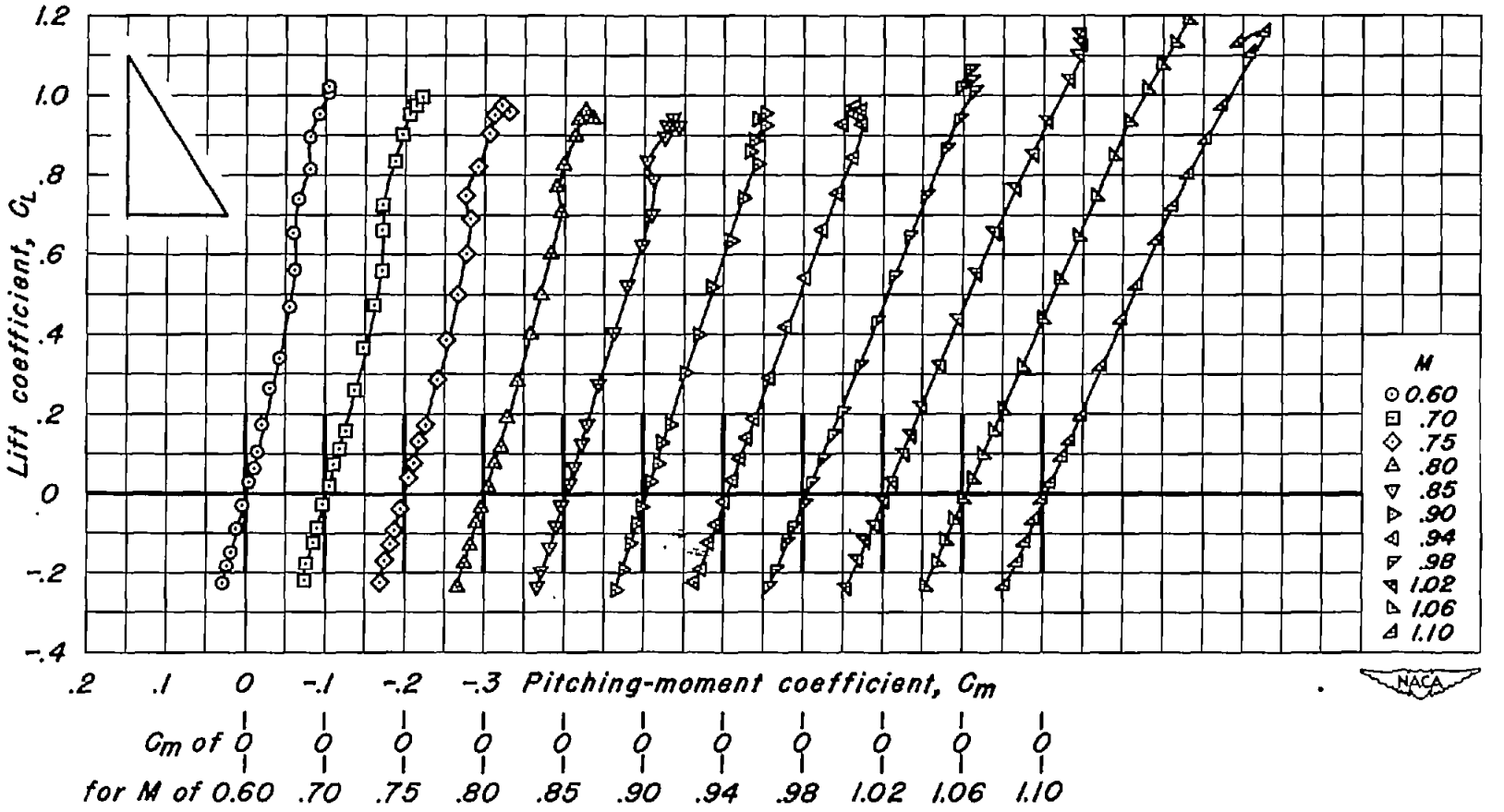

(a) NACA 63A002; λ, 0; A, 2.50.

Figure 10.- Variation of pitching-moment coefficient with lift coefficient for the wings of basic aspect ratio 2.50.

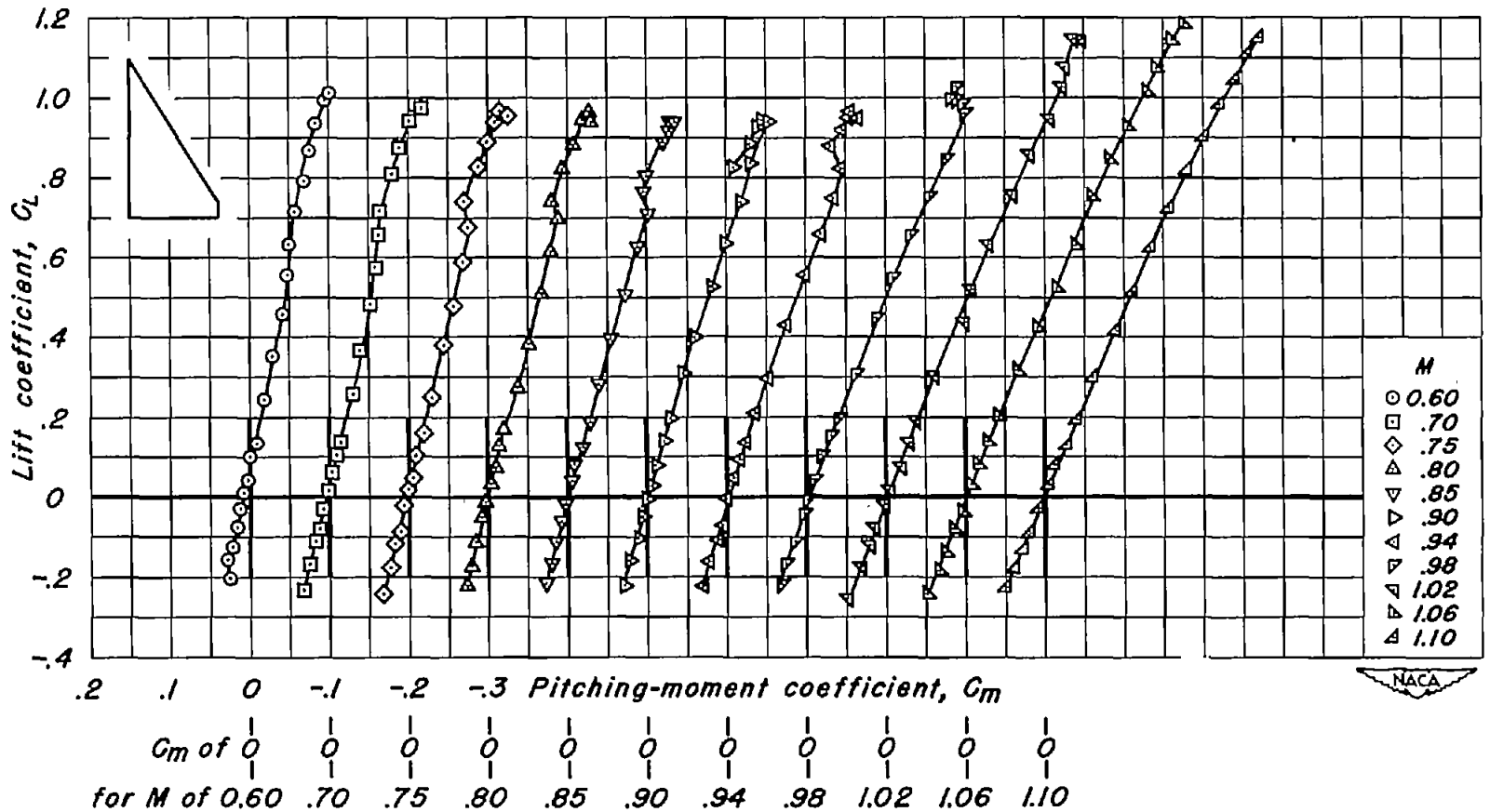

(b) NACA 63A002; λ, 0.1; A, 2.05.
Figure 10.- Continued.

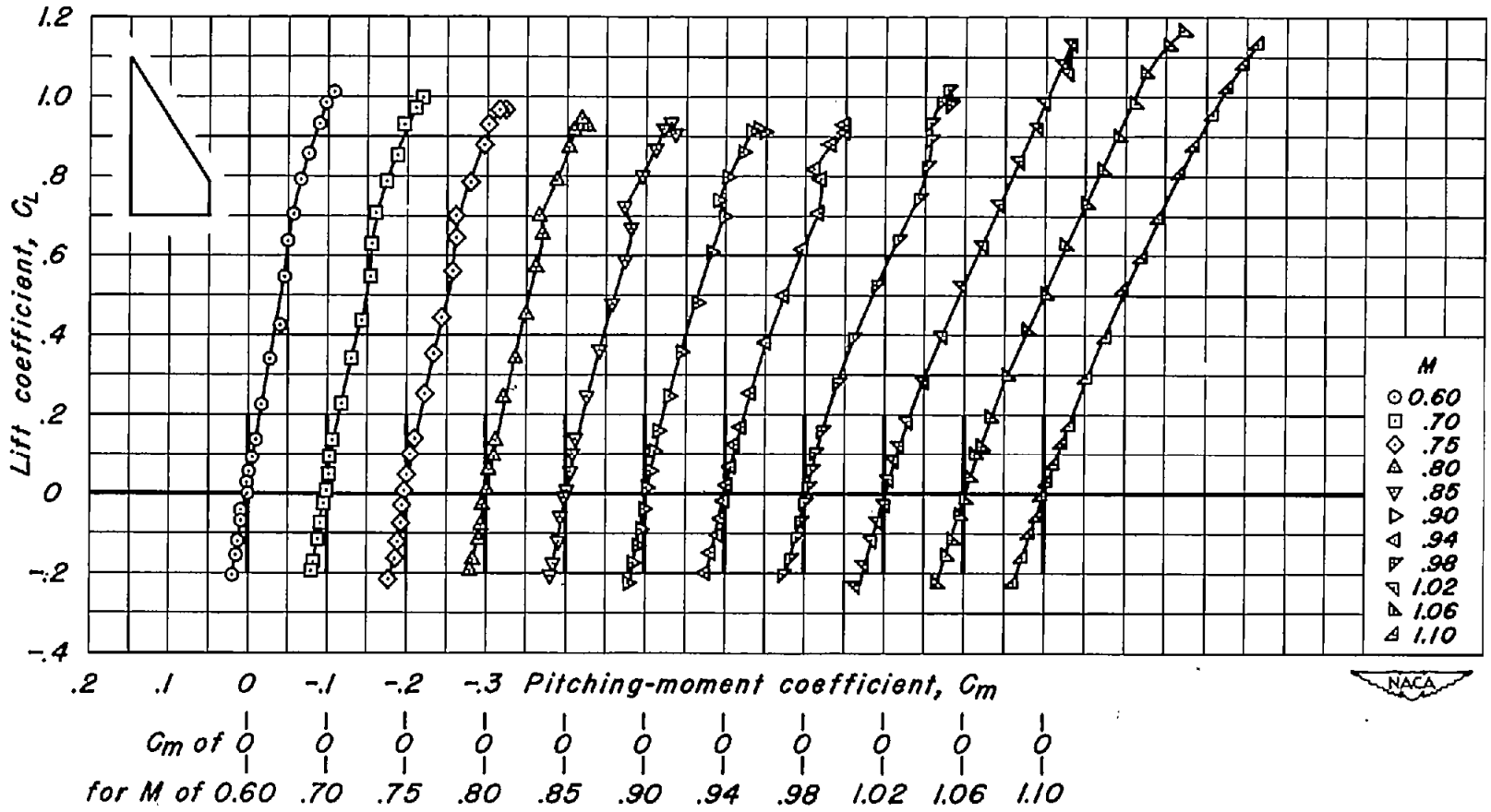

(c) NACA 63A002; λ, 0.2; A, 1.67.
Figure 10.- Continued.

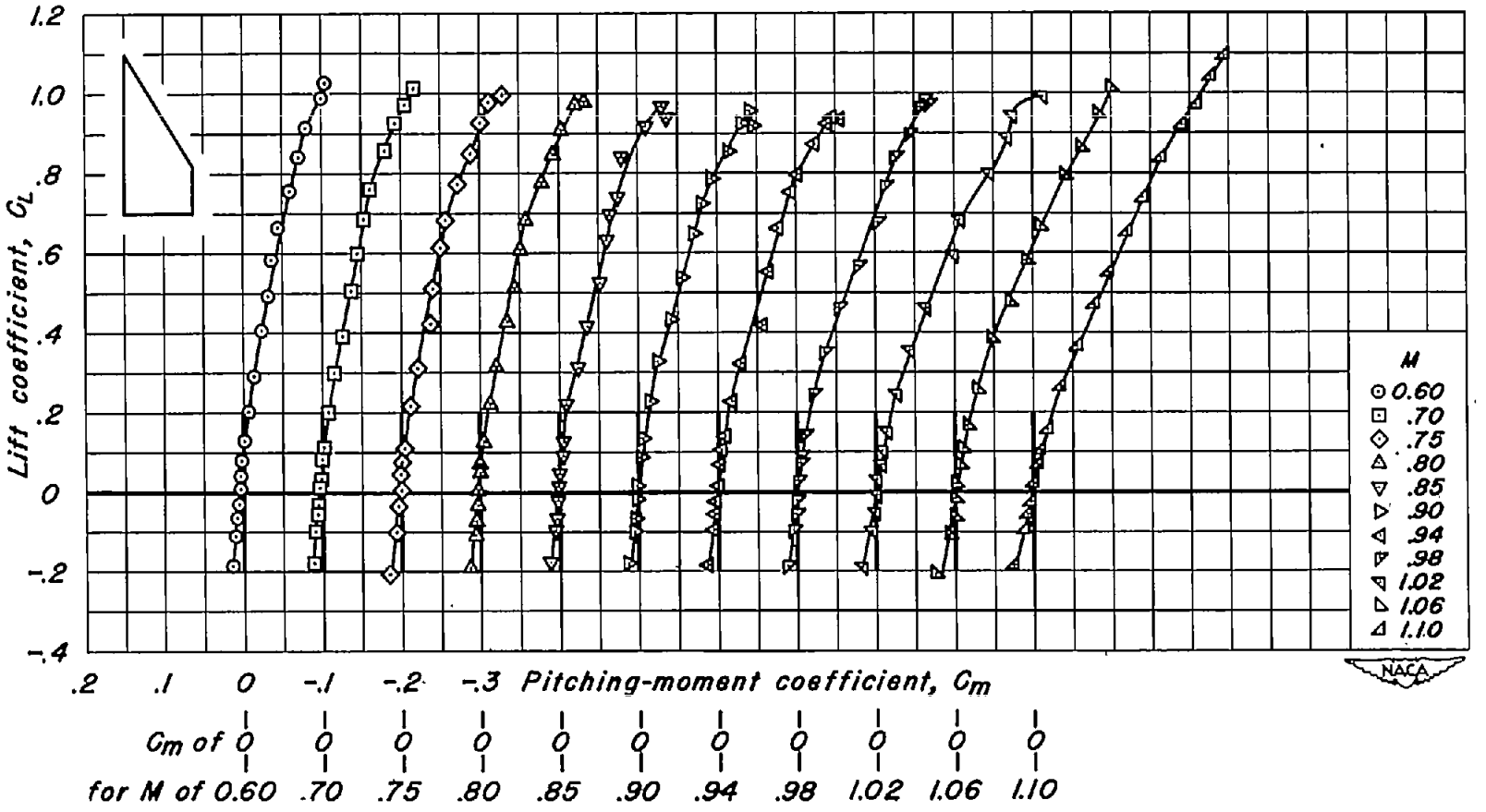

C_m of	0	0	0	0	0	0	0	0	0	0	0
for M of	0.60	.70	.75	.80	.85	.90	.94	.98	1.02	1.06	1.10

(d) NACA 63A002; λ, 0.3; A, 1.35.
Figure 10.- Continued.

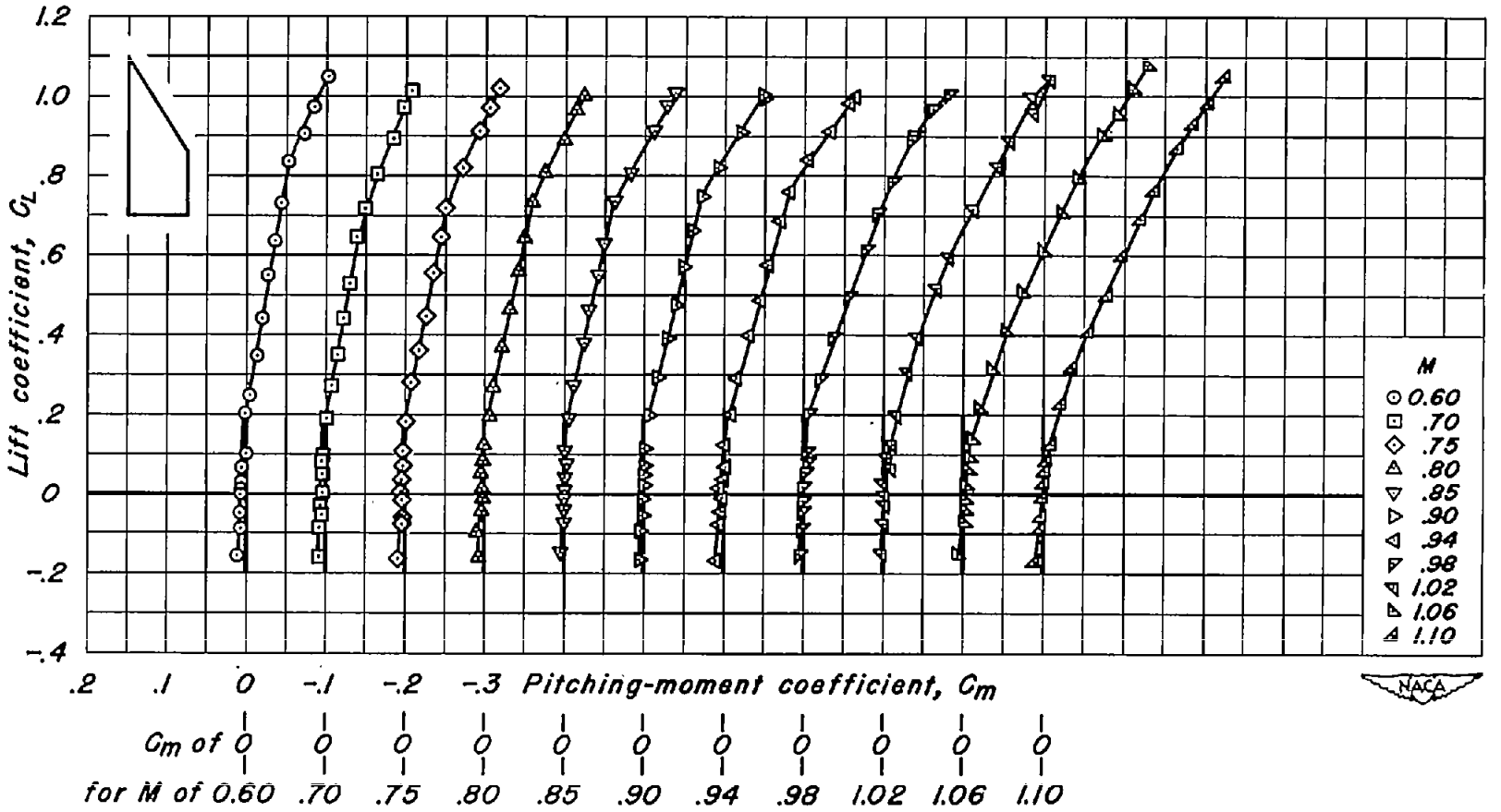

(e) NACA 63A002; λ, 0.4; A, 1.07

Figure 10.- Continued

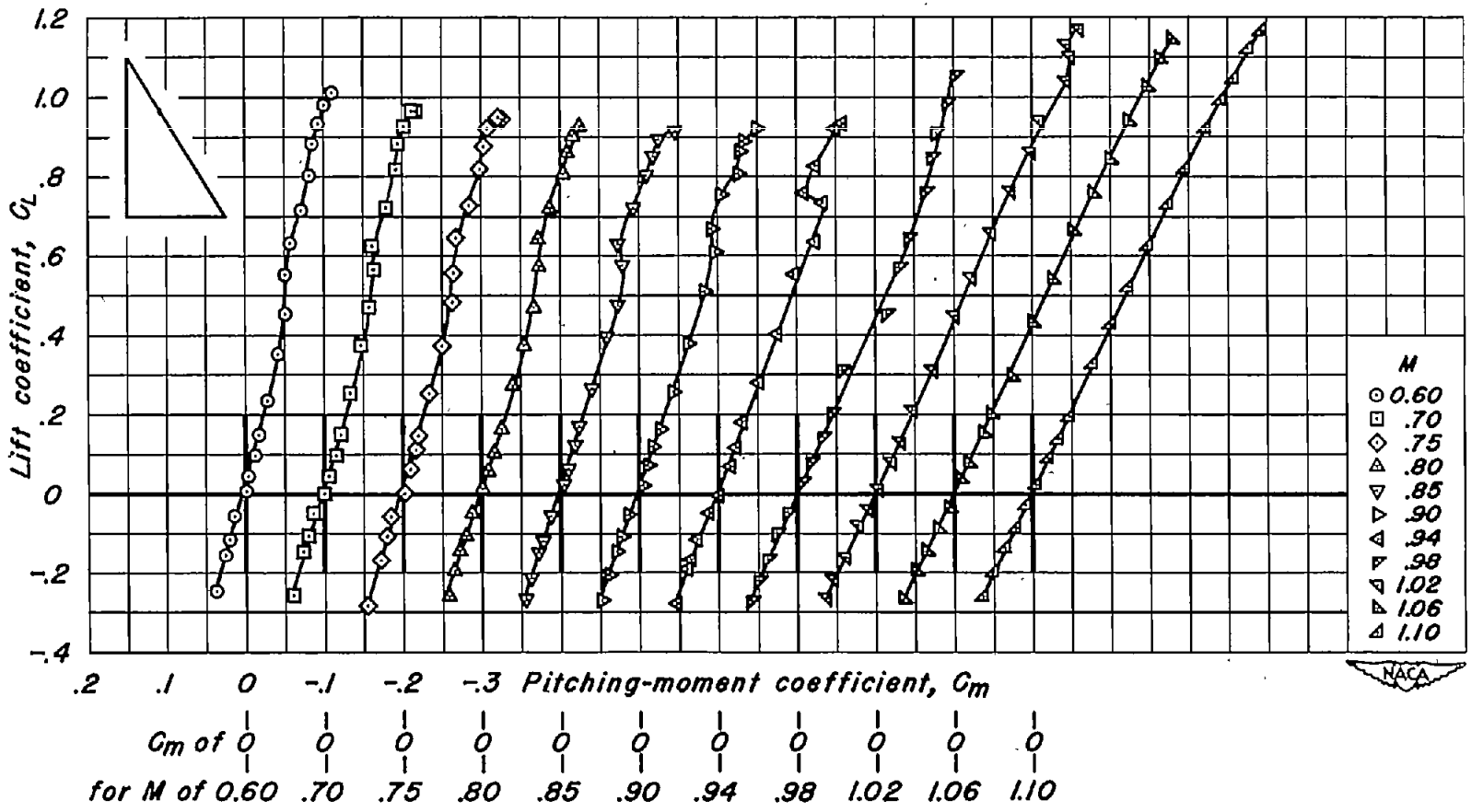

(f) NACA 63A004; λ, 0; A, 2.50.
Figure 10.- Continued.

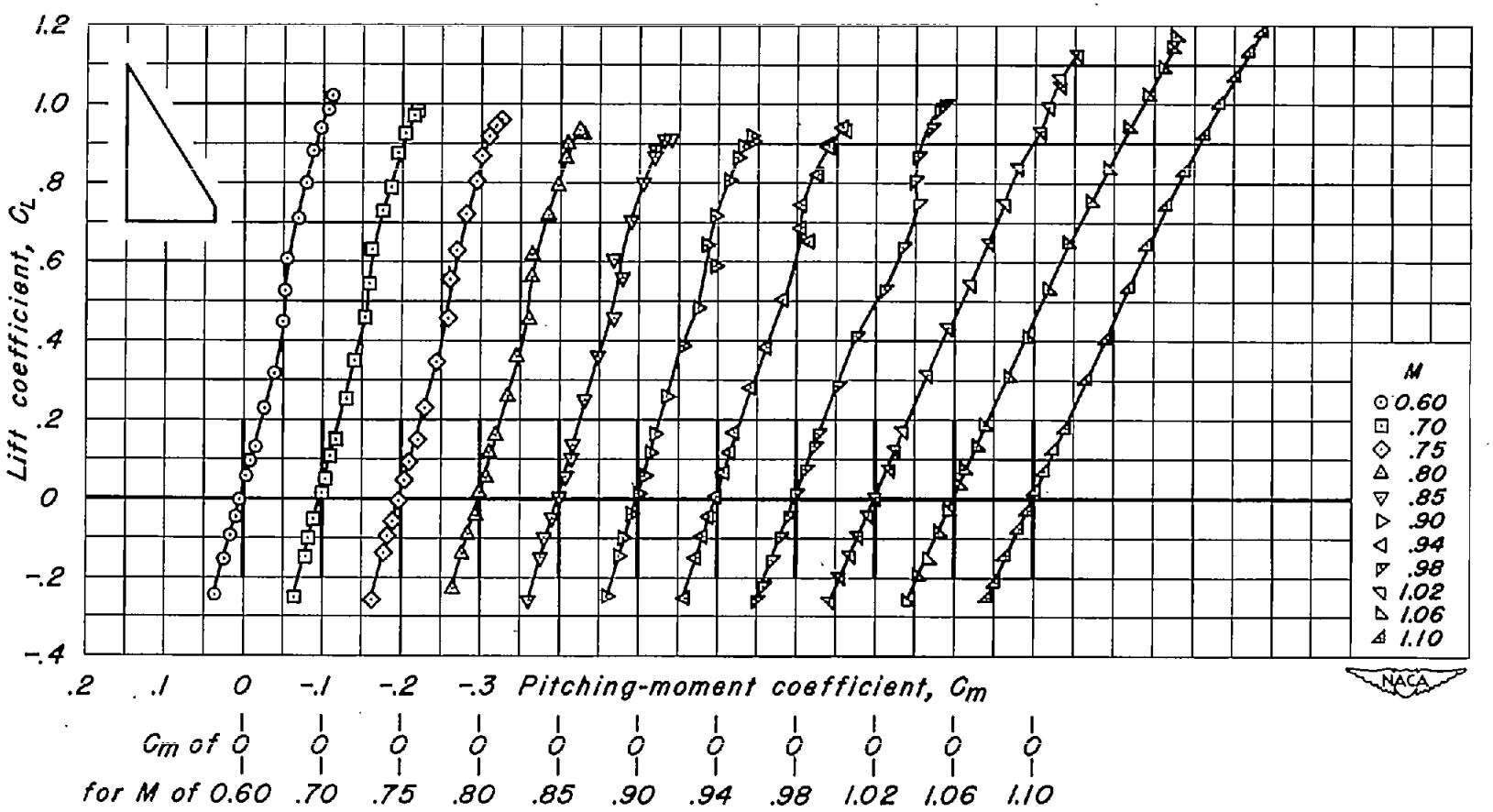

(g) NACA 63A004; λ, 0.1; A, 2.05.
Figure 10.- Continued.

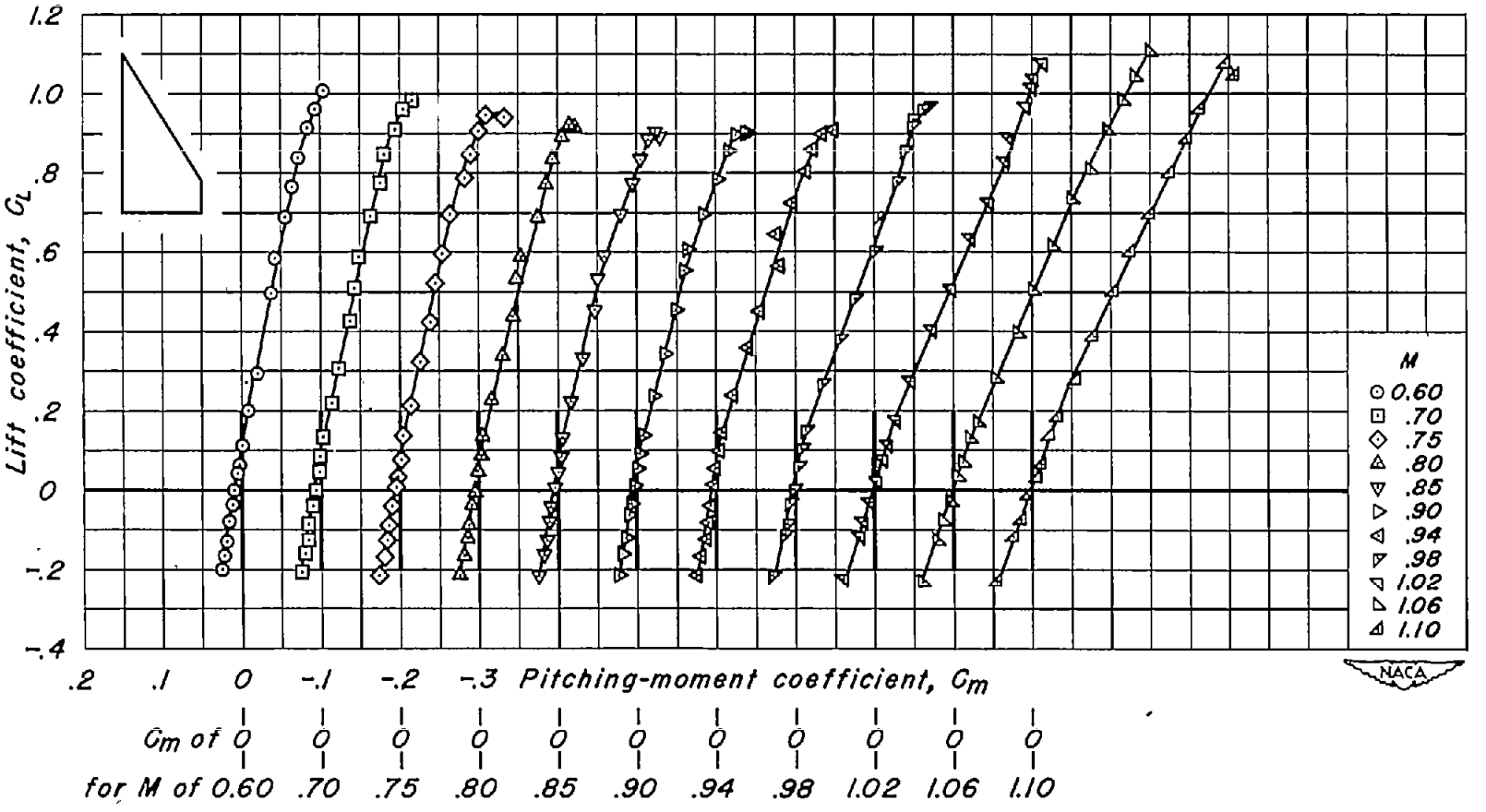

(h) NACA 63A004; λ, 0.2; A, 1.67.
Figure 10.- Continued.

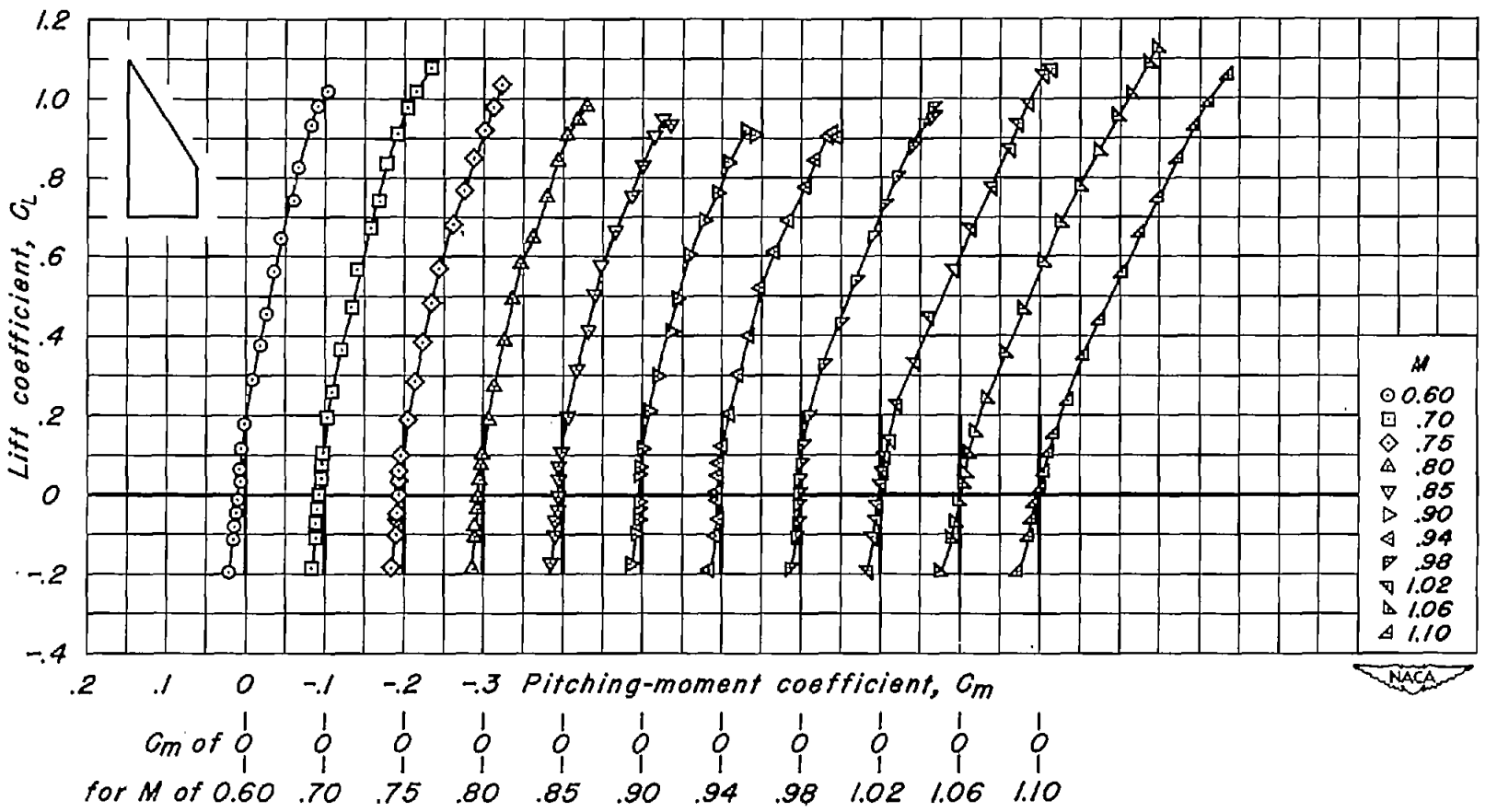

(i) NACA 63A004; λ, 0.3; A, 1.35.
Figure 10.- Continued.

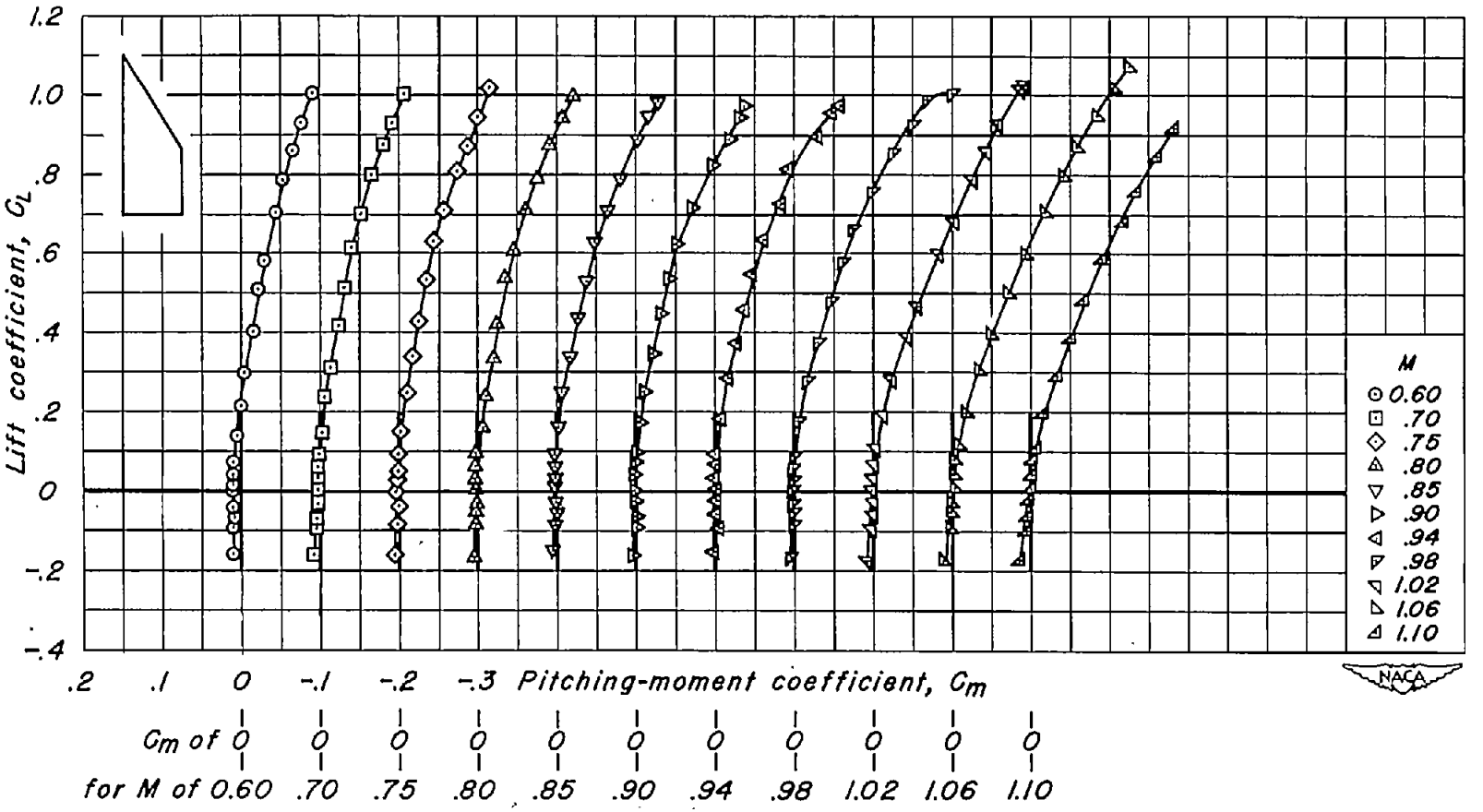

(j) NACA 63A004; λ, 0.4; A, 1.07.
Figure 10.- Continued.

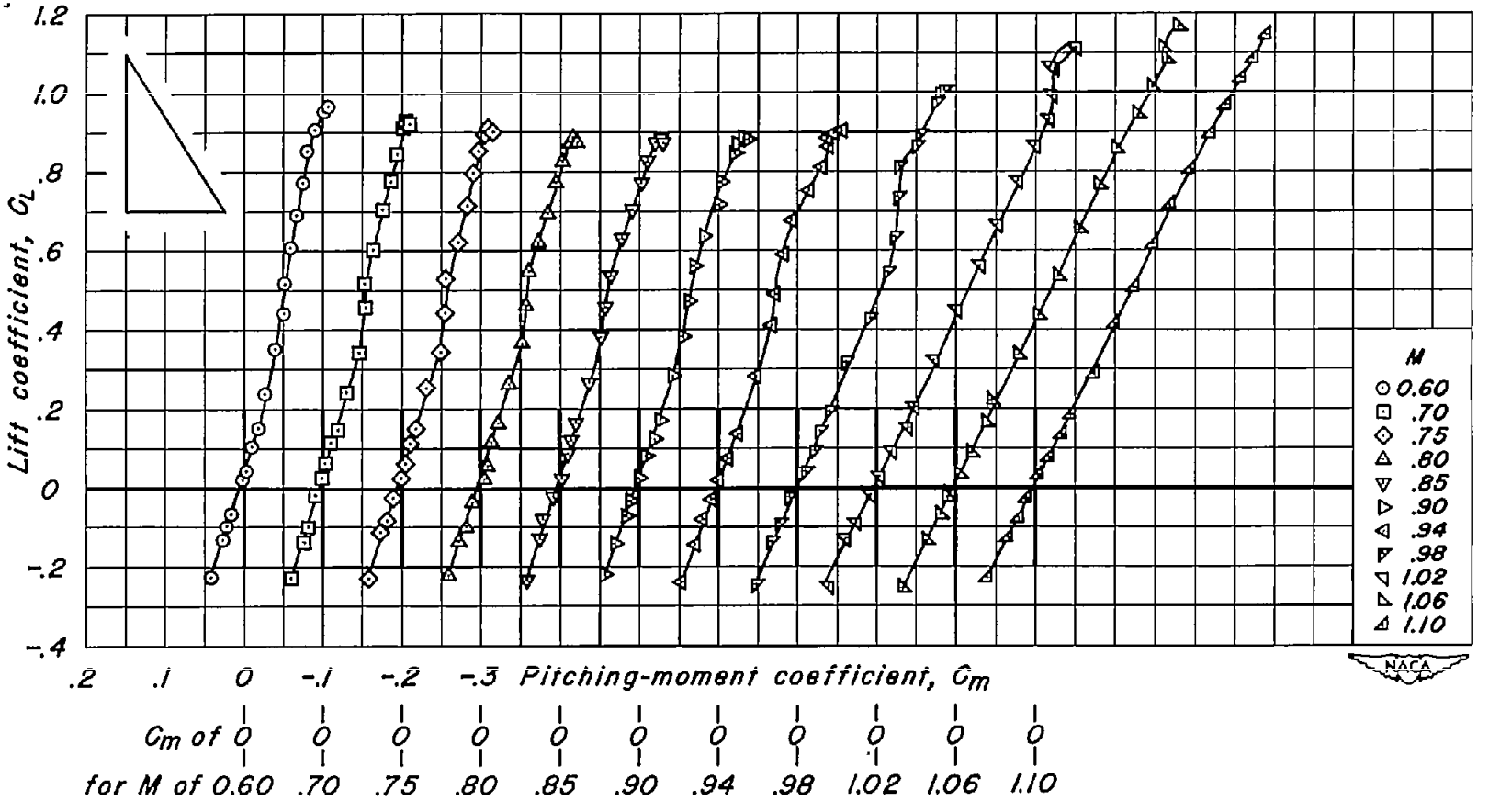

(k) NACA 63A006; λ, 0; A, 2.50.
Figure 10.- Continued.

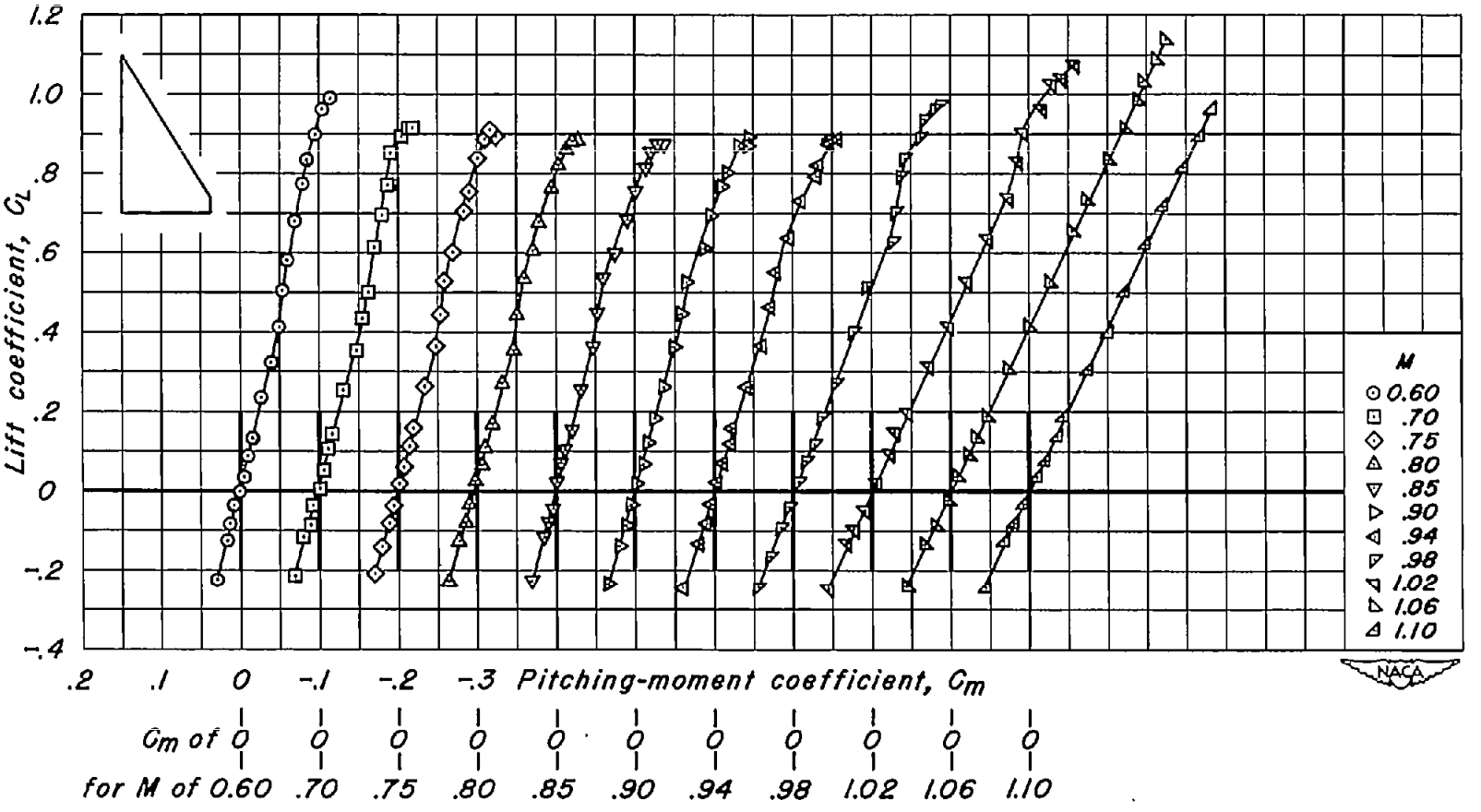

(l) NACA 63A006; λ, 0.1; A, 2.05.
Figure 10.- Continued.

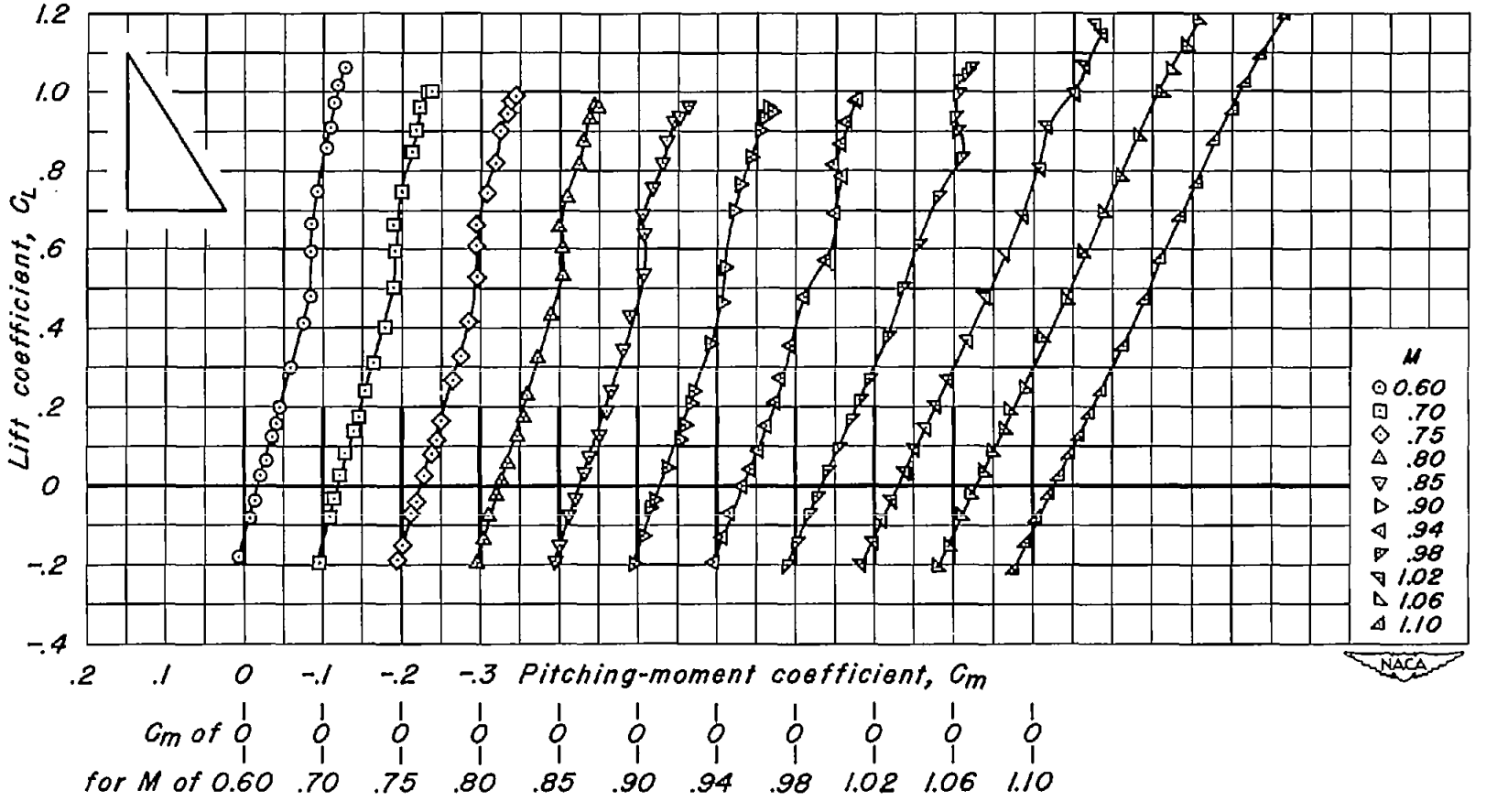

(m) NACA 63A(1.5)04; λ, 0; A, 2.50.
Figure 10.- Continued.

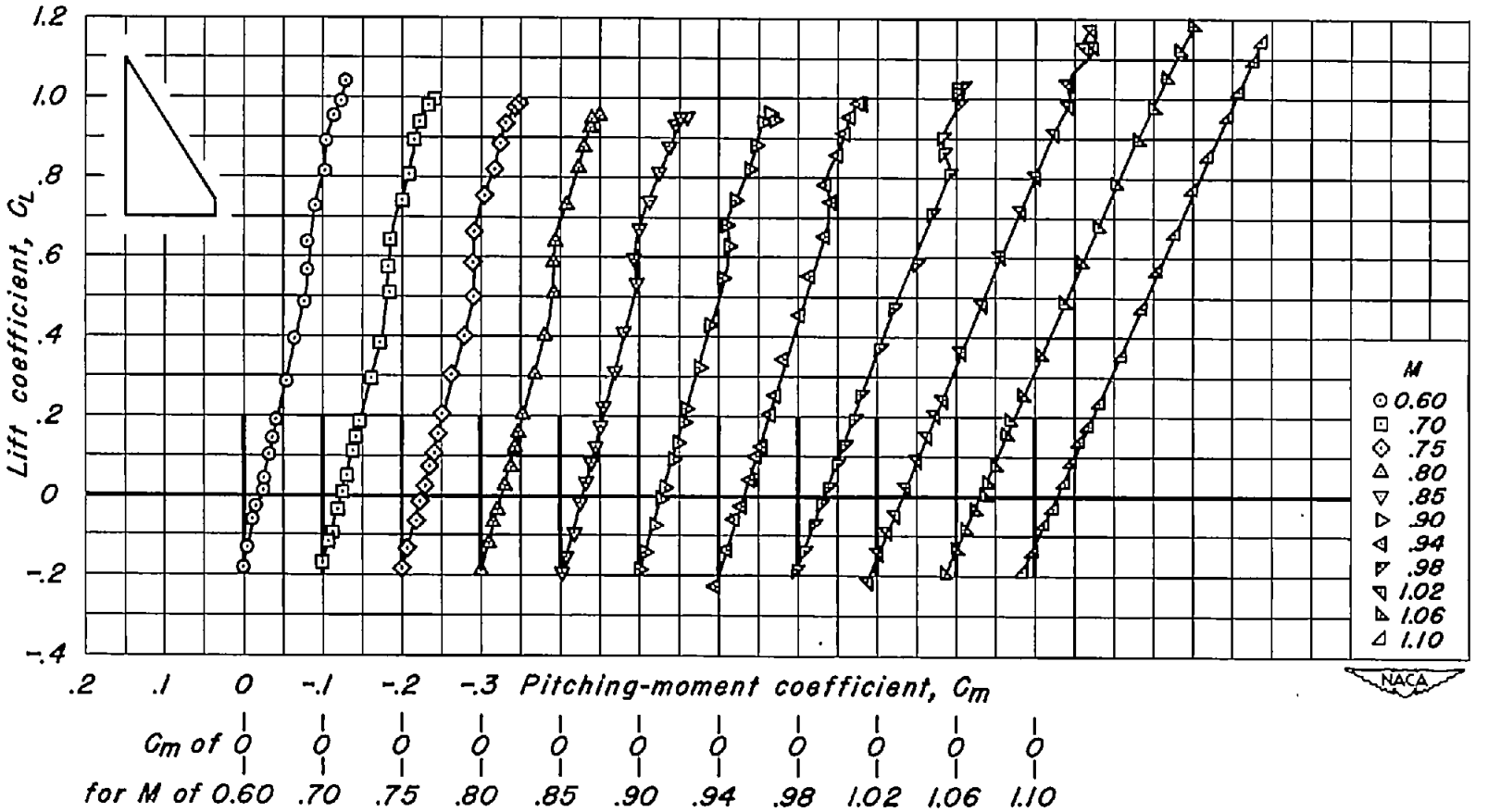

(n) NACA 63A(1.5)04; λ, 0.1; A, 2.05.
Figure 10.- Continued.

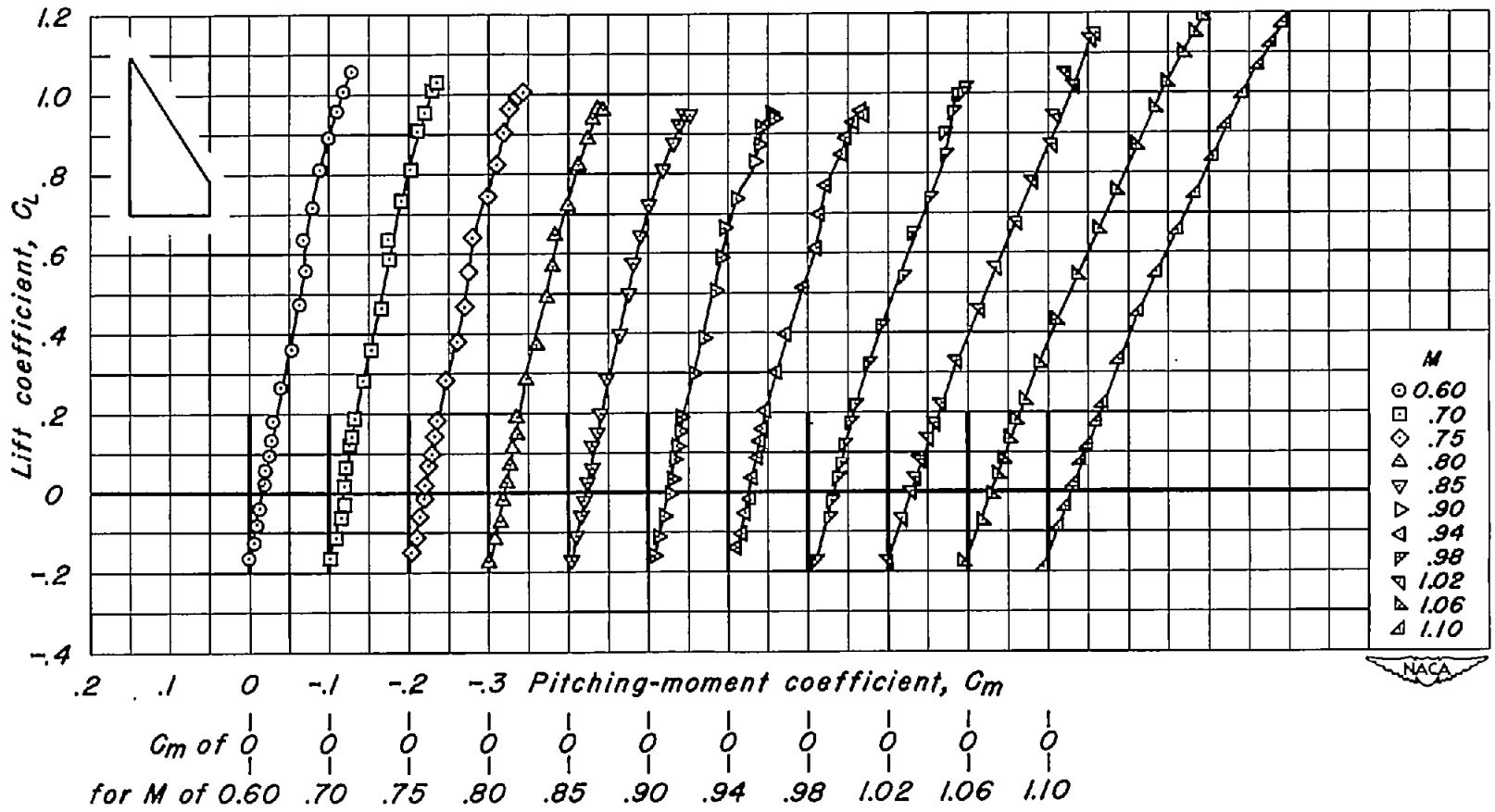

(o) NACA 63A(1.5)04, λ, 0.2; A, 1.67.
Figure 10.- Continued.

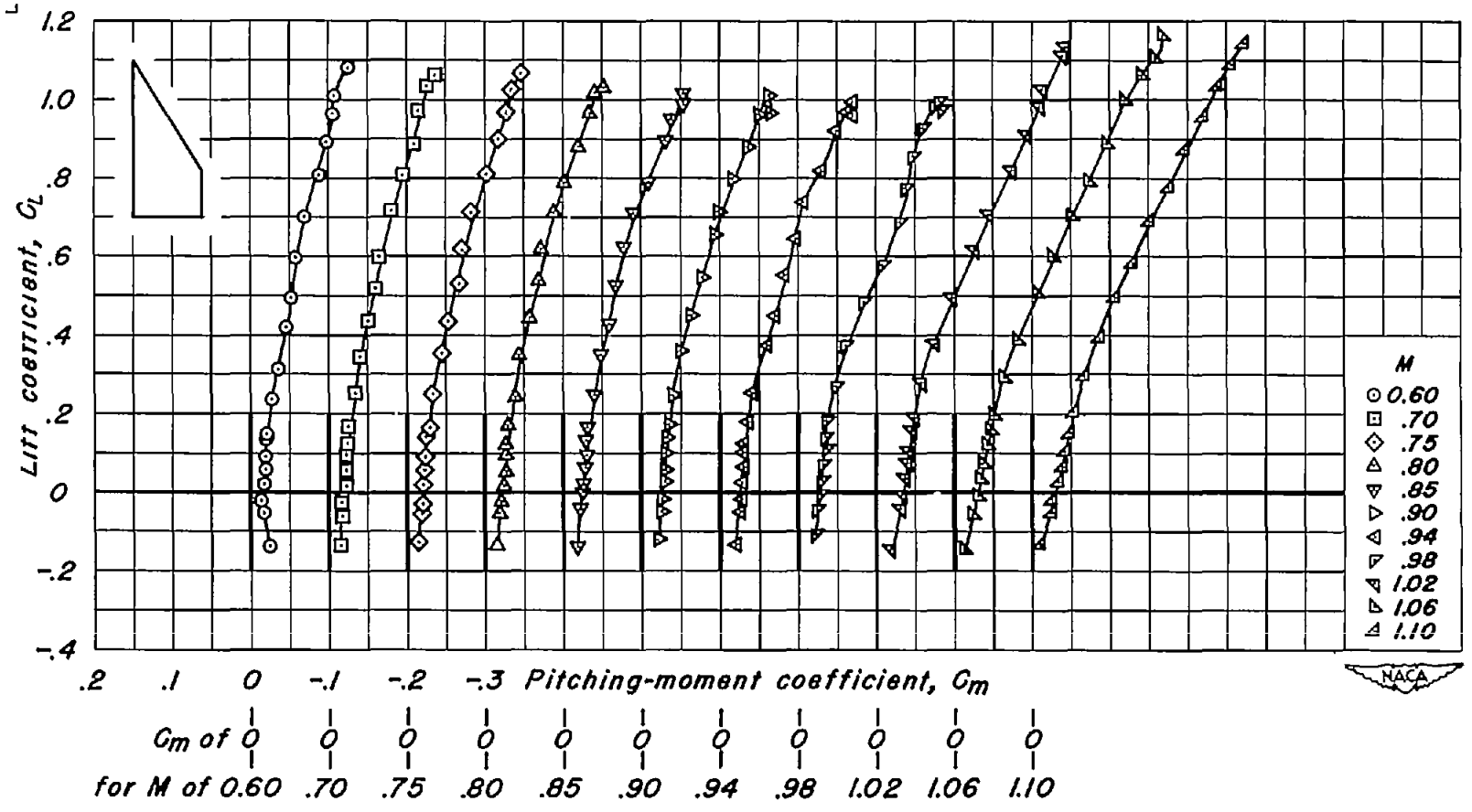

(p) NACA 63A(1.5)04; λ, 0.3; A, 1.35.
Figure 10.- Concluded.

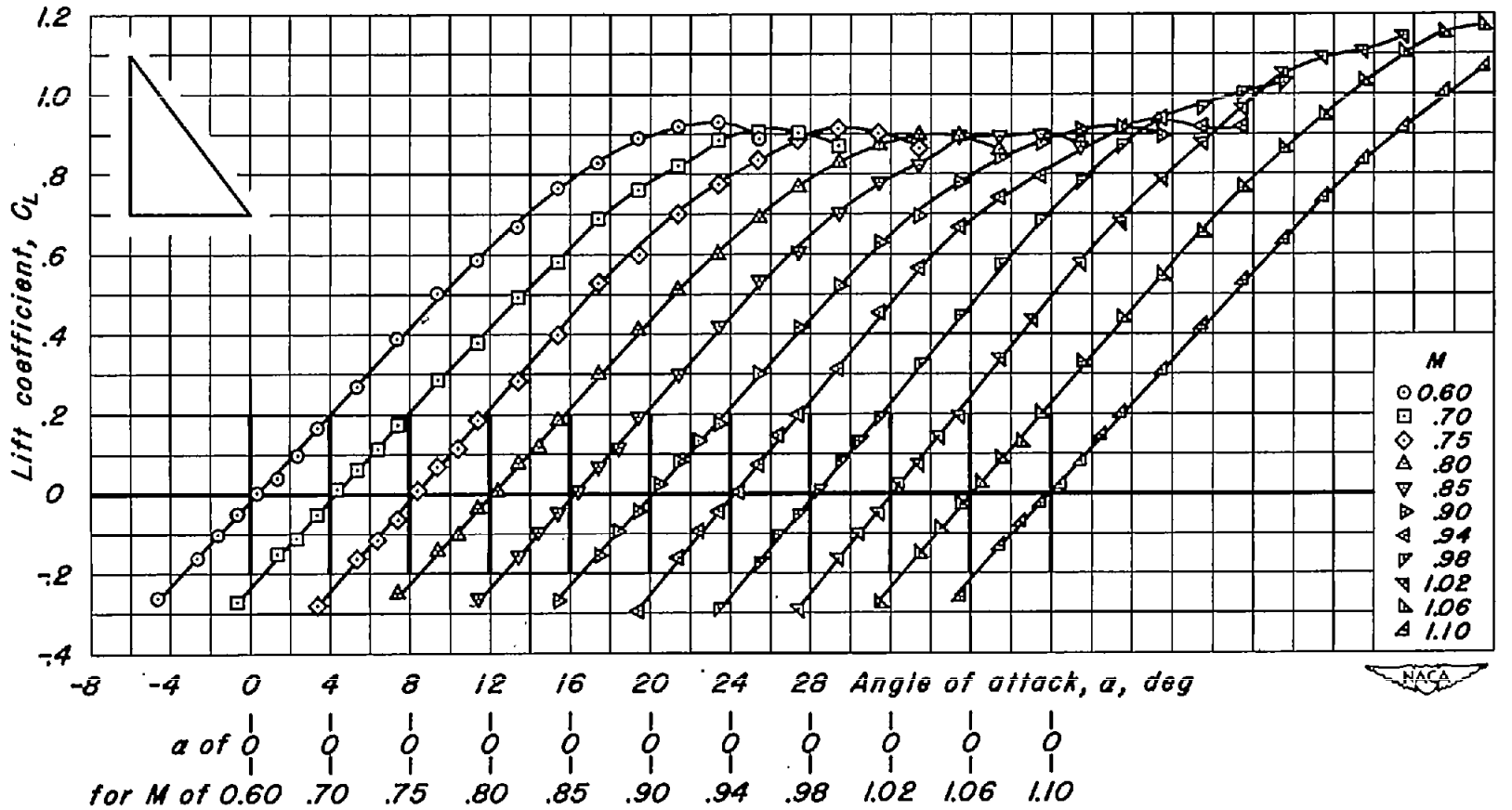

(a) NACA 63A002; λ, 0; A, 3.00.

Figure 11.- Variation of lift coefficient with angle of attack for the wings of basic aspect ratio 3.

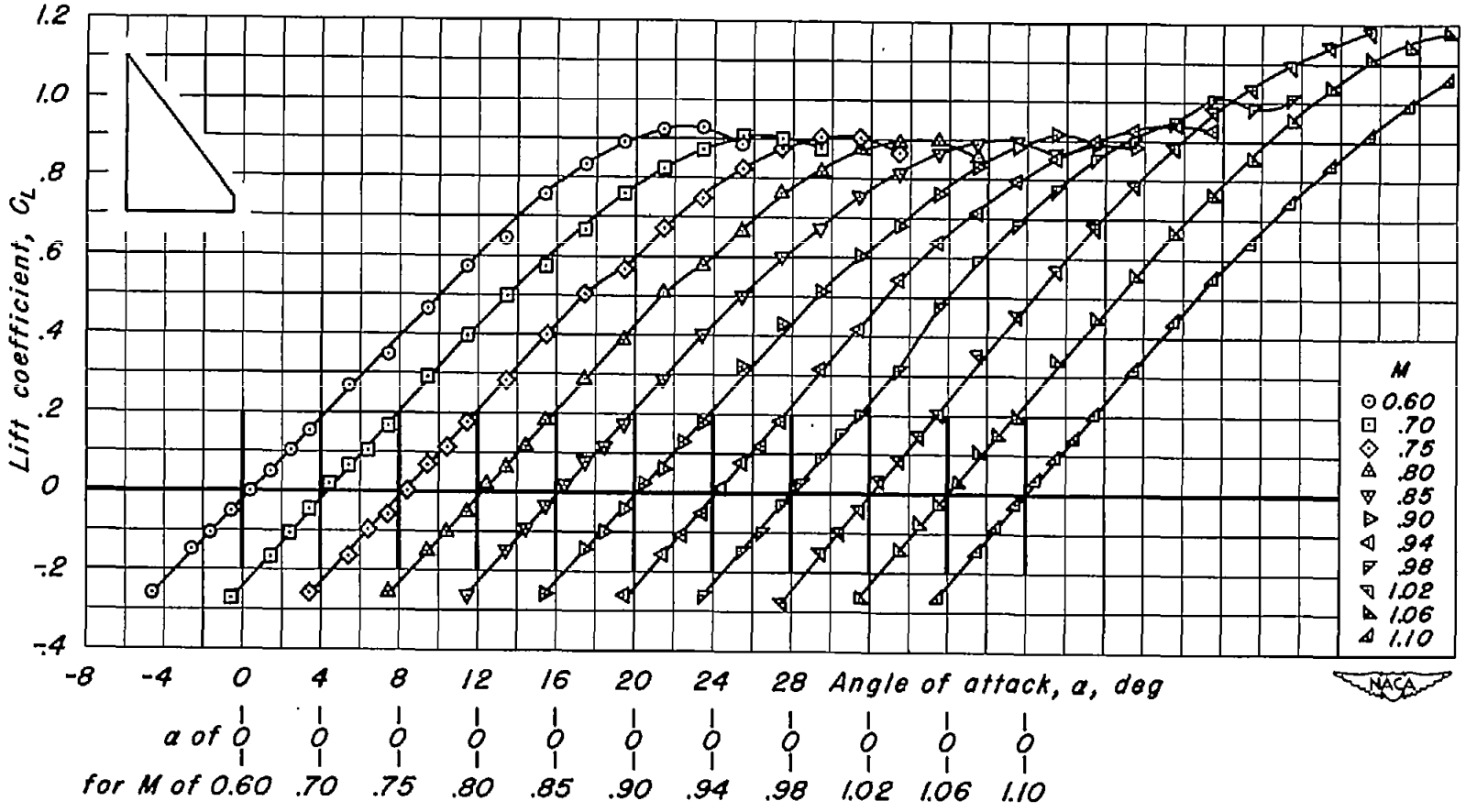

(b) NACA 63A002; λ, 0.1; A, 2.46.
Figure 11.- Continued.

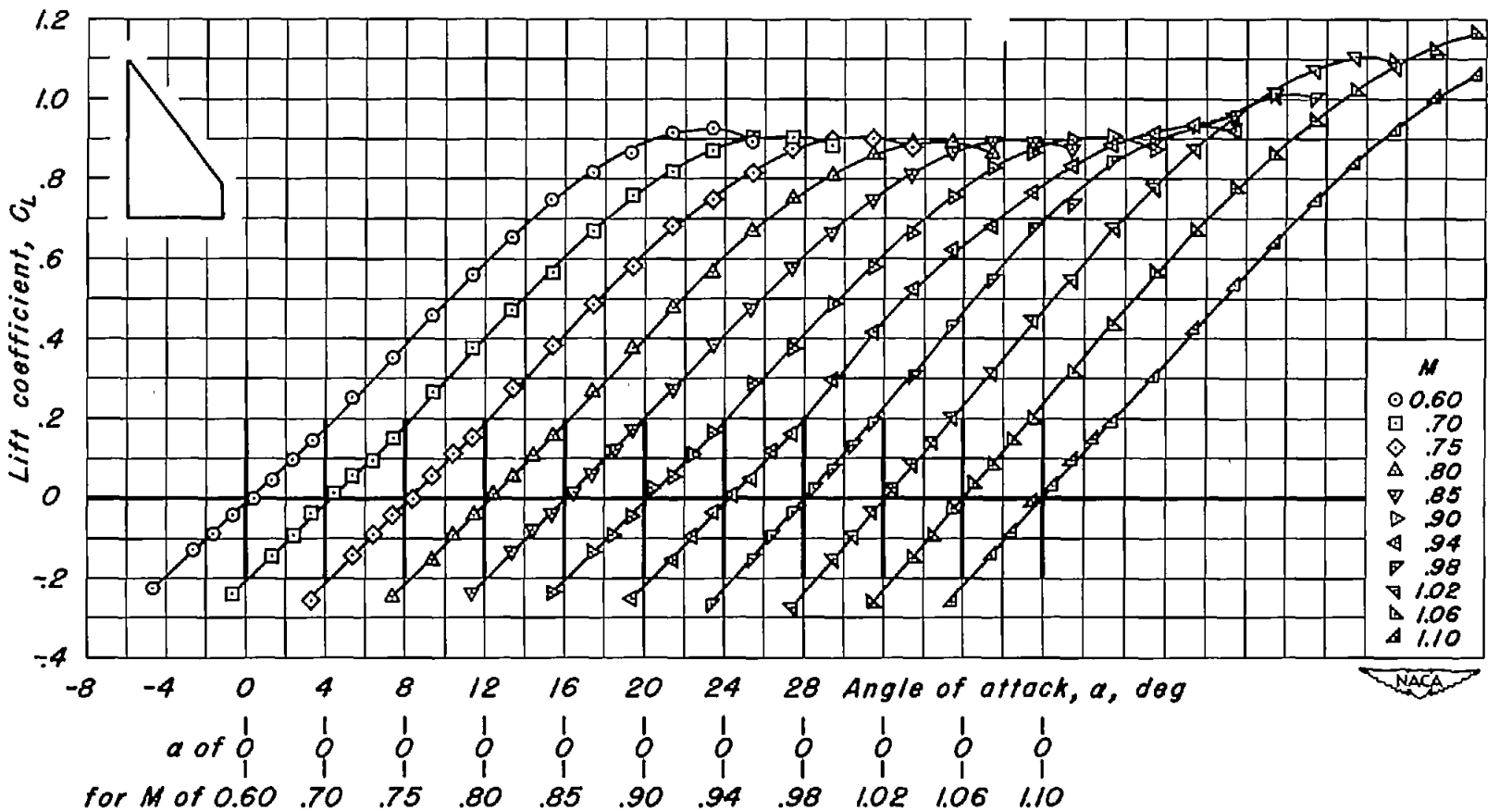

(c) NACA 63A002; λ, 0.2; A, 2.00.
Figure 11.- Continued.

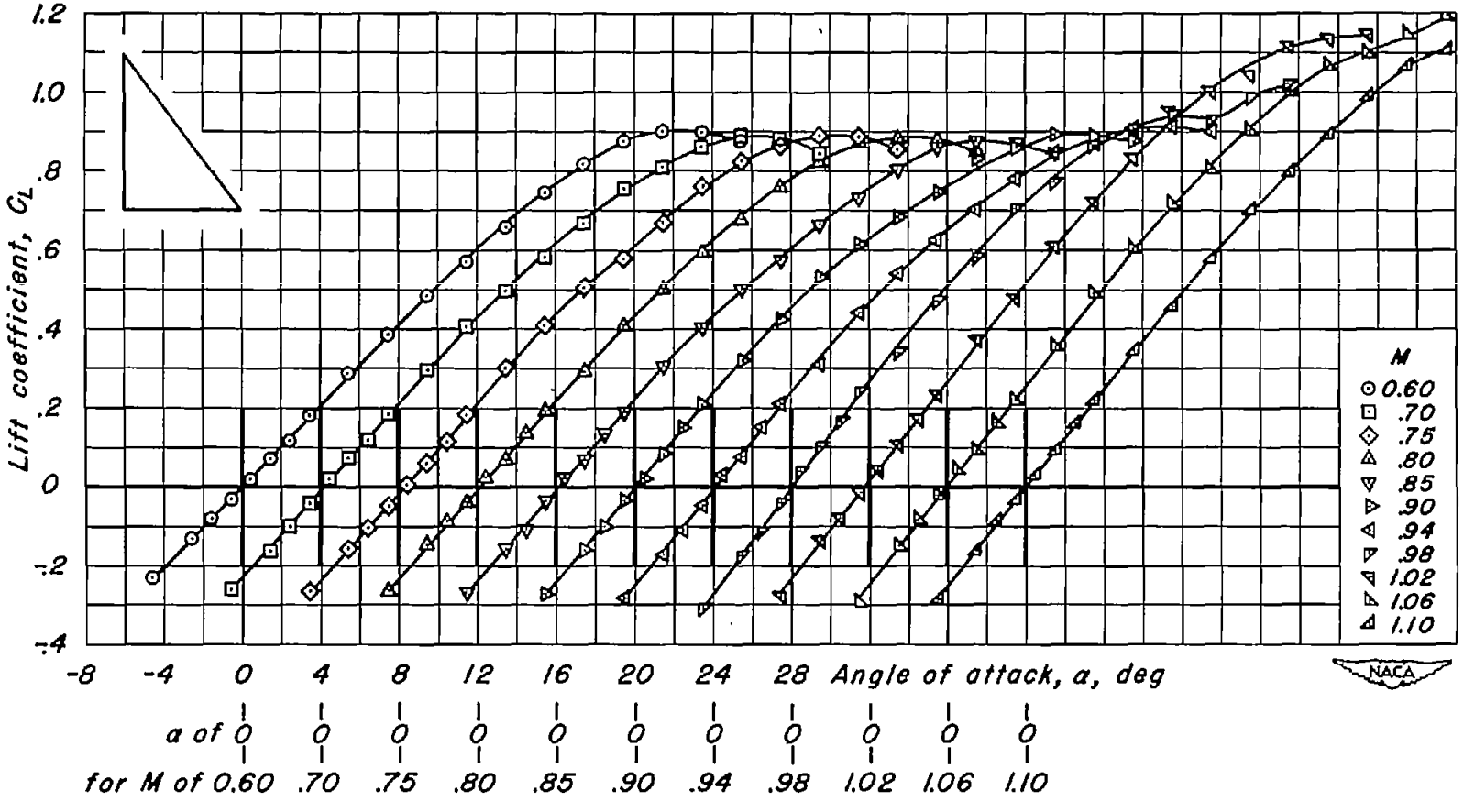

(d) NACA 63A004; λ, 0; A, 3.00.
Figure 11.- Continued.

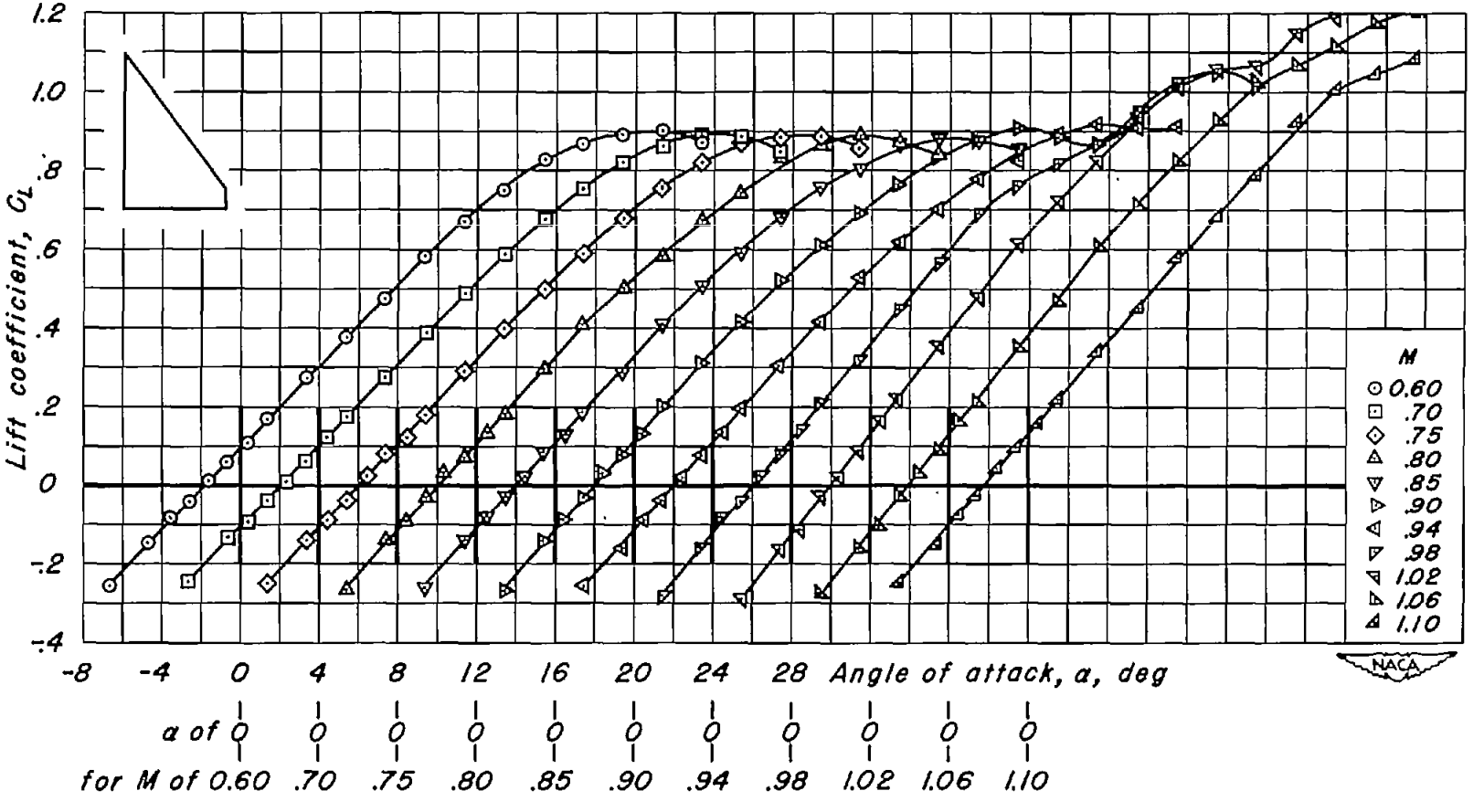

(e) NACA 63A004; λ, 0.1; A, 2.46.
Figure 11.- Continued.

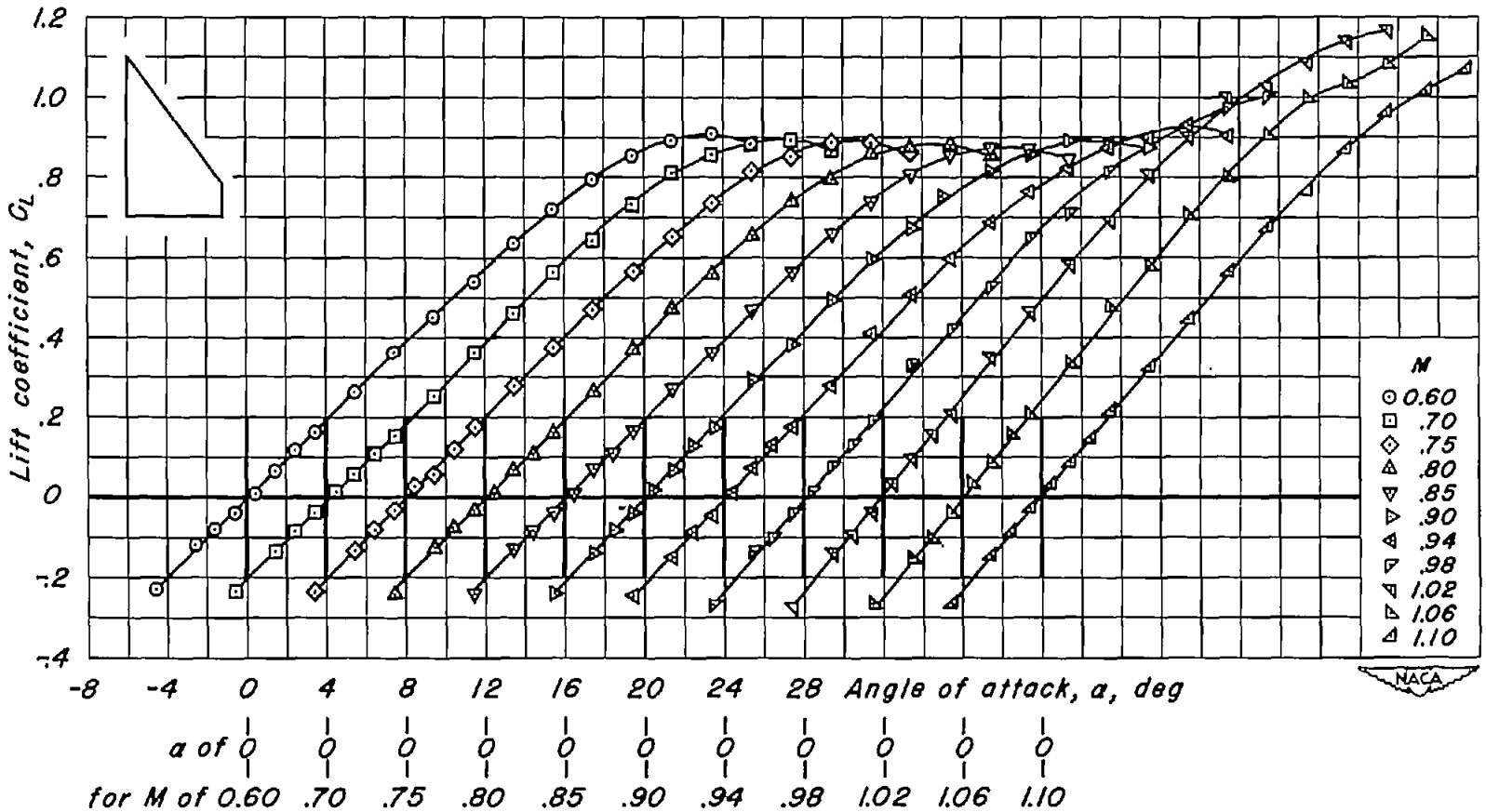

(f) NACA 63A004; λ, 0.2; A, 2.00.
Figure 11.- Continued.

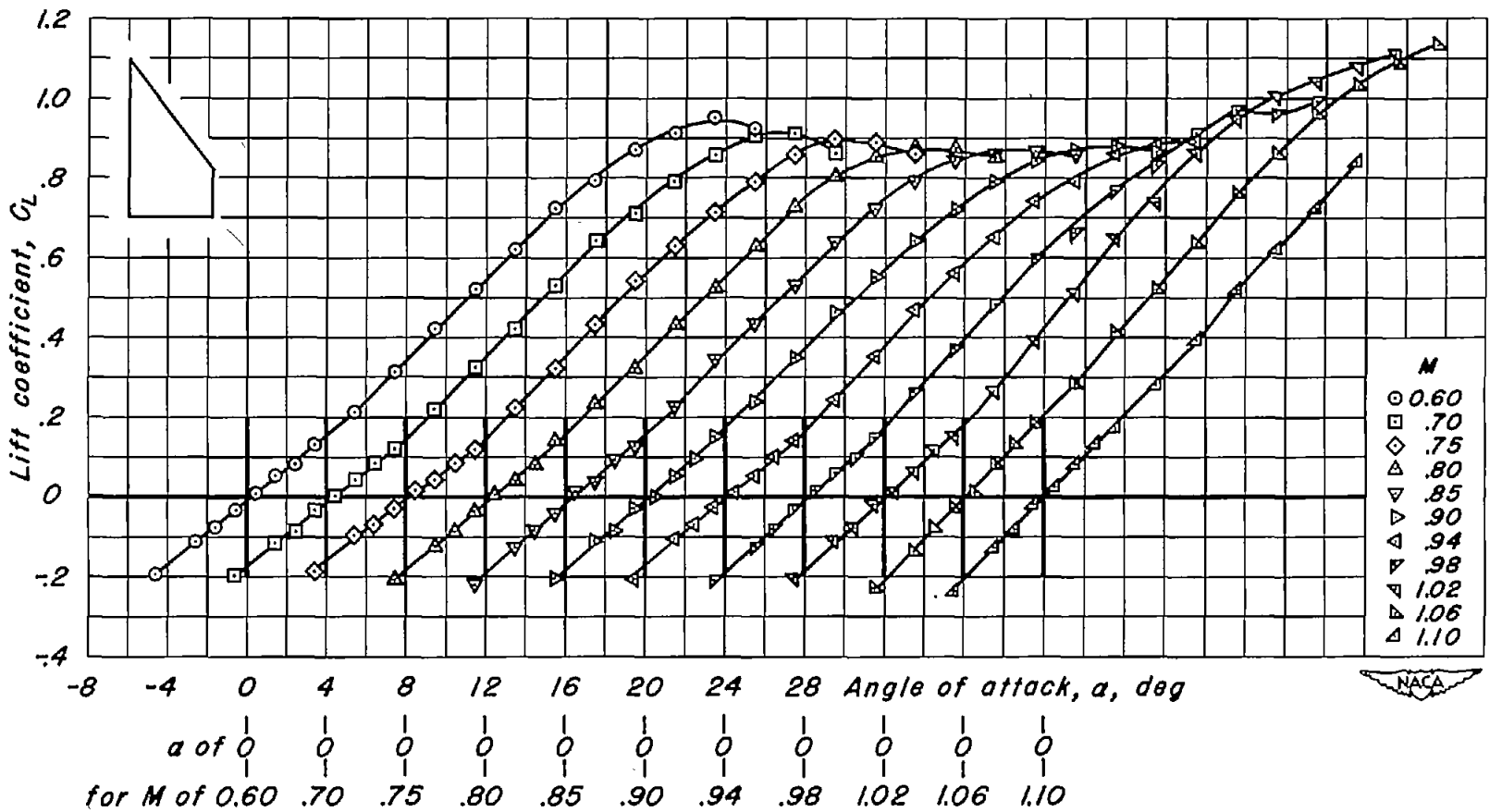

(g) NACA 63A004; λ, 0.3; A, 1.62.
Figure 11.- Continued.

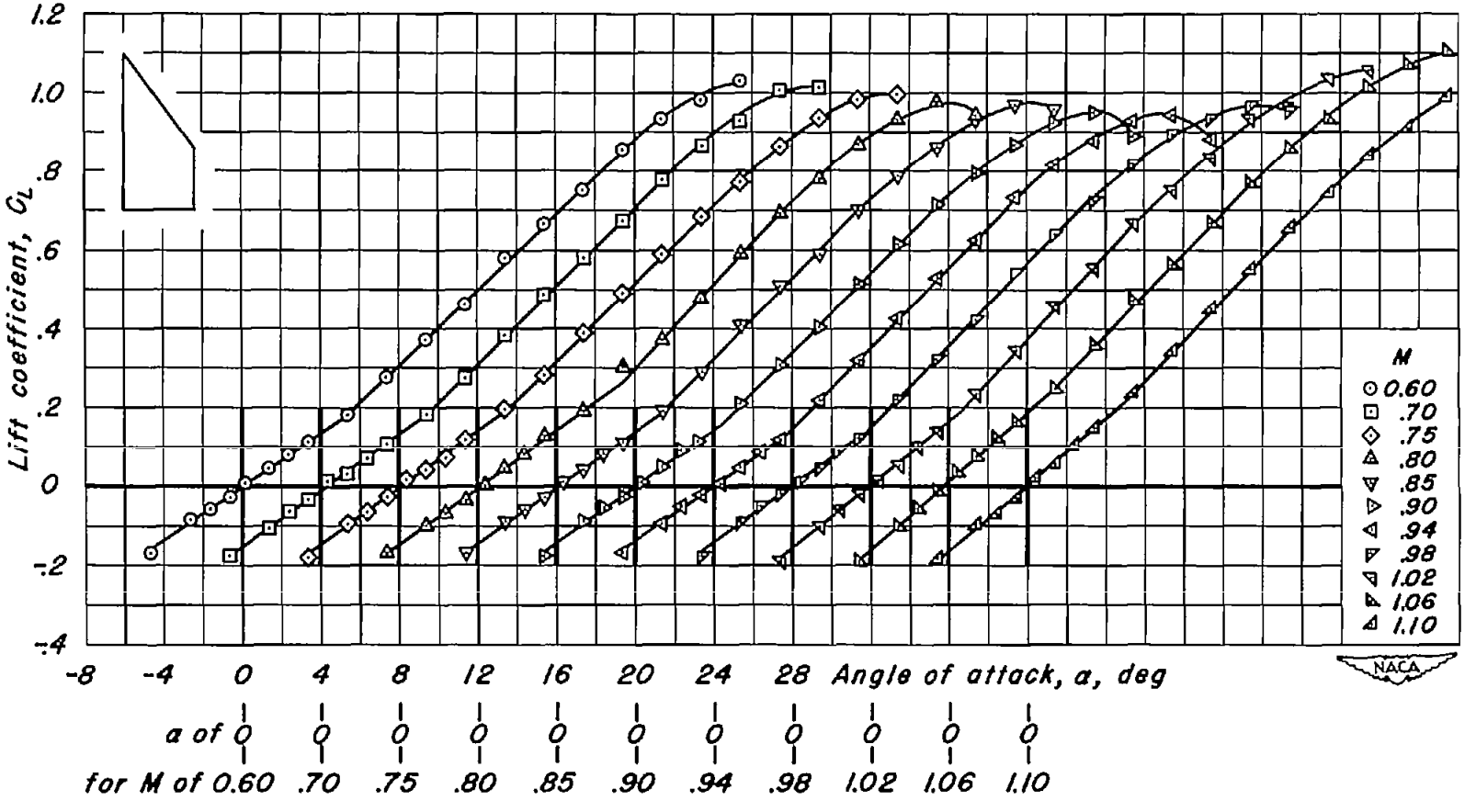

(h) NACA 63A004; λ, 0.4; A, 1.29.
Figure 11.- Continued.

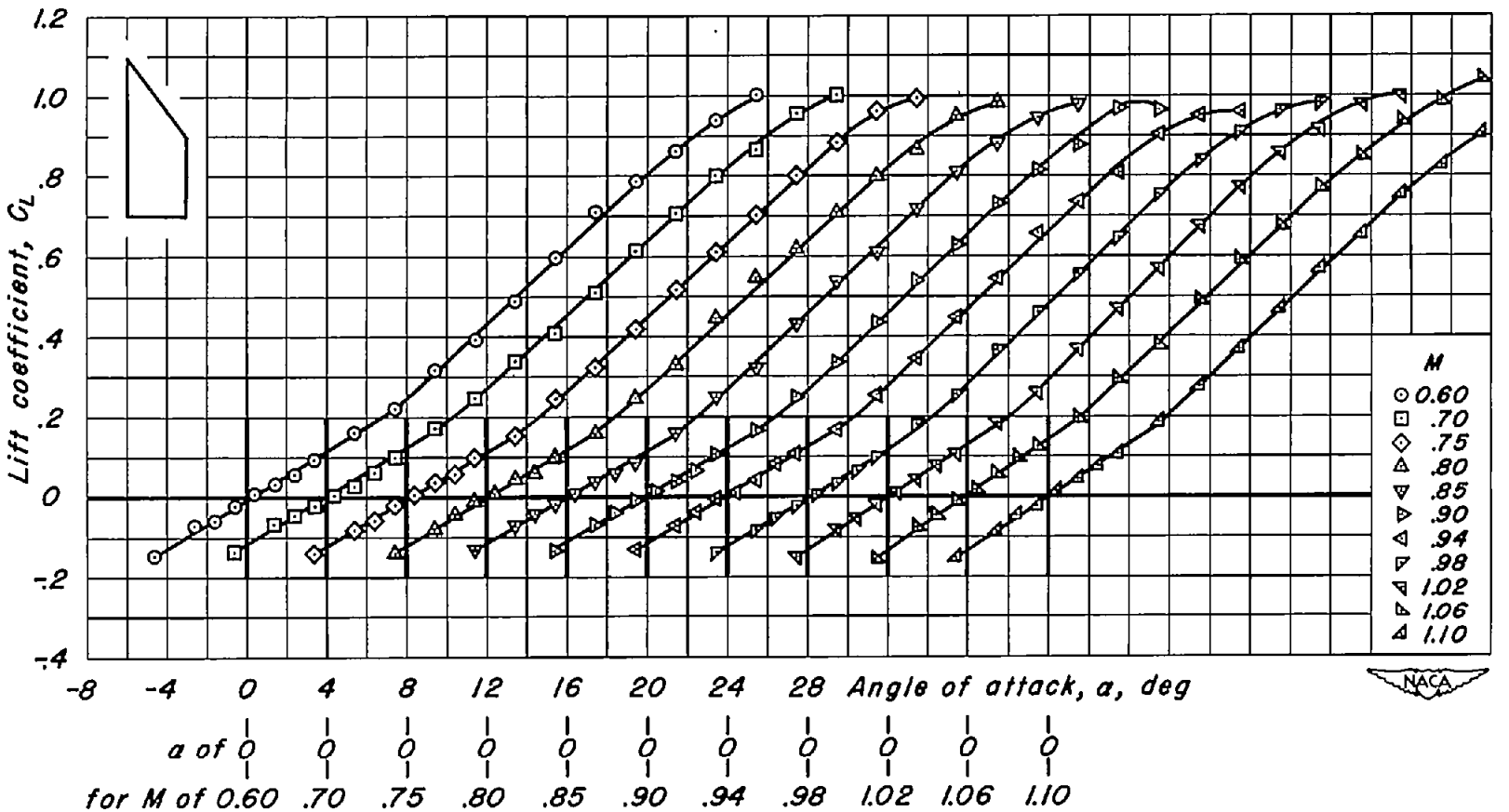

(i) NACA 63A004; λ, 0.5; A, 1.00.
Figure 11.- Continued.

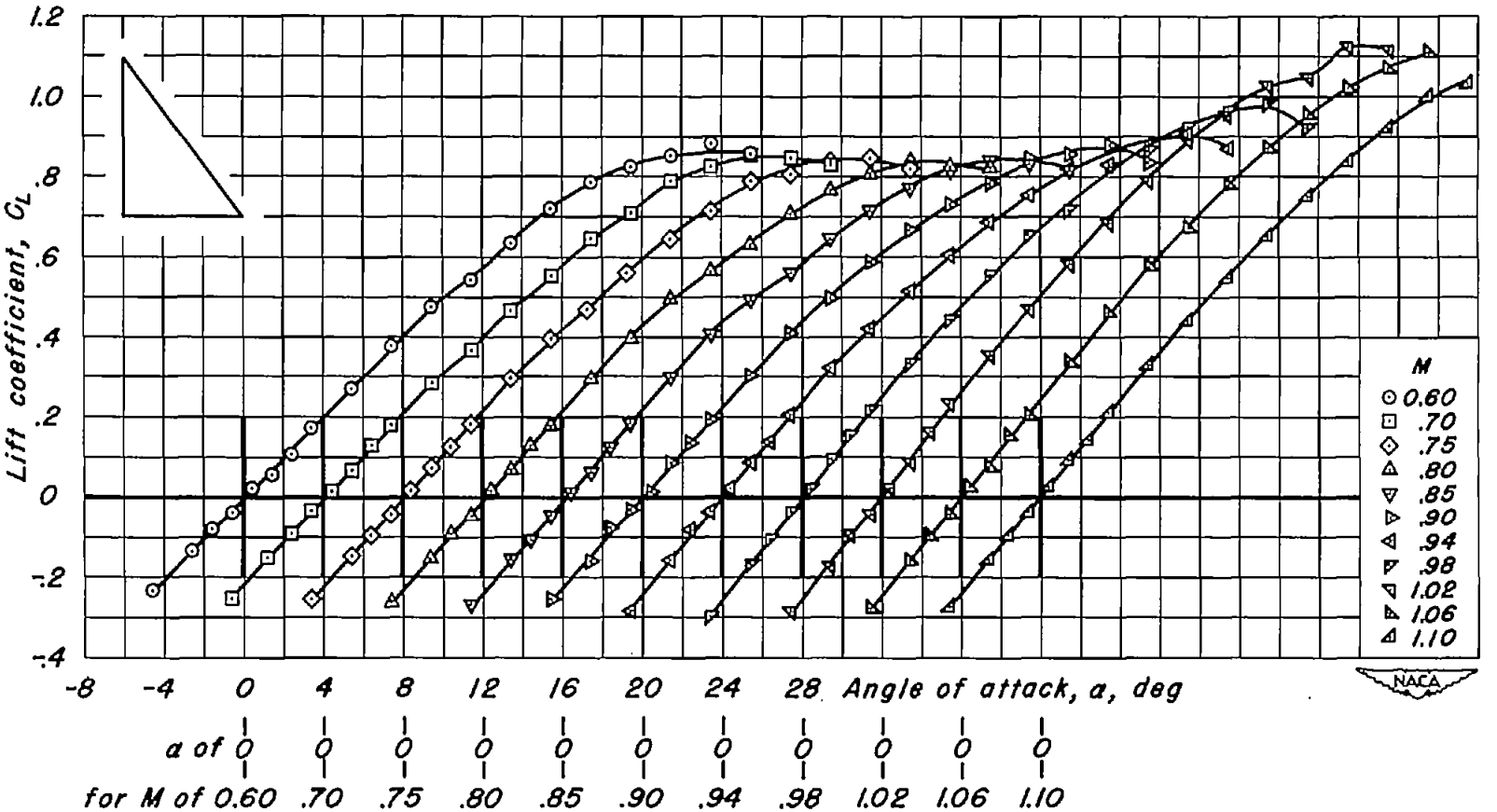

(j) NACA 63A006; λ, 0; A, 3.00.
Figure 11.- Continued.

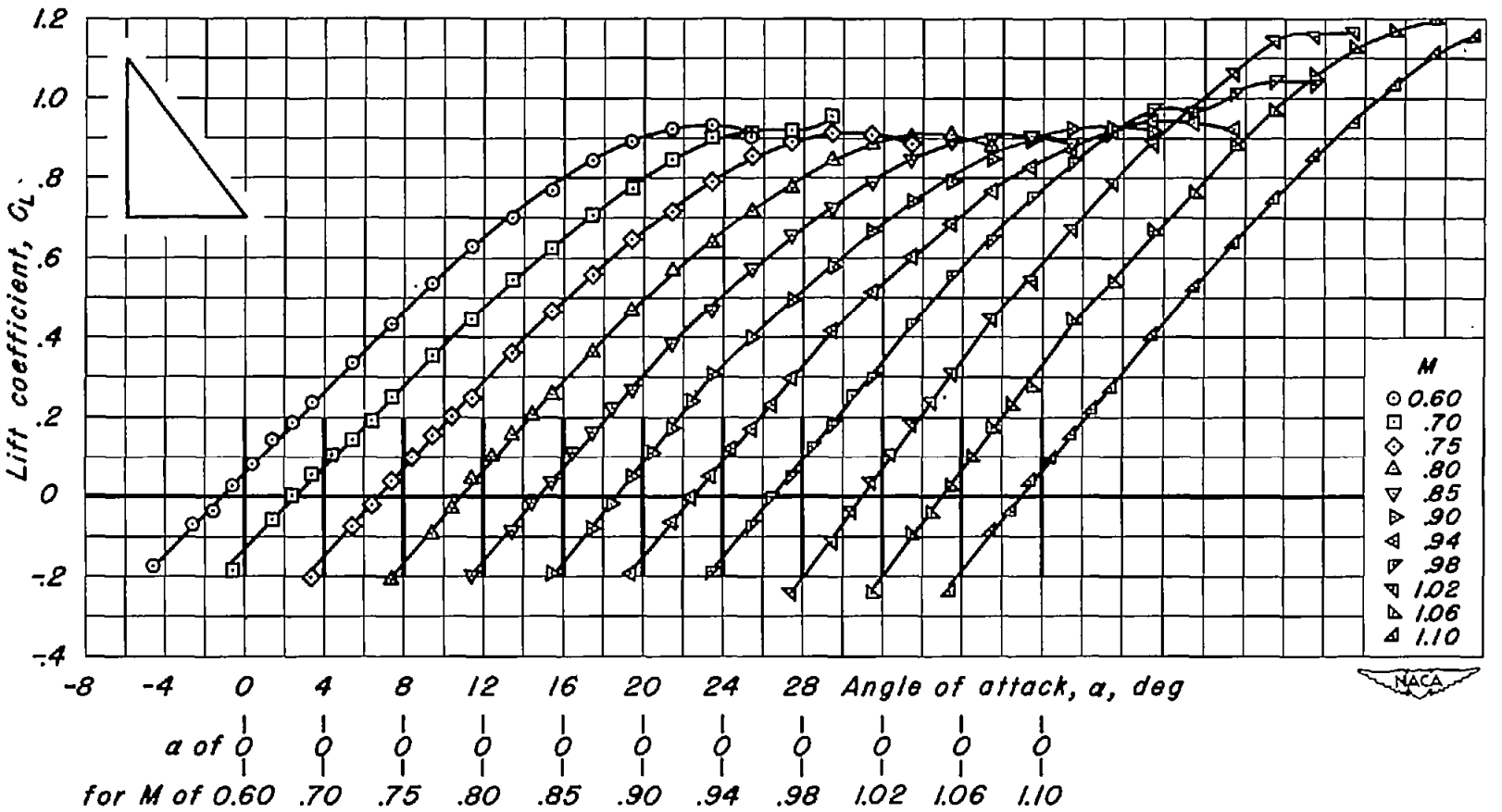

(k) NACA 63A(1.5)04; λ, 0; A, 3.00.
Figure 11.- Continued.

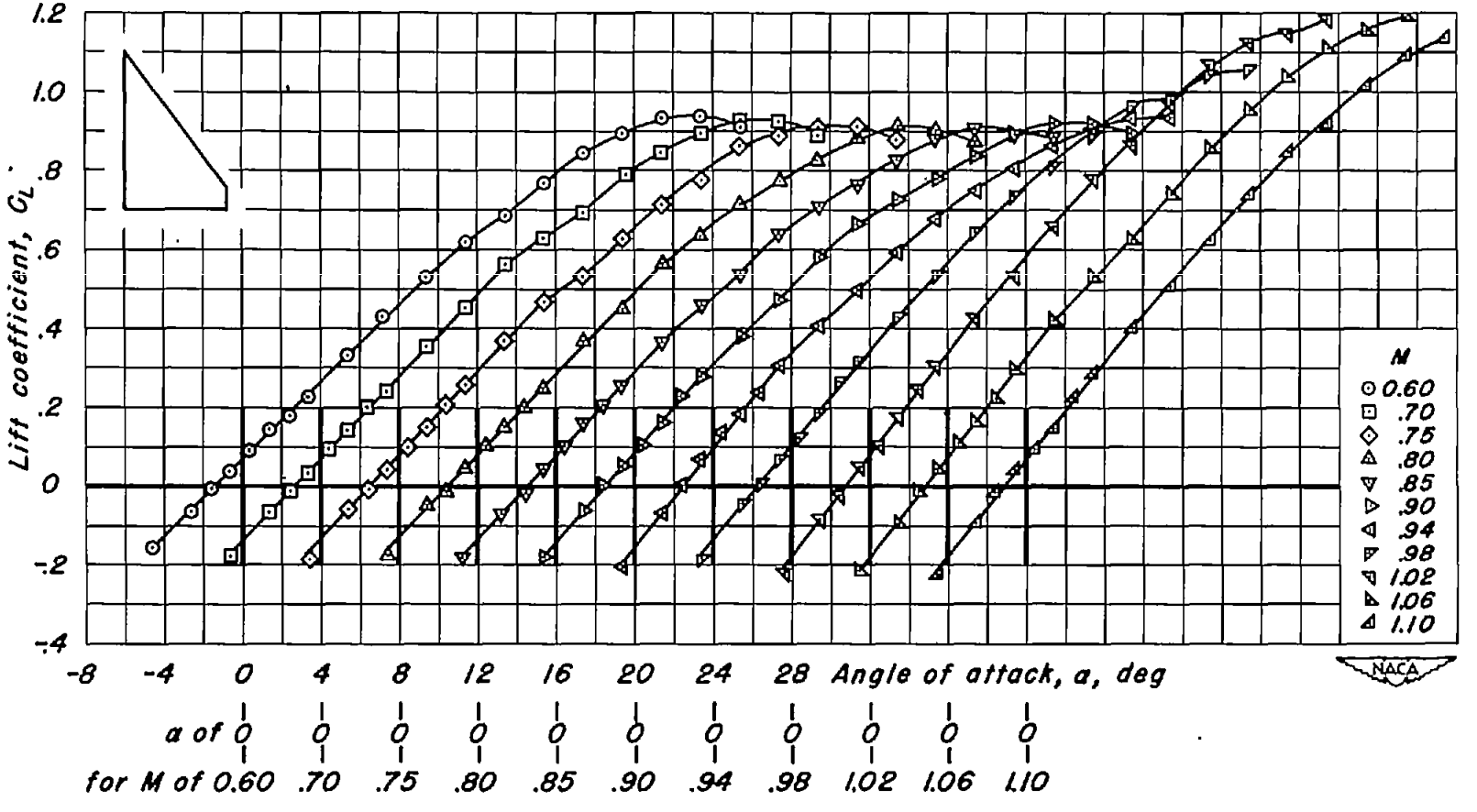

(l) NACA 63A(1.5)04; λ, 0.1; A, 2.46.
Figure 11.- Continued.

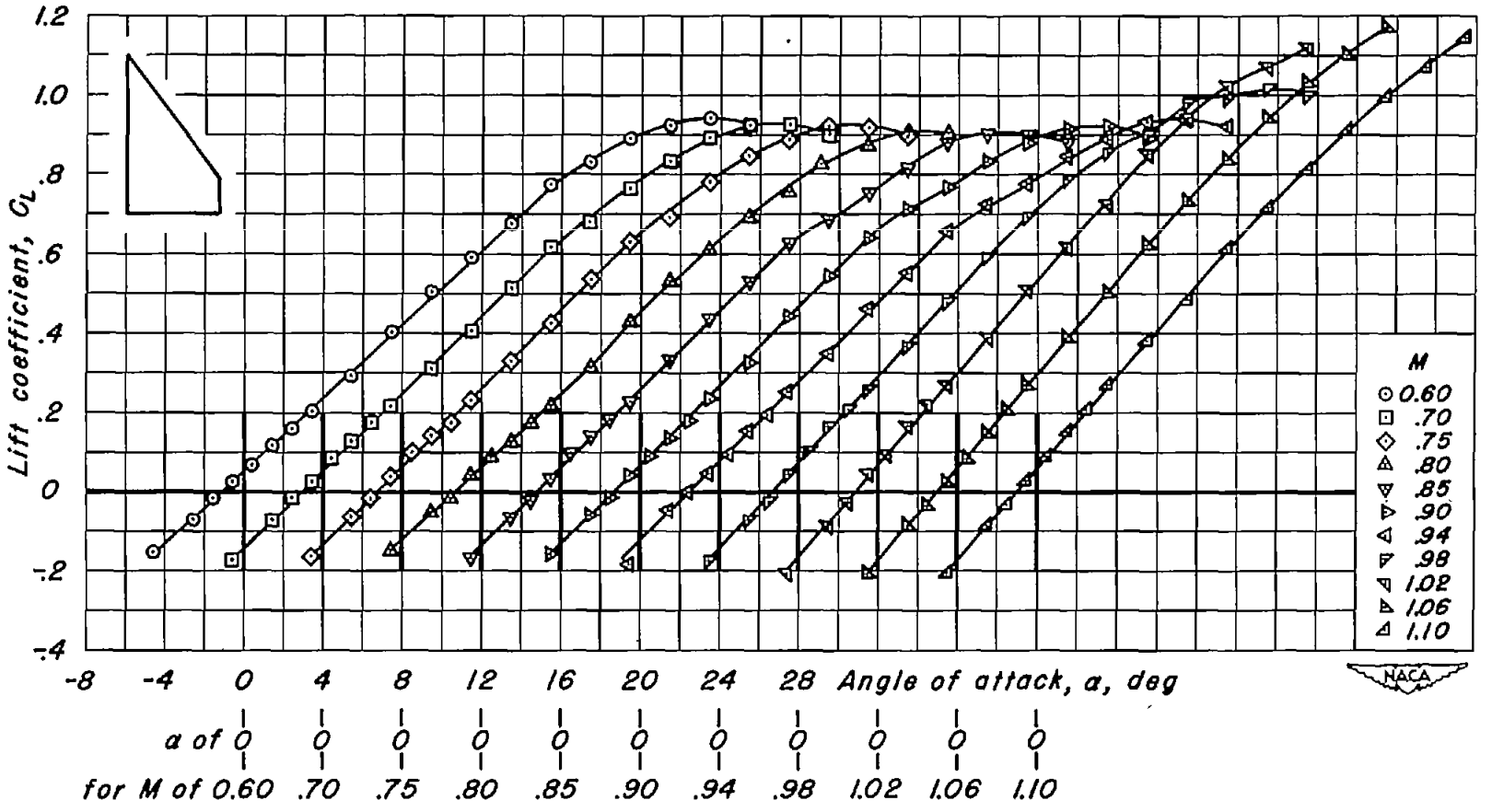

(m) NACA 63A(1.5)04; λ, 0.2; A, 2.00.
Figure 11.- Concluded.

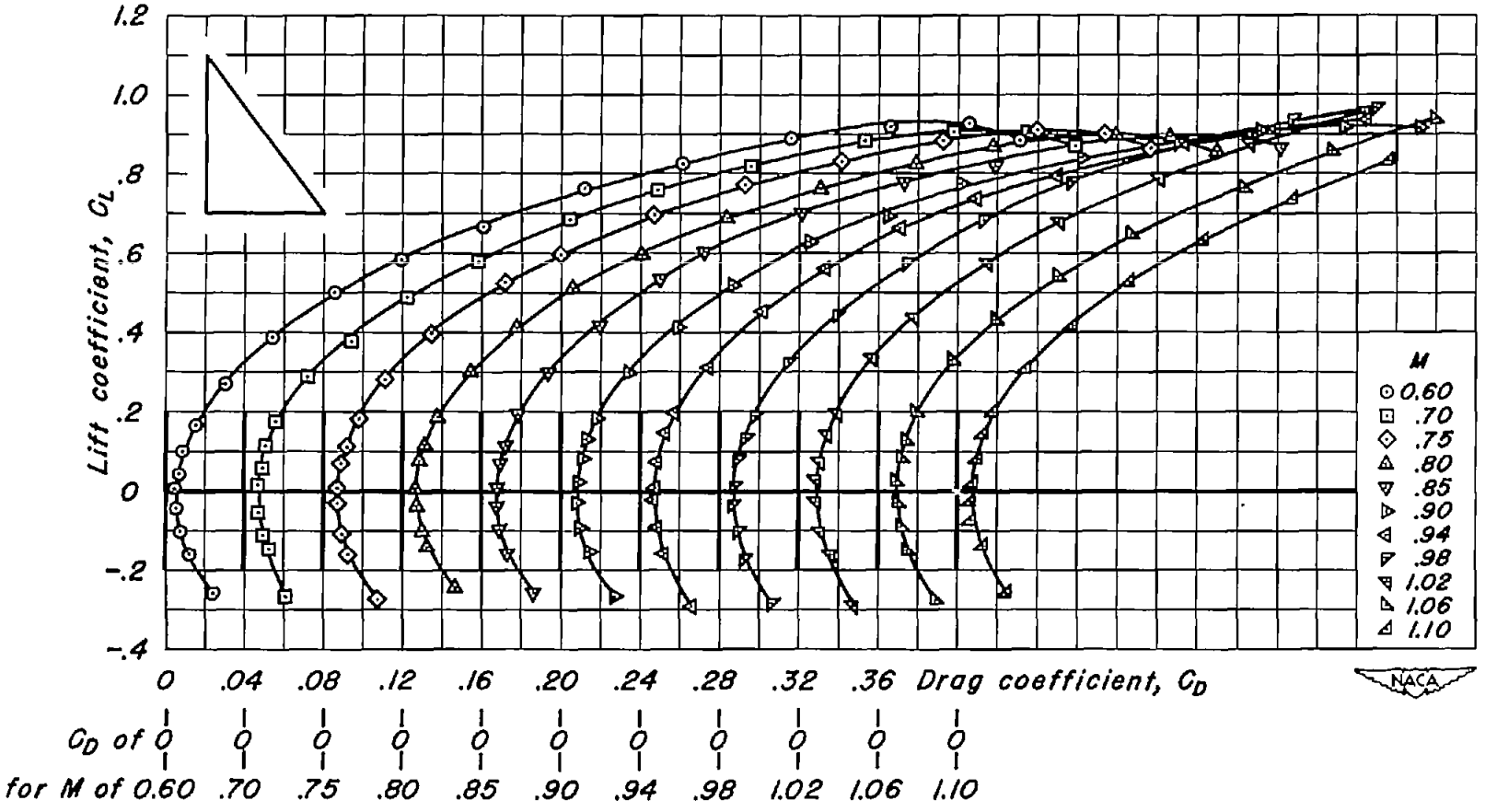

C_D of	0	0	0	0	0	0	0	0	0	0	0
for M of	0.60	.70	.75	.80	.85	.90	.94	.98	1.02	1.06	1.10

(a) NACA 63A002; λ, 0; A, 3.00.

Figure 12.- Variation of drag coefficient with lift coefficient for the wings of basic aspect ratio 3.

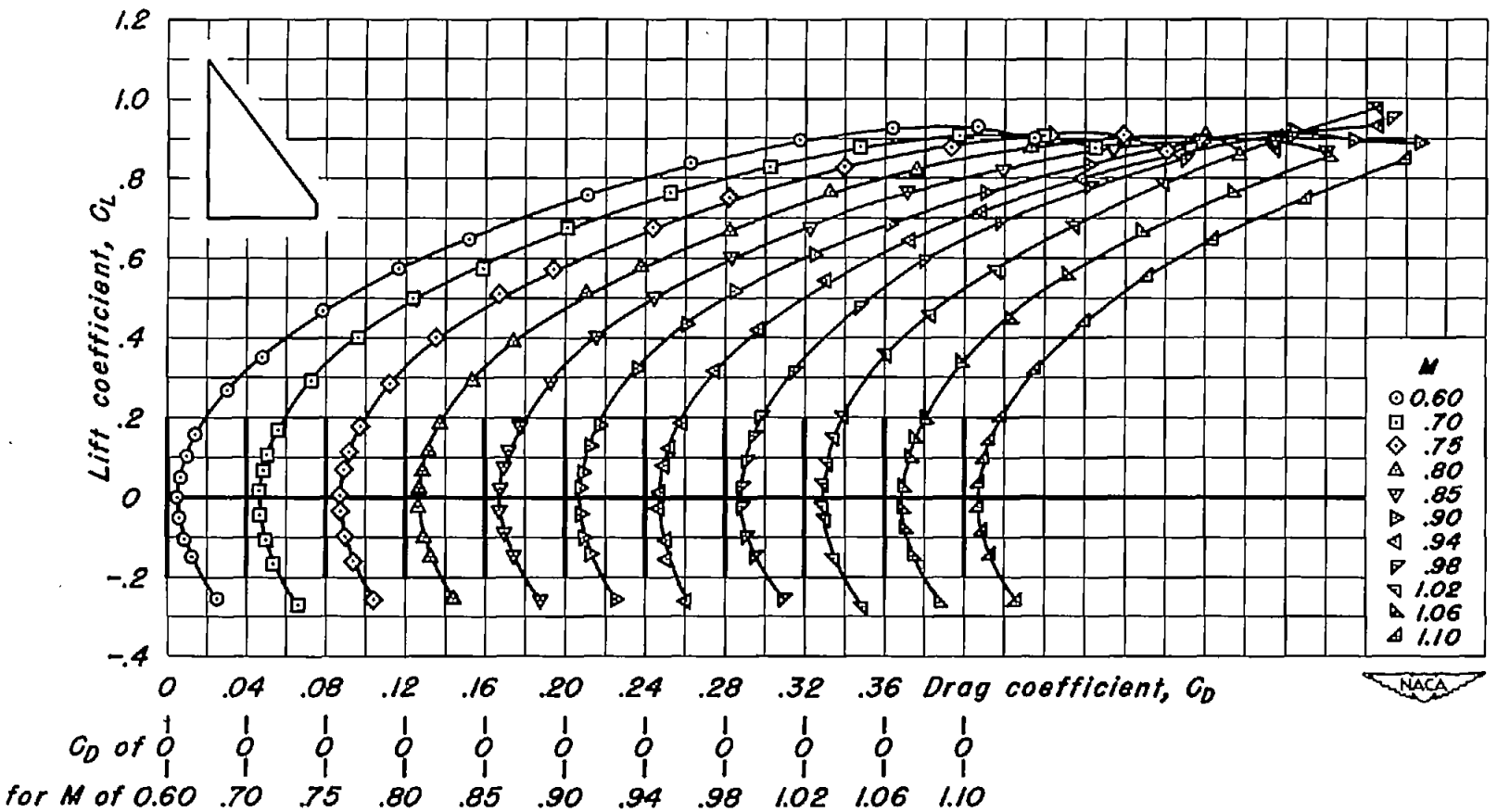

(b) NACA 63A002; λ, 0.1; A, 2.46.
Figure 12.- Continued.

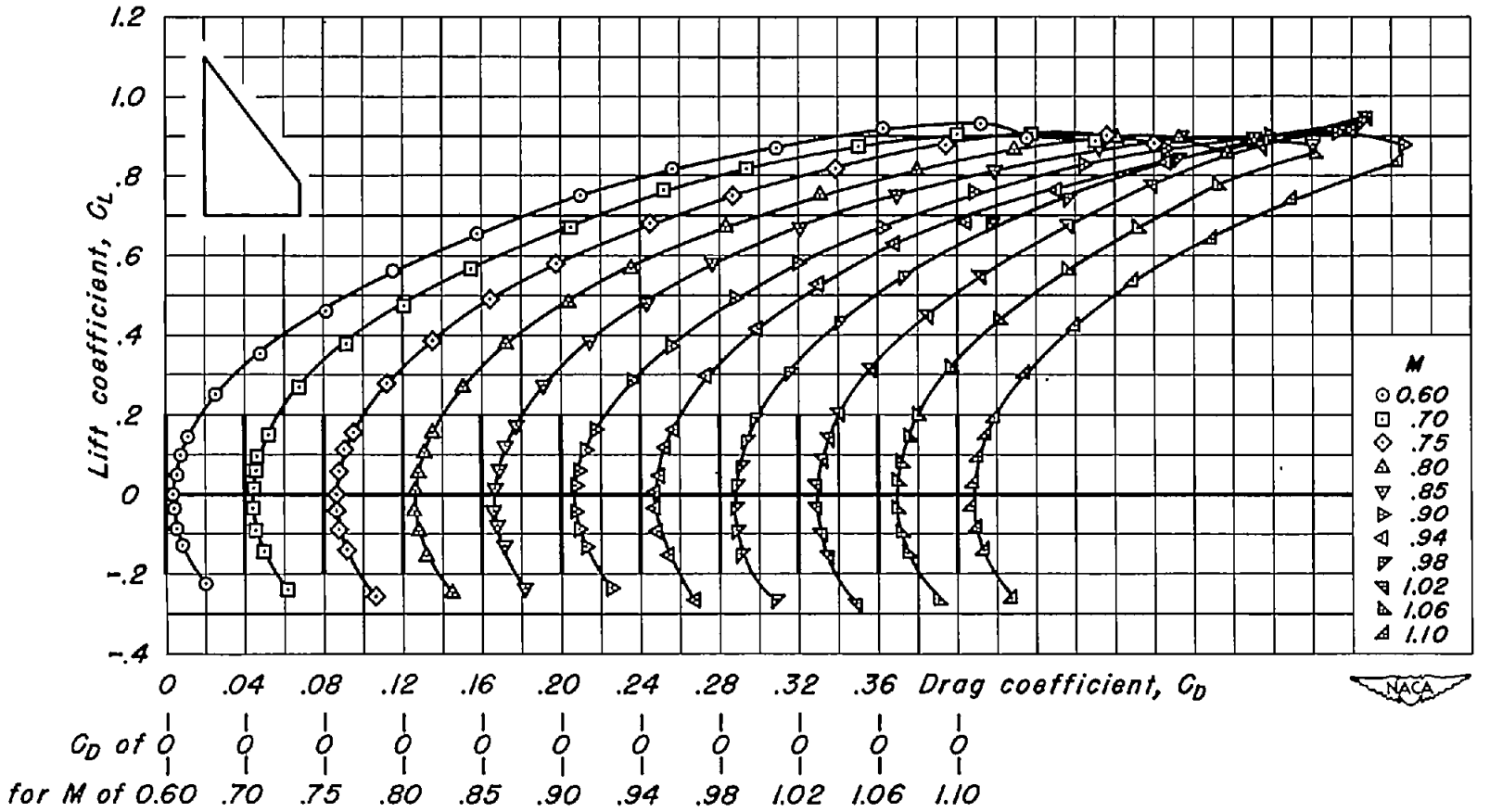

(c) NACA 63A002; λ, 0.2; A, 2.00.
Figure 12. Continued.

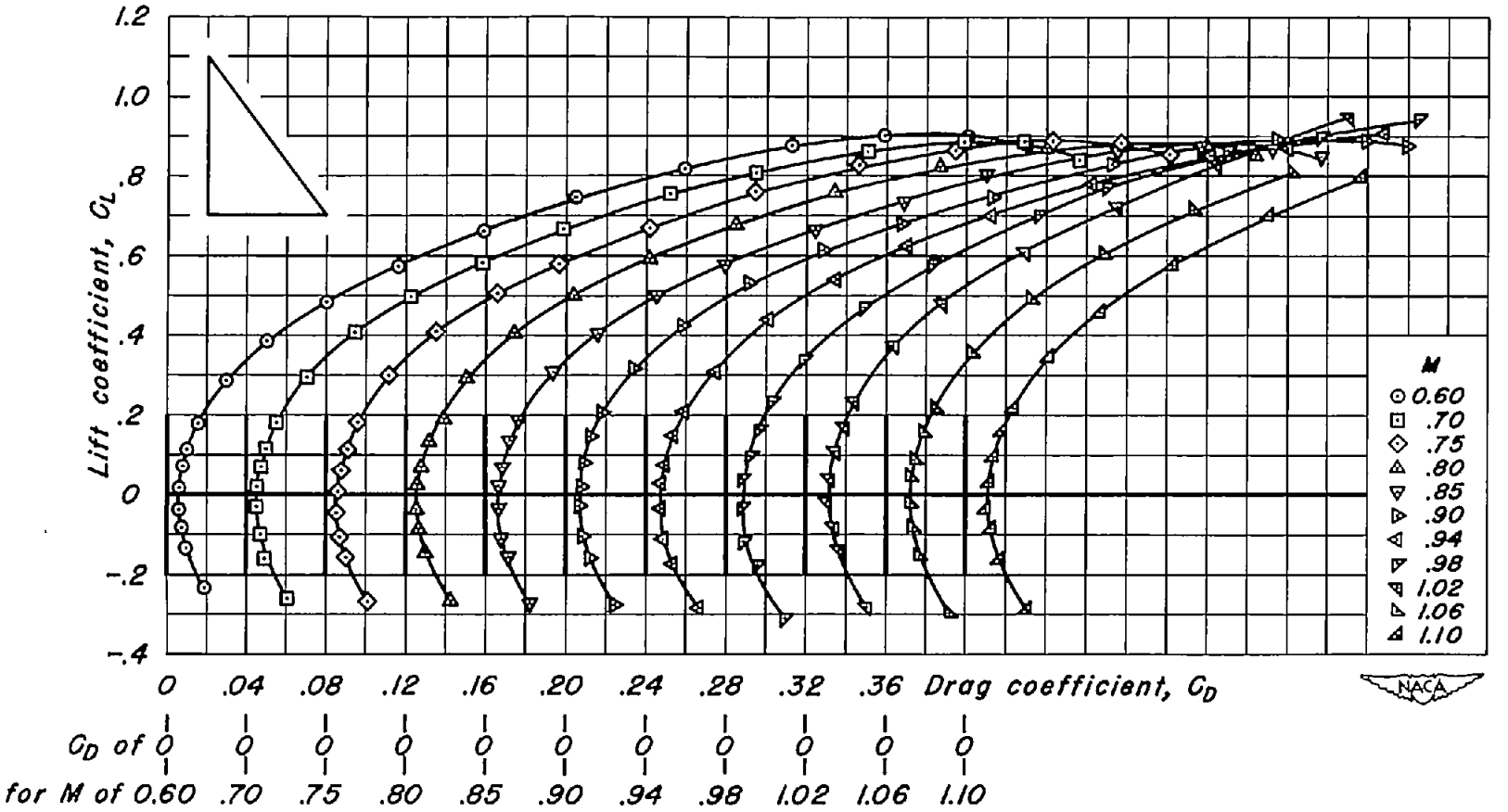

(d) NACA 63A004; λ, 0; A, 3.00.
Figure 12.- Continued.

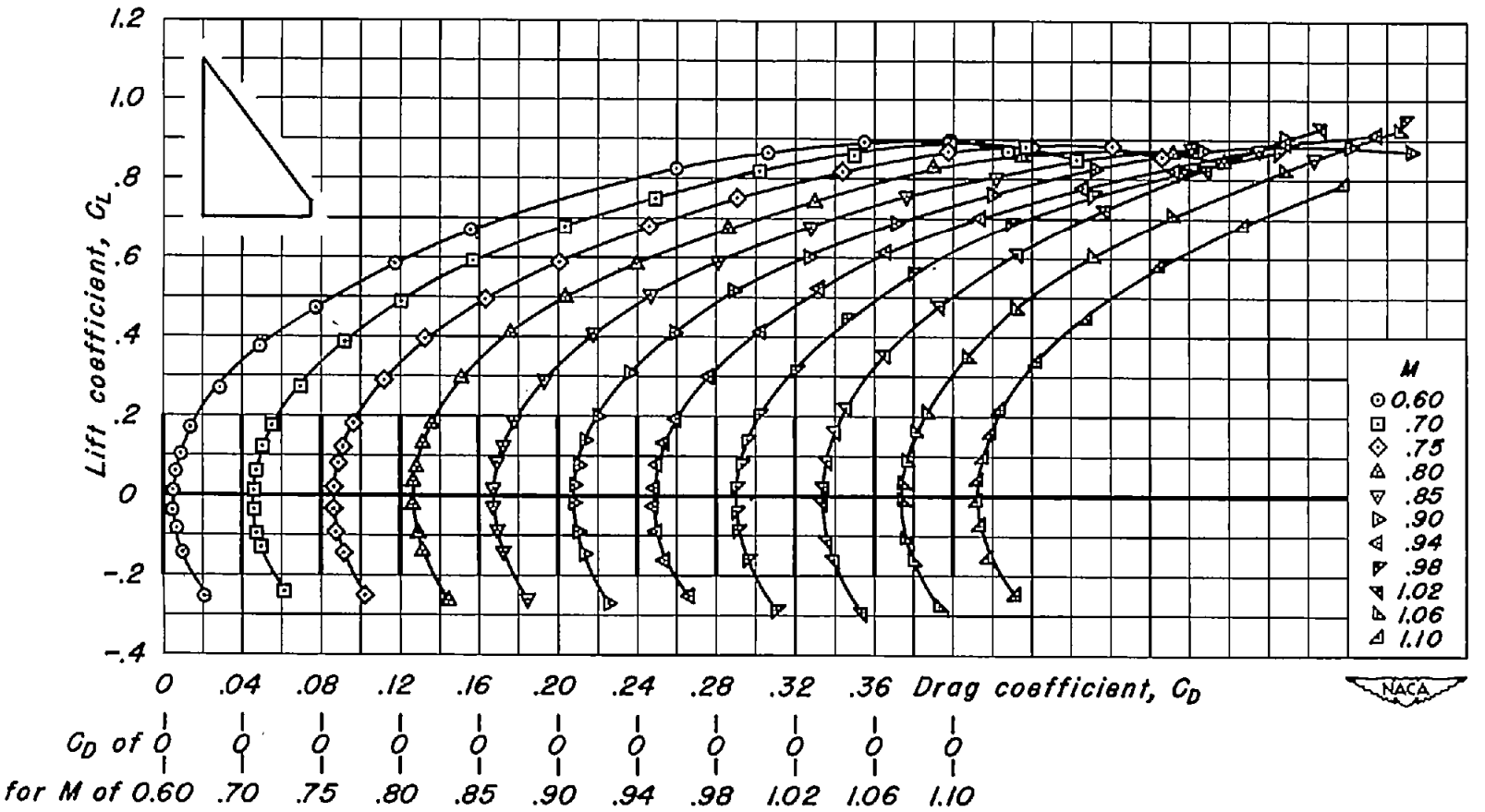

(e) NACA 63A004; λ, 0.1; A, 2.46.
Figure 12.- Continued.

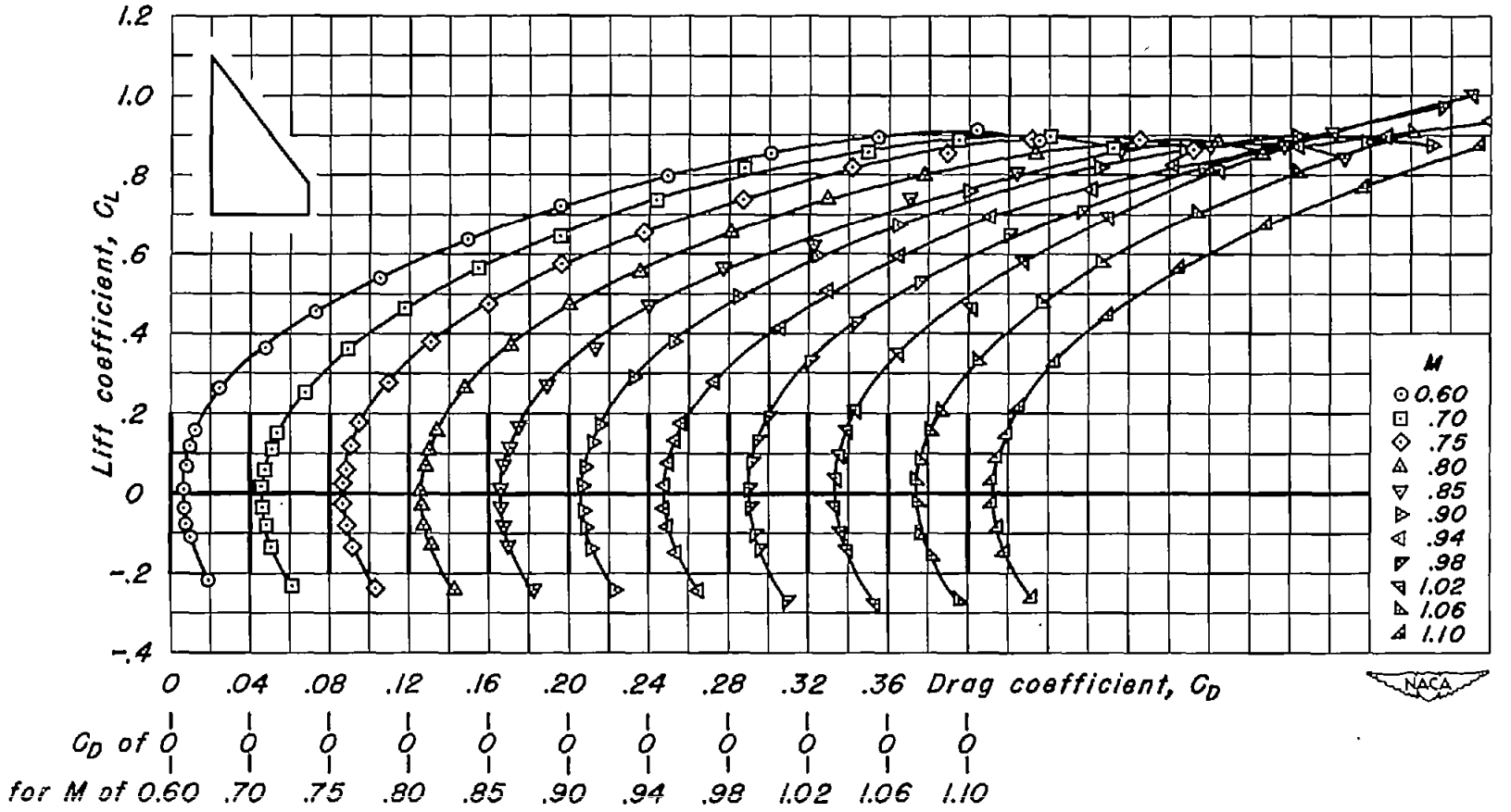

(f) NACA 63A004; λ, 0.2; A, 2.00.
Figure 12.- Continued.

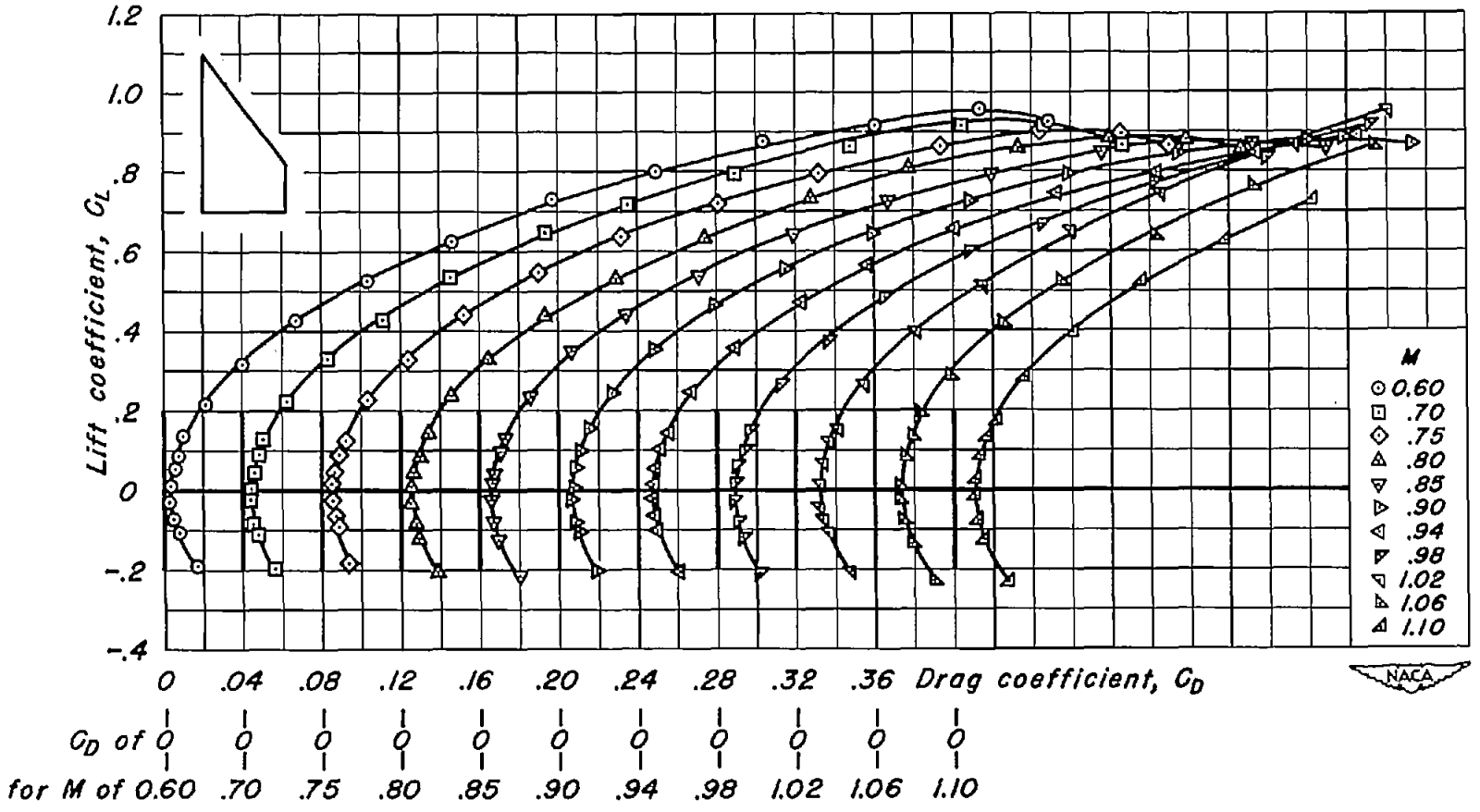

C_D of	0	0	0	0	0	0	0	0	0	0	0
for M of	0.60	.70	.75	.80	.85	.90	.94	.98	1.02	1.06	1.10

(g) NACA 63A004; λ, 0.3; A, 1.62.
Figure 12.- Continued.

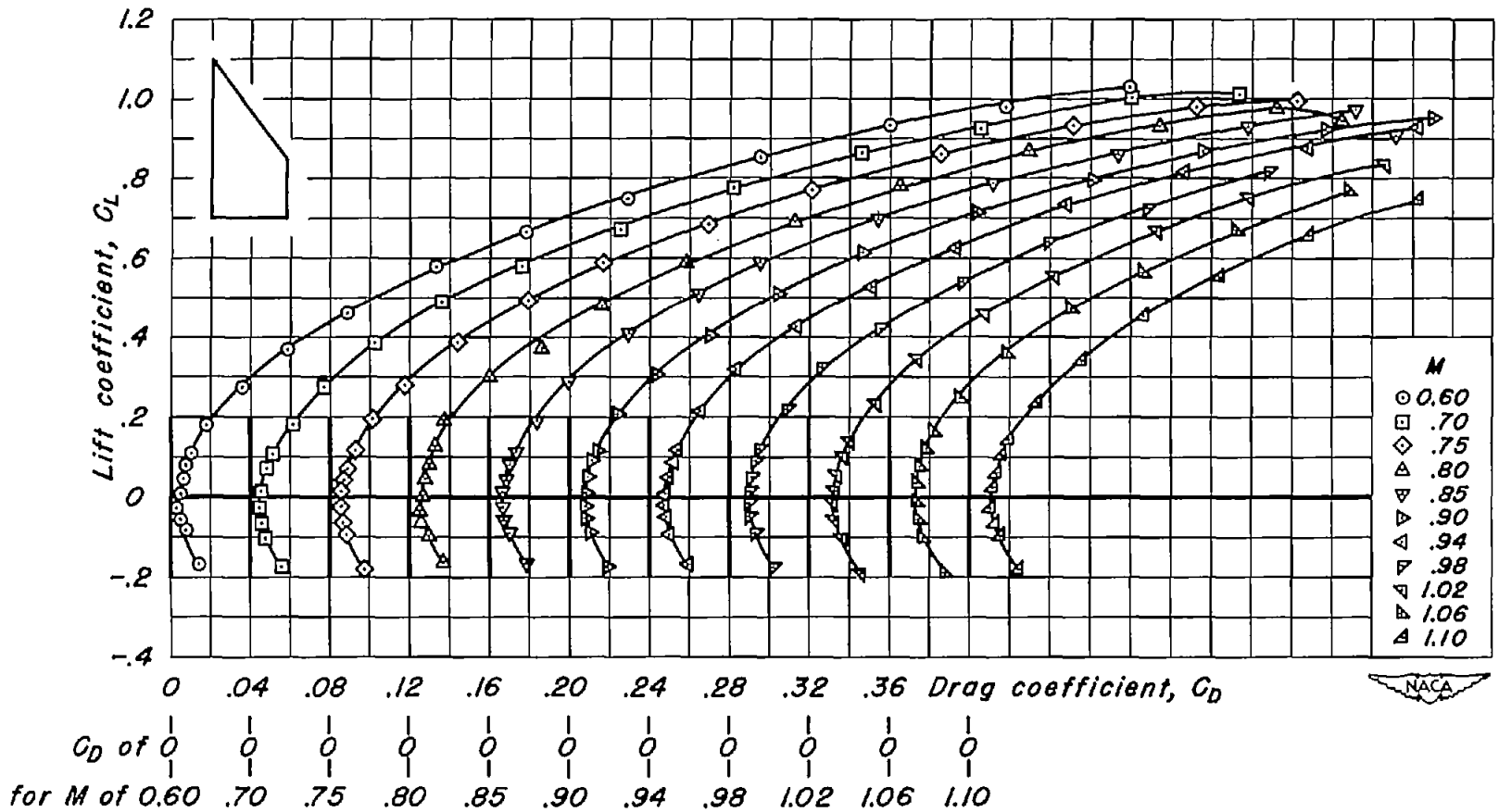

(h) NACA 63A004; λ, 0.4; A, 1.29.
Figure 12.- Continued.

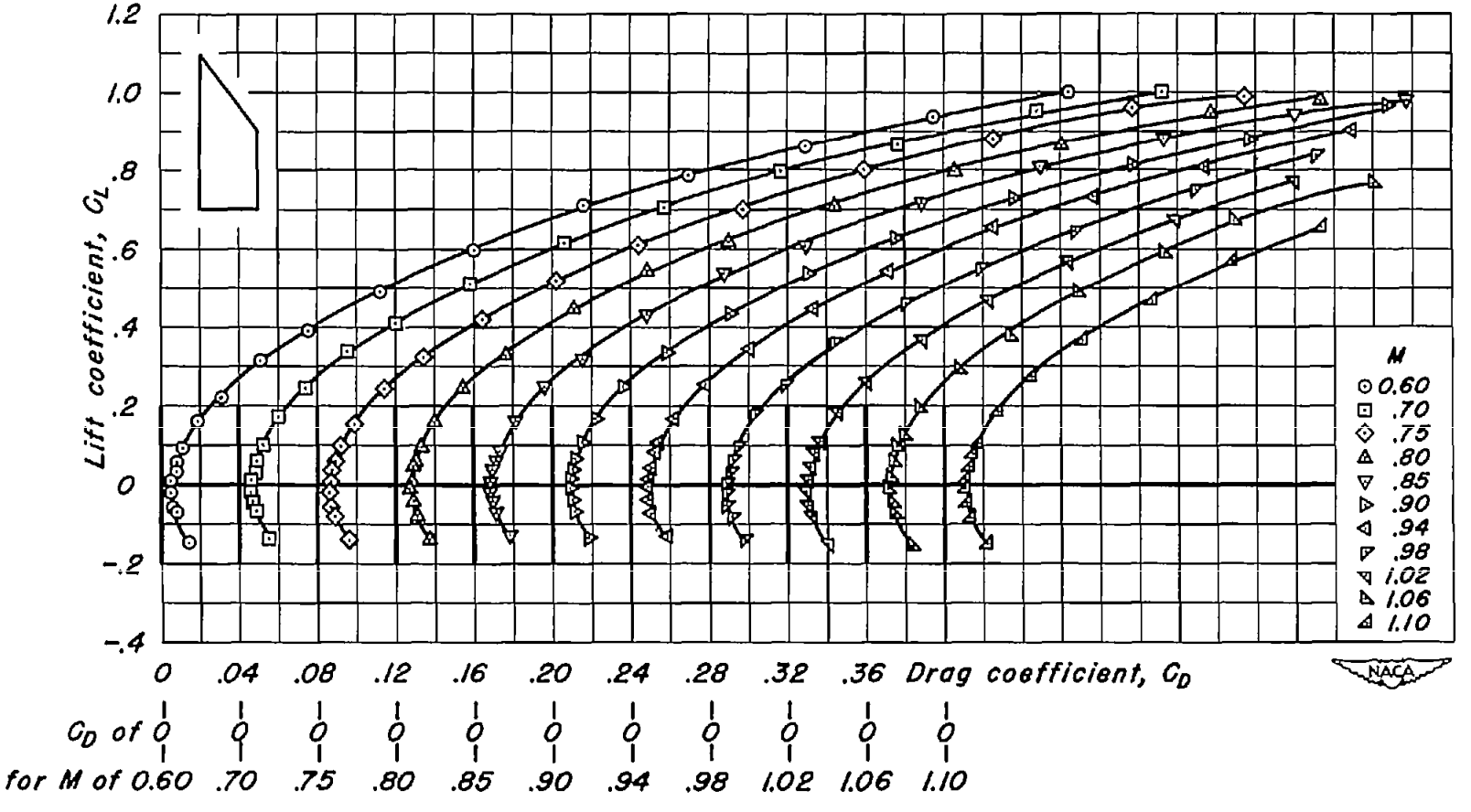

(i) NACA 63A004; λ, 0.5; A, 1.00.
Figure 12.- Continued.

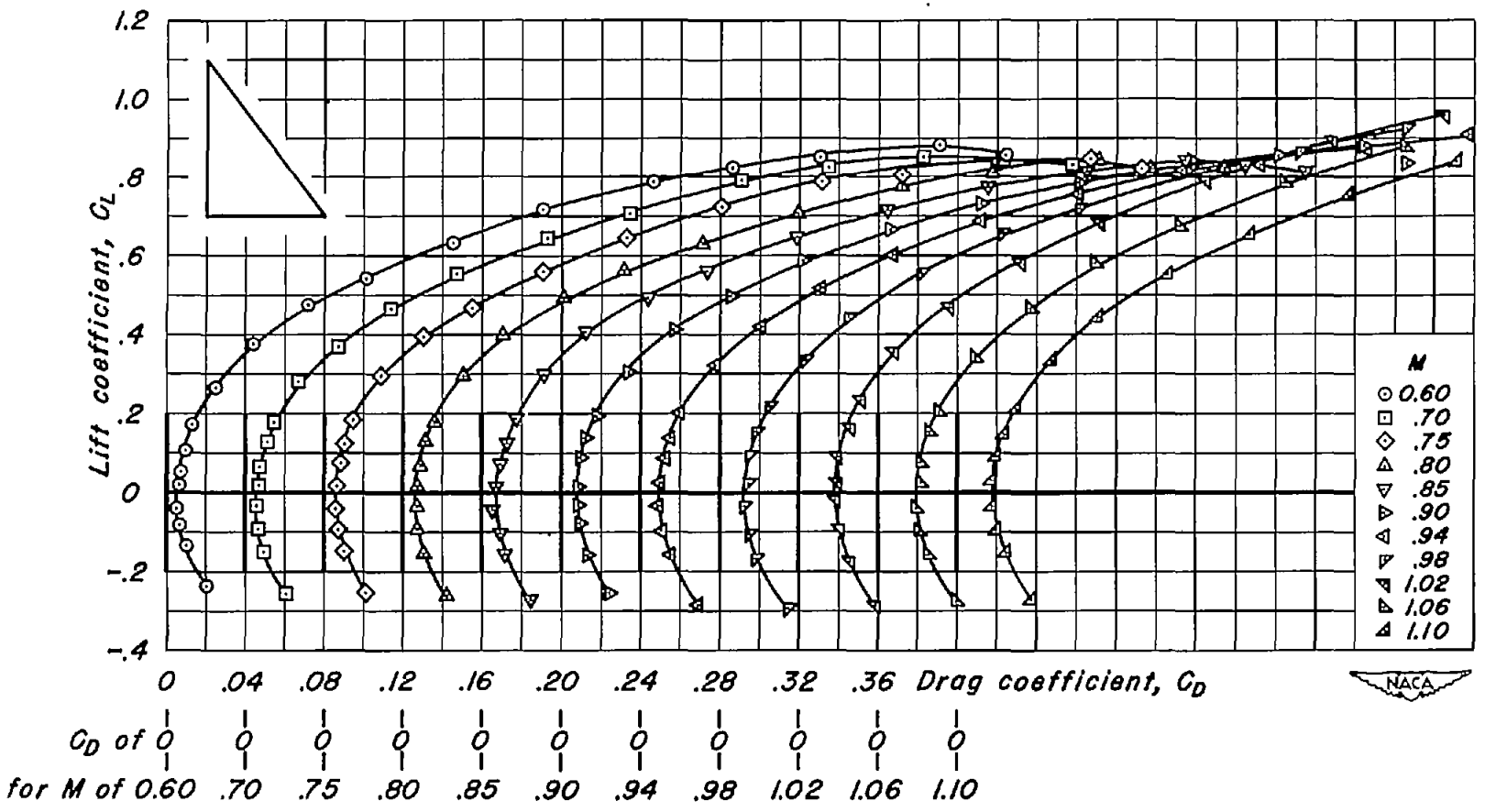

(j) NACA 63A006; λ, 0; A, 3.00.
Figure 12.- Continued.

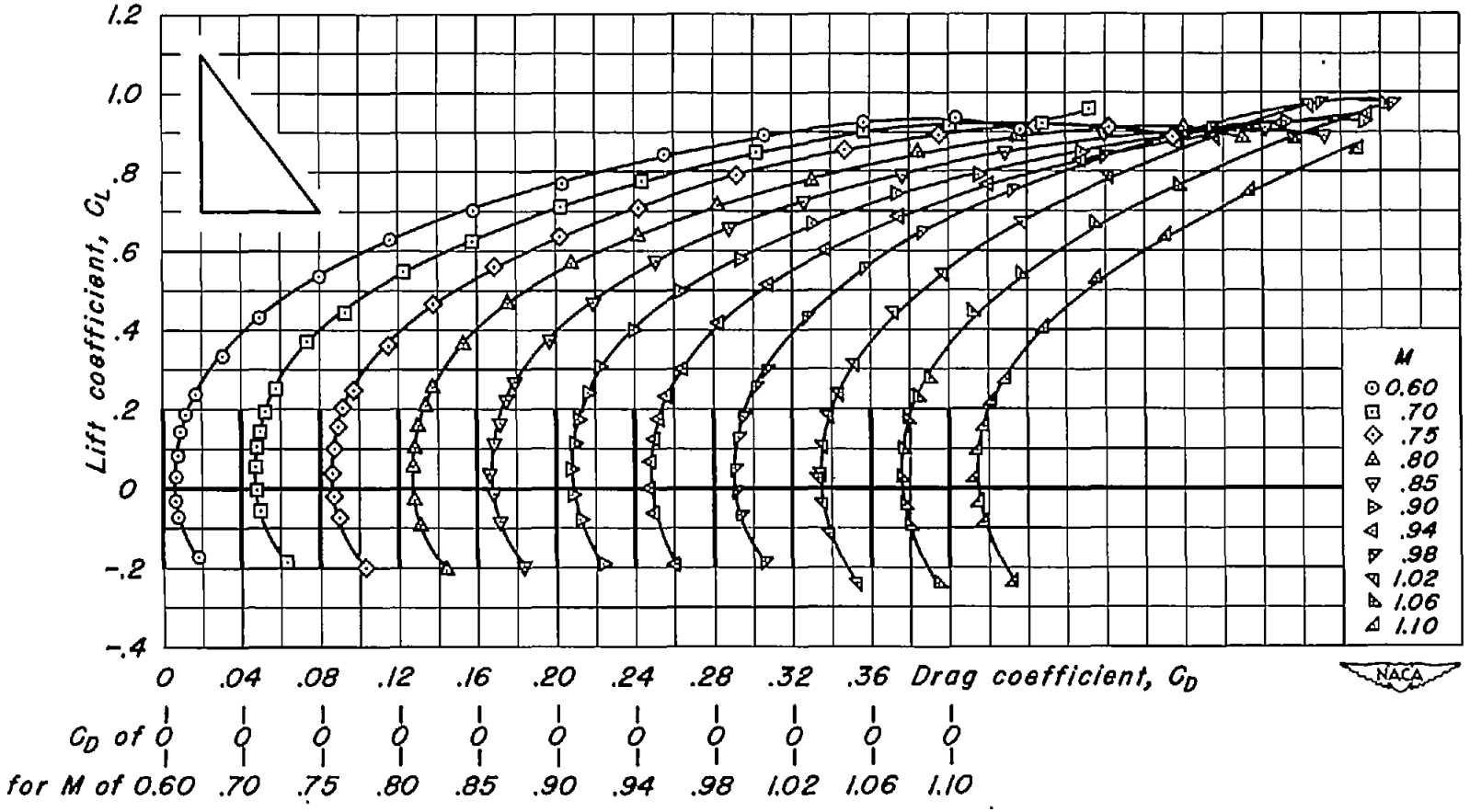

(k) NACA 63A(1.5)04; λ, 0; A, 3.00.
Figure 12.- Continued.

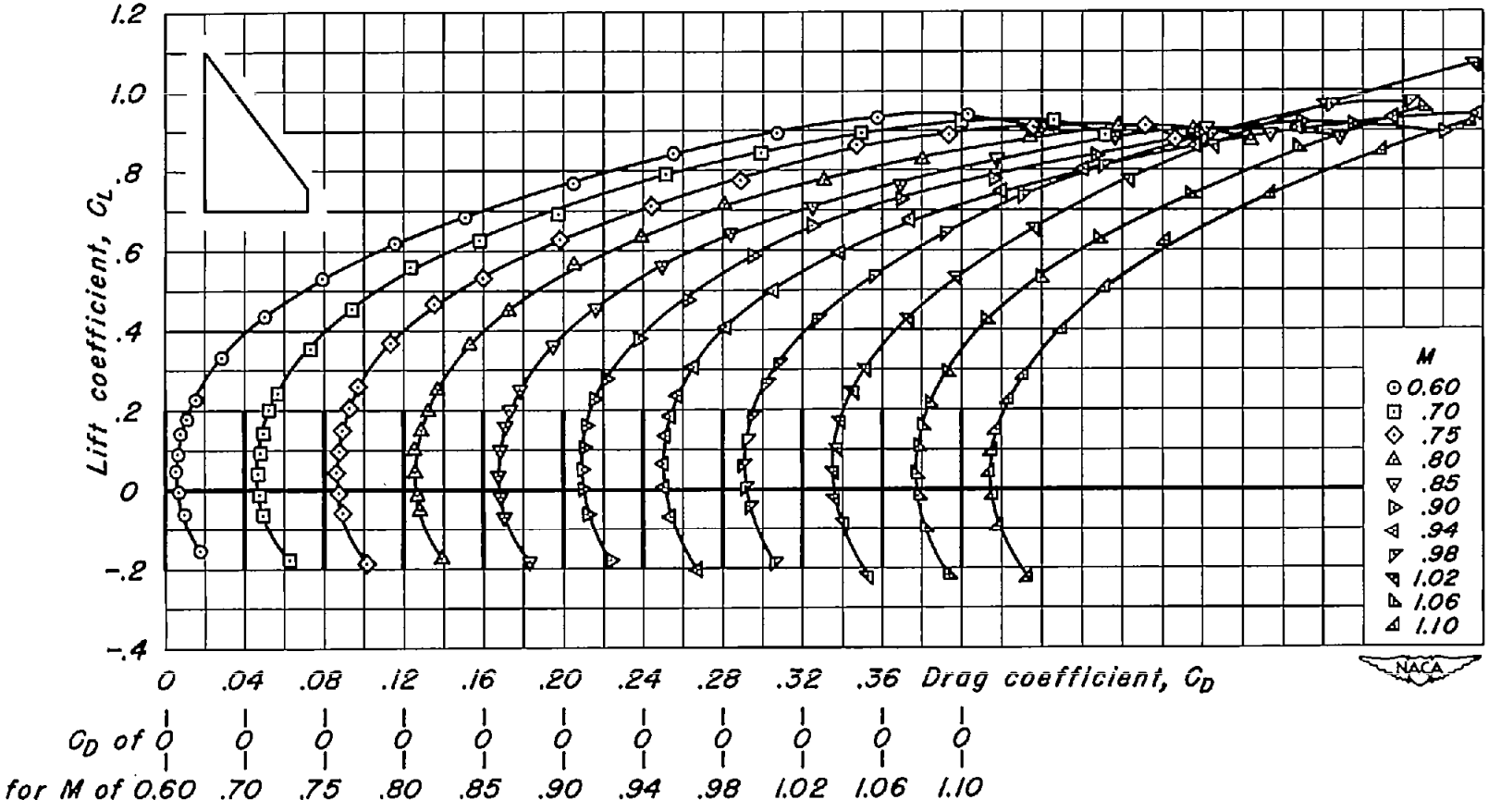

(l) NACA 63A(1.5)04; λ, 0.1; A, 2.46.
Figure 12.- Continued.

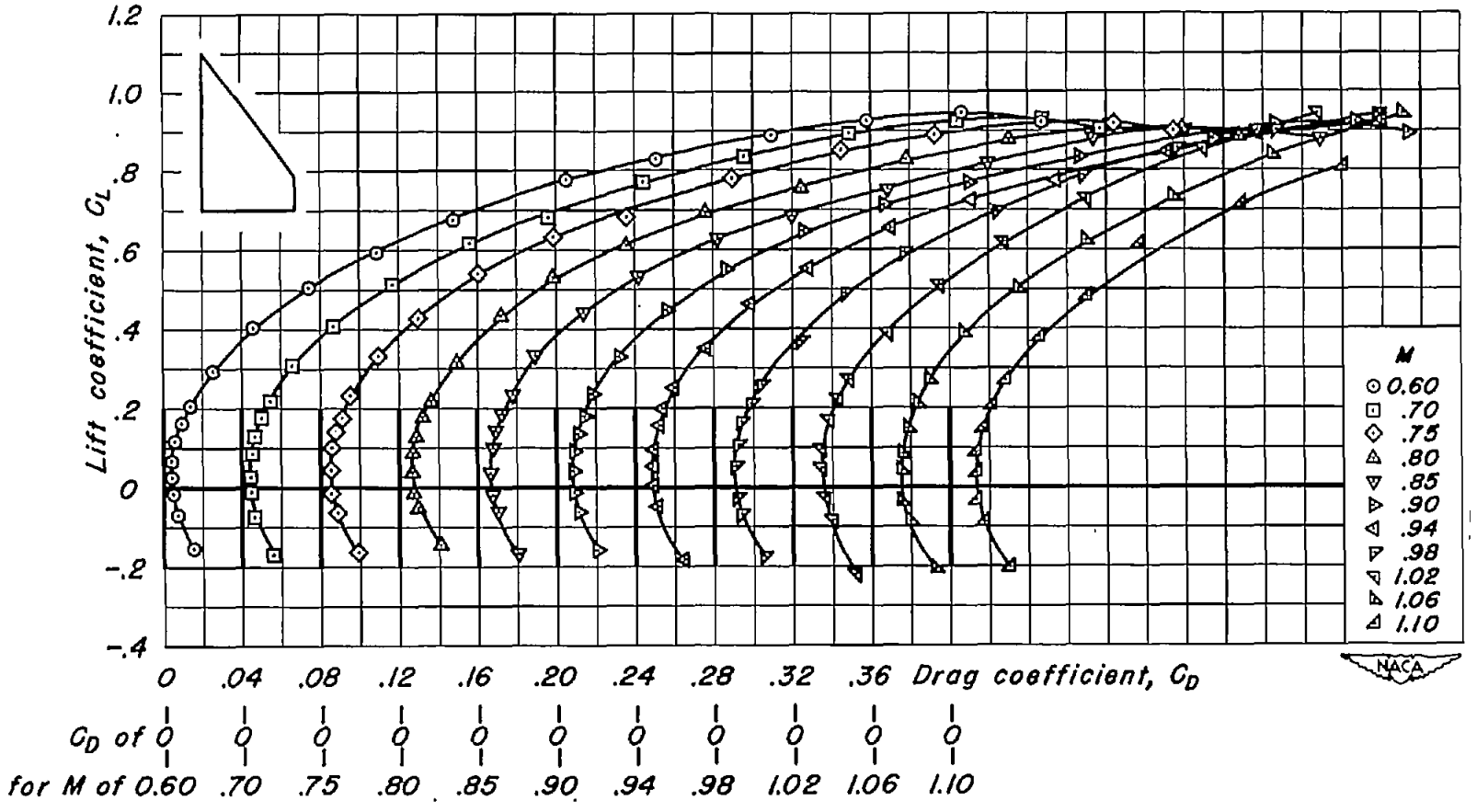

(m) NACA 63A(1.5)04; λ, 0.2; A, 2.00.
Figure 12.- Concluded.

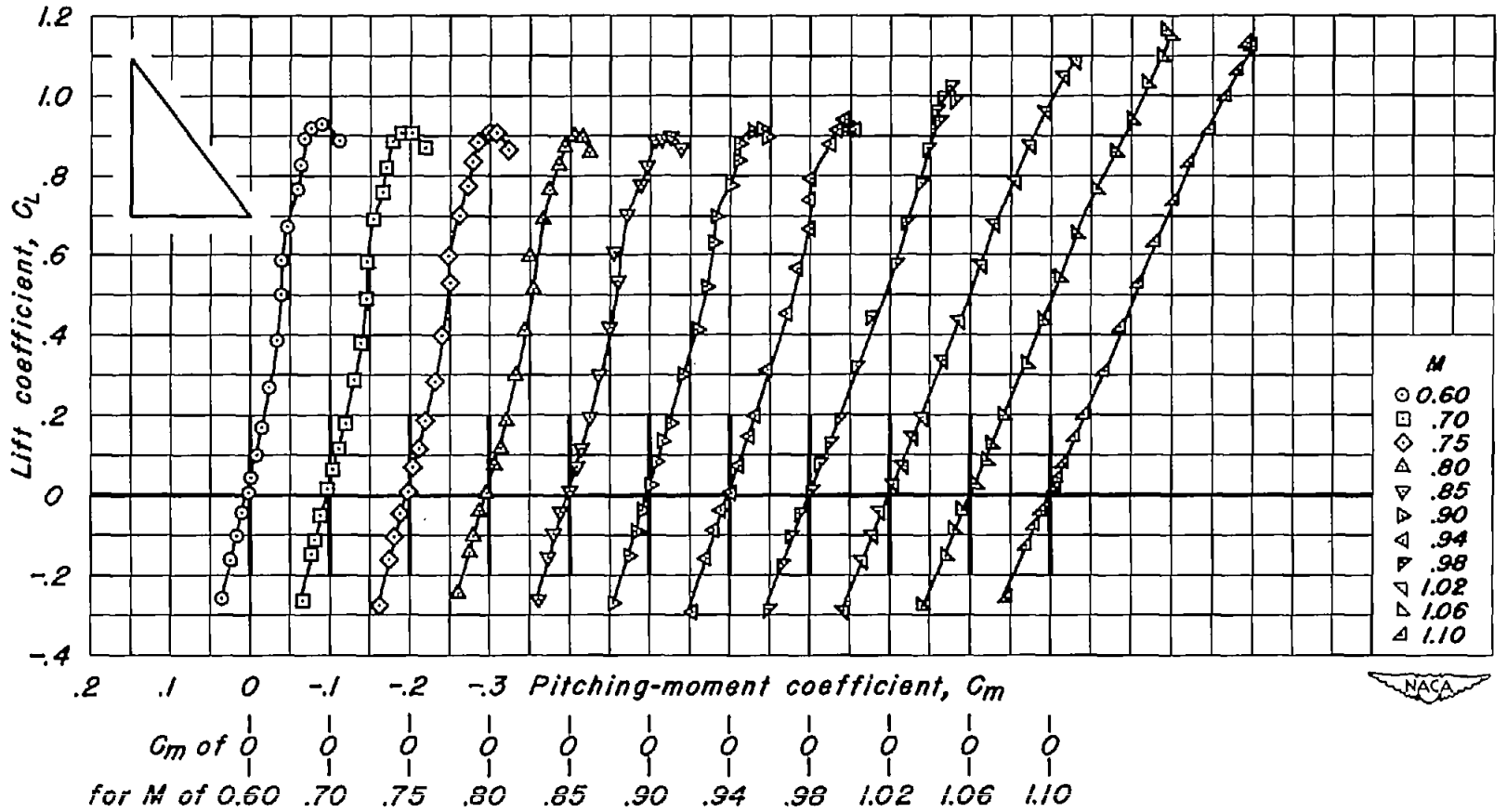

(a) NACA 63A002; λ, 0; A, 3.00.

Figure 13.- Variation of pitching-moment coefficient with lift coefficient for the wings of basic aspect ratio 3.

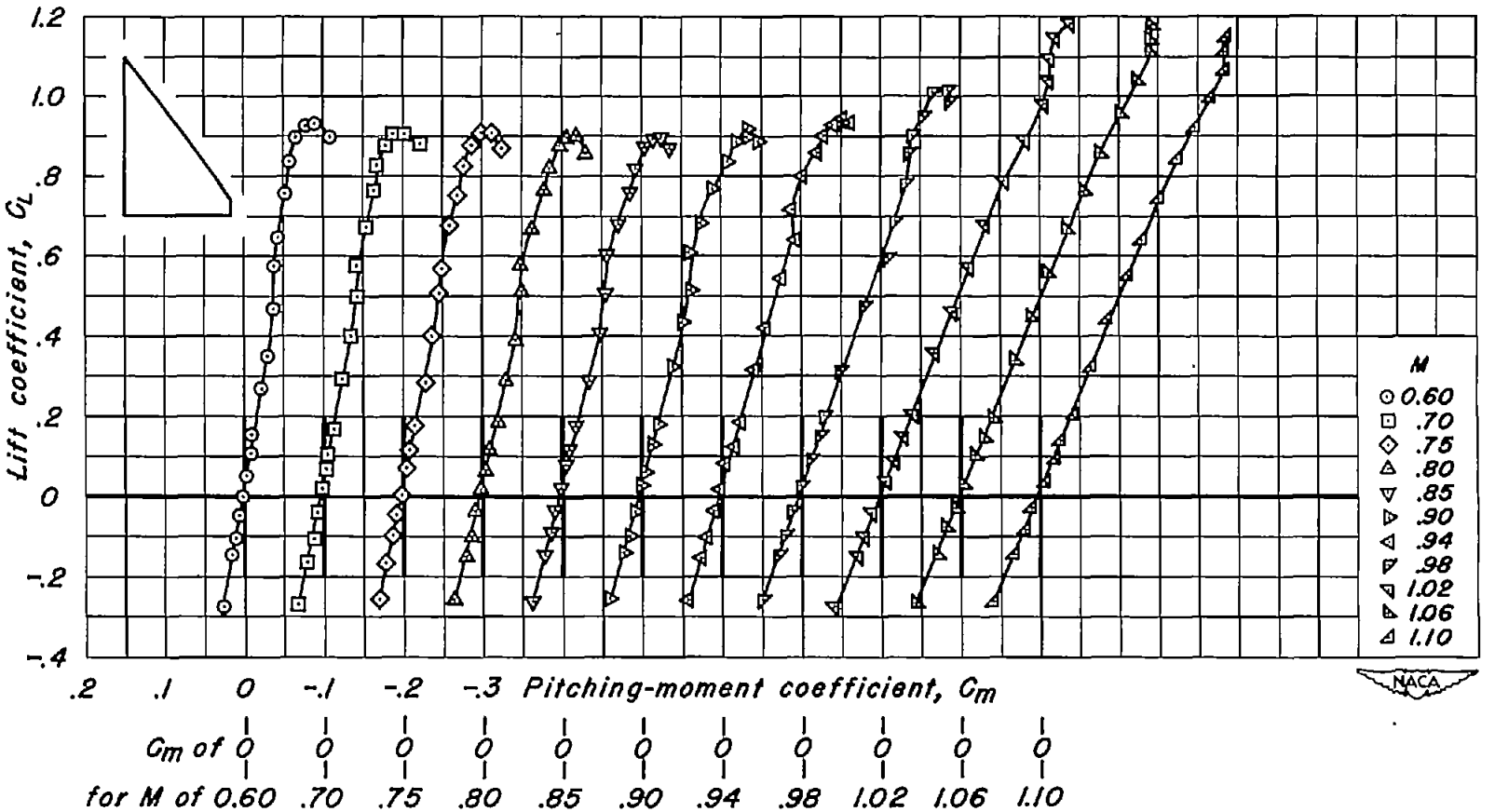

(b) NACA 63A002; λ, 0.1; A, 2.46.
Figure 13.- Continued.

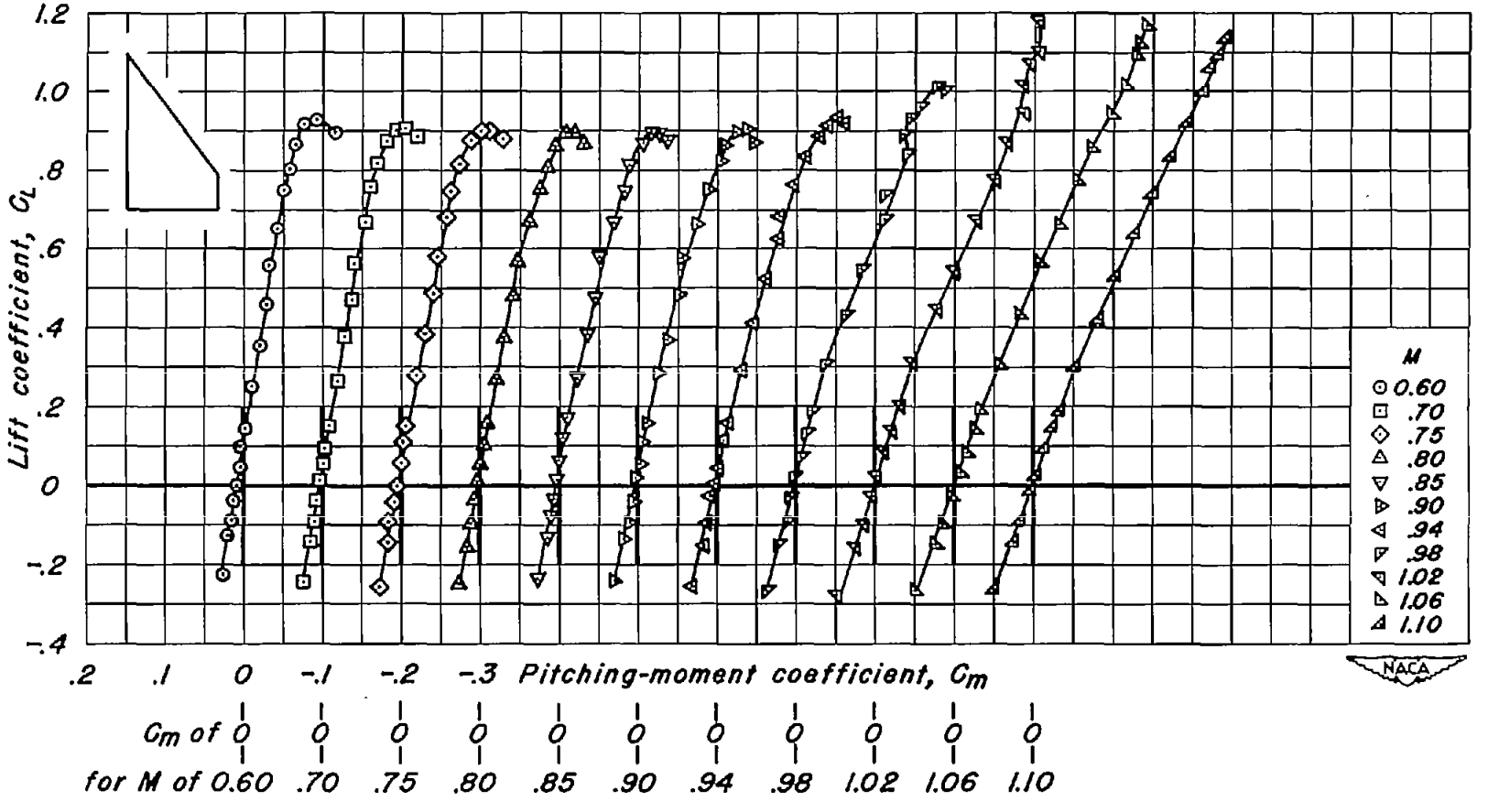

(c) NACA 63A002; λ, 0.2; A, 2.00.
Figure 13.- Continued.

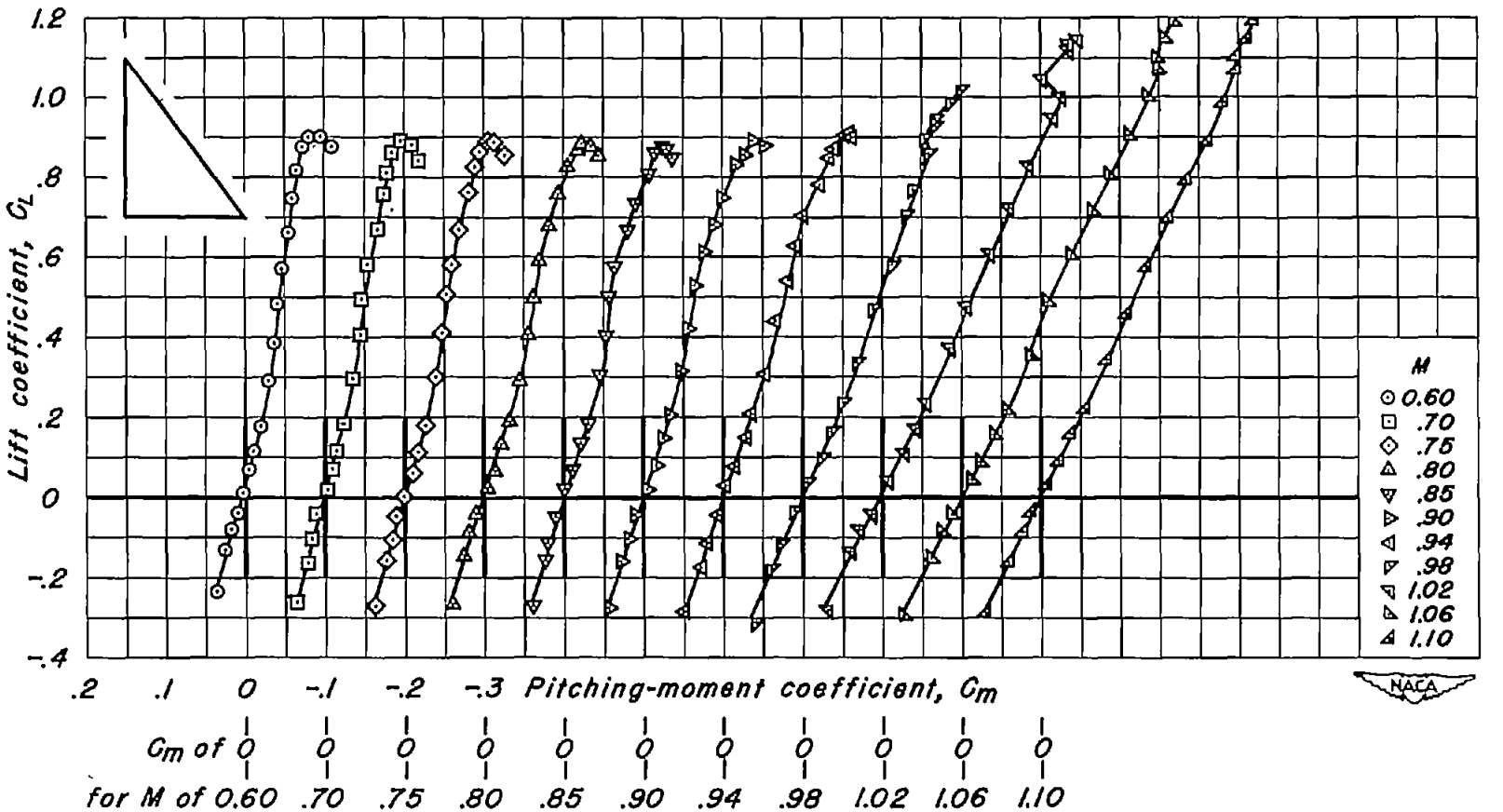

(d) NACA 63A004; λ, 0; A, 3.00.
Figure 13.- Continued.

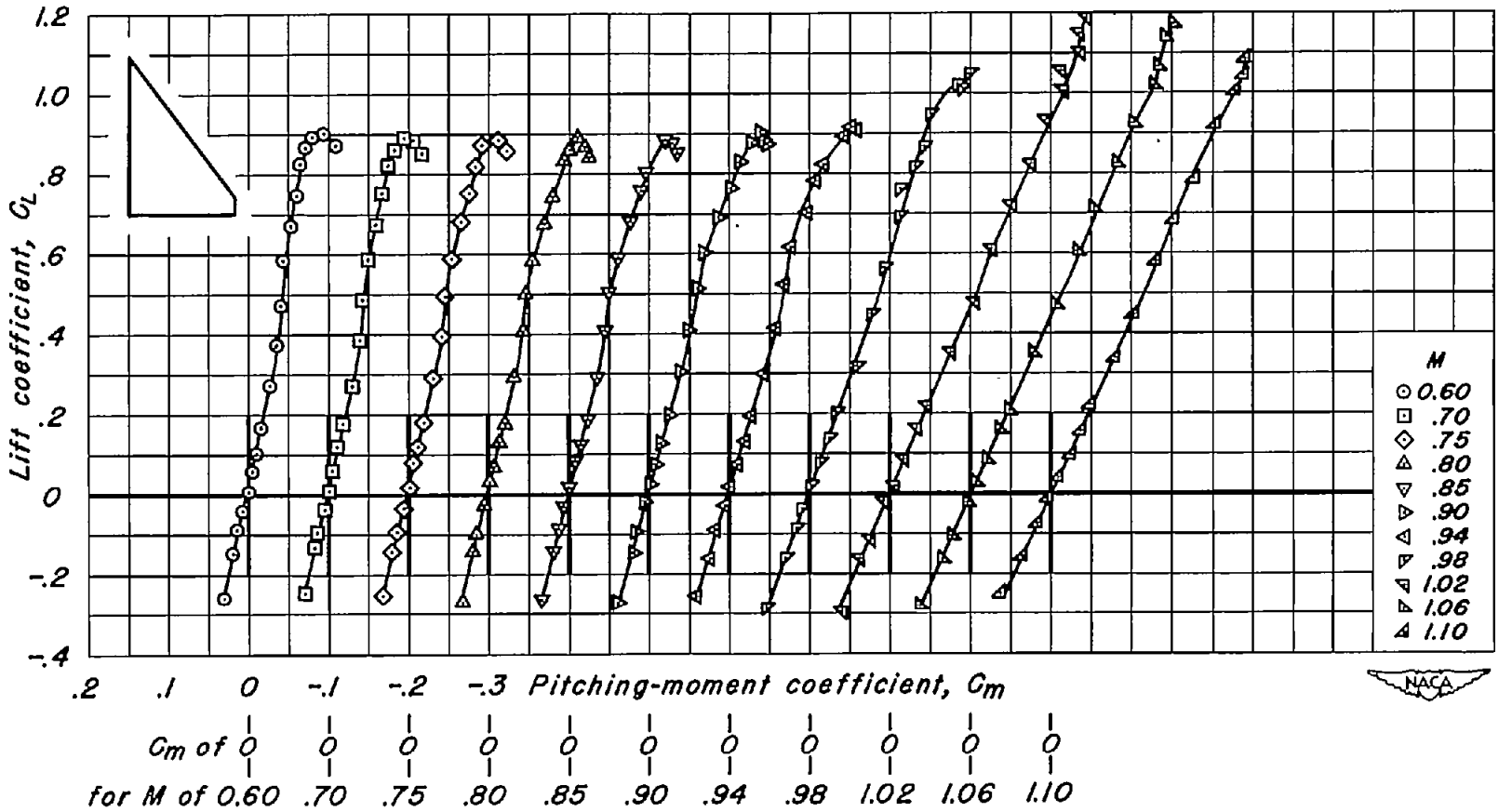

(e) NACA 63A004; λ, 0.1; A, 2.46.
Figure 13.- Continued.

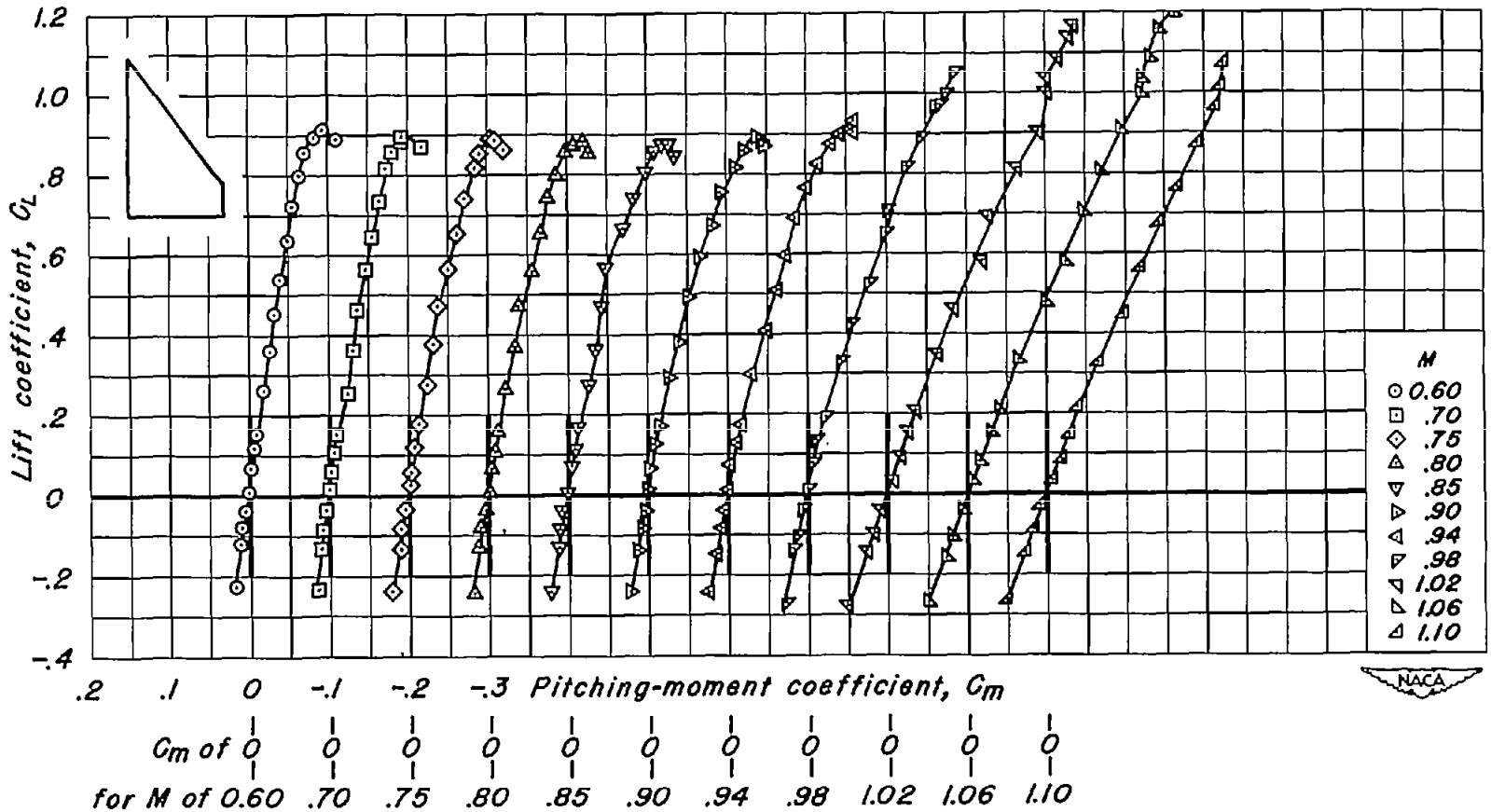

(f) NACA 63A004; λ, 0.2; A, 2.00.
Figure 13.- Continued.

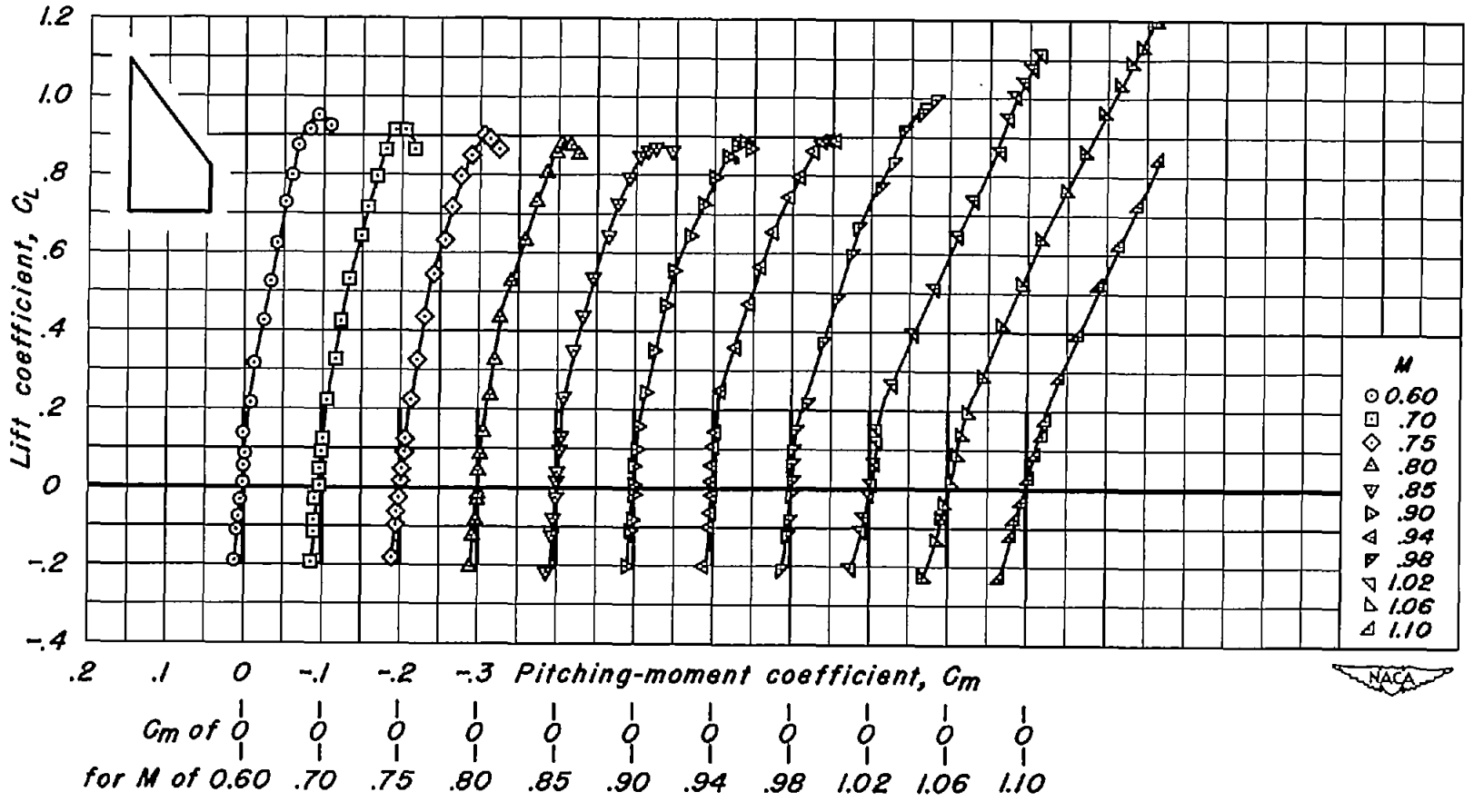

(g) NACA 63A004; λ, 0.3; A, 1.62.
Figure 13.- Continued.

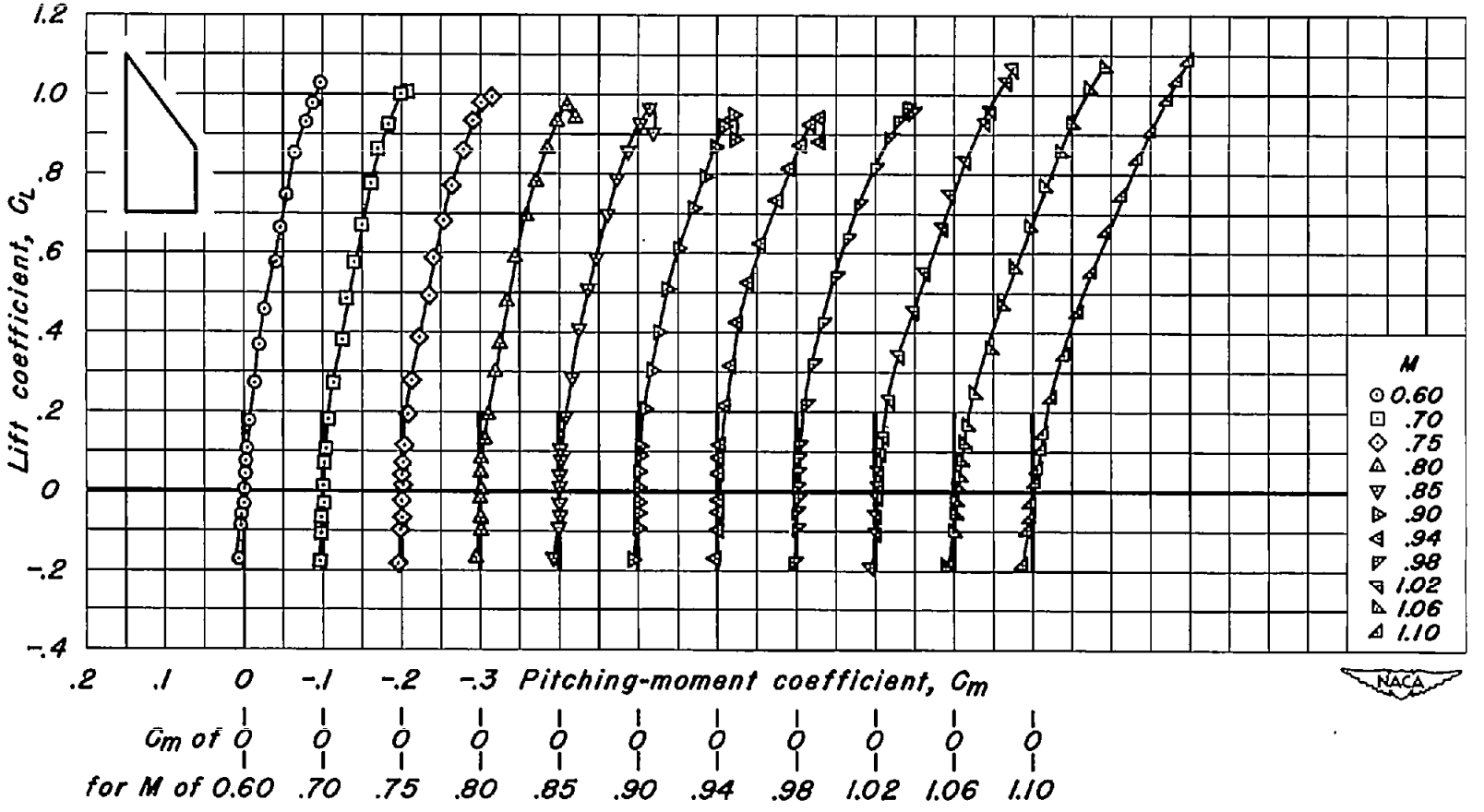

(h) NACA 63A004; λ, 0.4; A, 1.29.
Figure 13.- Continued.

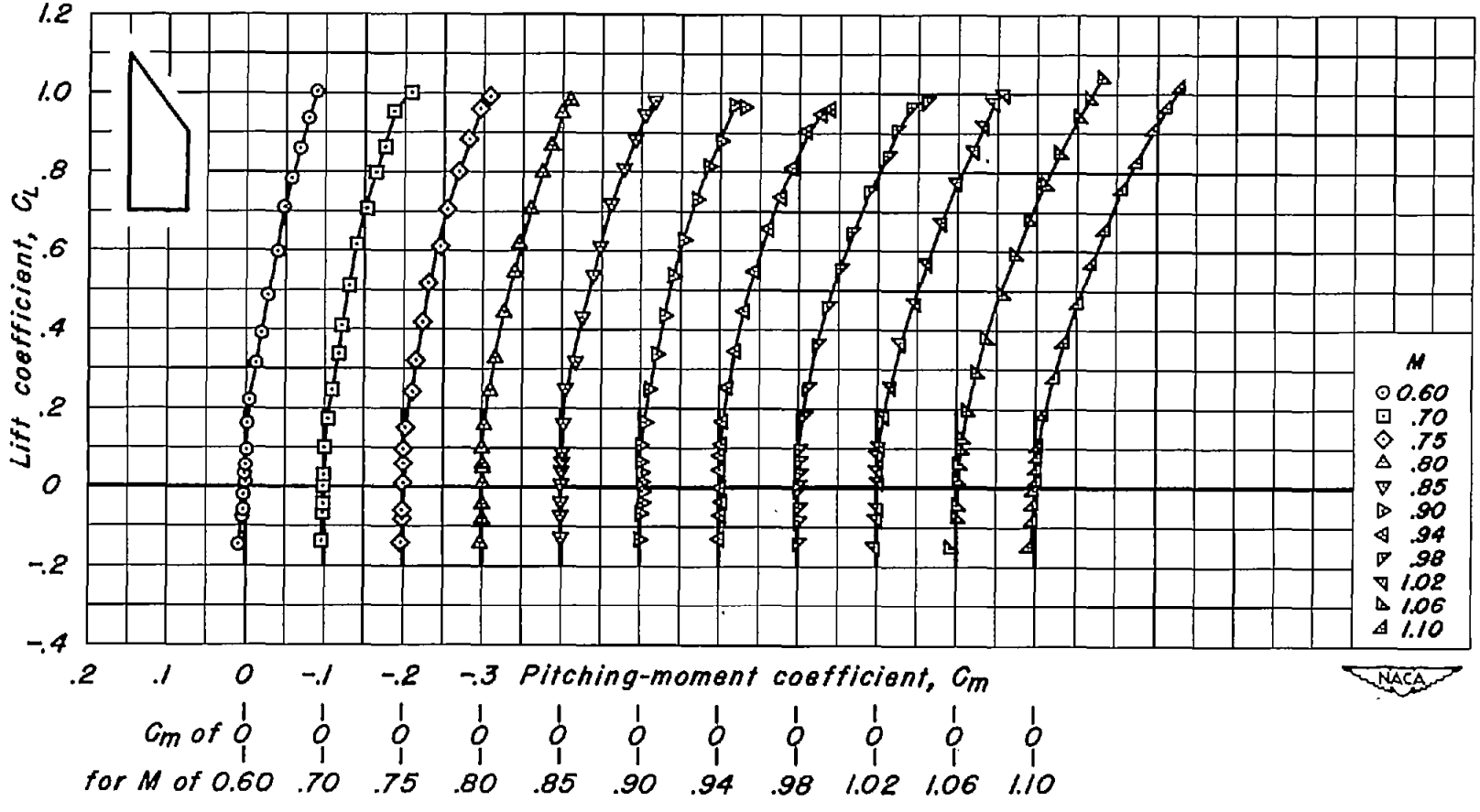

(i) NACA 63A004; λ, 0.5; A, 1.00.
Figure 13.- Continued.

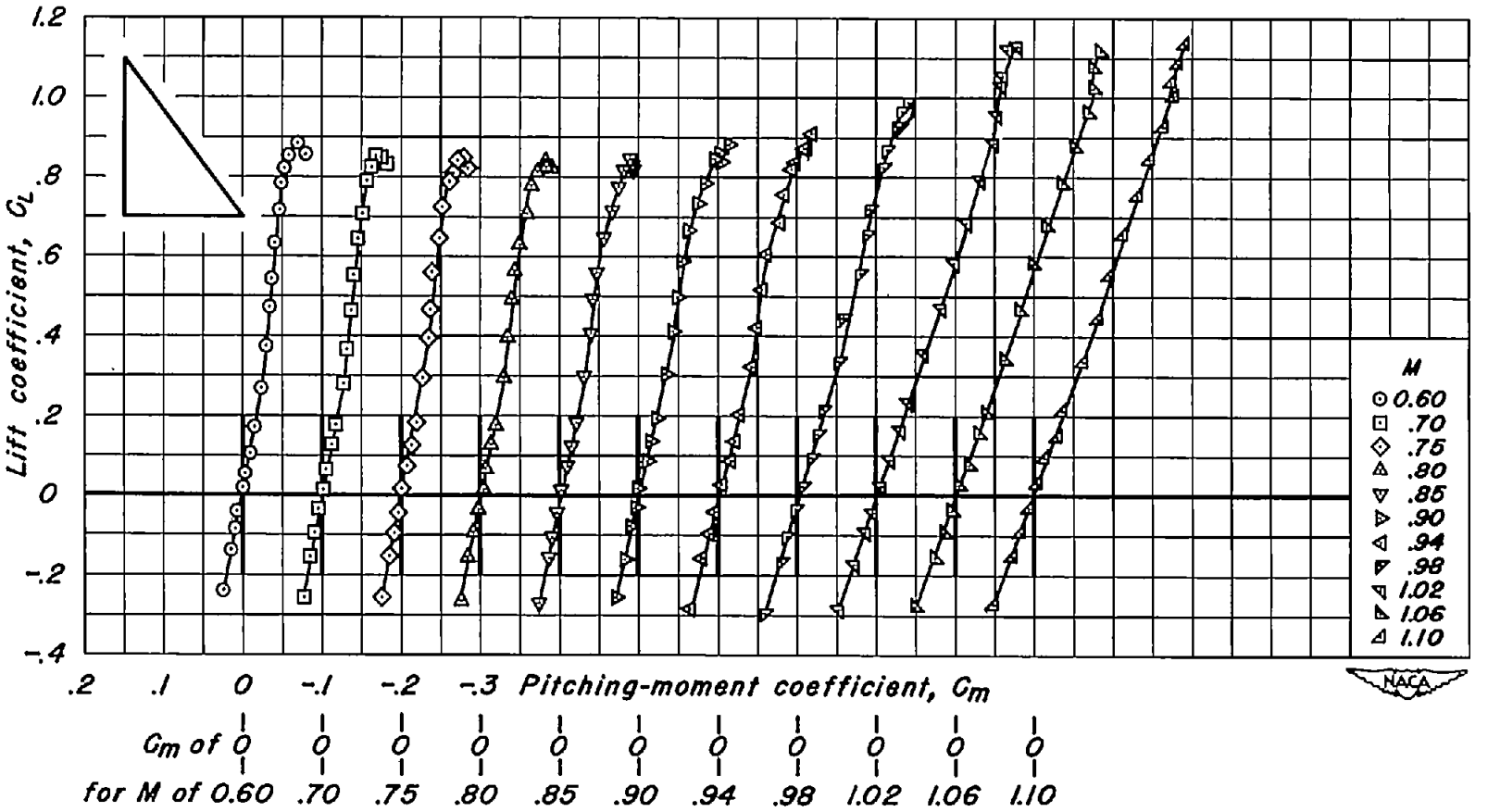

(j) NACA 63A006; λ, 0; A, 3.00.
Figure 13.- Continued.

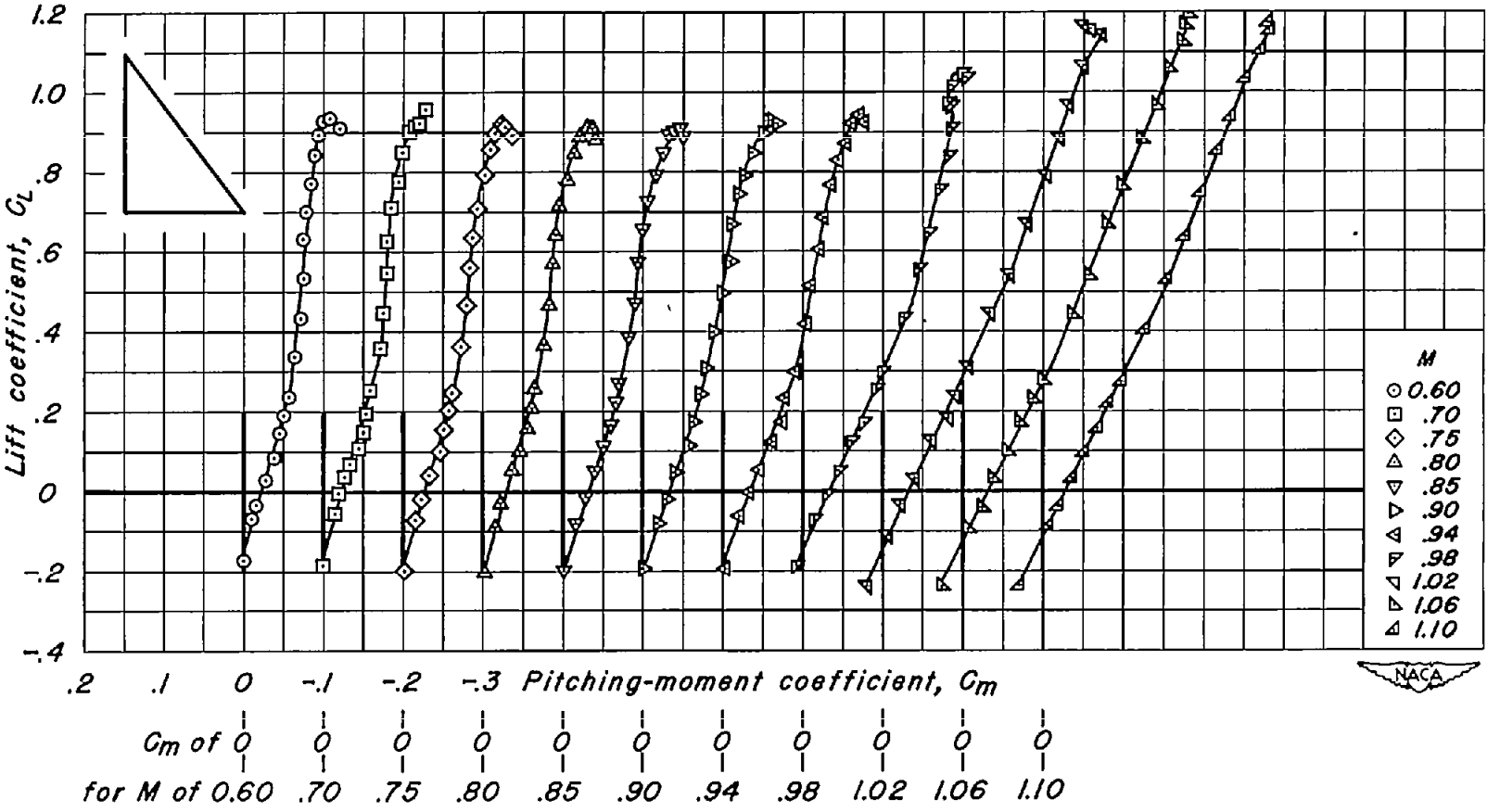

(k) NACA 63A(1.5)04; λ, 0; A, 3.00.
Figure 13.- Continued.

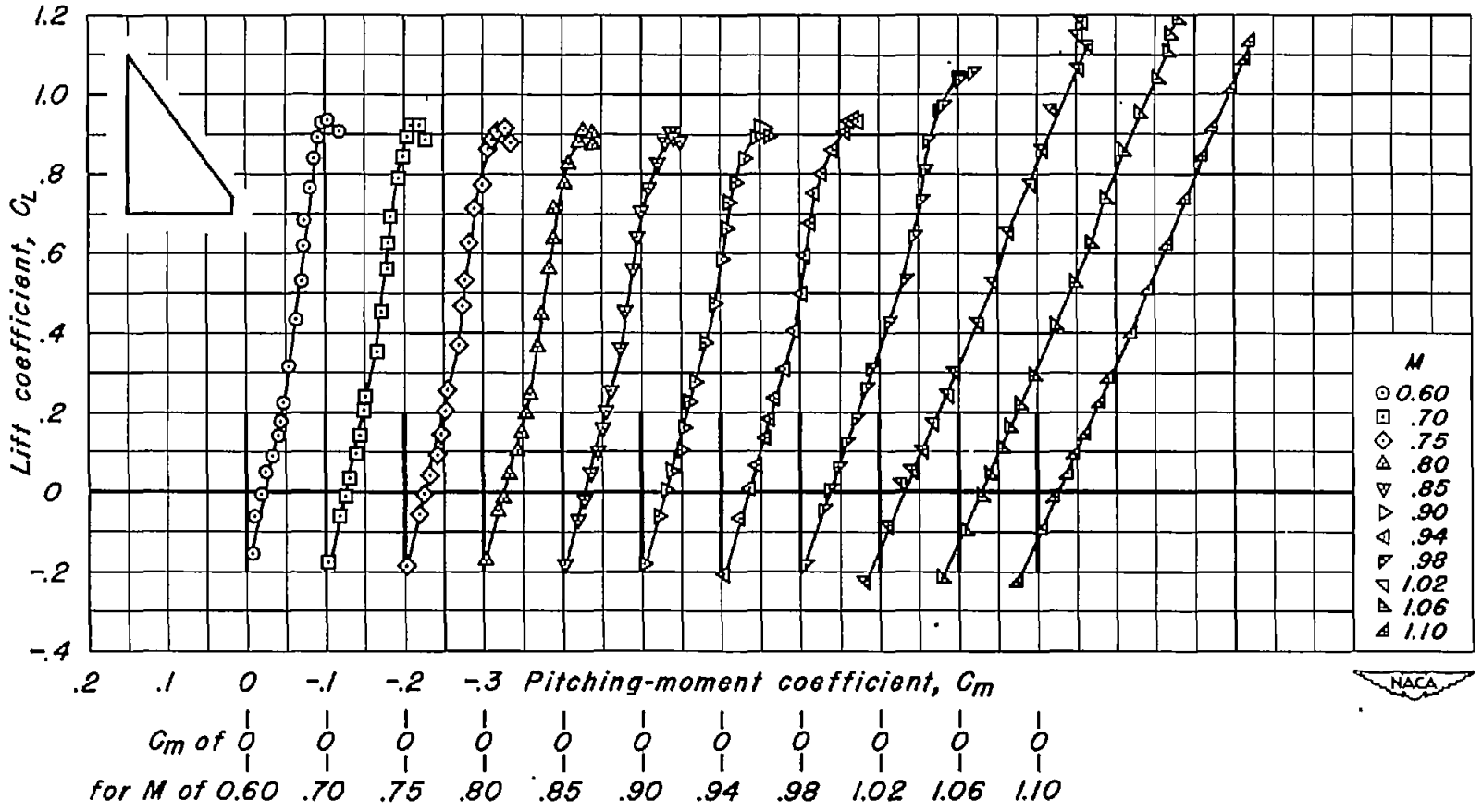

(1) NACA 63A(1.5)04; λ, 0.1; A, 2.46.
Figure 13.- Continued.

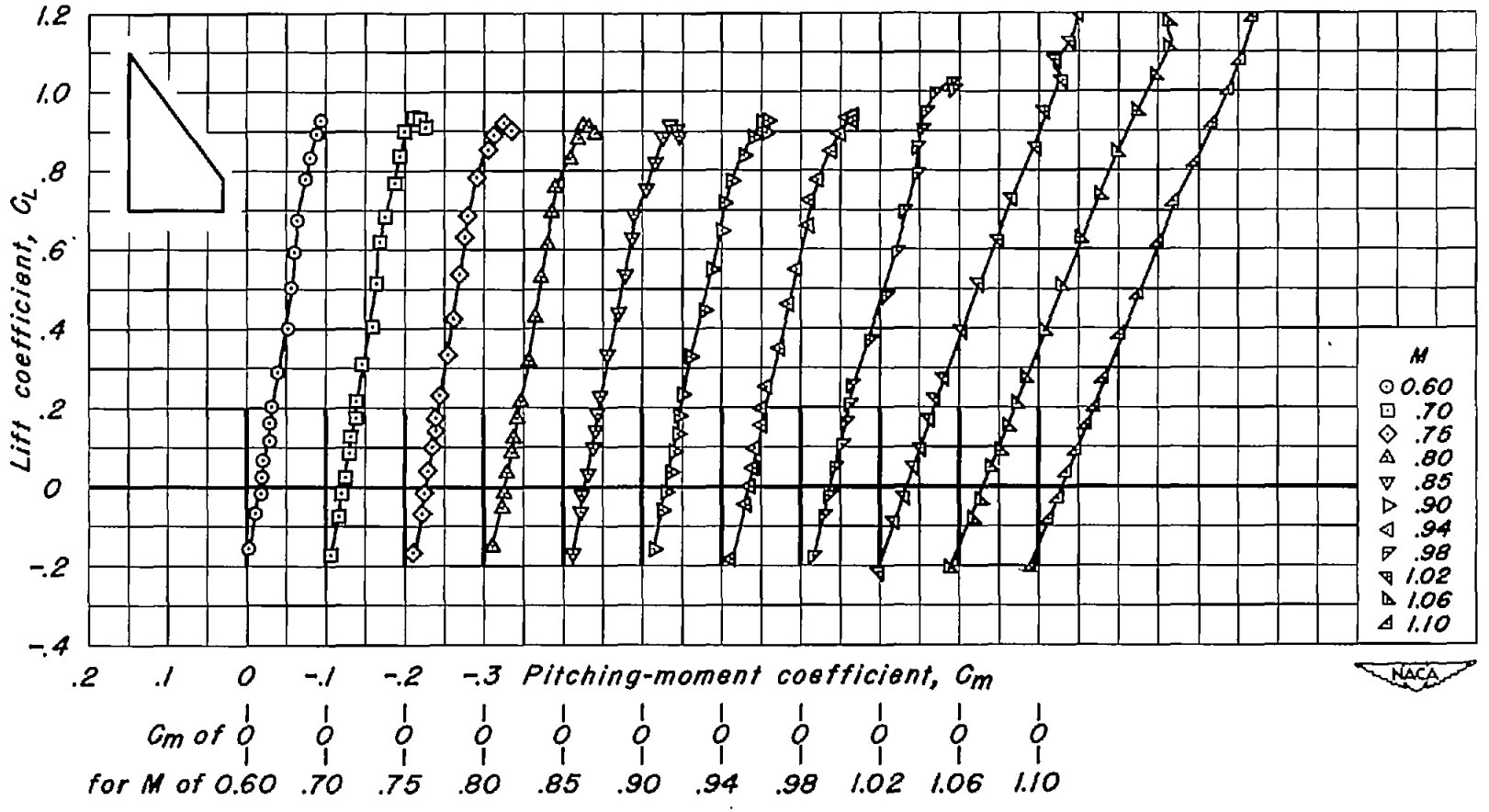

(m) NACA 63A(1.5)04; λ, 0.2; A, 2.00.
Figure 13.- Concluded.

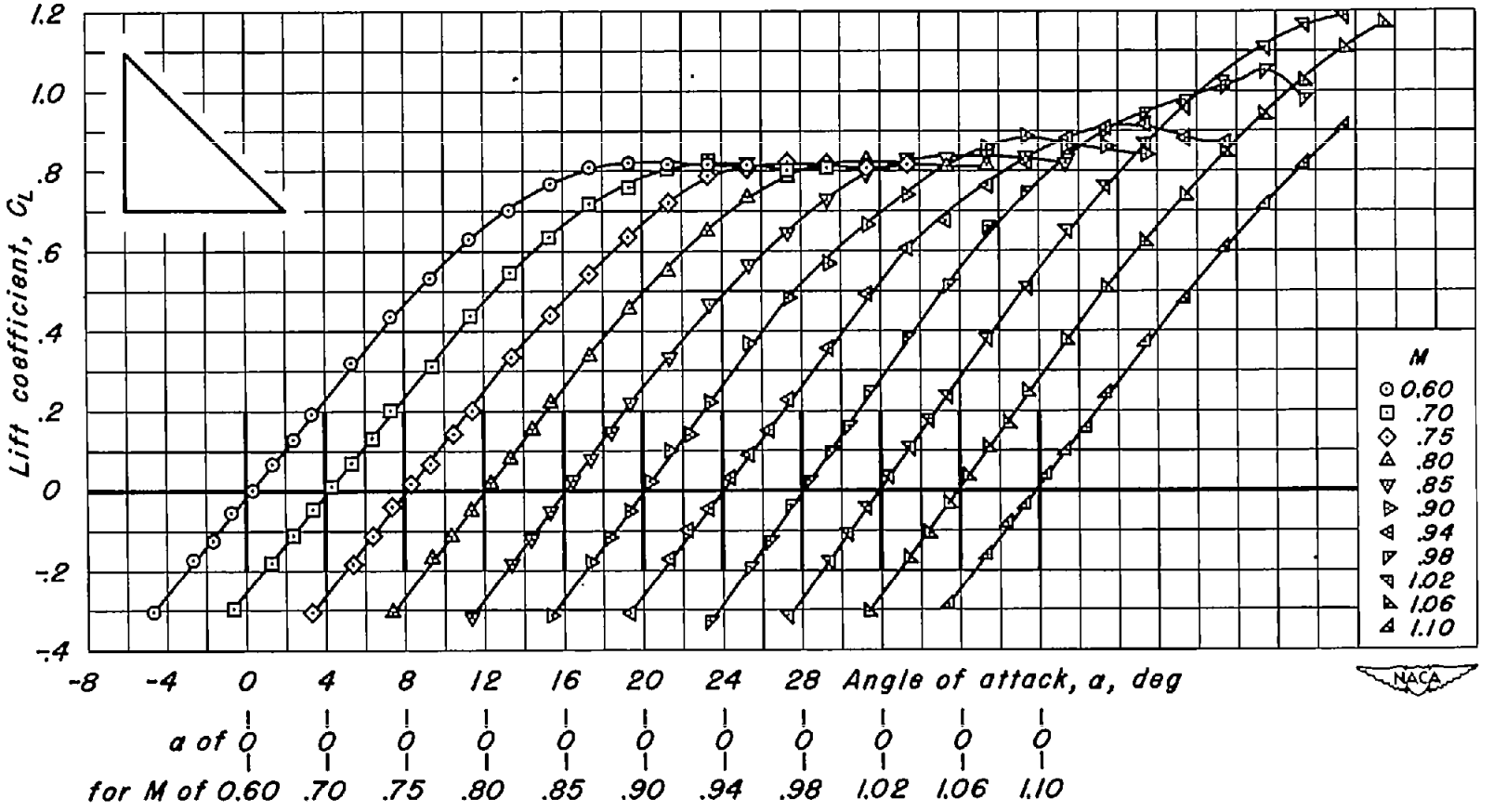

(a) NACA 63A002; λ, 0; A, 4.00.

Figure 14.- Variation of lift coefficient with angle of attack for the wings of basic aspect ratio 4.

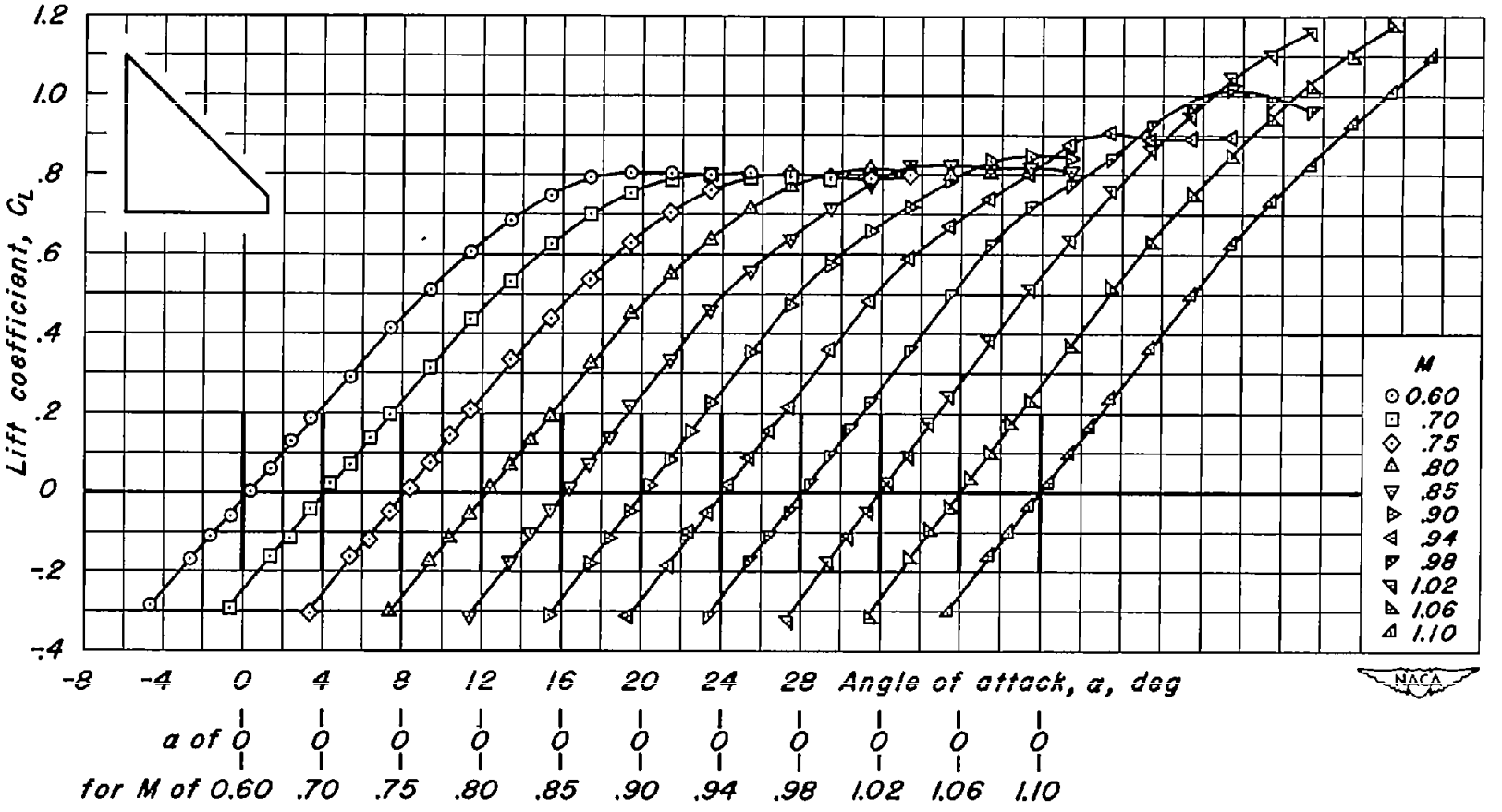

(b) NACA 63A002; λ, 0.1; A, 3.27.
Figure 14.- Continued.

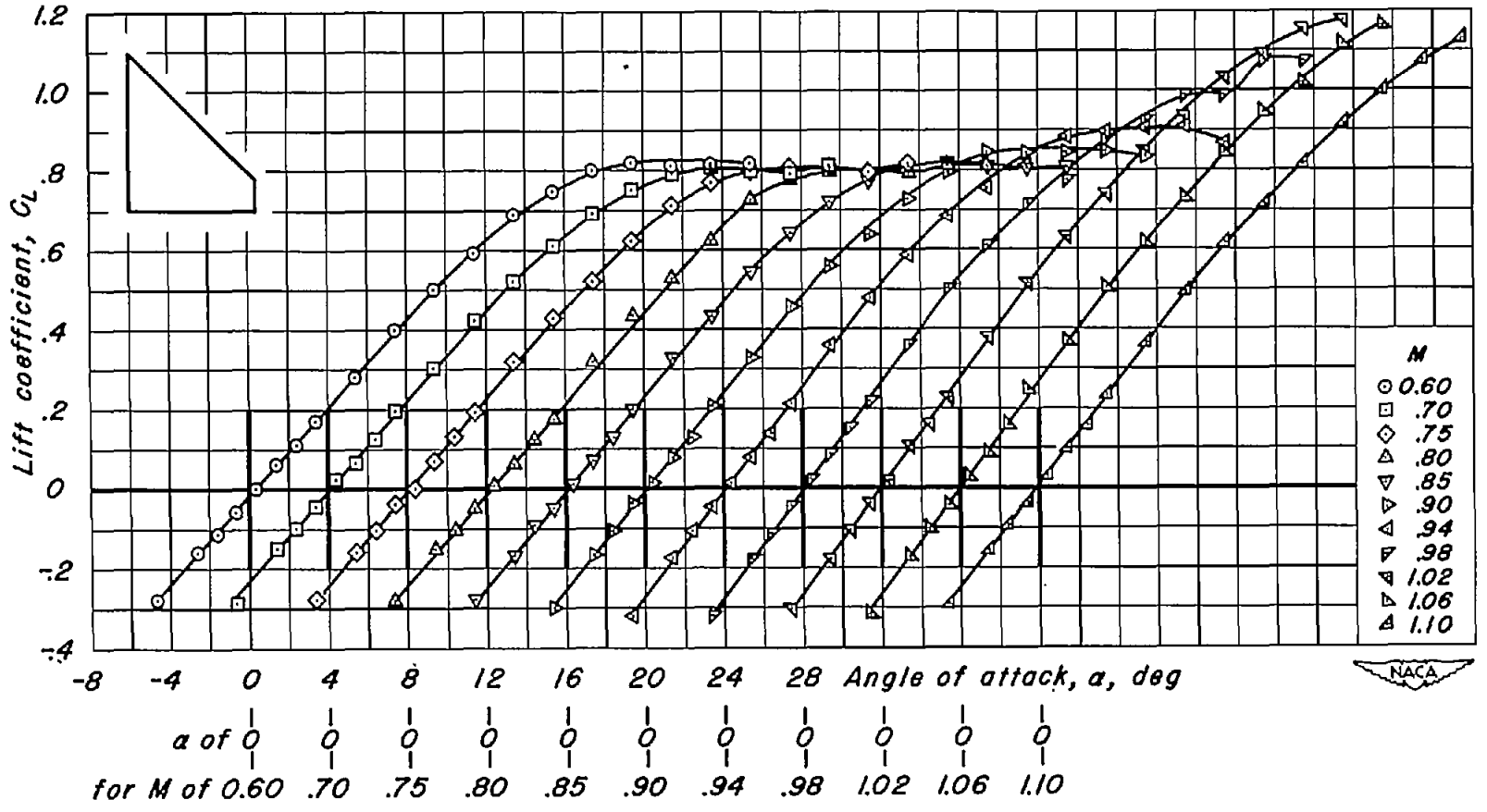

(c) NACA 63A002; λ, 0.2; A, 2.67.
Figure 14.- Continued.

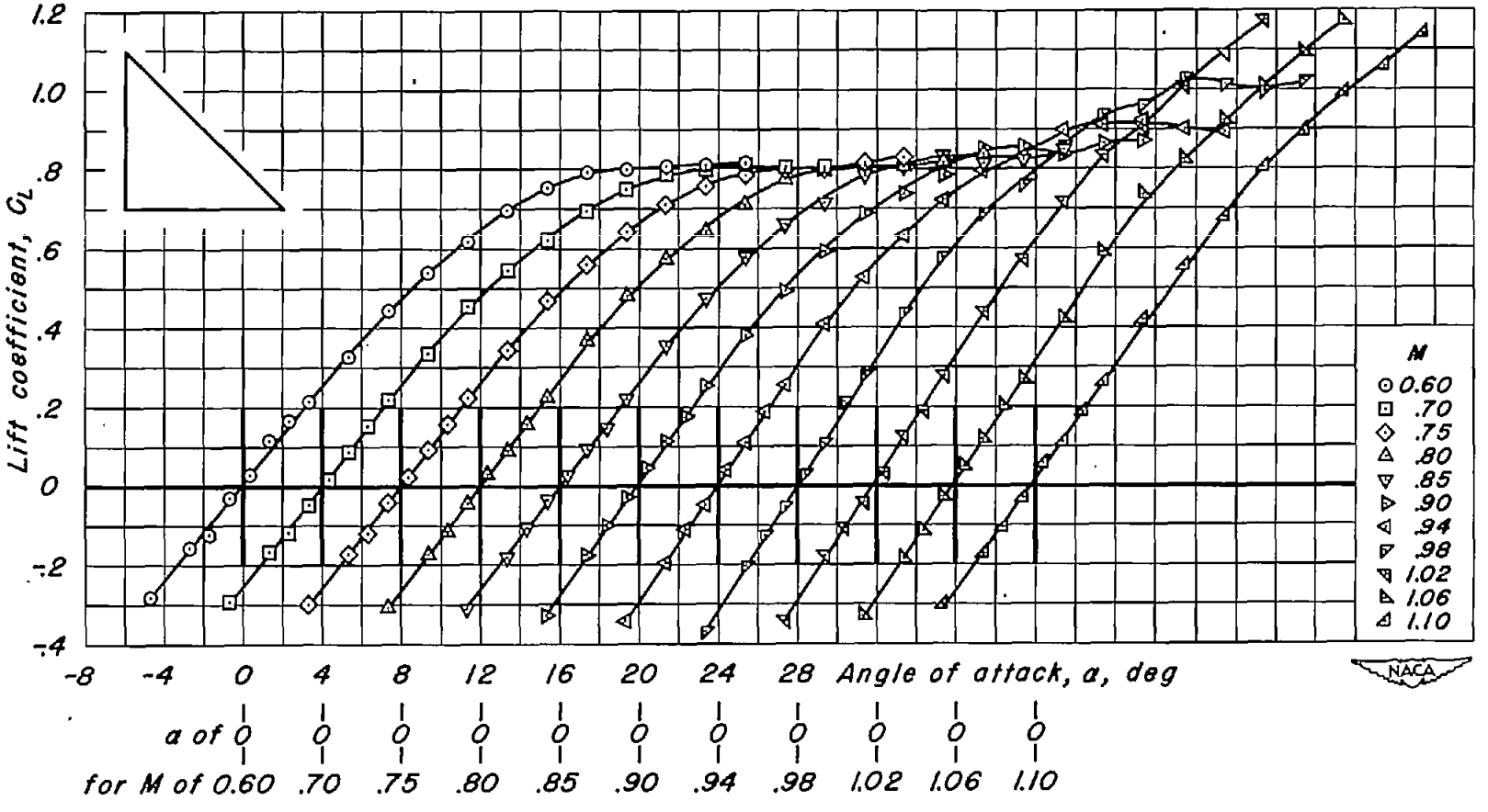

(d) NACA 63A004; λ, 0; A, 4.00.
Figure 14.- Continued.

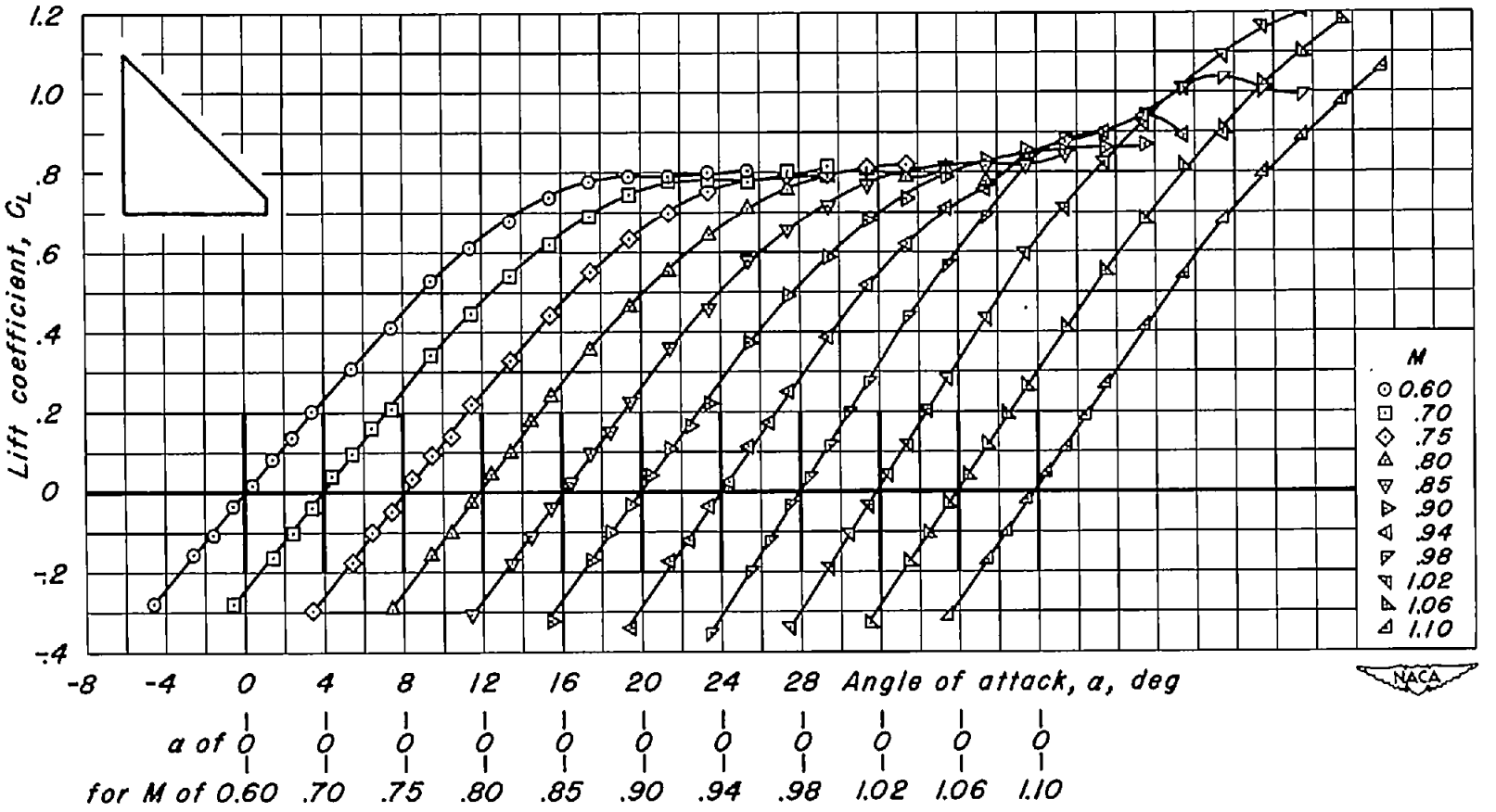

(e) NACA 63A004; λ, 0.1; A, 3.27.
Figure 14.- Continued.

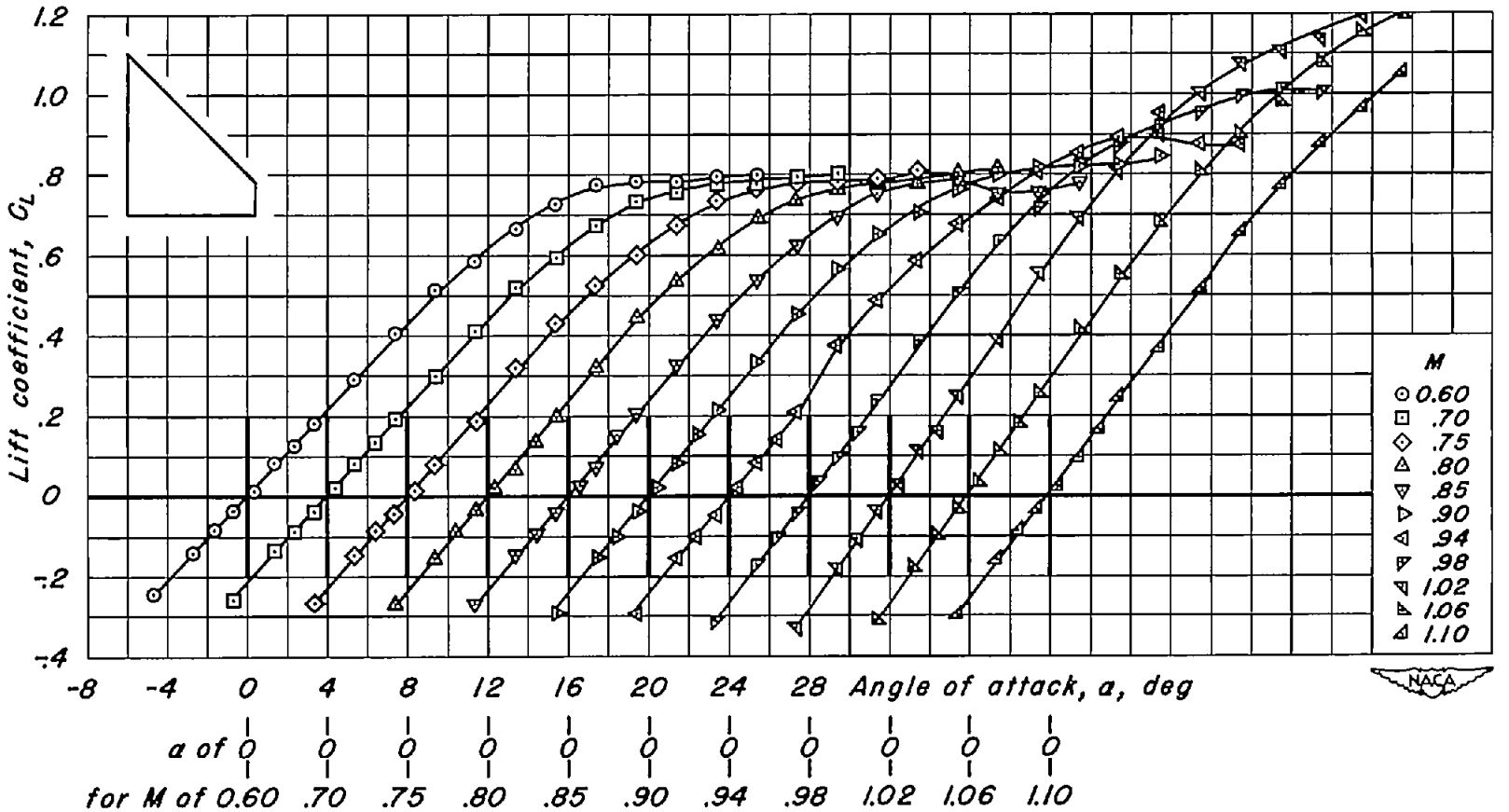

(f) NACA 63A004; λ, 0.2; A, 2.67.
Figure 14.- Continued.

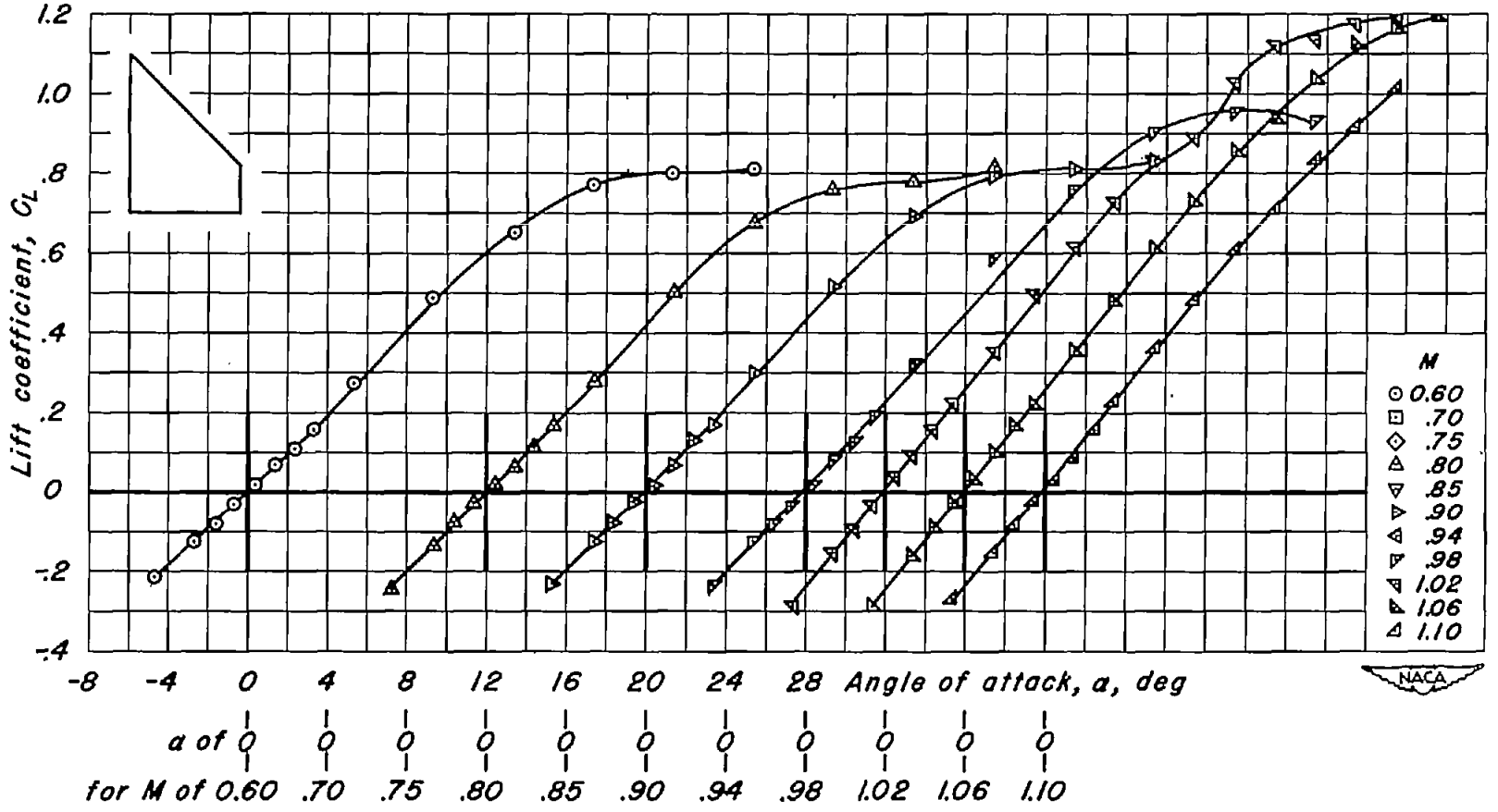

(g) NACA 63A004; λ, 0.3; A, 2.15.
Figure 14.- Continued.

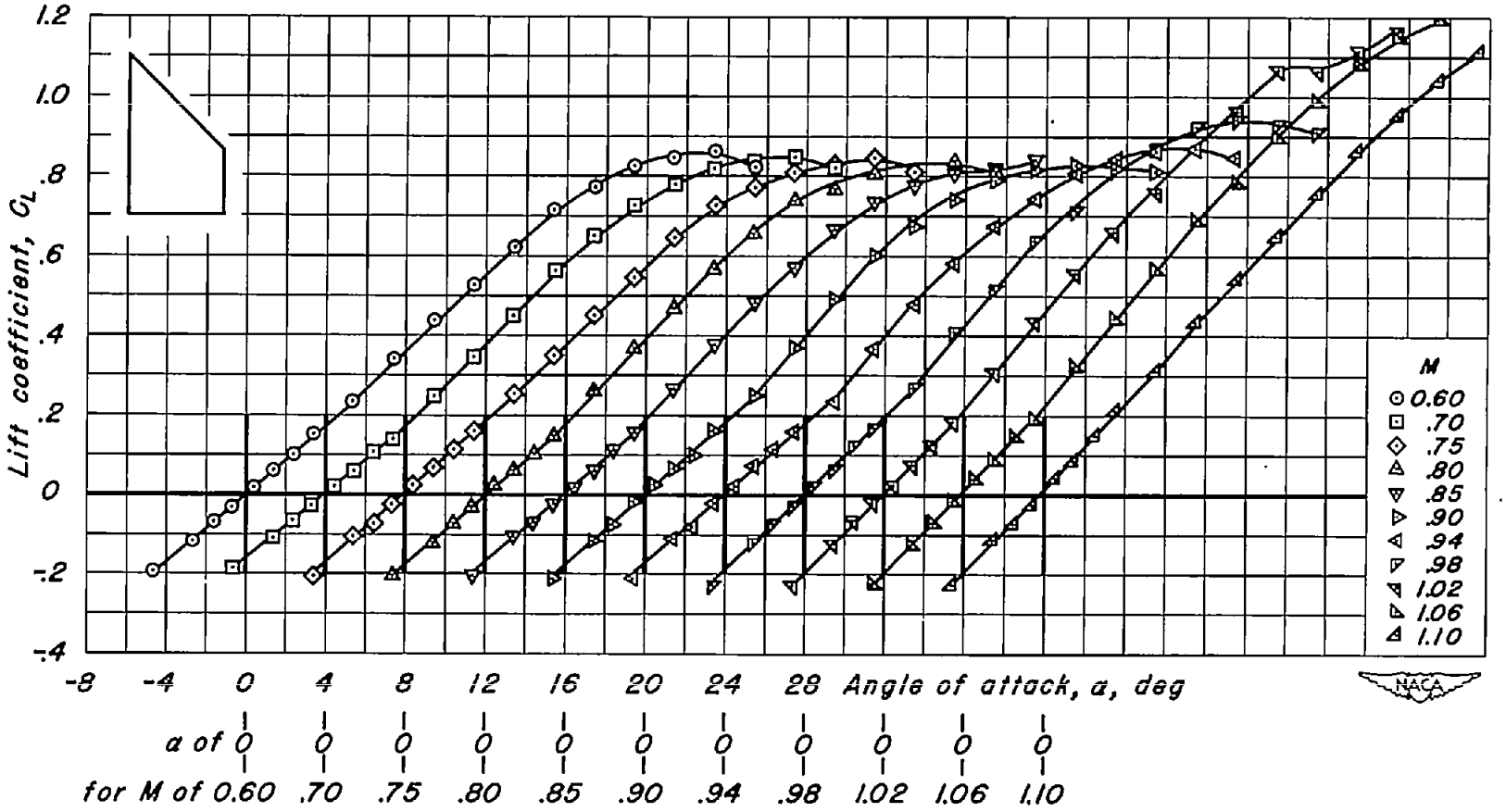

(h) NACA 63A004; λ, 0.4; A, 1.71.
Figure 14.- Continued.

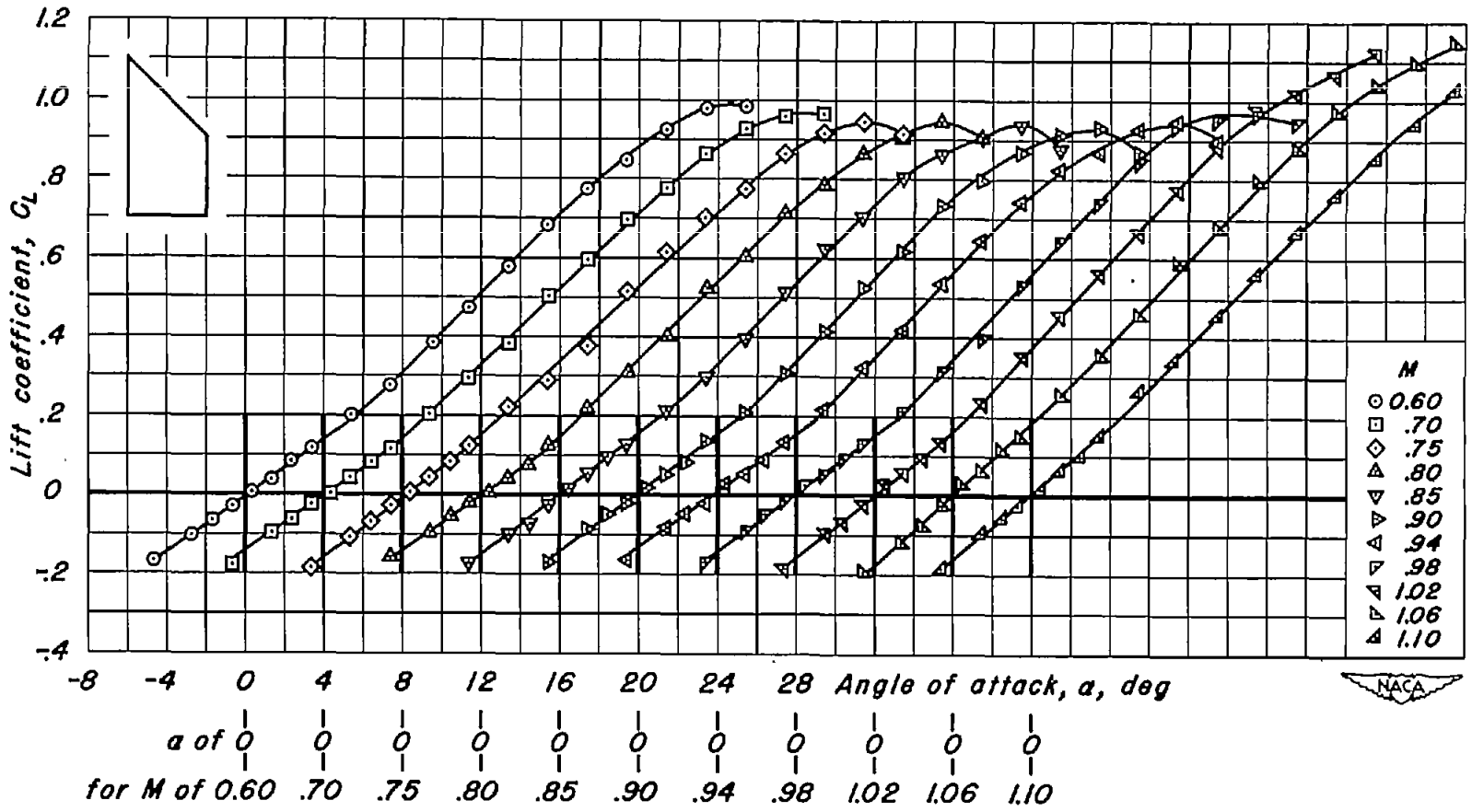

(l) NACA 63A004; λ, 0.5; A, 1.33.
Figure 14.- Continued.

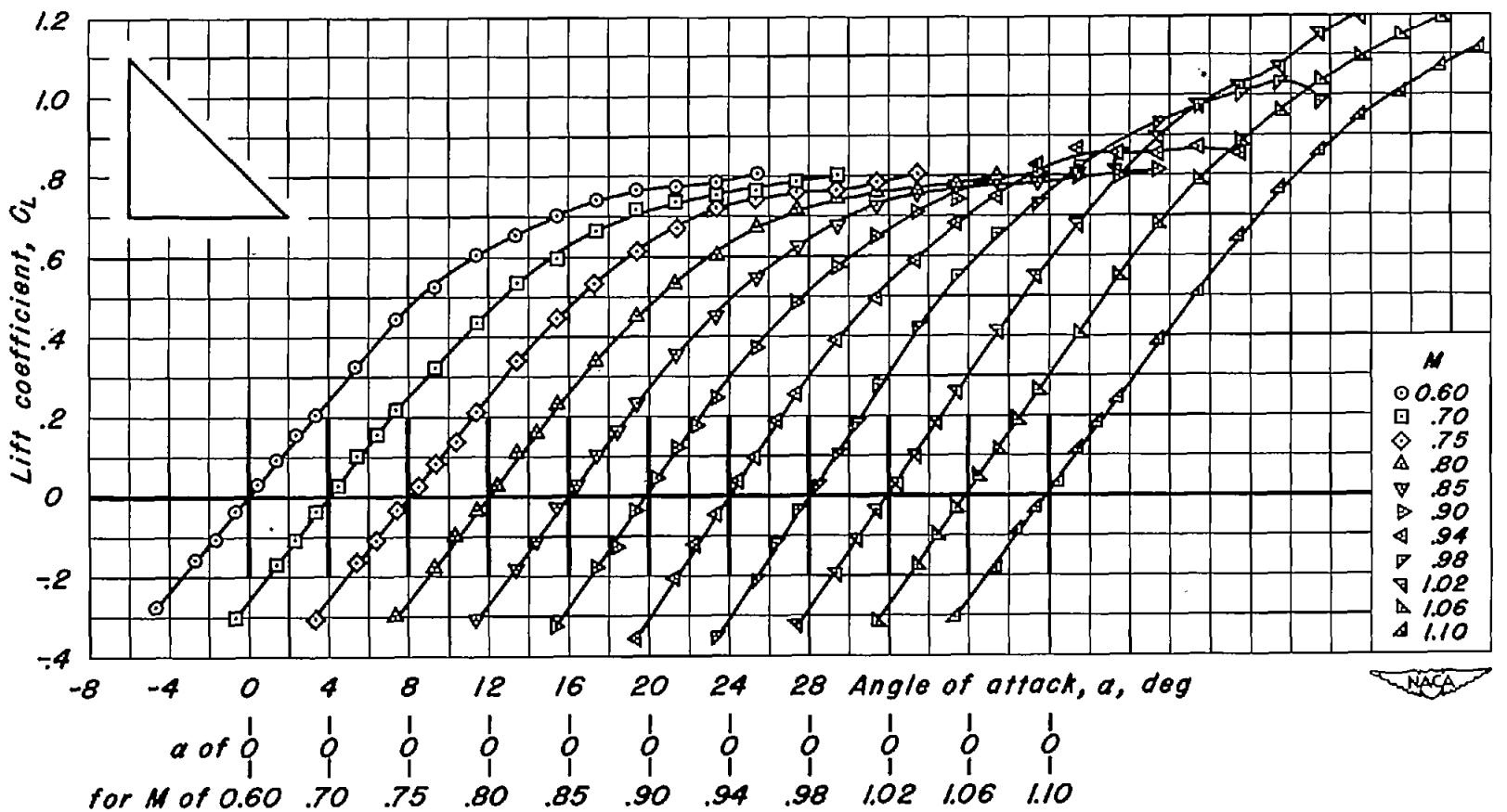

(j) NACA 63A006; λ, 0; A, 4.00.
Figure 14.- Continued.

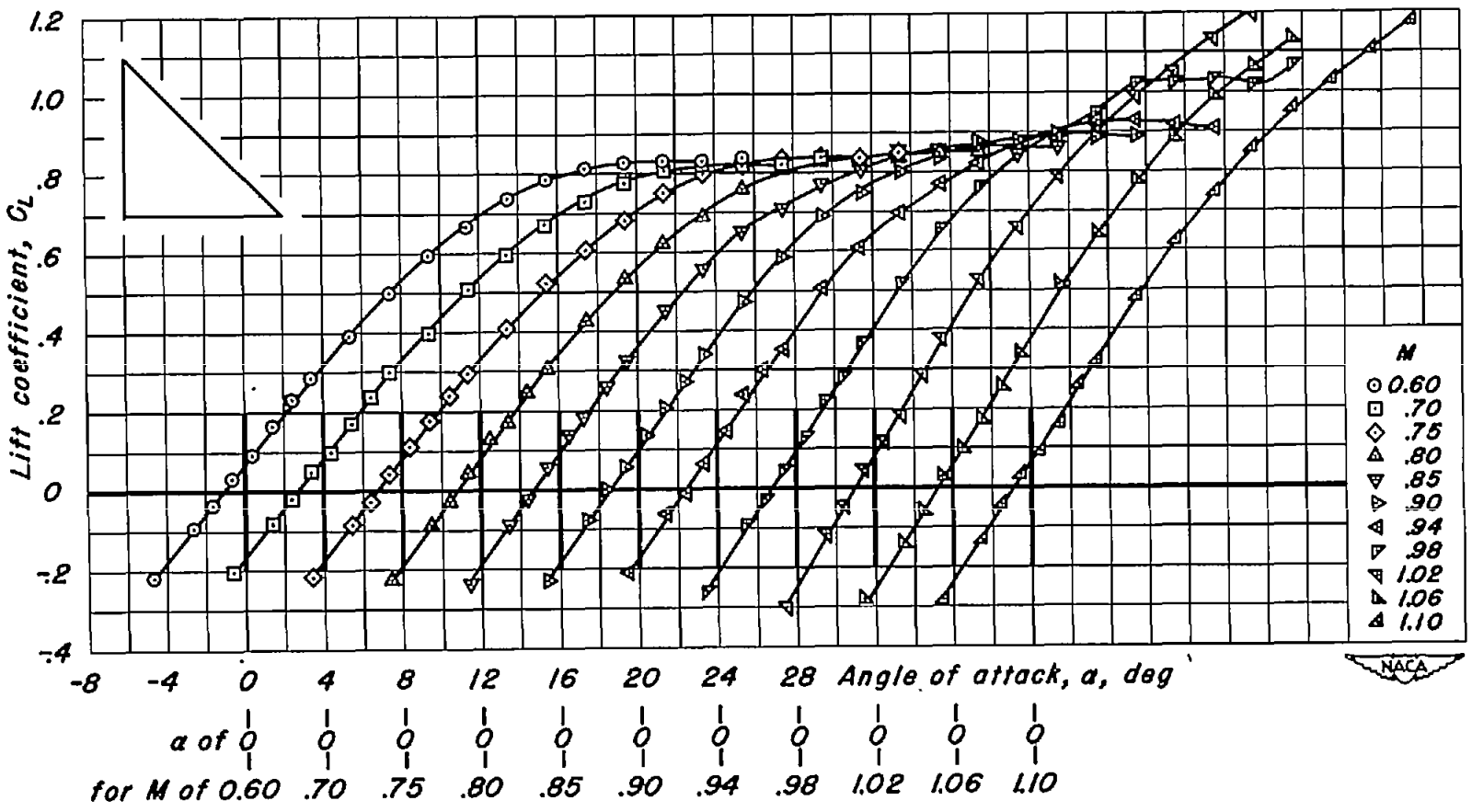

(k) NACA 63A(1.5)04; λ, 0; A 4.00.
Figure 14.- Continued.

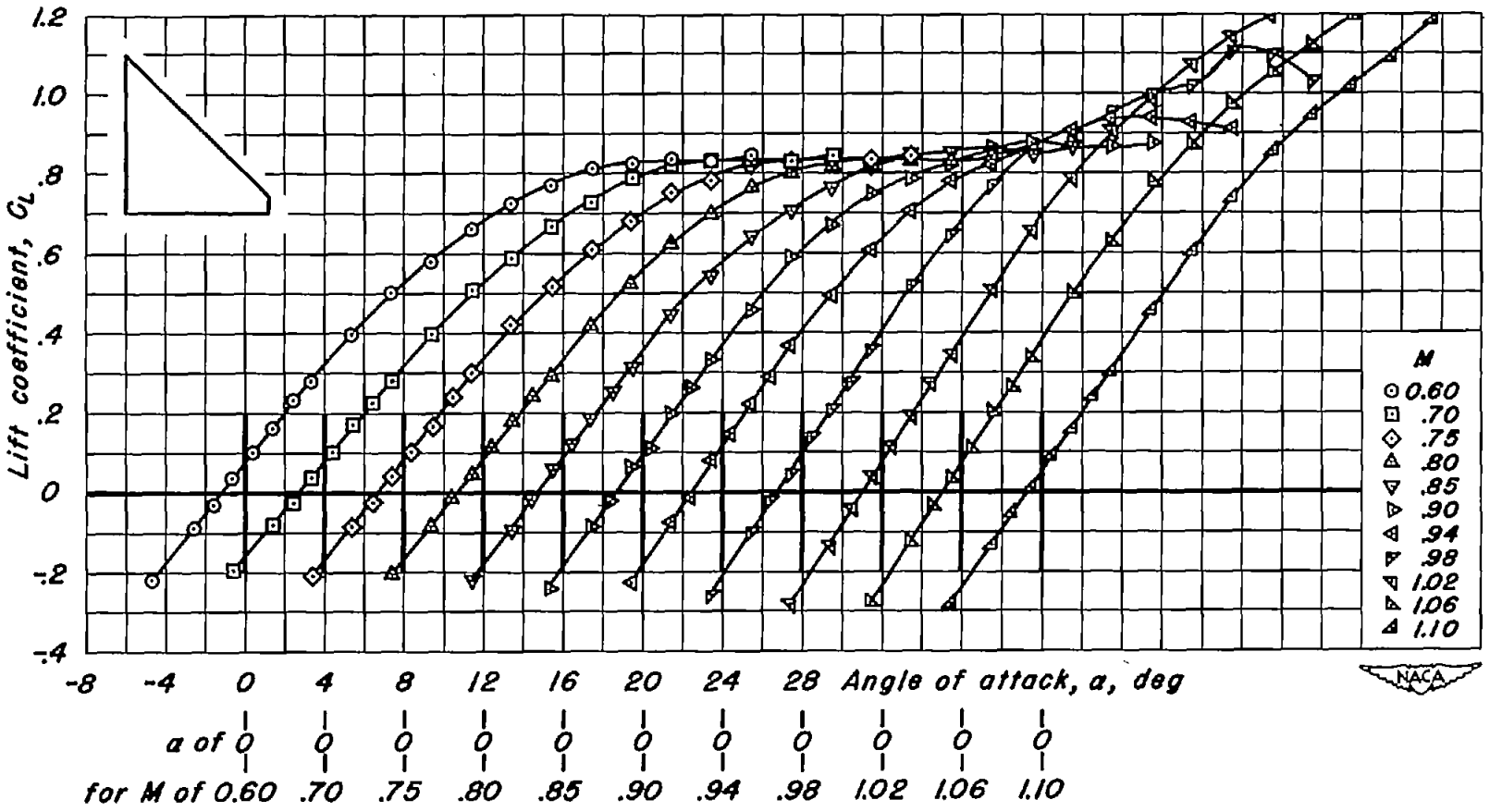

(l) NACA 63A(1.5)04; λ, 0.1; A, 3.27.
Figure 14.- Continued.

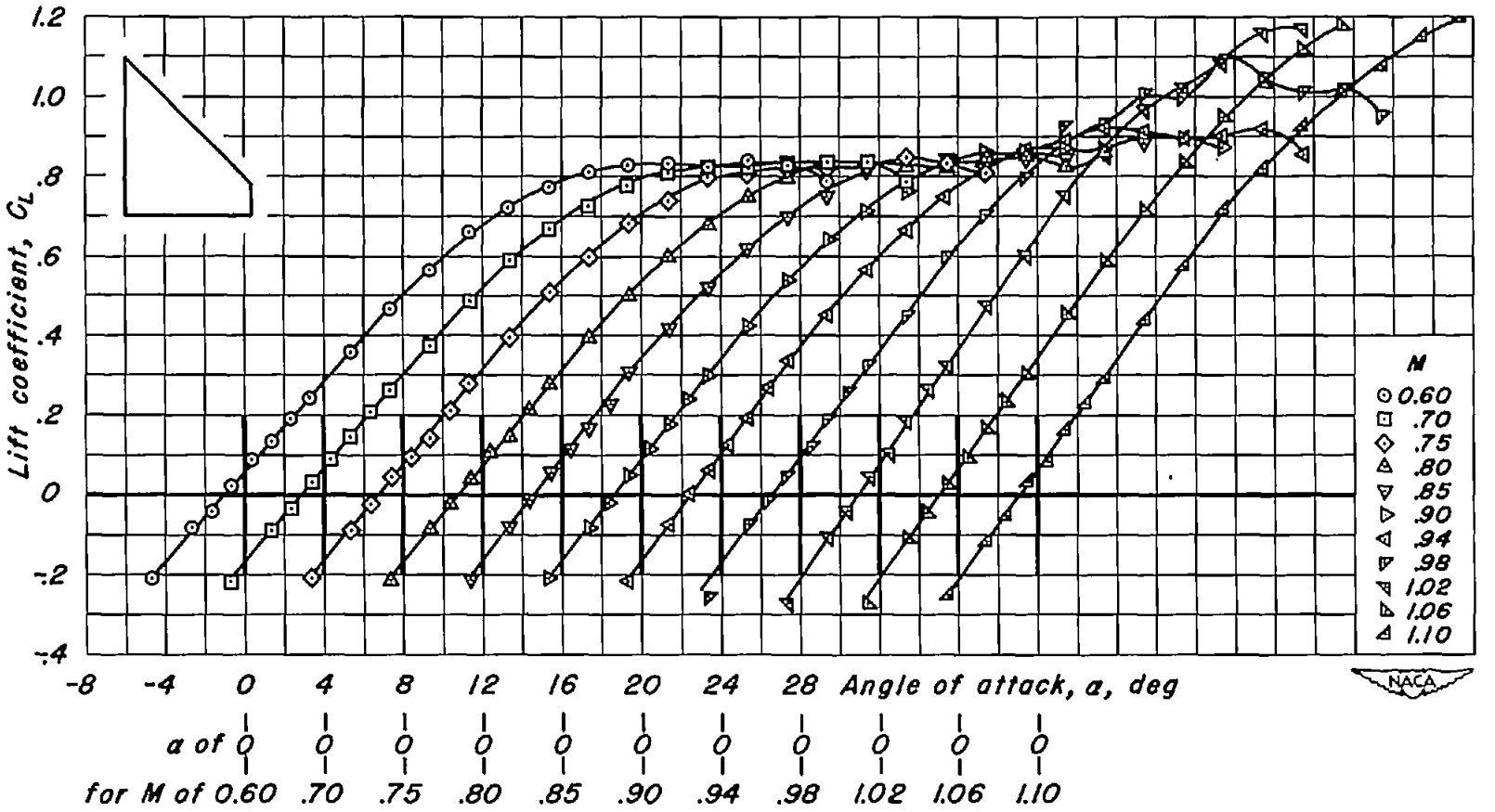

(m) NACA 63A(1.5)04; λ, 0.2; A, 2.67.
Figure 14.- Concluded.

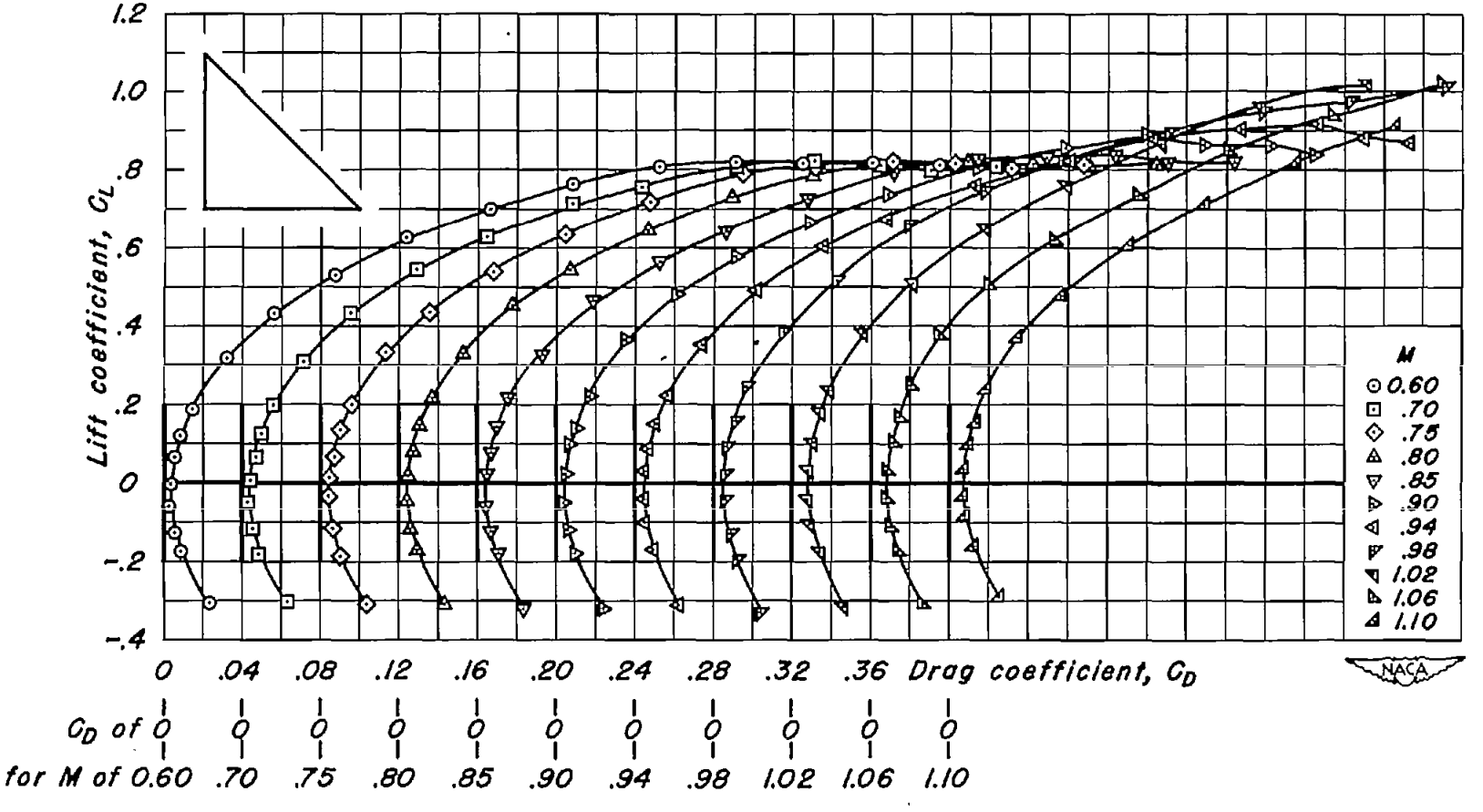

(a) NACA 63A002; λ, 0; A, 4.00.

Figure 15.- Variation of drag coefficient with lift coefficient for the wings of basic aspect ratio 4.

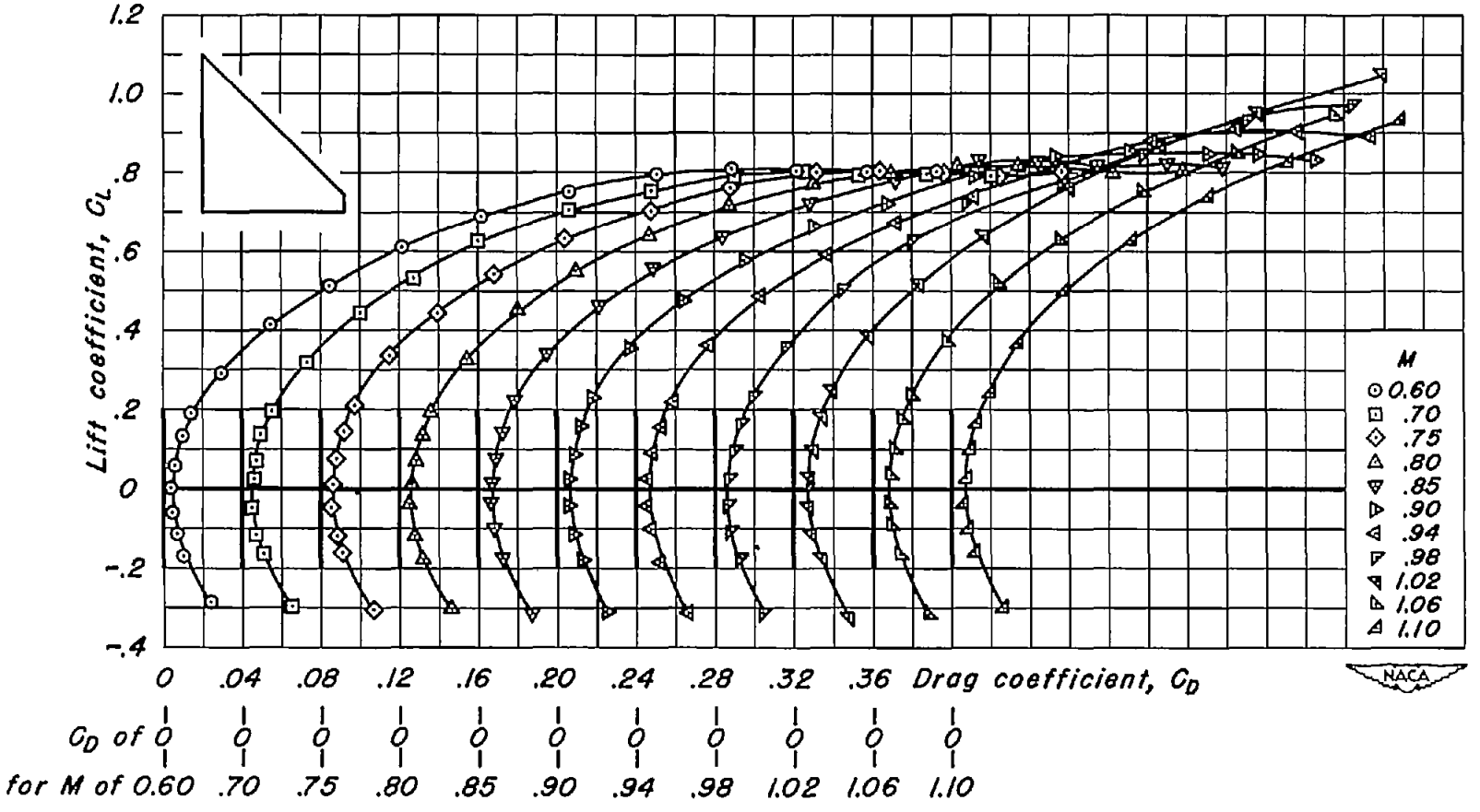

(b) NACA 63A002; λ, 0.1; A, 3.27.
Figure 15.- Continued.

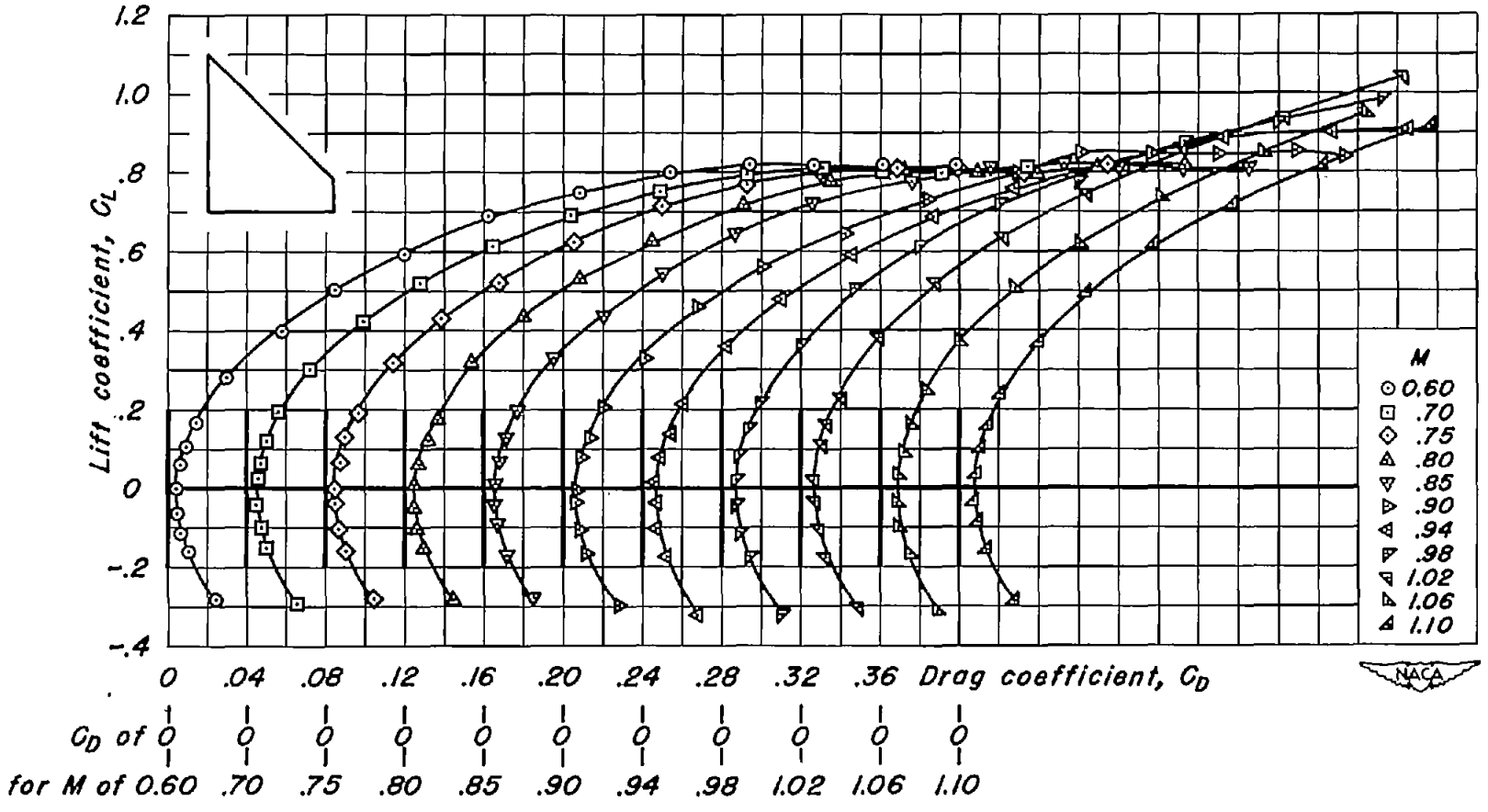

(c) NACA 63A002; λ, 0.2; A, 2.67.
Figure 15.- Continued.

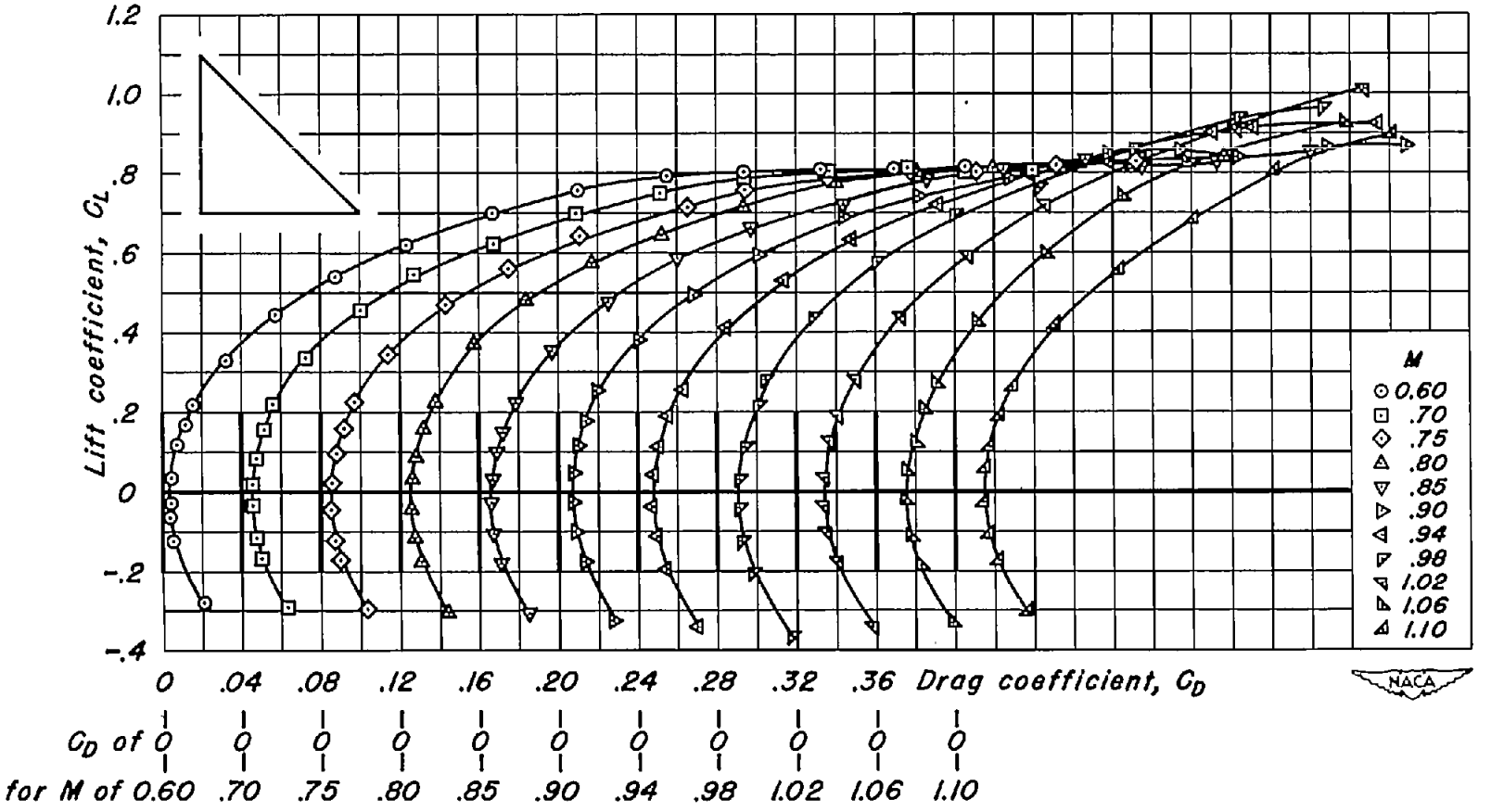

(d) NACA 63A004; λ, 0; A, 4.00.
Figure 15.- Continued.

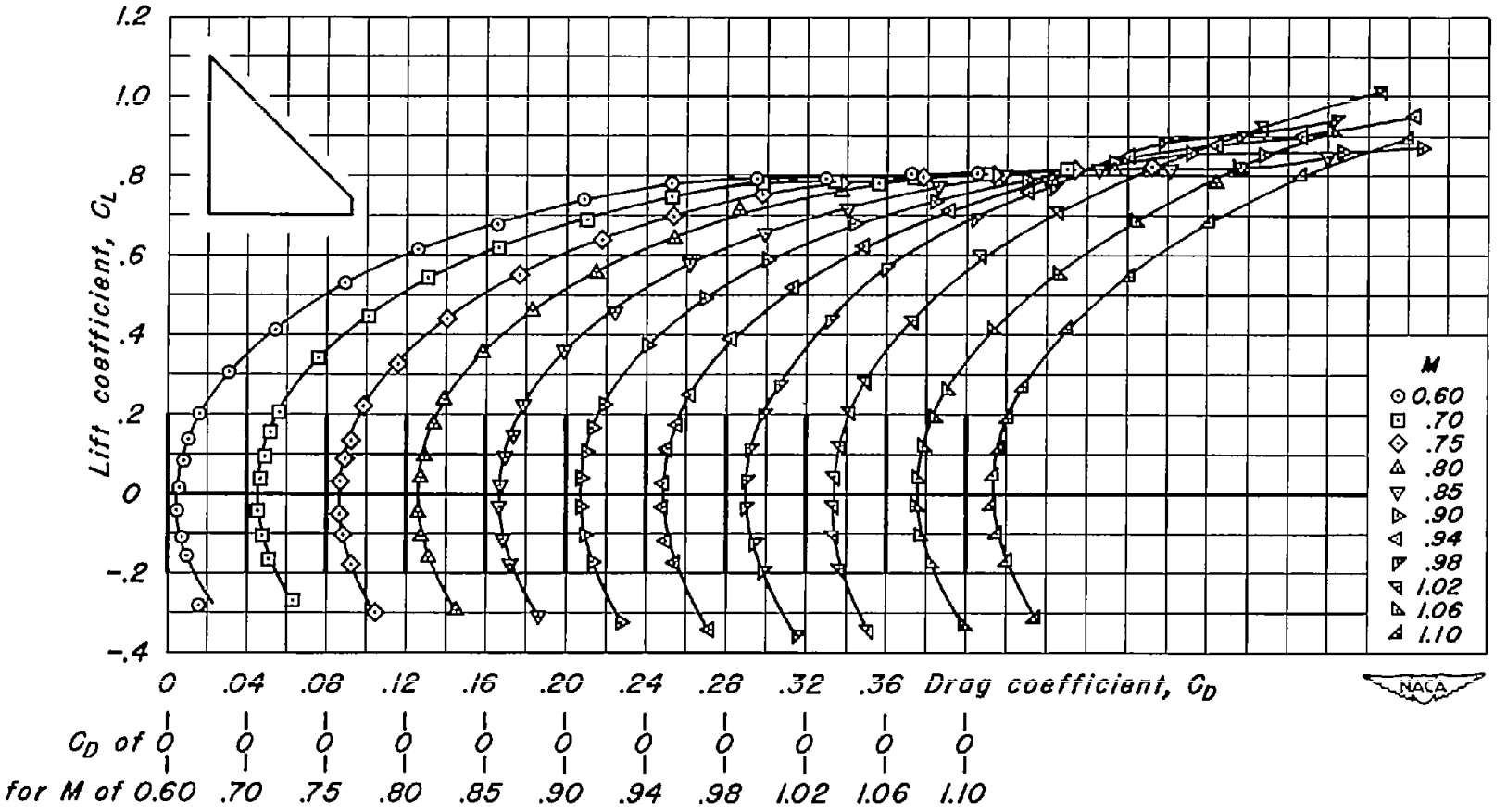

C_D of	0	0	0	0	0	0	0	0	0	0	0
for M of	0.60	.70	.75	.80	.85	.90	.94	.98	1.02	1.06	1.10

(e) NACA 63A004; λ, 0.1; A, 3.27.
Figure 15.- Continued.

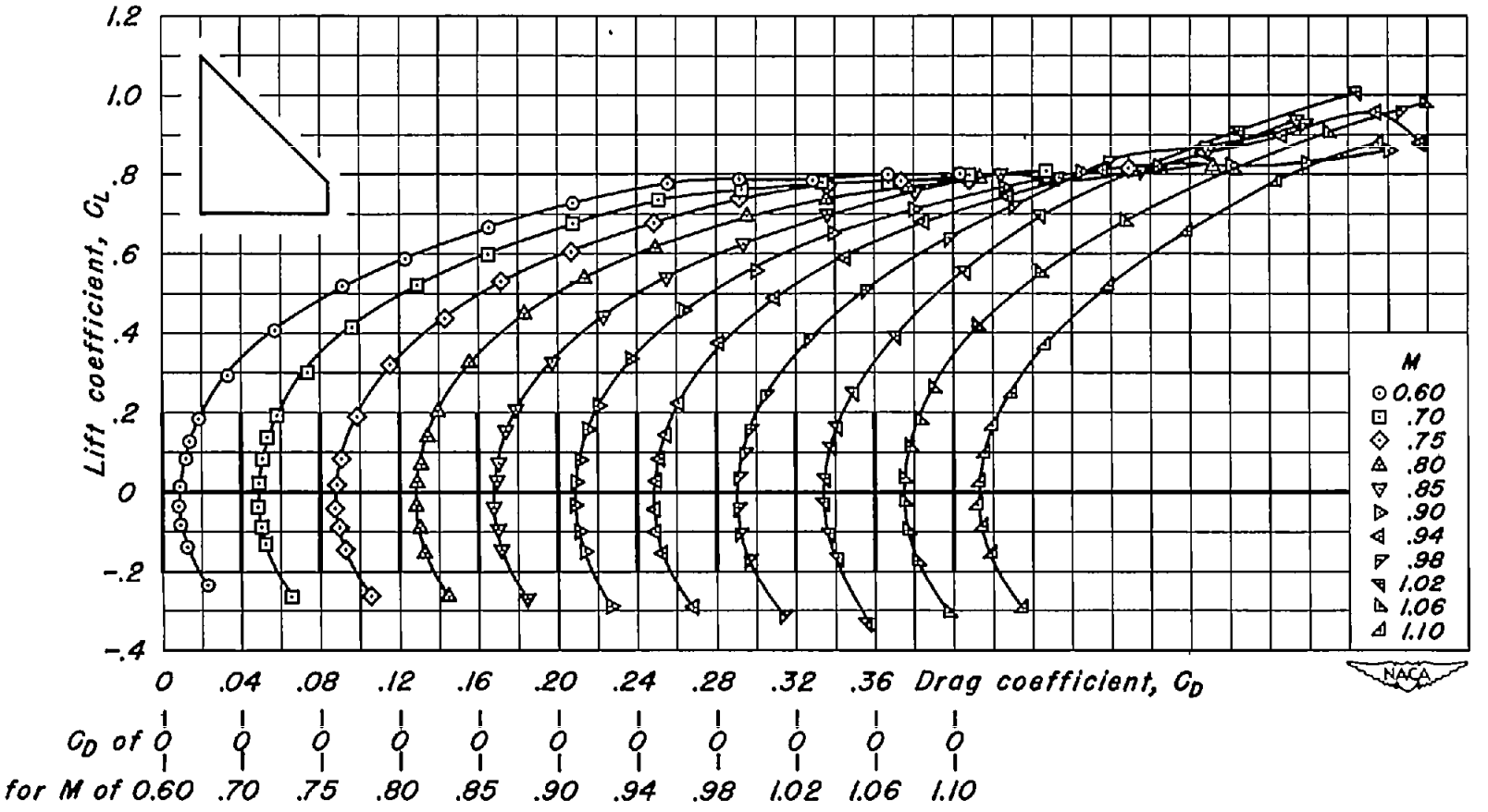

(f) NACA 63A004; λ, 0.2; A, 2.67.
Figure 15.- Continued.

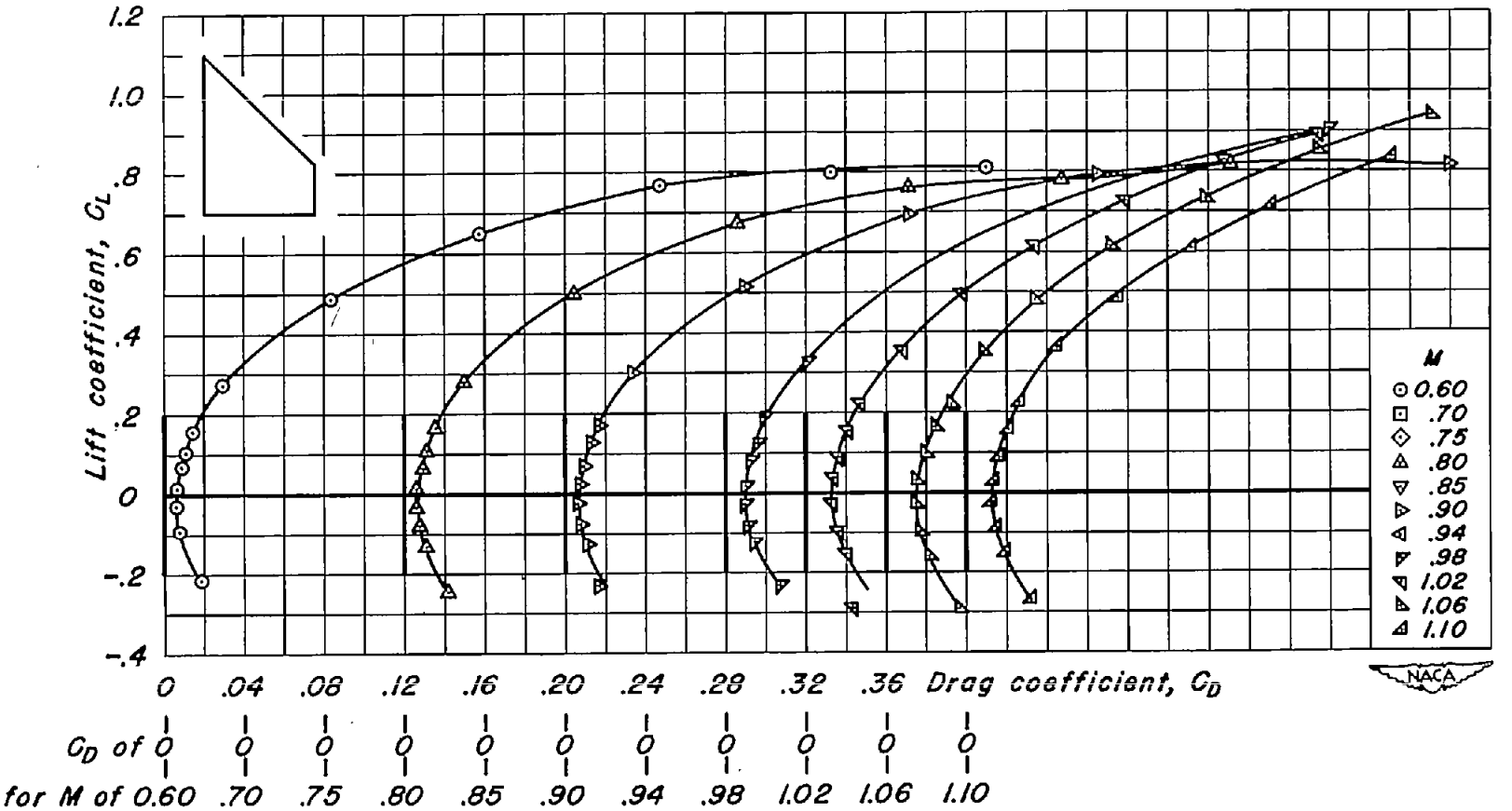

(g) NACA 63A004; λ, 0.3; A, 2.15.
Figure 15.- Continued.

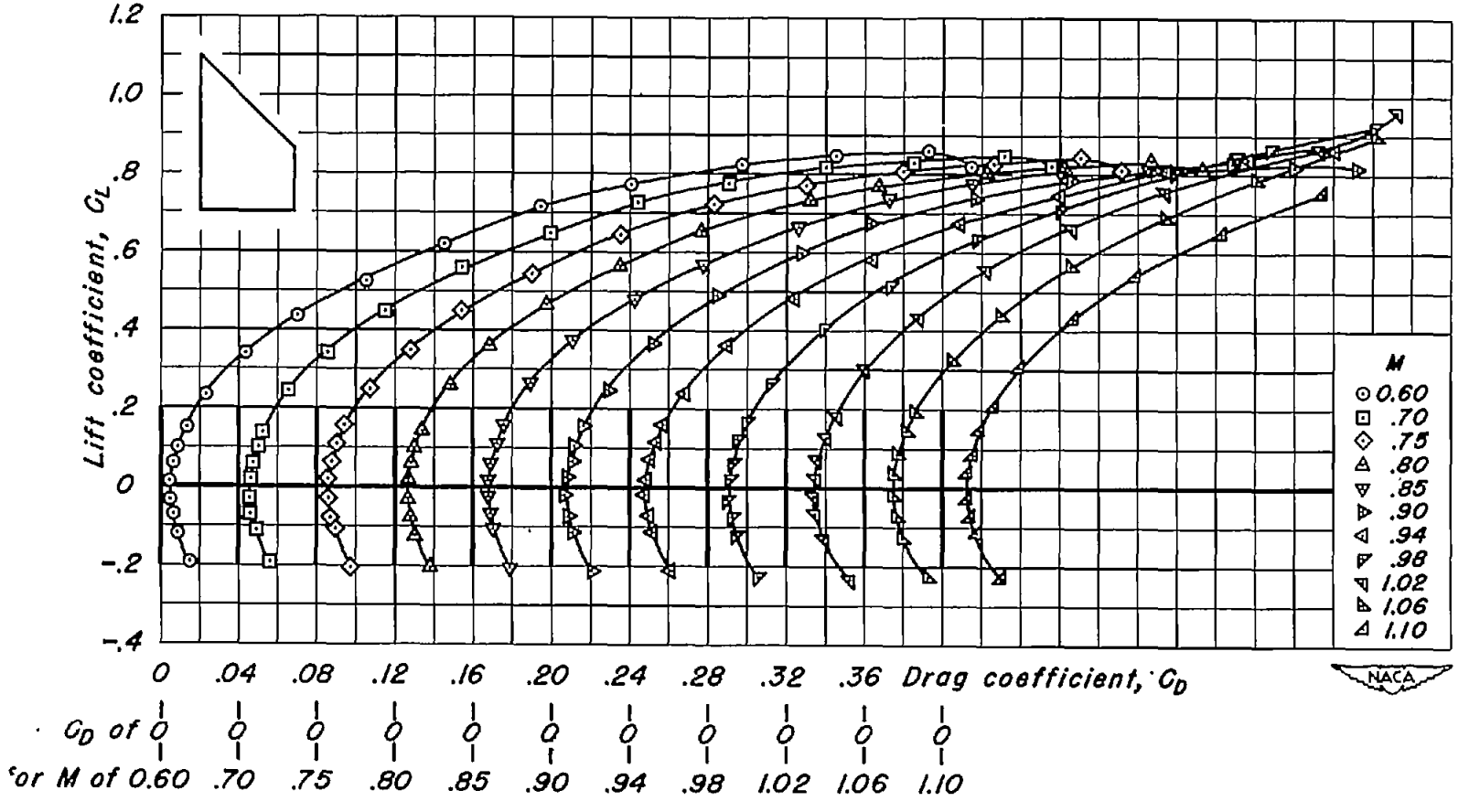

(h) NACA 63A004; λ, 0.4; A, 1.71.
Figure 15.- Continued.

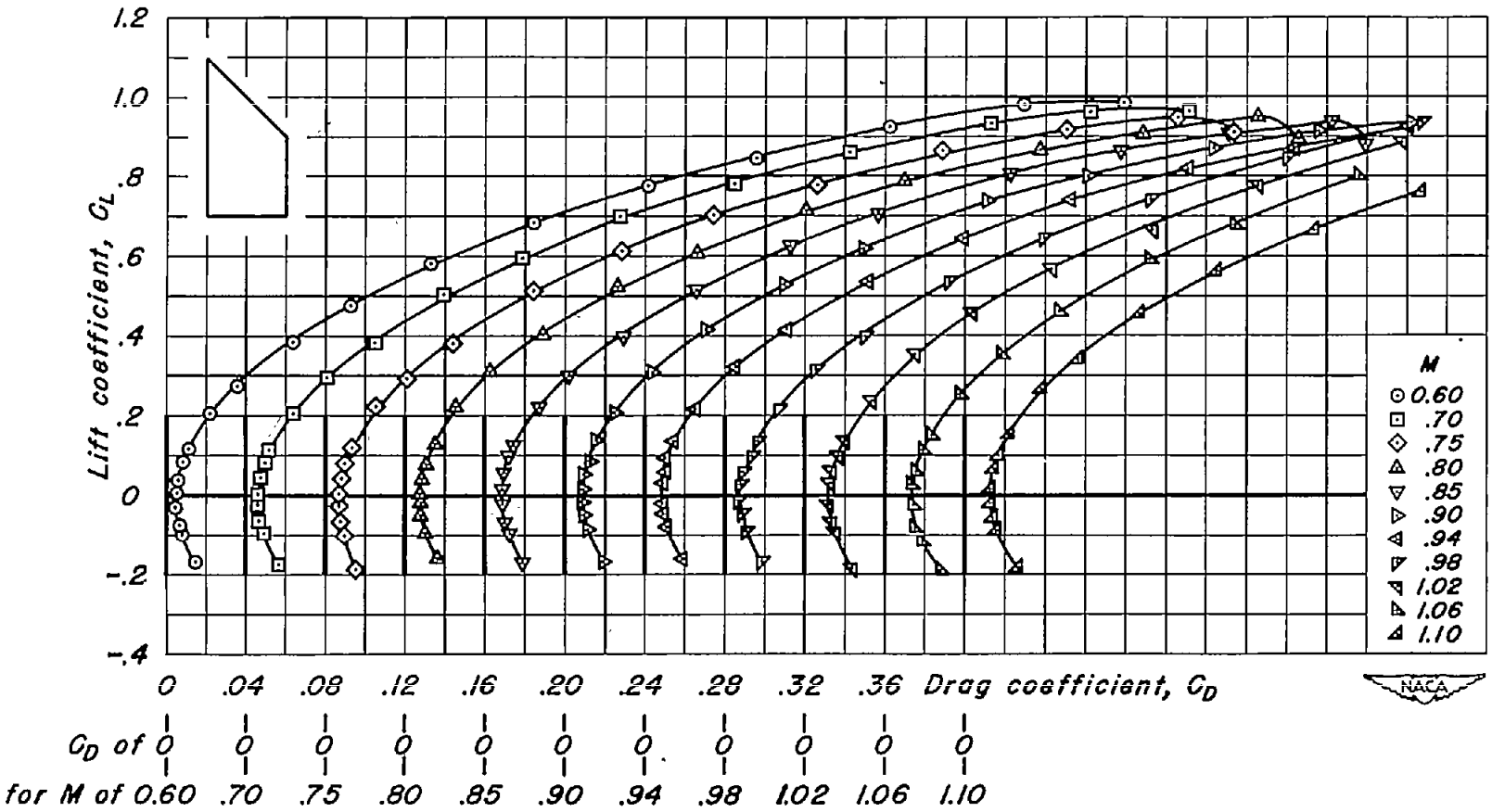

C_D of	0	0	0	0	0	0	0	0	0	0	0
for M of	0.60	.70	.75	.80	.85	.90	.94	.98	1.02	1.06	1.10

(i) NACA 63A004; λ, 0.5; A, 1.33.
Figure 15.- Continued.

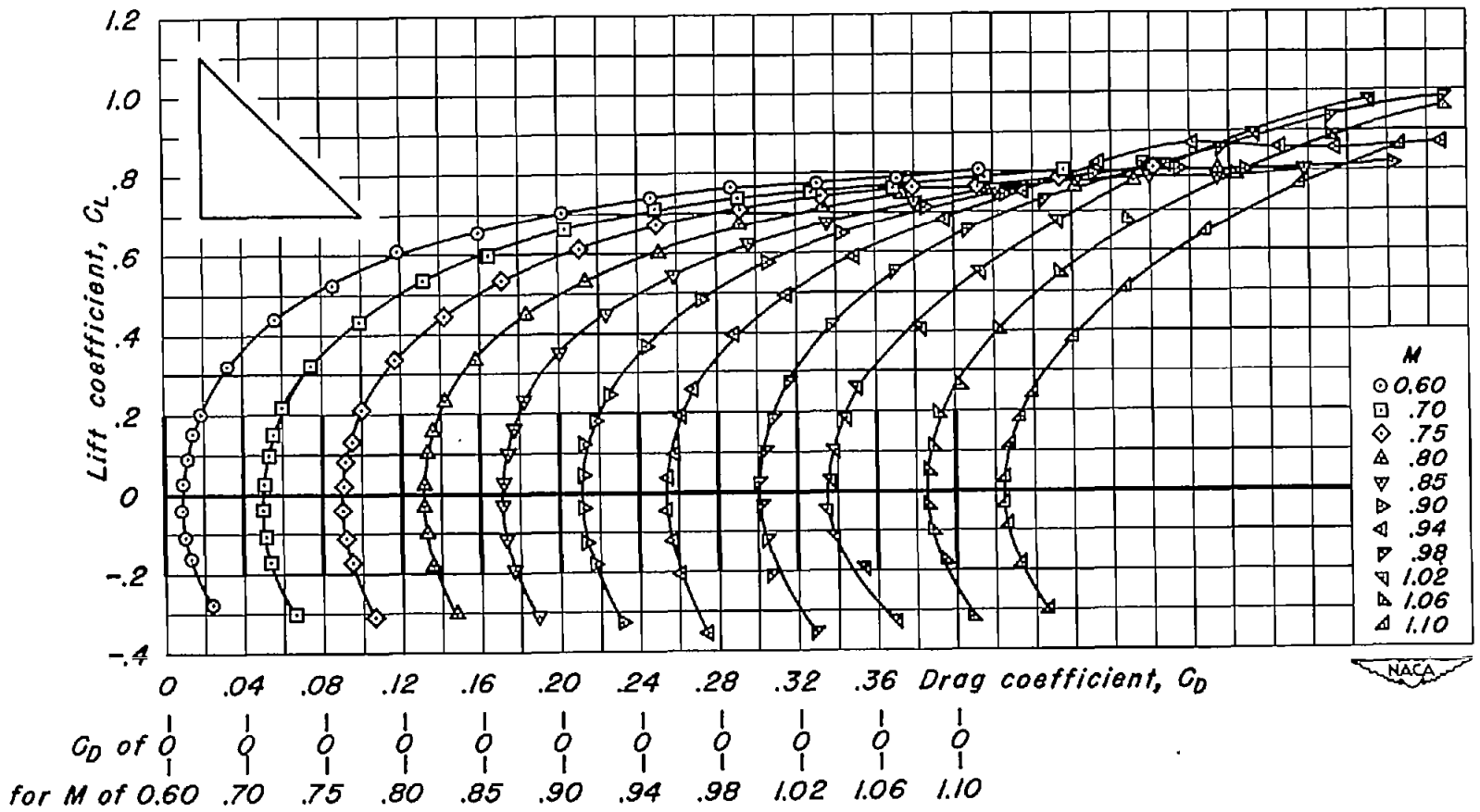

(j) NACA 63A006; λ, 0; A, 4.00.
Figure 15.- Continued.

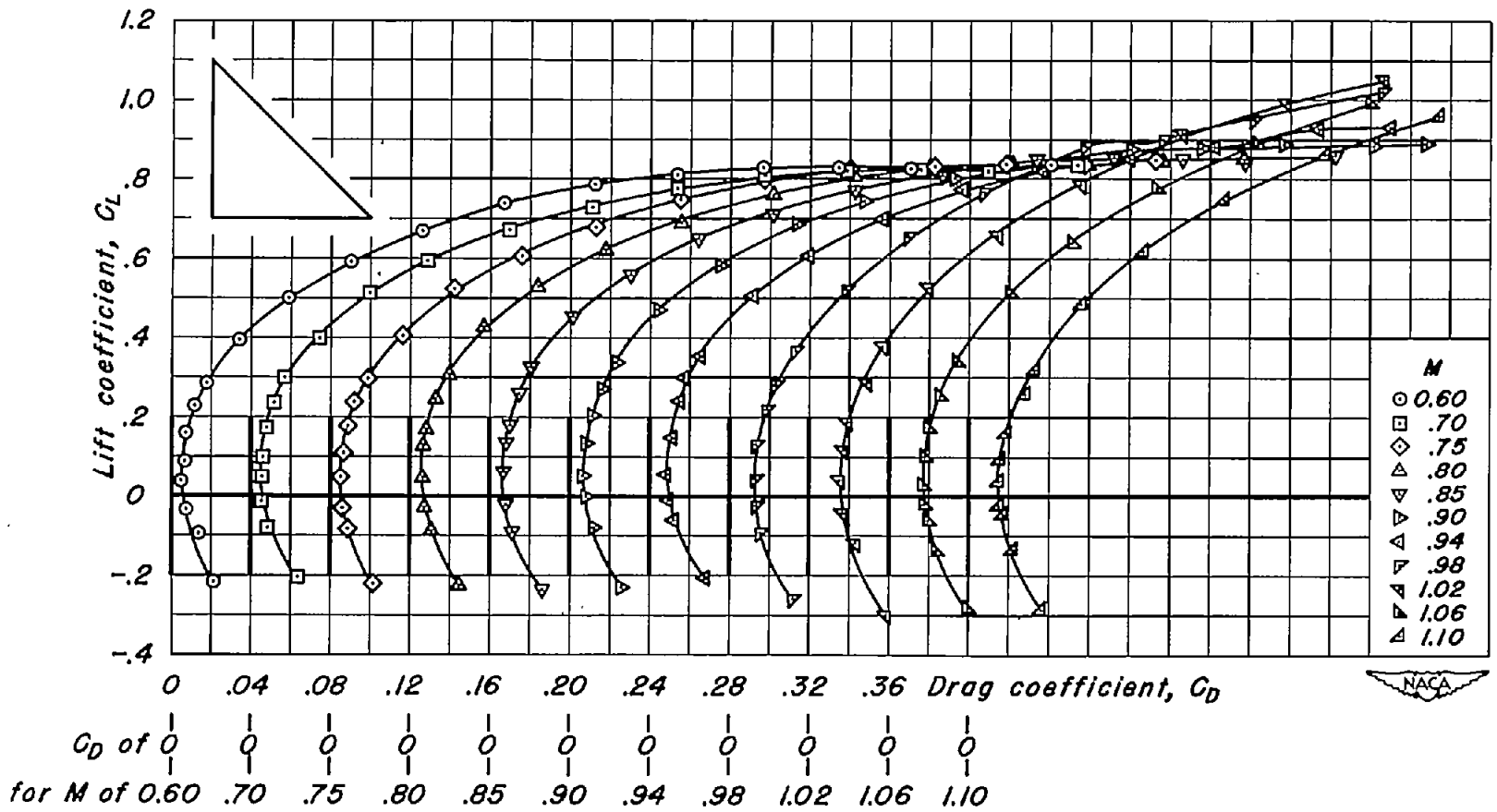

C_D of	0	0	0	0	0	0	0	0	0	0	0
for M of	0.60	.70	.75	.80	.85	.90	.94	.98	1.02	1.06	1.10

(k) NACA 63A(1.5)04; λ, 0; A, 4.00.
Figure 15.- Continued.

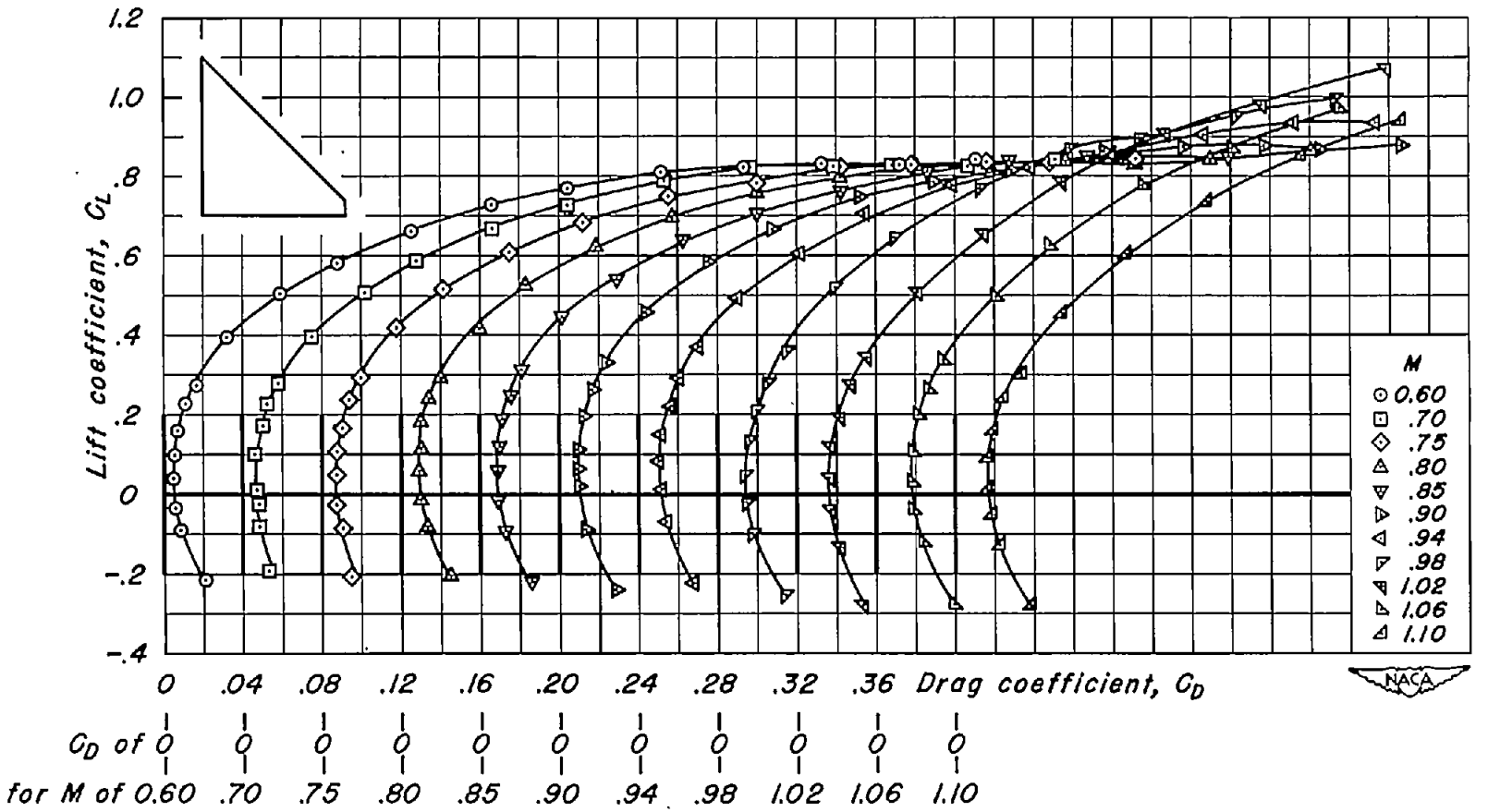

C_D of 0 0 0 0 0 0 0 0 0 0 0
for M of 0.60 .70 .75 .80 .85 .90 .94 .98 1.02 1.06 1.10

(l) NACA 63A(1.5)04; λ, 0.1; A, 3.27.
Figure 15.- Continued.

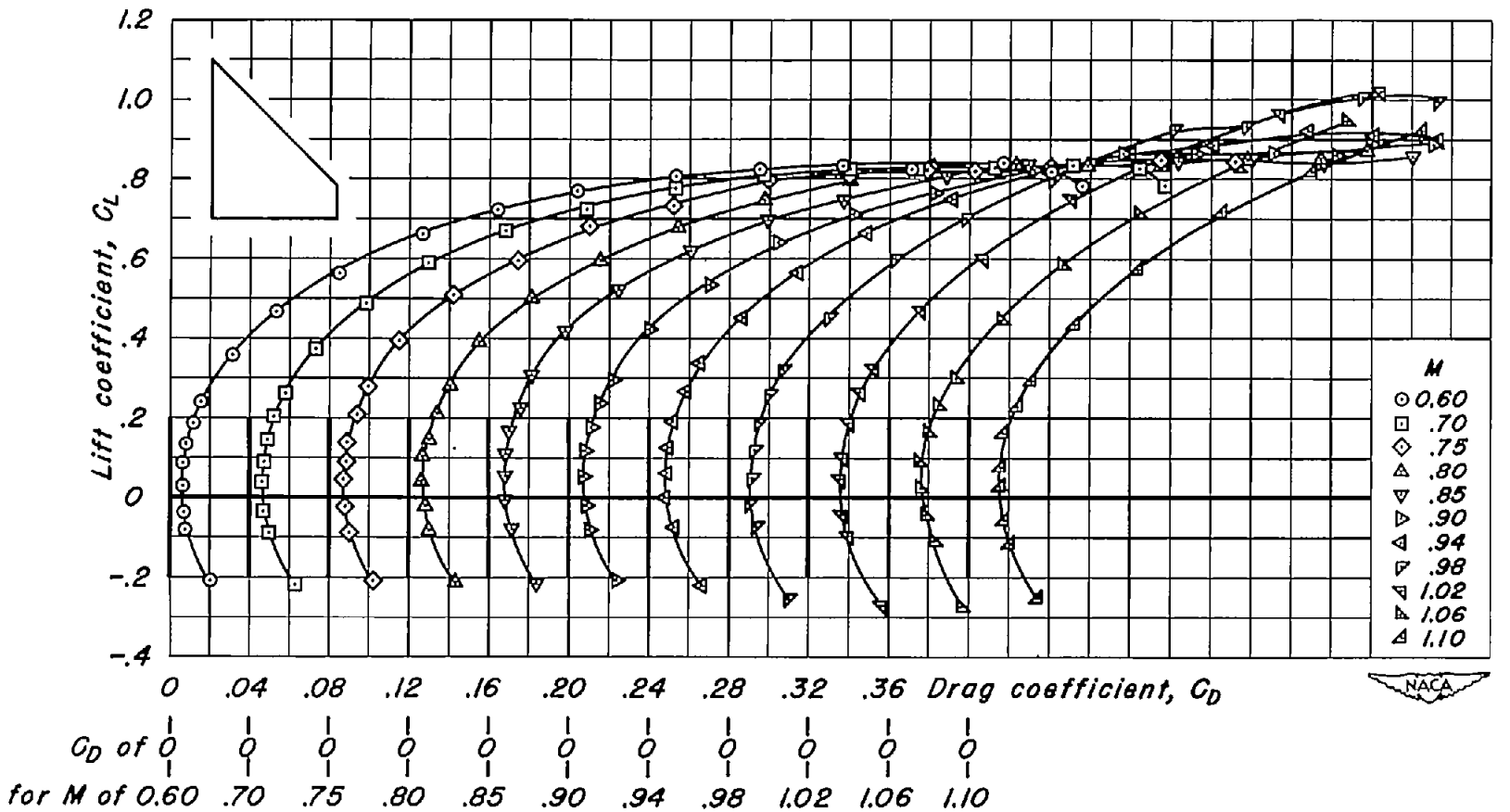

C_D of 0 0 0 0 0 0 0 0 0 0 0
for M of 0.60 .70 .75 .80 .85 .90 .94 .98 1.02 1.06 1.10

(m) NACA 63A(1.5)04; λ, 0.2; A, 267.
Figure 15.- Concluded.

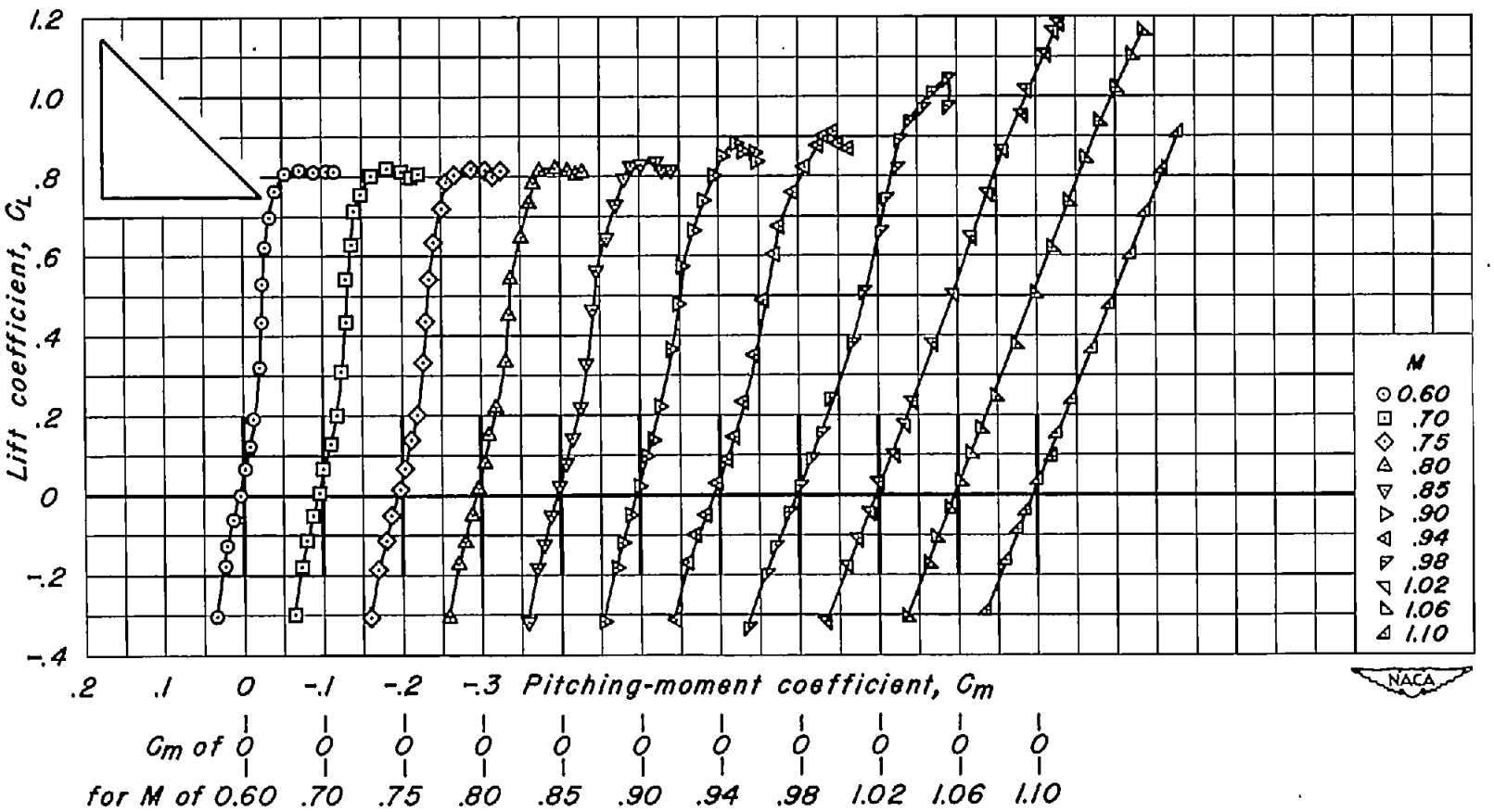

(a) NACA 63A002; λ, 0; A, 4.00.

Figure 16.- Variation of pitching-moment coefficient with lift coefficient for the wings of basic aspect ratio 4.

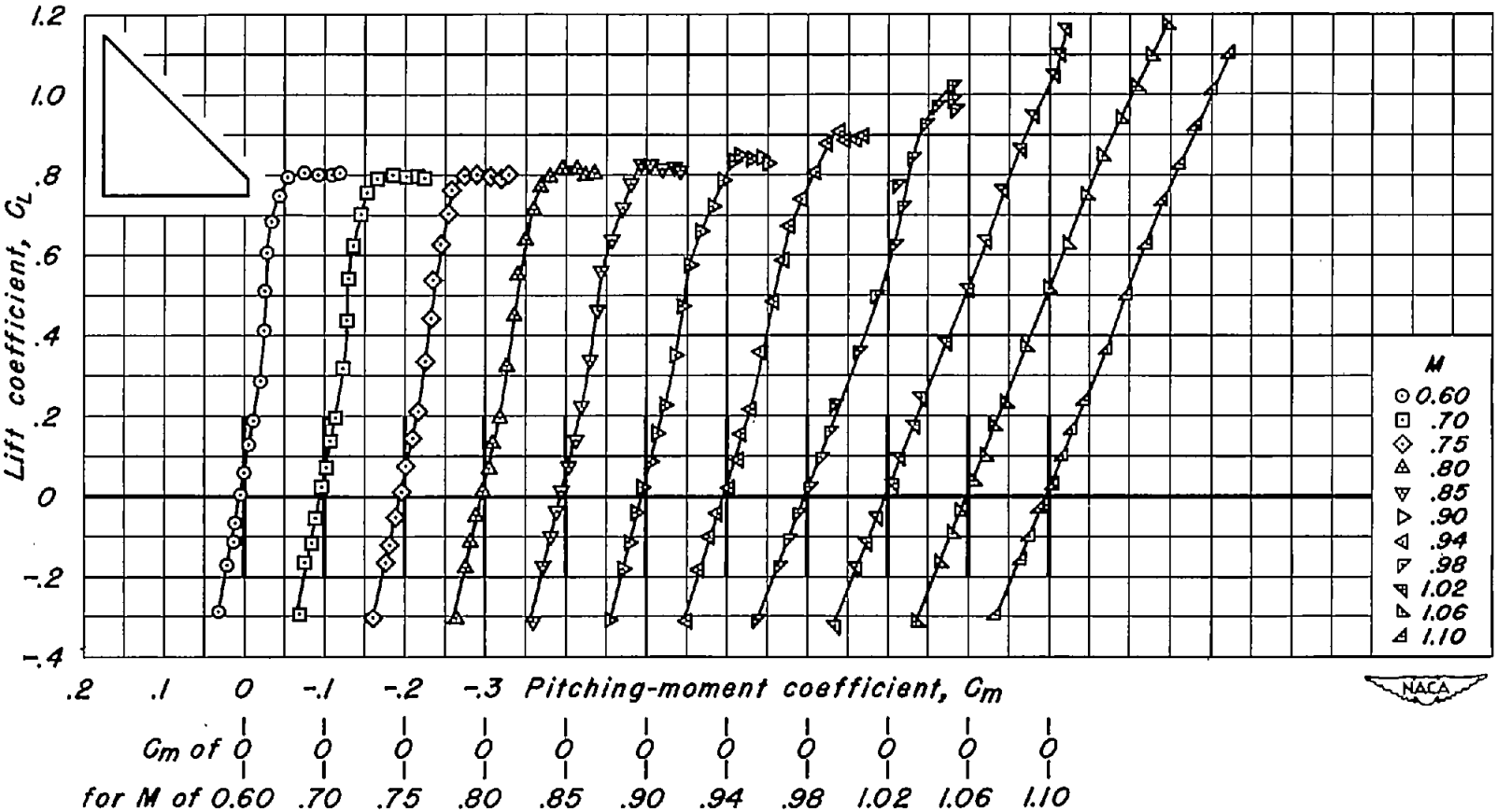

(b) NACA 63A002; λ, 0.1; A, 3.27.
Figure 16.- Continued.

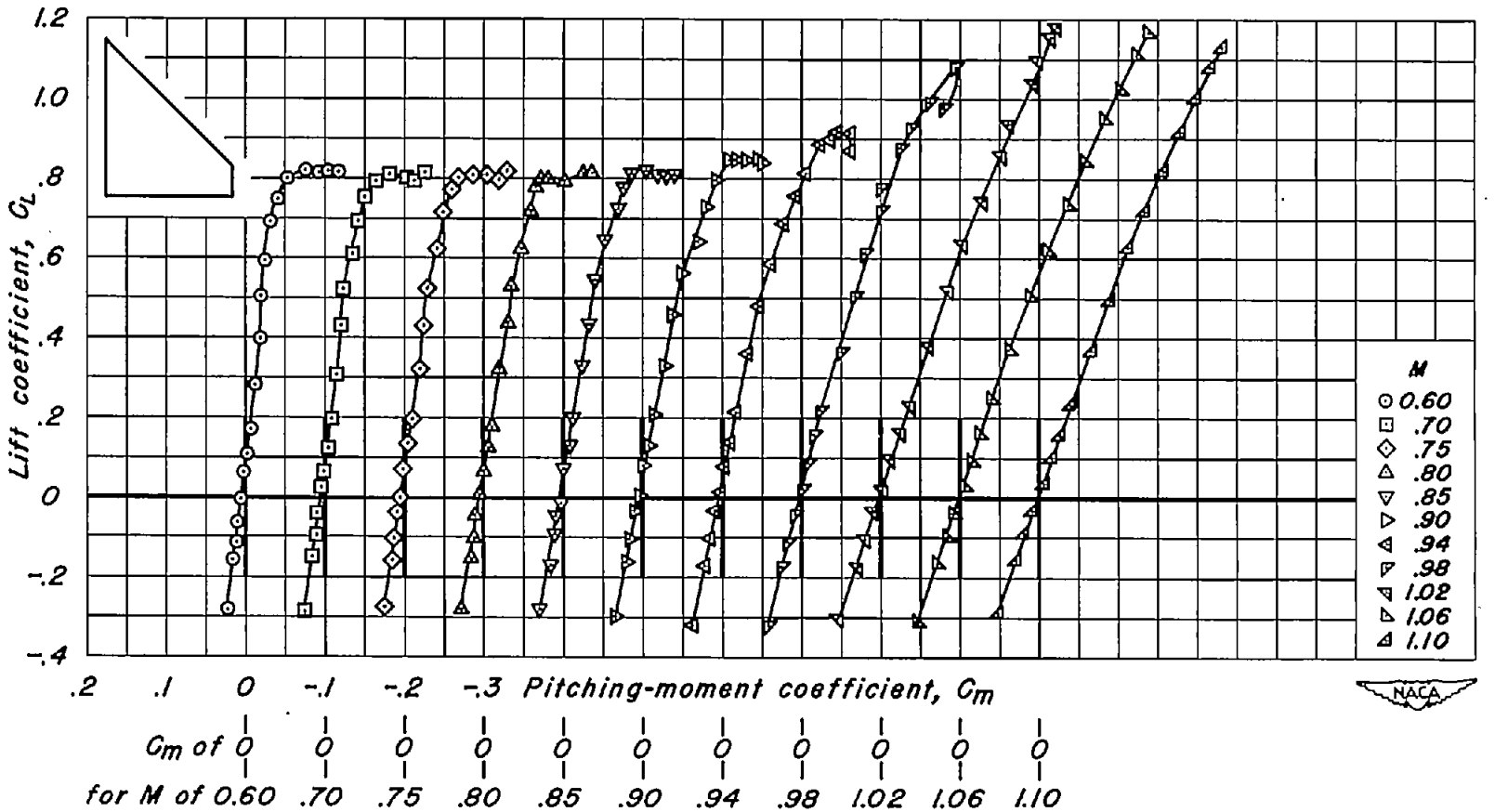

(c) NACA 63A002; λ, 0.2; A, 2.67.
Figure 16.- Continued.

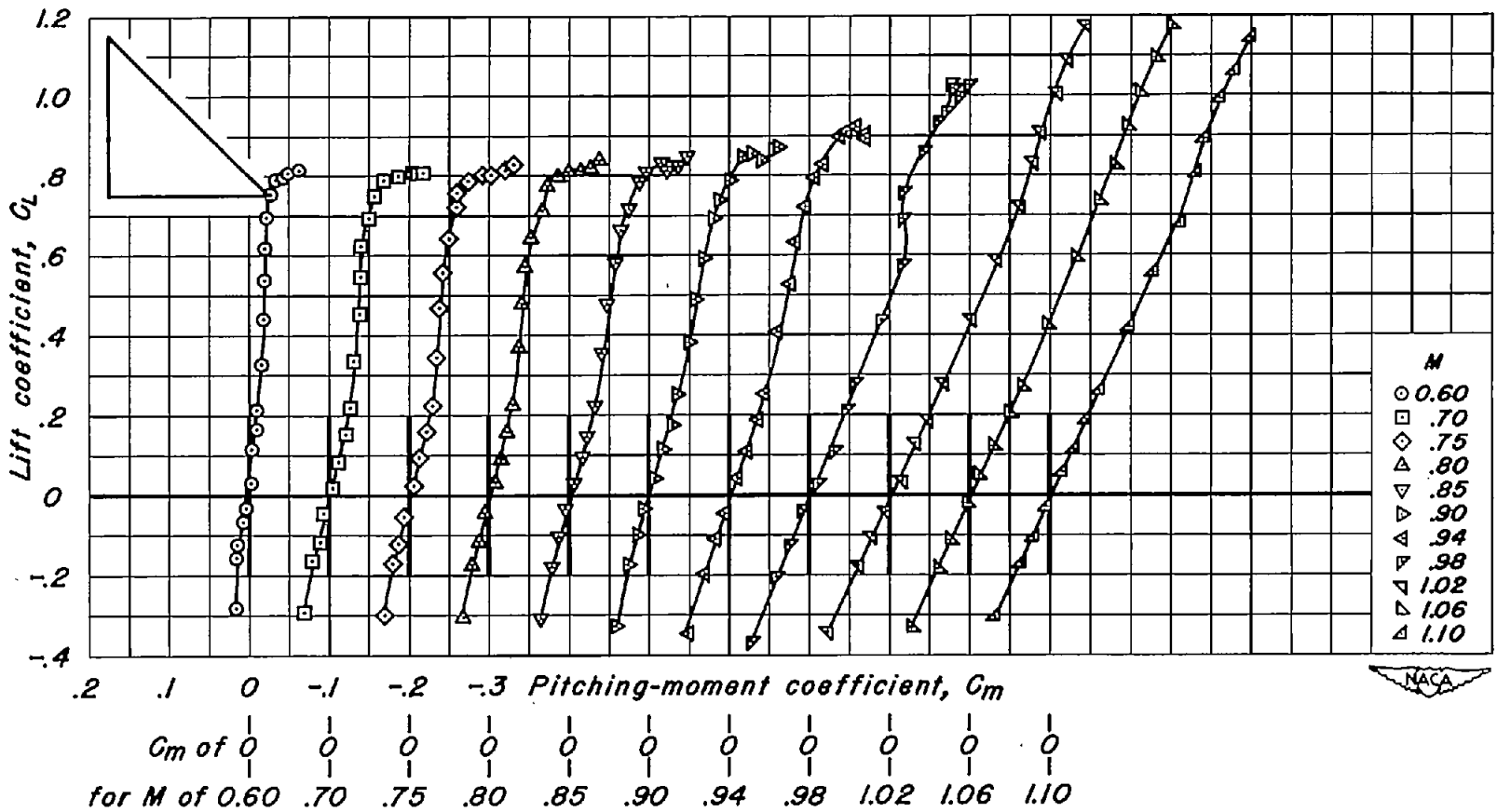

(d) NACA 63A004; λ, 0; A, 4.00.
Figure 16.- Continued.

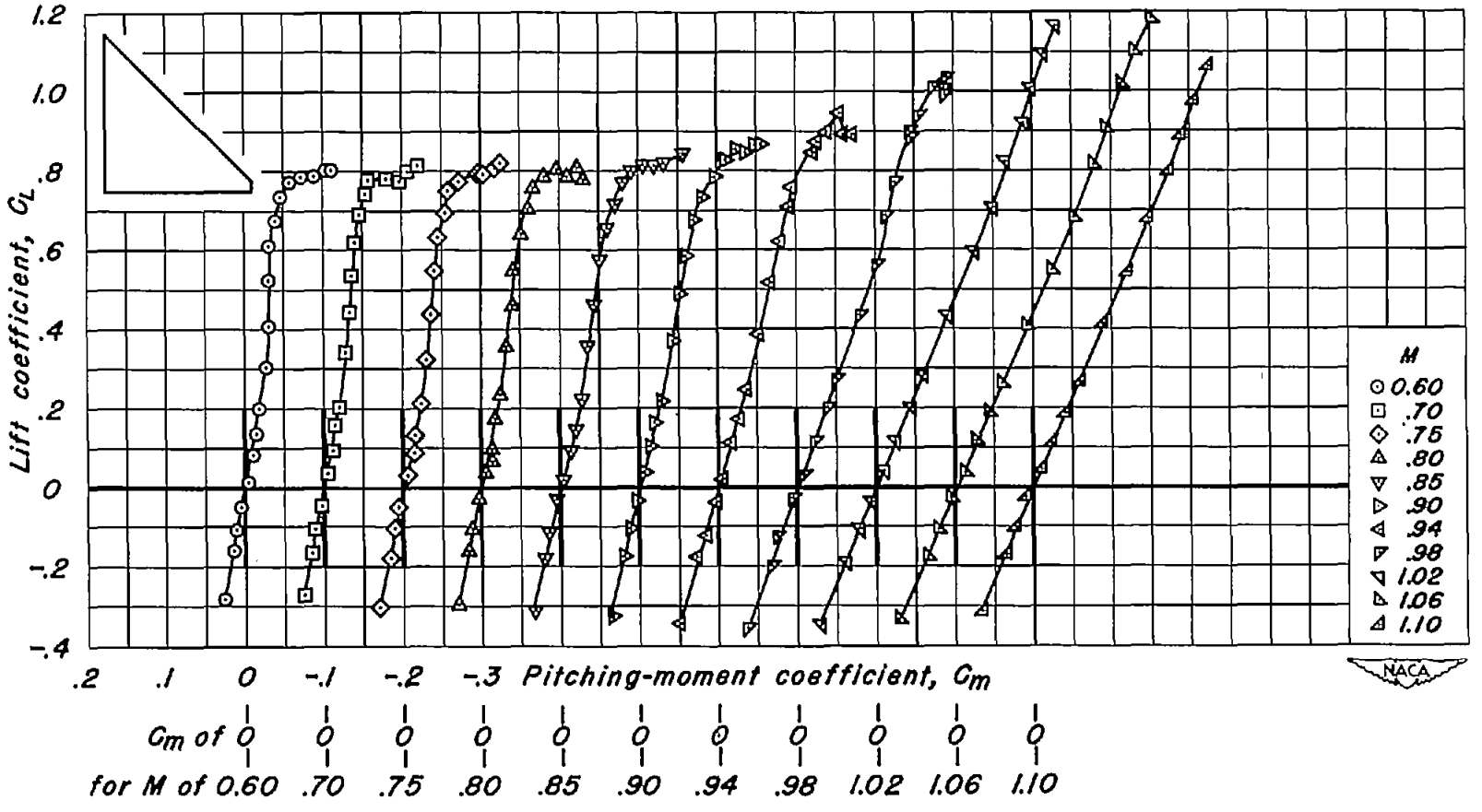

(e) NACA 63A004; λ, 0.1; A, 3.27.
Figure 16.- Continued.

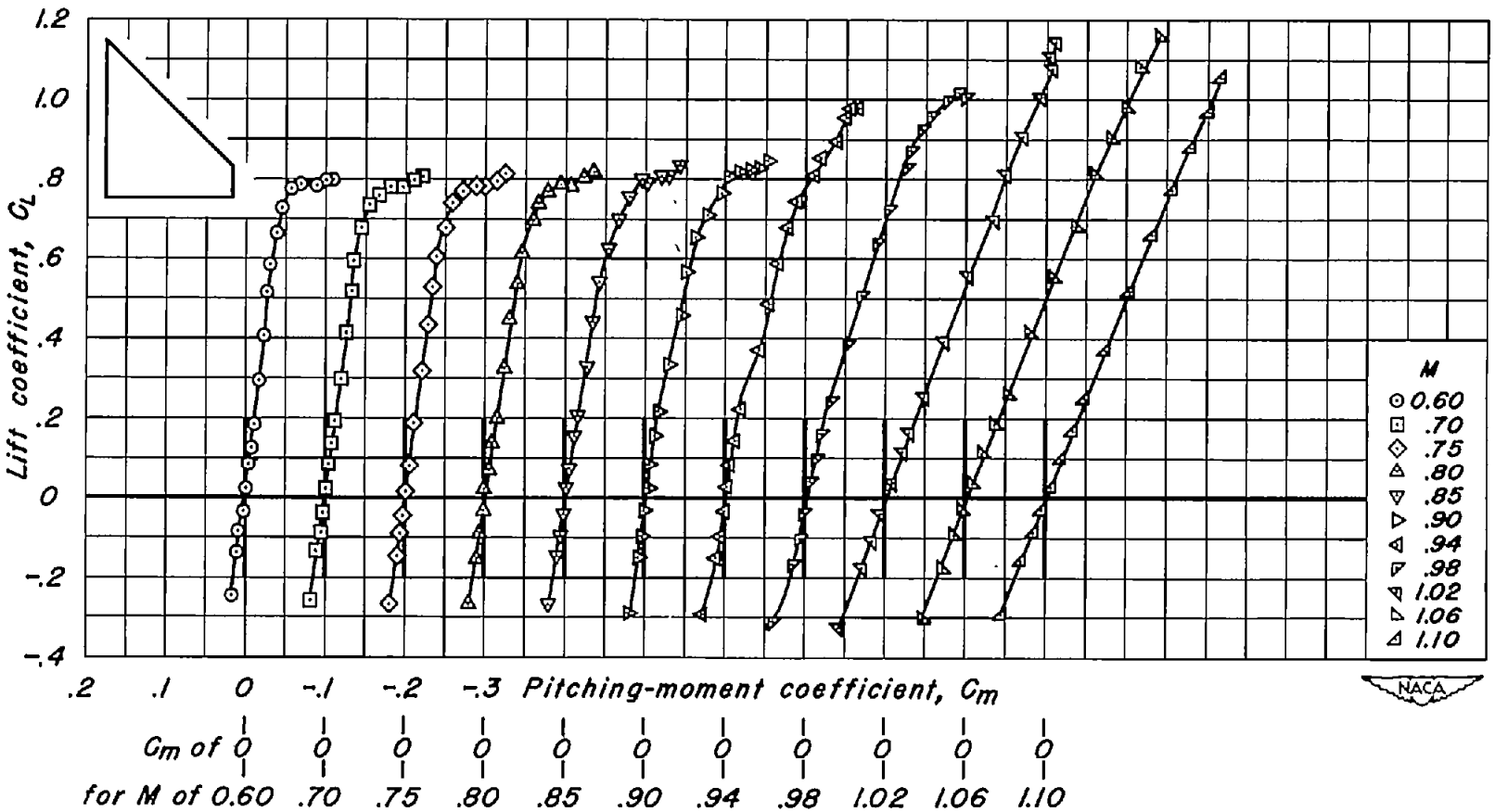

(f) NACA 63A004; λ, 0.2; A, 2.67.
Figure 16.- Continued.

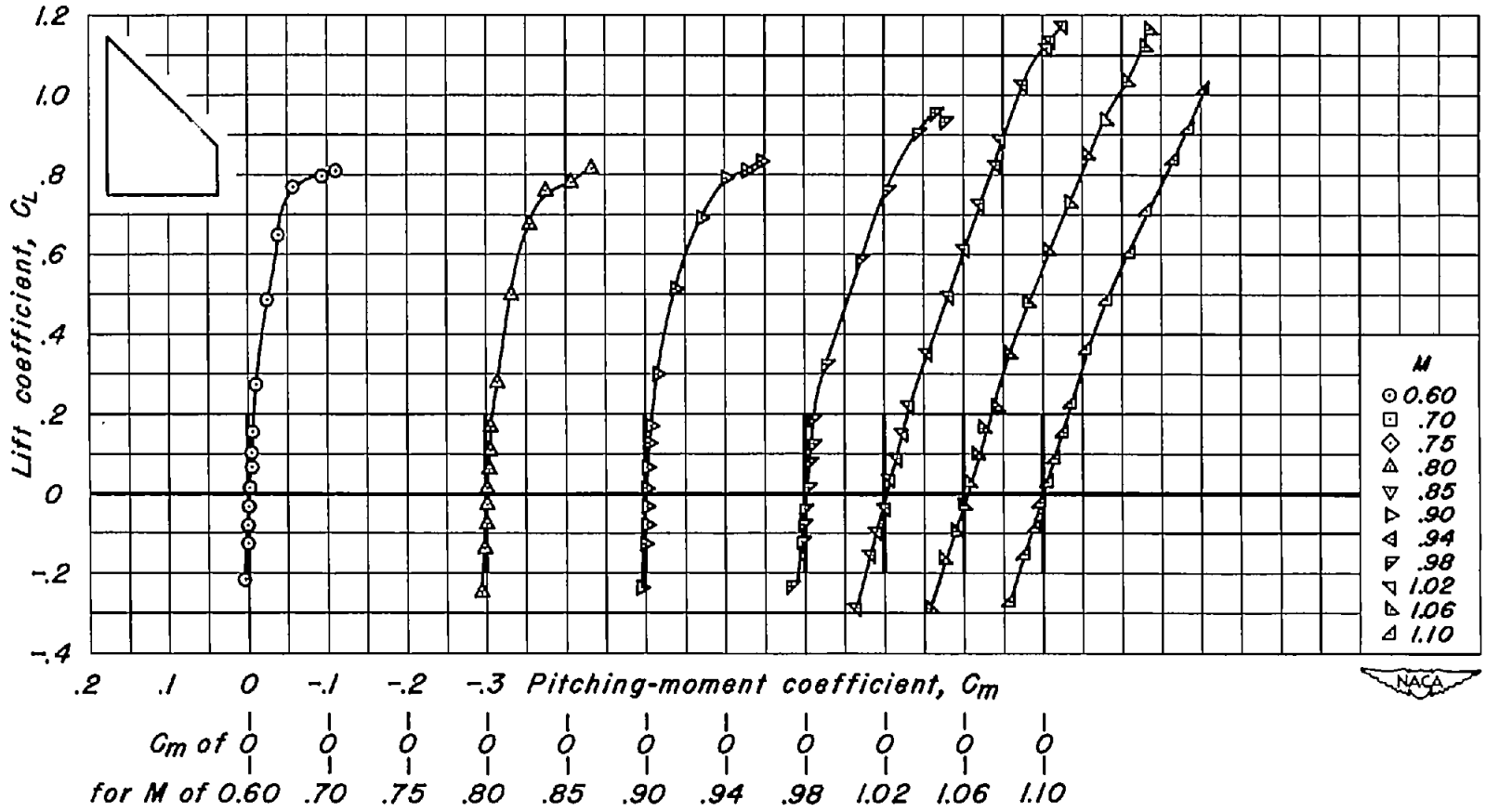

(g) NACA 63A004; λ, 0.3; A, 2.15.
Figure 16.- Continued.

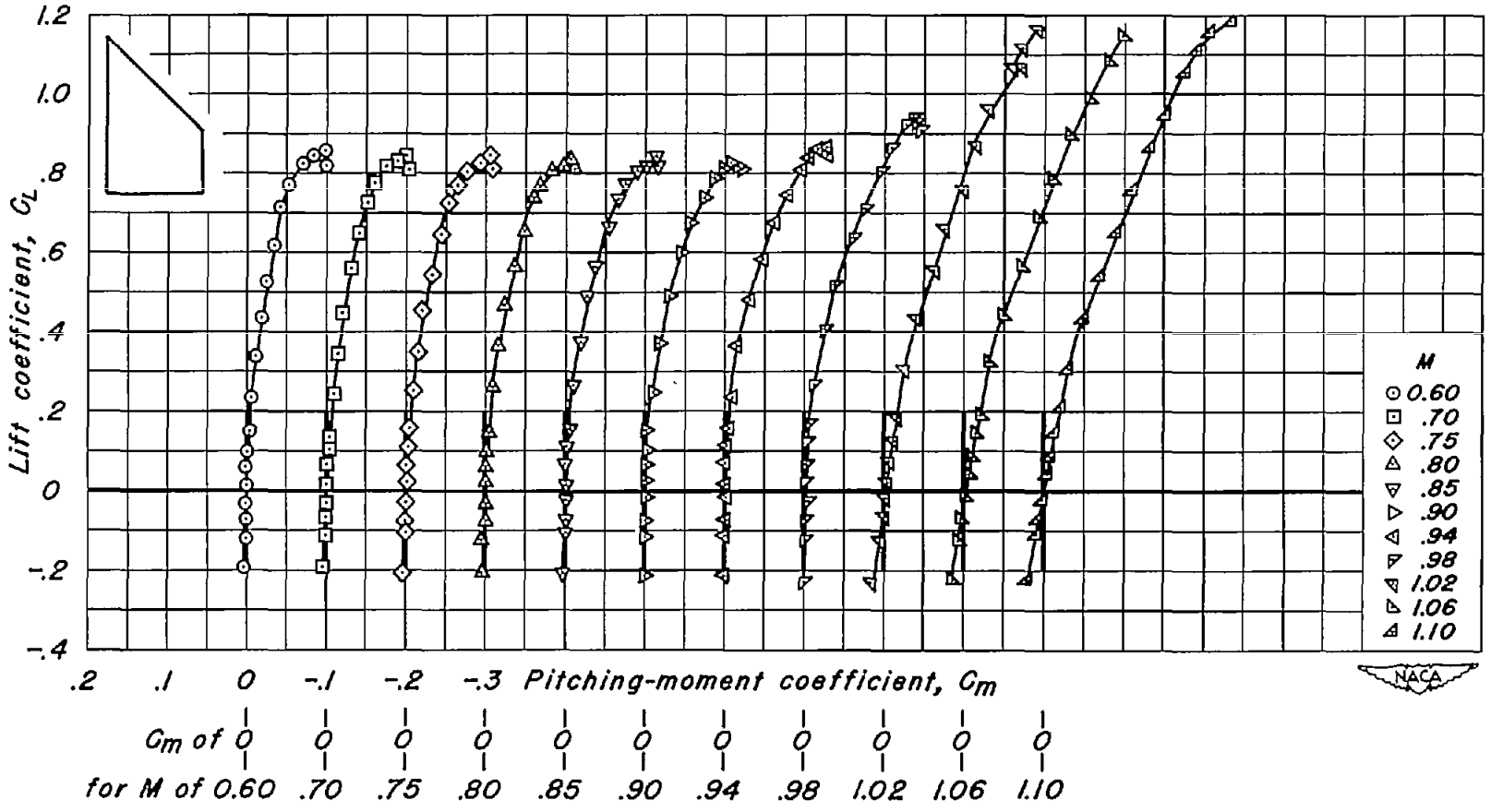

(h) NACA 63A004; λ, 0.4; A, 1.71.
Figure 16.- Continued.

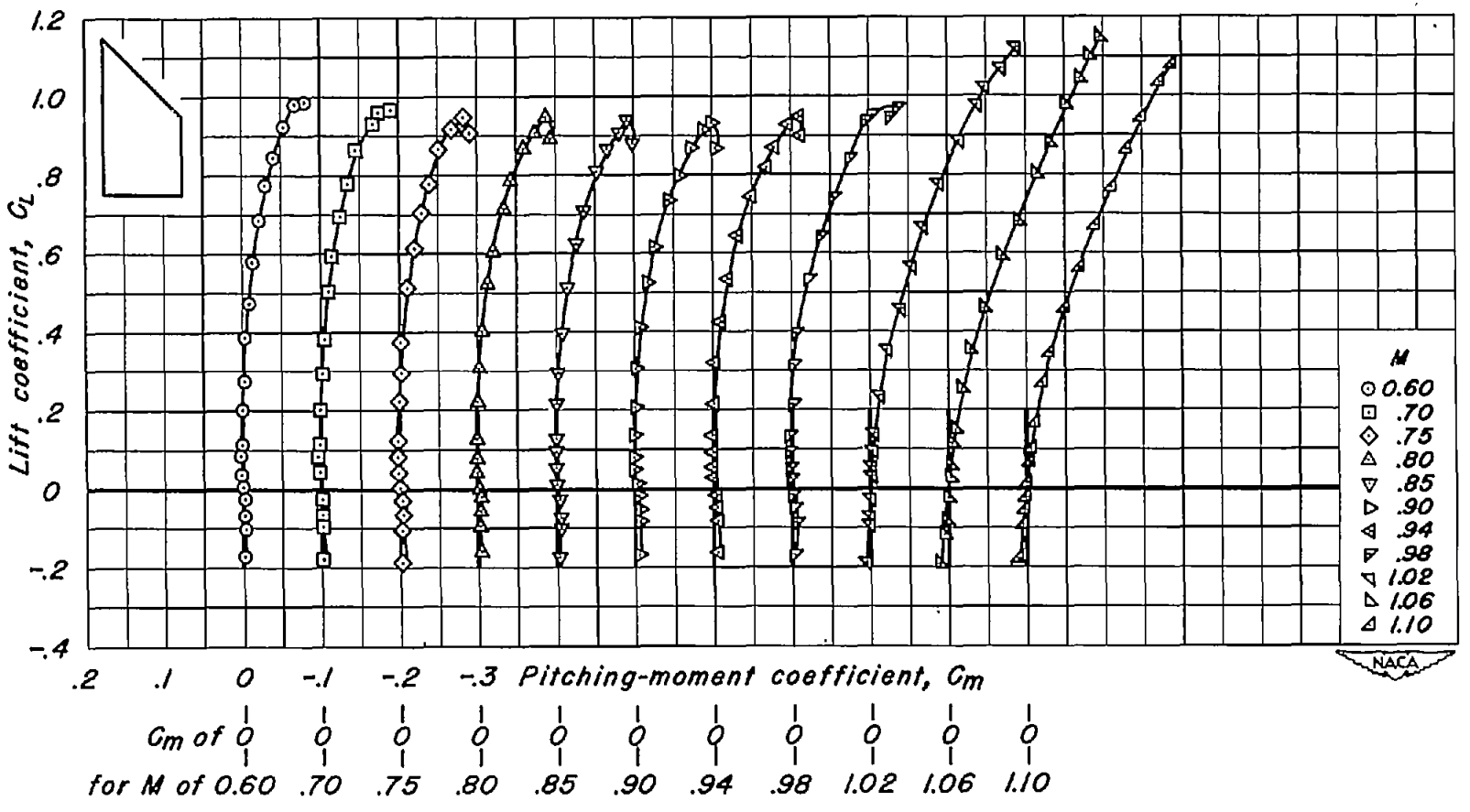

(i) NACA 63A004; λ, 0.5; A, 1.33.
Figure 16.- Continued.

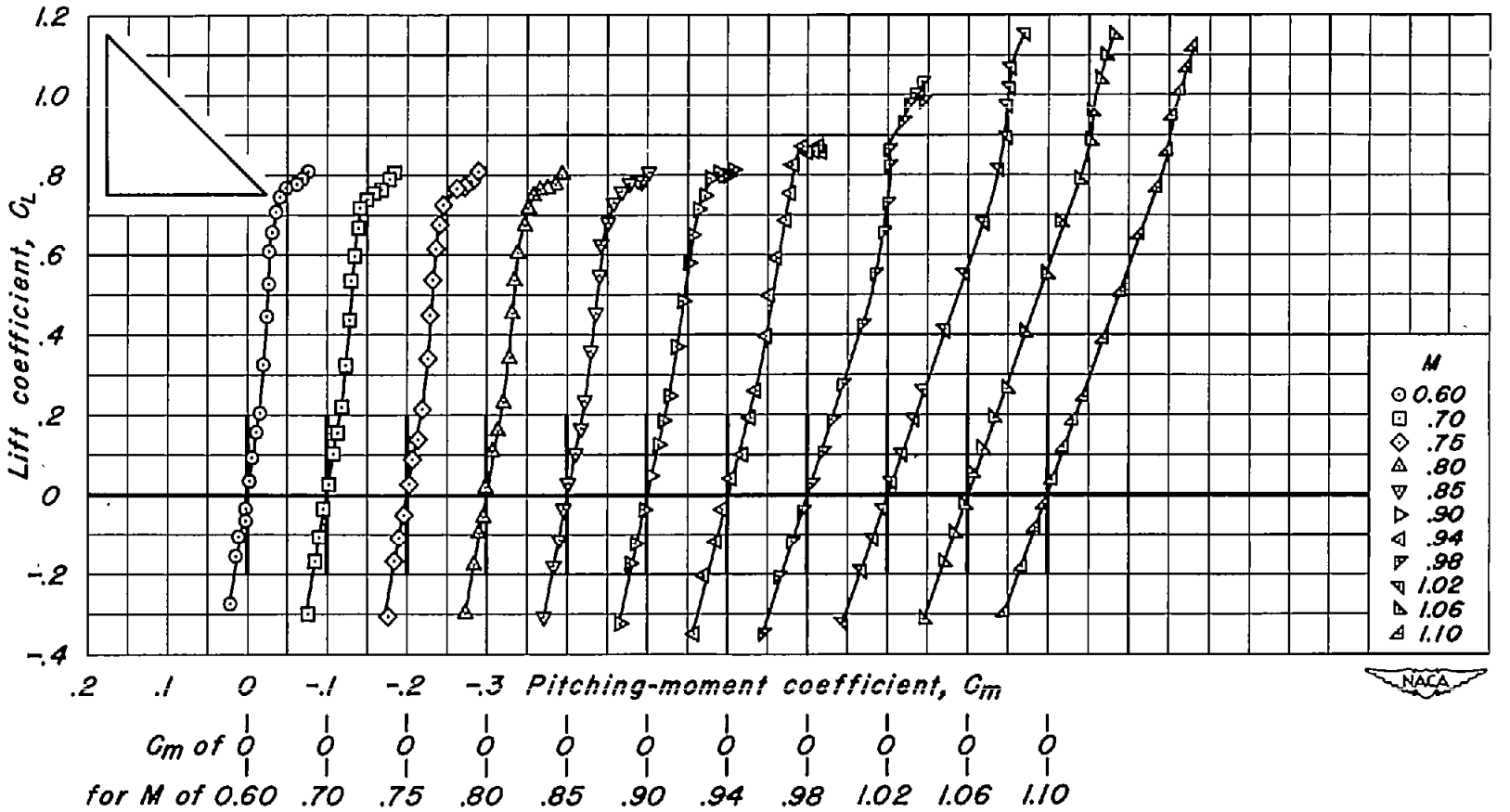

C_m of	0	0	0	0	0	0	0	0	0	0	0
for M of	0.60	.70	.75	.80	.85	.90	.94	.98	1.02	1.06	1.10

(j) NACA 63A006; λ, 0; A, 4.00.
Figure 16.- Continued.

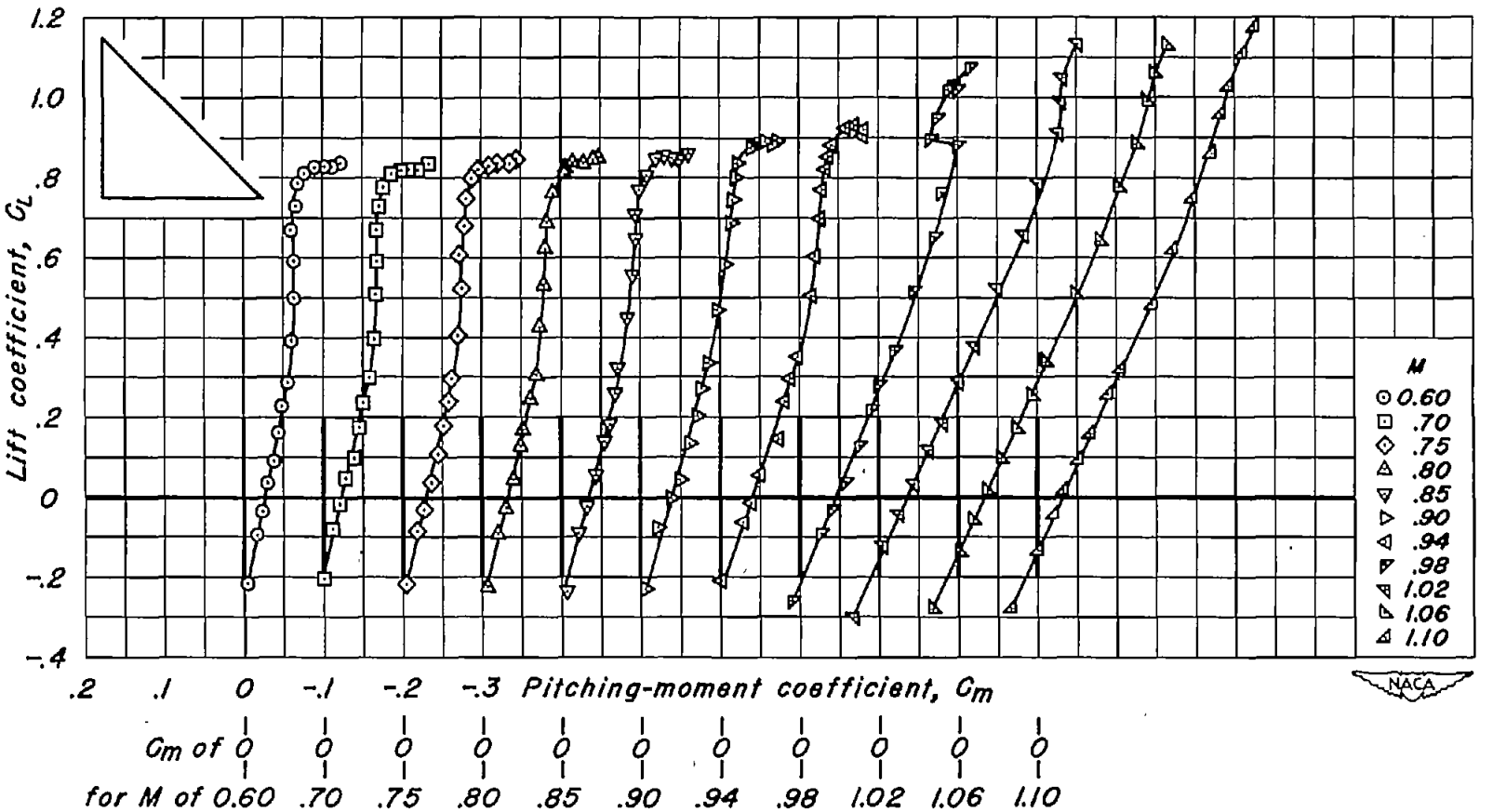

(k) NACA 63A(1.5)04; λ, 0; A, 4.00.
Figure 16.- Continued.

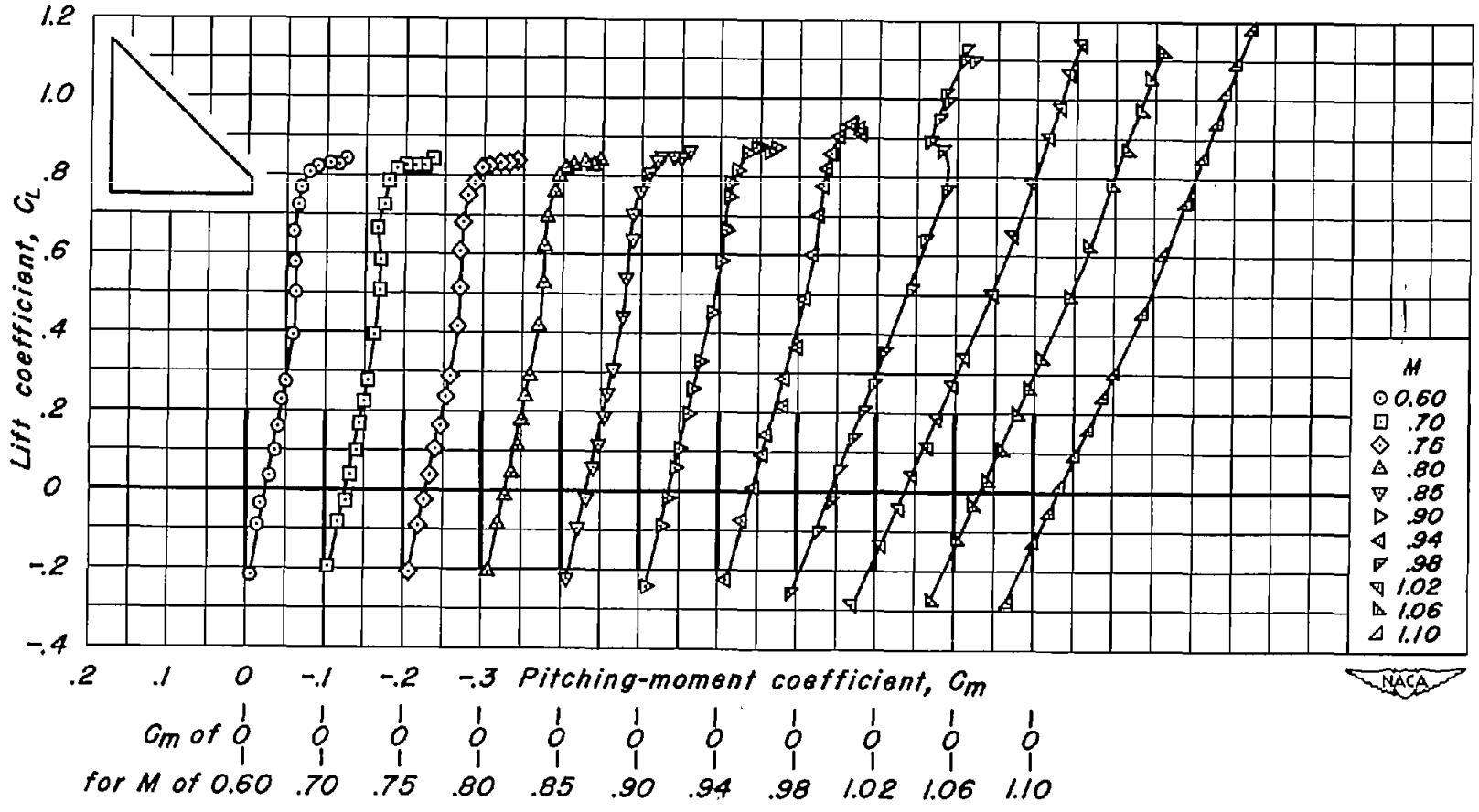

(l) NACA 63A(1.5)04; λ, 0.1; A, 3.27.
Figure 16.- Continued.

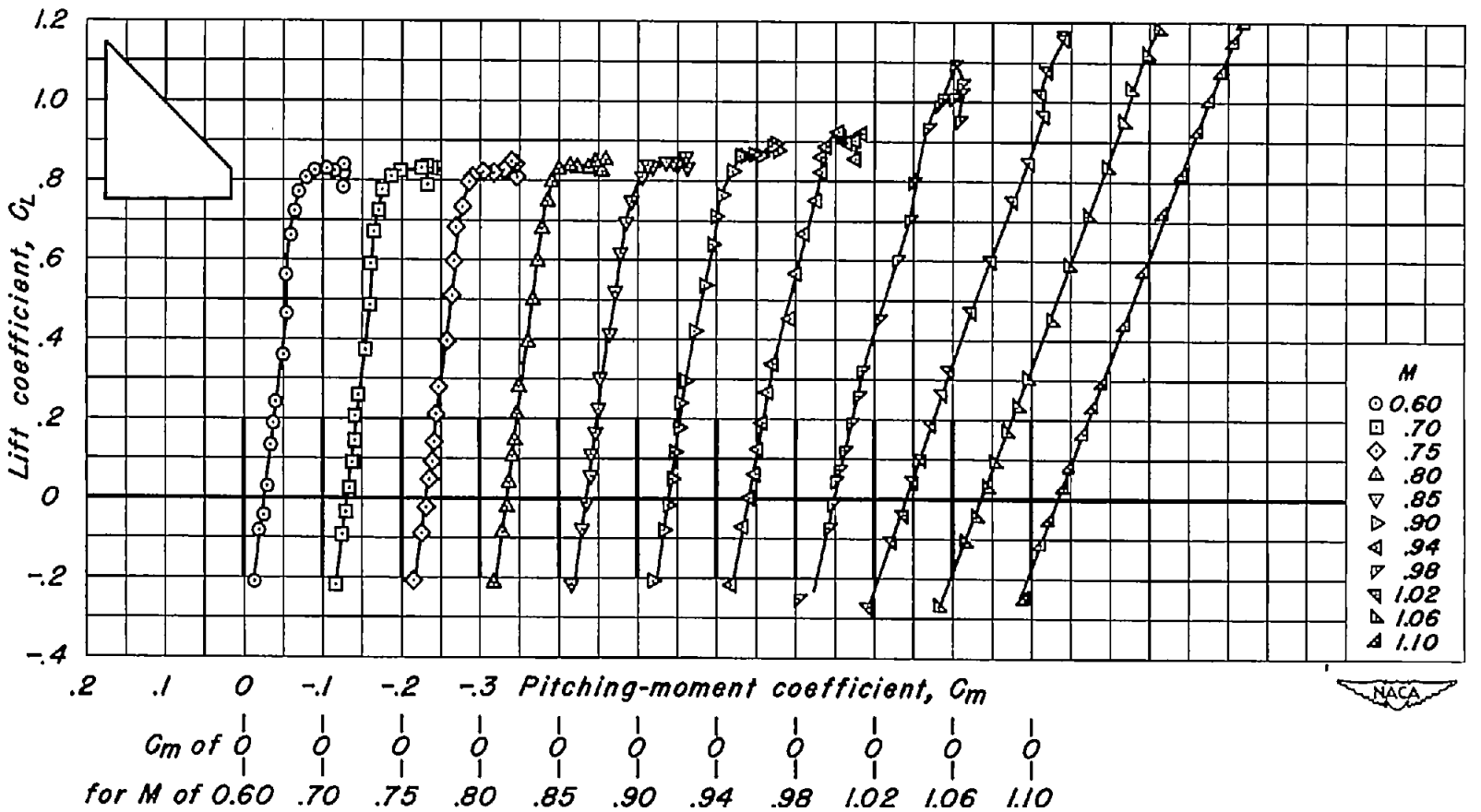

(m) NACA 63A(1.5)04; λ, 0.2; A, 2.67.
Figure 16.- Concluded.

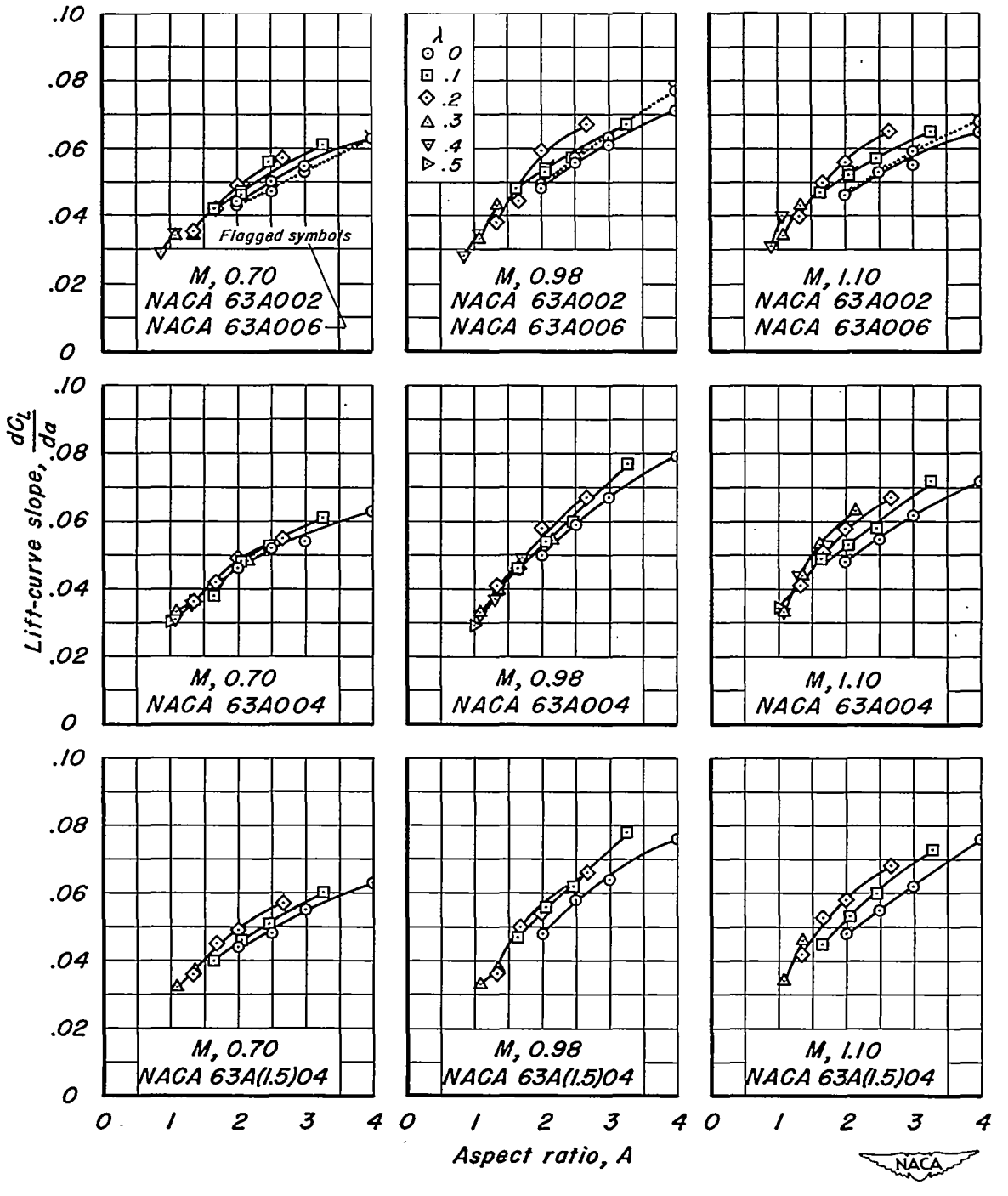

Figure 17.- Variation of lift-curve slope with aspect ratio.

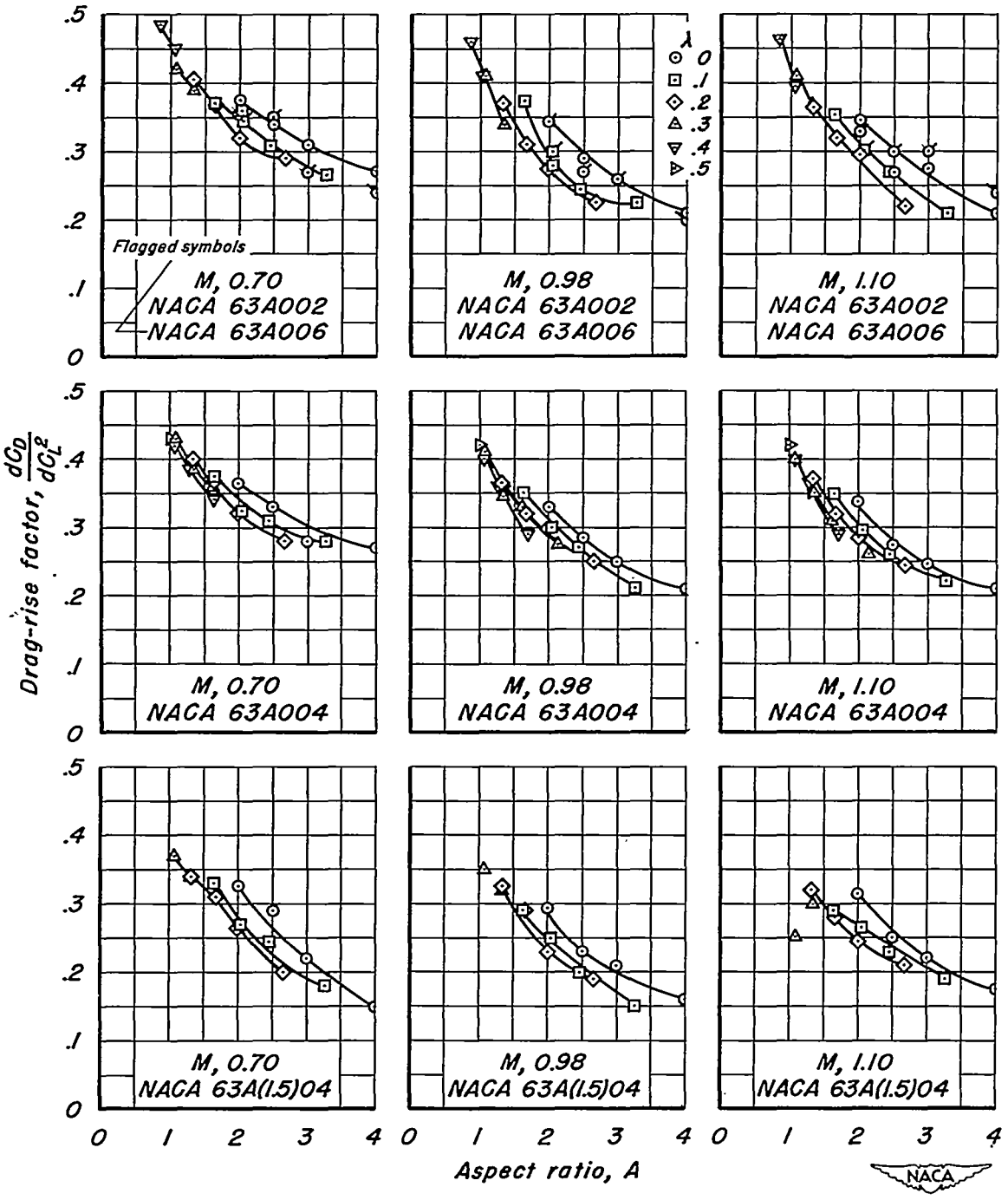

Figure 18.- Variation of drag-rise factor with aspect ratio.

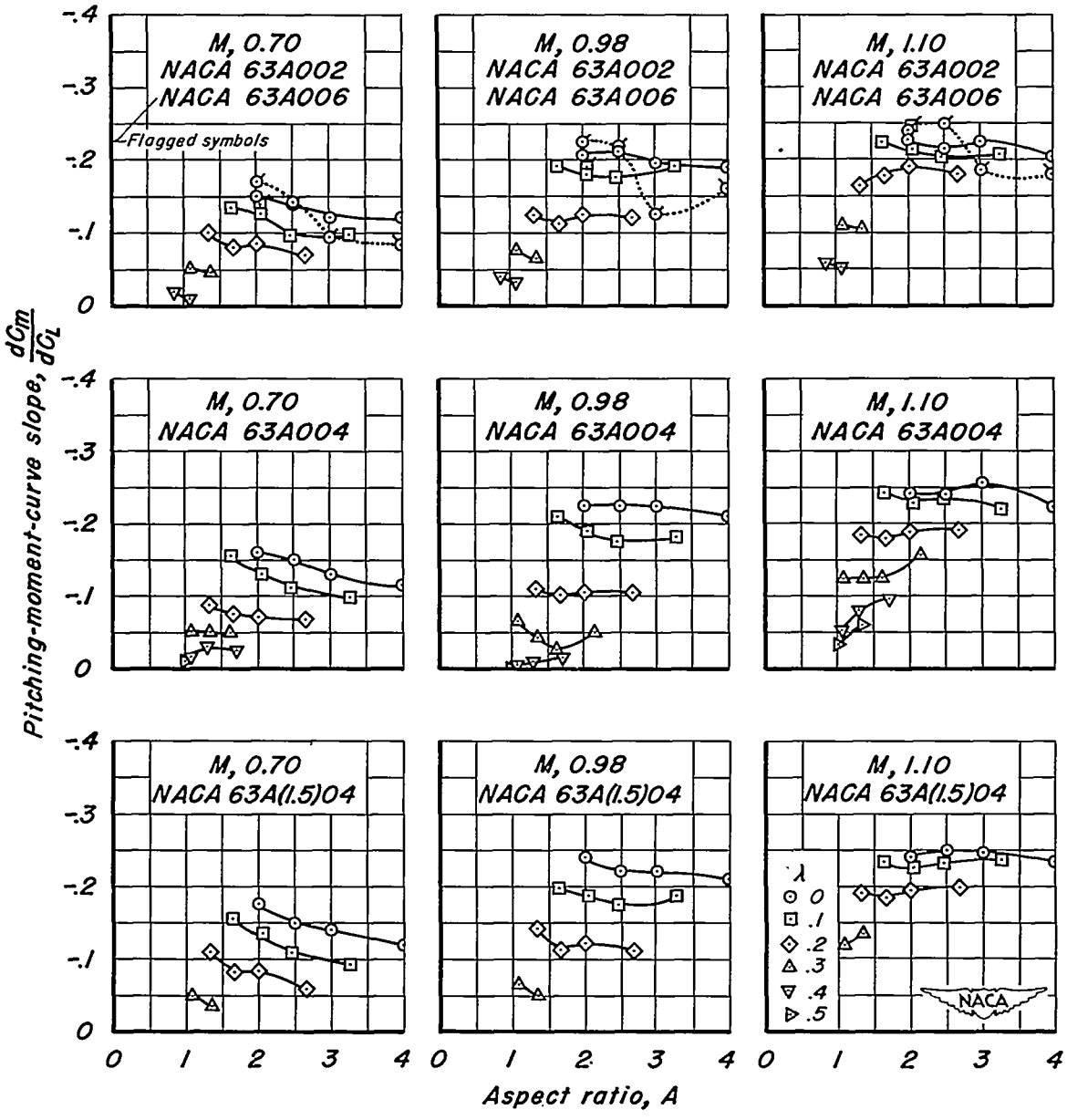

Figure 19.- Variation of pitching-moment-curve slope with aspect ratio.